Correlates of tuberculosis and non-tuberculosis morbidity and immunity in sub-Saharan African HIV-exposed, uninfected infants

By Saori Christina Iwase (IWSSAO001)

Dissertation Submitted for the Degree of

Ph.D. (Med) in Clinical Sciences and Immunology

Supervisor: Dr. Heather Jaspan

Co-supervisor: Dr. Anna-Ursula Happel

Institute of Infectious Disease and Molecular Medicine

Department of Pathology

Division of Immunology

Faculty of Health Sciences

University of Cape Town

October 2023

PLAGIARISM DECLARATION

I, Saori Christina Iwase, hereby declare that the work, on which this dissertation is based on, is my original work (except where acknowledgements indicate otherwise) and that neither the whole work nor any part of it has been, is being, or is to be submitted for another degree in this or any other university.

I authorize the university to reproduce for the purpose of research either the whole or any portion of the contents in any manner whatsoever.

Signature: Signed by candidate

Date: 29 October 2023

DEDICATION

This dissertation is dedicated to my late father, Masaaki Iwase.

His unconditional love, endless support and countless sacrifices

have propelled me to where I am today.

TABLE OF CONTENTS

INCLUSION OF PUBLICATIONS

I confirm that I have been granted permission by the University of Cape Town's Doctoral Degrees Board to include the following publications in my Ph.D. dissertation, and where co-authorships are involved, my co-authors have agreed that I may include the publications.

1. **Saori C. Iwase**, Paul T. Edlefsen, Lynnette Bhebhe, Kesego Motsumi, Sikhulile Moyo, Anna-Ursula Happel, Danica Shao, Nicholas Mmasa, Sara Schenkel, Melanie A. Gasper, Melanie Dubois, Megan A. Files, Chetan Seshadri, Fergal Duffy, John Aitchison, Mihai G. Netea, Jennifer Jao, Donald W. Cameron, Clive M. Gray, Heather B. Jaspan, Kathleen M. Powis., 2023. **T-SPOT.TB reactivity in Southern African children with and without *in utero* HIV exposure**. Clinical Infectious Diseases, ciad356, http://doi.org/10.1093/cid/ciad356

2. **Saori C. Iwase**, Sophia Osawe, Anna-Ursula Happel, Clive M. Gray, Jonathan Blackburn, Susan P. Holmes, Alash'le Abimiku, Heather B. Jaspan., 2024. **Longitudinal gut microbiota composition of South African and Nigerian infants in relation to tetanus vaccine responses**. Microbiology Spectrum, 12:e03190-23, https://doi.org/10.1128/spectrum.03190-23

Saori Christina Iwase (IWSSAO001)

Date: 29 October 2023

ACKNOWLEDGMENTS

First and foremost, I would like to express my sincere gratitude to my supervisors, Dr. Heather Jaspan and Dr. Anna-Ursula Happel, for their patience and valuable guidance throughout the program and for giving me the opportunity to study at the University of Cape Town under their supervision. Working with you has been inspirational.

I am grateful to former and current Jaspan Lab members in Cape Town and Seattle for their continuous support. In particular, Bryan Brown, Melanie Gasper, Colin Feng, and Christina Balle for sharing their wisdom and knowledge. I would also like to thank Profs. Clive Gray, Alash'le Abimiku, and Drs. Kathleen Powis, Sonwa Dzanibe, Paul Edlefsen, Danica Shao, Sophia Osawe, Elisa Nemes, and Melissa Murphy for sharing their data, scripts, and expertise at different stages of my academic journey. My gratitude extends to all the study personnel involved in the InFANT and Karabo studies and the BCG randomized trial. Most importantly, all the mothers and babies who kindly participated in these studies. Without them, none of this work would be possible.

Thank you to the student office members and others who often came and stopped by for the chat, laughter, moral support, and encouragement. To my friends outside the lab, thank you for your friendship and memorable times.

To my family and my husband's family, thank you for your continuous care, support, and assistance in every way possible. To my beloved husband, Ishkar Singh, words cannot describe how much I am grateful for your unwavering support and encouragement. Thank you for being there for me throughout the highs and lows of this academic journey.

Finally, my sincere appreciation goes to the Yoshida Scholarship Foundation, National Institute of Allergy and Infectious Diseases (NIAID), Dr. Heather Jaspan, and Dr. Kathleen Powis for the financial support.

LIST OF ABBREVIATIONS

ADCC	Antibody-dependent cellular cytotoxicity
AIDS	Acquired immunodeficiency syndrome
AKT	Protein kinase B
AMPs	Antimicrobial proteins
ANCOM-BC	Analysis of Compositions of Microbiomes with Bias Correction
aP	Acellular pertussis
AP-1	Activator protein 1
APCs	Antigen-presenting cells
Areg	Amphiregulin
ART	Antiretroviral therapy
ASVs	Amplicon sequence variants
BCG	Bacillus Calmette-Guérin
BCR	B-cell receptor
BMI	Body mass index
bp	Base pair
C-section	Cesarean section
$CaCl_2$	Calcium chloride
CFP-10	Culture filtrate protein-10
ChIP	Chromatin immunoprecipitation
CI	Confidence interval
ConA	Concanavalin A
COX2	Cyclooxygenase-2
CTLA-4	Cytotoxic T-lymphocyte-associated protein 4
CPC	Chromosomal passenger complex
CUT&RUN	Cleavage Under Targets And Release Using Nuclease
CUT&Tag	Cleavage Under Targets And Tagmentation
DC-SIGN	Dendritic cell-specific intercellular adhesion molecule-3-grabbing nonintegrin
DCs	Dendritic cells
DNA	Deoxyribonucleic acid
DNMT	DNA methyltransferase
DT	Diphtheria toxoid
DUBs	Deubiquitinating enzymes
EBF	Exclusively breastfed
EDTA	Ethylenediaminetetraacetic acid
ELISA	Enzyme-linked immunosorbent assay
EPI	Expanded Programme of Immunization
ESAT-6	Early secreted antigenic target 6 kDa

FACS	Fluorescence-activated cell sorting
FcRn	Fc receptor
FCS	Fetal calf serum
FDCs	Follicular dendritic cells
Foxp3	Forkhead box P3
g	G-force
GALT	Gut-associated lymphoid tissue
GATA3	GATA binding protein 3
GI	Gastrointestinal
GPR	G-protein-coupled receptor
H2AT120ph	Phosphorylation on histone H2A at threonine 120
H2Aub1	Monoubiquitylation on histone H2A
H2Bub1	Monoubiquitylation on histone H2B
H3K14Ac	Acetylation of histone H3 at lysine 14
H3K27Ac	Acetylation of histone H3 at lysine 27
H3K27me3	Trimethylation of histone H3 at lysine 27
H3K36me3	Trimethylation of histone H3 at lysine 36
H3K4me1	Monomethylation of histone H3 at lysine 4
H3K4me2	Dimethylation of histone H3 at lysine 4
H3K4me3	Trimethylation of histone H3 at lysine 4
H3K79me3	Trimethylation of histone H3 at lysine 79
H3K9Ac	Acetylation of histone H3 at lysine 9
H3K9me2	Dimethylation of histone H3 at lysine 9
H3K9me3	Trimethylation of histone H3 at lysine 9
H3S10ph	Phosphorylation on histone H3 at serine 10
H3T3ph	Phosphorylation on histone H3 at threonine 3
H4K16Ac	Acetylation of histone H4 at lysine 16
HAT	Histone acetyltransferase
HDACs	Histone deacetylases
HDMs	Histone demethylases
HEPES	4-(2-hydroxyethyl)-1-piperazineethanesulfonic acid
hg38	Genome Reference Consortium Human Build 38
HIF-1α	Hypoxia-inducible factor-1α
HIV	Human immunodeficiency virus
HLA	Human leukocyte antigen
HMOs	Human milk oligosaccharides
HMTs	Histone methyltransferases
hr(s)	Hour(s)
HREC	Human Research Ethics Committee
HSPCs	Hematopoietic stem and progenitor cells

Hz	Hertz
ICOS	Inducible co-stimulator
IBD	Inflammatory bowel disease
ID2	Inhibitor of DNA Binding 2
IECs	Intestinal epithelial cells
IELs	Intraepithelial lymphocytes
IFN-γ	Interferon-gamma
IGRAs	Interferon-gamma release assays
IgV	Immunoglobulin variable region
IGV	Integrative Genomics Viewer
iHEU	Infants who are HIV-exposed but uninfected
iHUU	Infants who are HIV-unexposed and uninfected
IL	Interleukin
ILCs	Innate lymphoid cells
InFANT	Innate Factors Associated with Nursing Transmission study
IQR	Interquartile range
IU	International units
kB	Kilobase
kbp	Kilobase pair
KCl	Potassium chloride
kDa	Kilodalton
KEGG	Kyoto Encyclopedia of Genes and Genomes
kg	Kilogram
LAB	Lactic acid bacteria
LASSO	Least Absolute Shrinkage and Selection Operator
LAT	Linker for activation of T cells
LAG-3	Lymphocyte activation gene 3
LCK	Lymphocyte cell-specific protein tyrosine kinase
LFC	Log_e fold change
LINE	Long interspersed nuclear element
lncRNA	Long non-coding RNA
LPS	Lipopolysaccharides
LTBI	Latent tuberculosis infection
M	Molar
M cells	Microfold cells
MACS2	Model-based Analysis for ChIP-Seq 2
MAMPs	Microbe-associated molecular patterns
mg	Milligram
$MgCl_2$	Magnesium chloride
MHC	Major histocompatibility complex

min(s)	Minute(s)
miRNA	Micro RNA
ml	Millilitre
mM	Millimolar
mm^3	Cubic millimetre
MNase-pA	Micrococcal nuclease conjugated protein A
$MnCl_2$	Manganese(II) chloride
mRNA	Messenger RNA
Mtb	Mycobacterium tuberculosis
mTOR	Mammalian target of rapamycin
MUC2	Mucin 2
NaCl	Sodium chloride
ncRNA	Non-coding RNA
NCRs	Natural cytotoxicity receptors
NEC	Necrotizing enterocolitis
NFATC2	Nuclear factor of activated T cells 2
NFκB	Nuclear factor kappa B
ng	Nanogram
NGS	Next-generation sequencing
NK	Natural killer cells
NKT	Natural killer T cells
nm	Nanometre
NOD	Nucleotide-binding oligomerization domain
nt	Nucleotide
pA-Tn5	Tn5 transposasae conjugated protein A
PAM	Partitioning around medoids
PAMPs	Pathogen-associated molecular patterns
PBMCs	Peripheral blood mononuclear cells
PBS	Phosphate-buffered saline
PCA	Principal component analysis
PCI	phenol:chloroform:isoamyl alcohol
PCoA	Principal coordinate analysis
PCR	Polymerase chain reaction
PEP	Post-exposure prophylaxis
PERMANOVA	Permutational multivariate analysis of variance
PHA	Phytohaemagglutinin
PI3K	Phosphoinositide 3-kinases
pIgR	Polymeric immunoglobulin receptor
piRNA	Piwi-interacting RNA
PLHIV	People living with HIV

PPD	Purified protein derivative
PPs	Peyer's patches
PRRs	Pattern recognition receptors
QFT	QuantiFERON-TB Gold
qPCR	Quantitative real-time polymerase chain reaction
Rap1	Ras-related protein 1
RD	Regions of difference
RIG-I	Retinoic acid-inducible gene I
RISC	RNA-induced silencing complex
RNA	Ribonucleic acid
RORγt	Retinoic acid-related orphan receptor gamma
ROS	Reactive oxygen species
RPMI	Roswell Park Memorial Institute medium
rpm	Revolutions per minute
rRNA	Ribosomal RNA
RT	Room temperature
SCFAs	Short-chain fatty acids
SCID	Severe combined immunodeficiency
SD	Standard deviation
SDS	Sodium dodecyl sulfate
SEACR	Sparse Enrichment Analysis for CUT&RUN
SFCs	Spot-forming cells
SHM	Somatic hypermutation
SIgA	Secretory IgA
SINE	Small interspersed nuclear element
siRNA	Small interfering RNA
STAT	Signal transducer and activator of transcription
TB	Tuberculosis
TBI	Tuberculosis infection
TCRs	T cell receptors
TE	Tris-EDTA buffer
TFH	T follicular helper cells
TFs	Transcription factors
TGF-β	Transforming growth factor-beta
Th	T helper cells
TJs	Tight junctions
TLRs	Toll-like receptors
TNF-α	Tumor necrosis factor-alpha
Tregs	Regulatory T cells
Tris-HCl	Tris hydrochloride

TST	Tuberculin skin test
TT	Tetanus toxoid
U	Units
Ub	Ubiquitin
UCSC	University of California Santa Cruz
UTR	Untranslated region
vs.	Versus
W1	1 week of age
W15	15 weeks of age
Wflz	Weight-for-length z score
WHO	World Health Organization
wP	Whole-cell pertussis
ZAP-70	Zeta-chain-associated protein kinase 70
α	Alpha
β	Beta
γ	Gamma
µg	Microgram
µl	Microliter
µM	Micromolar
%	Per cent
°C	Degrees Celsius

LIST OF FIGURES

LIST OF TABLES

ABSTRACT

Correlates of tuberculosis and non-tuberculosis morbidity and immunity in sub-Saharan African HIV-exposed, uninfected infants

Background:

Perinatal HIV transmission has been considerably reduced due to successful intervention programs. Consequently, there is a growing population of infants who are HIV-exposed but uninfected (iHEU), particularly in sub-Saharan Africa. These infants experience an increased risk of morbidity compared to infants who are HIV-unexposed and uninfected (iHUU), predominantly due to infectious diseases. Although the mechanisms underlying this increased vulnerability remain unclear, it may be associated with their altered immunity and/or gut microbiota.

Bacillus Calmette-Guérin (BCG) vaccination is an effective intervention to prevent severe tuberculosis (TB) disease in children. BCG vaccination also enhances heterologous protective immunity against infections through epigenetic reprogramming of innate immune cells (known as "trained innate immunity"). However, whether iHEU receive comparable protection from BCG-induced immunity against TB and non-TB infection as iHUU remains elusive.

Gut microbiota plays a critical role in immune development during infancy. A close relationship between gut microbiota and vaccine responses has been reported in iHUU, including tetanus toxoid (TT) vaccination. However, a limited number of studies longitudinally investigated the effect of *in utero* HIV exposure on the gut microbiota, and results are often conflicting. In addition, not many studies have compared the trajectory of gut microbiota between iHEU and iHUU across multiple countries. While several studies have indicated reduced immune responses against TT vaccination in iHEU compared to iHUU, the interplay between HIV exposure, gut microbiota, and vaccine response is largely unexplored.

Aims:

In this dissertation, we examined three potential contributing factors that may underlie the higher risk of morbidity observed among iHEU in sub-Saharan Africa. The specific aims were to examine

whether BCG affords the same protection against TB infection (TBI) and disease in iHEU (corresponds to Aim 1), effect of HIV exposure on longitudinal gut microbiota composition and its association with TT vaccine response (corresponds to Aim 2), and optimization of epigenetic assay protocol, intended for future investigation of BCG-induced histone modifications in iHEU (corresponds to Aim 3).

Methods and results:

To assess TBI prevalence among iHEU and iHUU, a total of 418 mother-infant pairs from South Africa and Botswana were included. All infants received BCG vaccination at birth as per standard of care. T-SPOT.TB (ELISpot-based interferon-gamma release assay) was performed using cryopreserved peripheral blood mononuclear cells (PBMCs) from infants aged 9-18 months. The prevalence of TBI did not differ by the infant HIV exposure status, with 10 cases (3.4%) among iHEU and four cases (3.2%) among iHUU, none with symptoms of active TB disease. This trend was the same across two different African countries where the burden of HIV and TB is high. However, because of the lower T-SPOT.TB positivity than initially anticipated, we were under powered to conclude the effect.

To assess whether gut microbial succession alters immunity in iHEU, we profiled longitudinal gut microbiota composition and associated this with TT vaccine responses in 354 mother-infant pairs from South Africa and Nigeria. Stool samples were collected at 1 and 15 weeks of life, and 16S ribosomal ribonucleic acid (rRNA) gene sequencing was performed. Plasma IgG anti-tetanus antibody titers were measured by enzyme-linked immunosorbent assay (ELISA). The effect of HIV exposure on infant gut microbiota composition was relatively modest compared to the impact of age and geographical factors. However, HIV exposure and specific gut microbes were independently associated with the TT vaccine response at 15 weeks of age. Results for South Africa and Nigeria differed, possibly due to higher maternal anti-tetanus IgG titers and hence infant baseline titers in Nigeria.

To optimize an epigenetic assay that can be applied to infant samples, monocytes and natural killer (NK) cells were isolated from cryopreserved PBMCs using fluorescence-activated cell sorting (FACS). Cleavage Under Targets and Tagmentation (CUT&Tag) was optimized for assessing the

histone modifications, acetylation of histone H3 at lysine 27 (H3K27Ac), trimethylation of histone H3 at lysine 4 (H3K4me3), and trimethylation of histone H3 at lysine 27 (H3K27me3; also used as a positive control). The optimized protocol was then applied to a subset of infant samples (n = 14; aged between six and seven weeks). Optimal input cell number, polymerase chain reaction (PCR) cycles, and sequencing depth were carefully determined for the CUT&Tag assay. These adjustments were necessary to achieve the assay's feasibility and data quality. The optimized CUT&Tag protocol and fine-tuned data analysis strategy successfully exhibited its capability to analyze multiple histone modifications using only 5,000 infant monocytes or NK cells as an input sample.

Conclusions:

Prenatal HIV exposure and gut microbiota may independently influence infant TT vaccine response. This supports the existing notion that iHEU exhibit altered immunity. Although previous studies have indicated that iHEU experience a higher risk of infection than iHUU, our data suggested that BCG vaccination was equally protective against TBI, irrespective of HIV exposure status. The optimized CUT&Tag protocol will offer a useful tool for investigating histone modifications using ultra-low input samples. This will be employed in the future study to explore whether iHEU exhibit comparable epigenetic modifications induced by BCG vaccination as for iHUU, providing valuable insight into whether iHEU receive similar non-specific protection from BCG vaccination compared to iHUU.

Chapter 1. Literature review

1.1. Human Immunodeficiency Virus (HIV) infection and disease

1.1.1. Epidemiology of HIV infection and disease

HIV is the causative agent of acquired immunodeficiency syndrome (AIDS). Due to the availability of antiretroviral therapy (ART), the number of people dying of AIDS has dramatically decreased. However, HIV infection is still a major public health issue, as approximately 39 million people are currently living with HIV and 630,000 people died from AIDS-related illnesses in 2022 worldwide [1]. sub-Saharan Africa accounts for two-thirds of new HIV infections, though the population of this region only makes up approximately 15% of the global population. HIV is predominantly spread through heterosexual transmission in sub-Saharan Africa, with adolescent girls and young women being particularly at high risk of HIV. In 2022, about 63% of new HIV infections were among women and girls living in sub-Saharan Africa [1].

1.1.2. Prevention of vertical HIV transmission

Vertical transmission of HIV occurs during pregnancy, delivery, or via breastfeeding. Children in sub-Saharan Africa account for nearly 90% of the population of children and adolescents living with HIV [2]. Without intervention, the vertical transmission rate can be as high as 45% [3]. Since 2013, Option B+ has been recommended by the World Health Organization (WHO) to combat vertical HIV transmission [4], whereby women with HIV should initiate lifelong ART regardless of CD4 count or clinical stage. In 2022, among the 1.2 million pregnant women with HIV, 82% were on ART globally [5]. Although its effectiveness is substantially dependent on the woman's adherence, Option B+ is shown to be a more effective approach to reducing vertical transmission than previous guidelines [4,6–11]. With the successful prevention programs, the vertical transmission rate in sub-Saharan Africa in 2021 ranged between 2-25% in 2021 [12]. Women with HIV are advised to exclusively breastfeed their infants for six months and to continue breastfeeding alongside complementary foods for 24 months or longer [13]. Furthermore, infants born to women with HIV receive daily oral ART (either nevirapine or zidovudine) for a period of two to six weeks after birth [14,15].

1.2. Tuberculosis (TB) infection and disease

1.2.1. Epidemiology of TB infection and disease

TB disease is an airborne infectious disease caused by *Mycobacterium tuberculosis* (Mtb). TB disease contributes to a major cause of mortality in the world. According to the WHO, an estimated 10 million people newly developed TB disease in 2018, with a global average of 130 cases per 100,000 population [16]. Most TB disease cases in 2018 occurred in South-East Asia (44%), Africa (24%), and the Western Pacific (18%), with smaller percentages in the Eastern Mediterranean (8%), Europe (3%), and the Americas (3%). WHO lists 30 high TB burden countries, which account for 87% of the world's TB disease cases. Among them, eight countries accounted for two-thirds of the total cases: Bangladesh, China, India, Indonesia, Nigeria, Pakistan, Philippines, and South Africa [16].

Among the global TB disease cases, 8.6% were people living with HIV (PLHIV) [16,17]. Estimated TB deaths in 2018 were 1.2 million among people without HIV and 251,000 among PLHIV. TB disease can affect people regardless of age group and sex, but males (15 years and older) accounted for the highest burden of 57% in 2018, whereas females (15 years and older) only consisted of 32%, and children (younger than 15 years) for 11% [16], and the prevalence increases with age [18]. About a quarter of the global population has been infected with Mtb, but most individuals infected with Mtb are asymptomatic and remain in a latent stage of infection. The risks of progressing to TB disease are about 5-10% in adults, 15% in adolescents, 24% in children aged between one and five years, and 43% in infants under the age of one [19]. As progression from an asymptomatic state to active TB disease is particularly rapid in the first five years of life [20,21], early diagnosis and initiation of treatment are crucial to mitigate the burden of TB disease in children [22].

1.2.2. Immune response against Mtb infection

Mtb is carried as airborne droplet nuclei when a person with active TB disease coughs. Transmission of Mtb occurs when the droplets are inhaled into the lower respiratory tract of the recipient host [23]. Mtb infection mainly causes pulmonary disease. However, extra-pulmonary disease can occur if the Mtb is disseminated from the lung to other tissues (such as lymph nodes, bone, and meninges) through the bloodstream and lymphatic system [24].

The primary immune response against Mtb infection is phagocytosis by alveolar macrophages and dendritic cells (DCs) through toll-like receptor (TLR) recognition. In addition, autophagy, apoptosis, and inflammasome assembly are induced to control Mtb infection [25]. Macrophages trigger pro-inflammatory responses and attract mononuclear cells to form a cluster of cells at the infection site, known as granuloma (**Figure 1.1**) [26]. T helper type 1 (Th1) cells are also recruited to the granuloma and help to develop the structure further [27]. Interferon-gamma (IFN-γ) secreted from Th1 cells is important for controlling Mtb infection [28]. In addition, Th1 immunity induces the secretion of tumor necrosis factor-alpha (TNF-α), which enhances the microbicidal activity of macrophages [29].

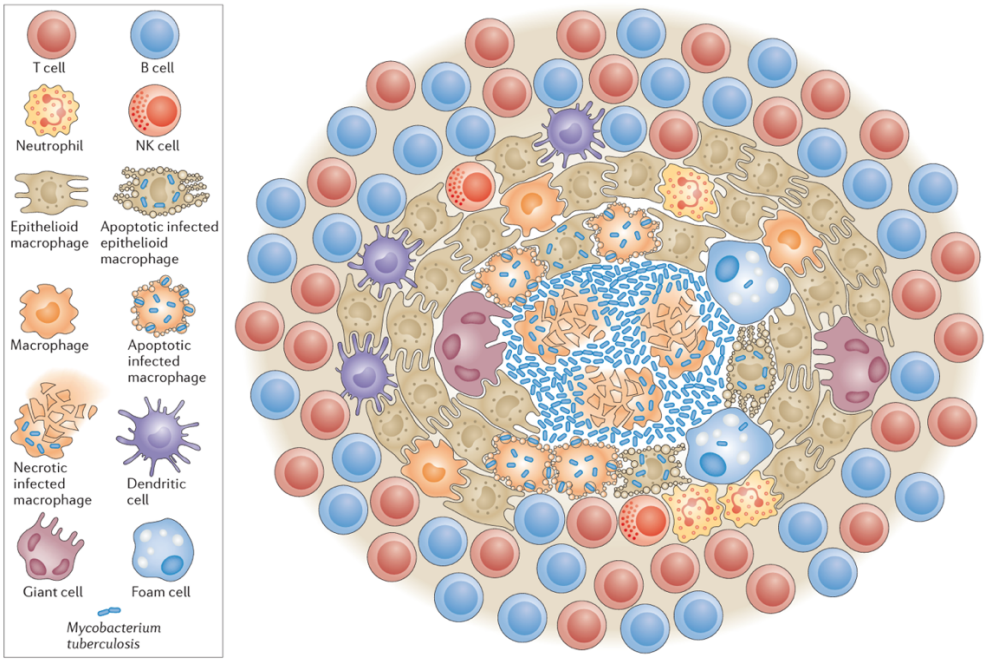

Figure 1.1. Structure of TB granuloma. Macrophages are recruited to the infection site, where they transform into epithelioid cells. These cells exhibit tightly interdigitated cell membranes, which helps to create a barrier to isolate the infection. Macrophages also transform into foam cells. Other immune cells, such as DCs, T cells, B cells, NK cells, and neutrophils, are also recruited to the granuloma. The center of the granuloma is necrotic and apoptotic due to the death of infected macrophages. Abbreviation: DCs, dendritic cells; NK cells, natural killer cells; TB, tuberculosis (Adapted from Ramakrishnan, 2012).

The cellular response in granulomas is orchestrated to prevent bacterial growth [30]. This state has been called latent TB infection (LTBI) [31,32] but is now more commonly called TB infection (TBI) [33–36] (**Figure 1.2**). A person with TBI is not infectious and does not present symptoms

of TB disease. However, this latent state can progress soon after infection or can be reactivated if the host immune system cannot suppress the growth of Mtb. Increased replication of Mtb causes necrotic macrophage death, leading to granulomatous lesions and dissemination of Mtb [37]. Mtb has adapted several mechanisms to evade the host immune responses, including blocking phagosome maturation, limiting antigen presentation, and delaying the priming of adaptive immunity [38–41].

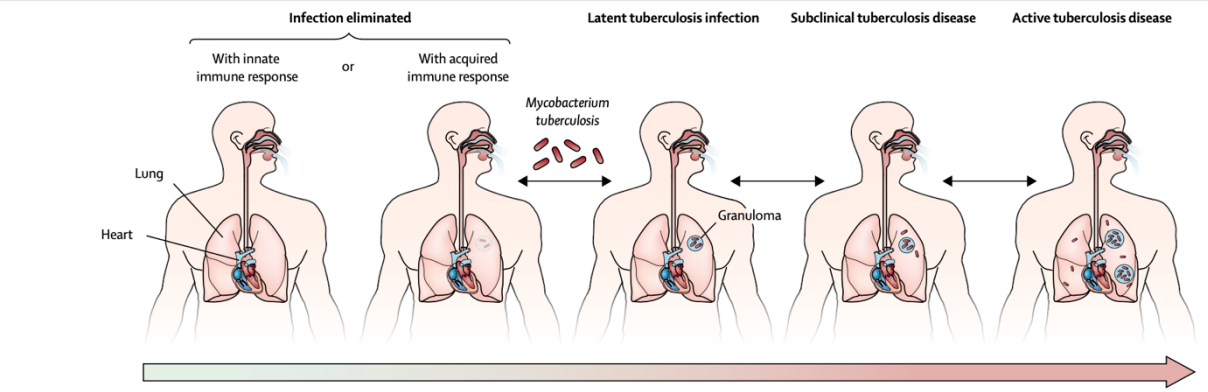

TST	Negative	Positive	Positive	Positive	Usually positive
IGRA	Negative	Positive	Positive	Positive	Usually positive
Culture	Negative	Negative	Negative	Intermittently positive	Positive
Sputum smear	Negative	Negative	Negative	Usually negative	Positive or negative
Infectious	No	No	No	Sporadically	Yes
Symptoms	None	None	None	Mild or none	Mild to severe
Preferred treatment	None	None	Preventive therapy	Multidrug therapy	Multidrug therapy

Figure 1.2. The spectrum of TB infection and disease. TB encompasses a wide spectrum of stages, from initial infection to active disease. The stages are dependent on the immune condition of the infected person. Upon exposure to Mtb, individuals may effectively eliminate pathogens through either an innate or acquired immune response. Positive results from TST or IGRA indicate the involvement of the acquired immune response in pathogen clearance. If the immune system fails to eradicate Mtb completely, the pathogen enters a latent state (used to be referred to as LTBI and recently as TBI). During the latent state, Mtb remains contained within the granuloma. Therefore, individuals with TBI do not exhibit symptoms but present positive TST or IGRA results. When the immune system cannot control the bacterial growth within the granuloma, the infected individuals progress to TB disease status. Abbreviation: IGRA, interferon-gamma release assay; LTBI, latent TB infection; Mtb, Mycobacterium tuberculosis; TB, tuberculosis; TBI, tuberculosis infection; TST, tuberculin skin test (Adapted from Furin, Cox, & Pai, 2019).

1.2.3. Detection methods for TBI

Currently, there are two methods of detecting TBI: the tuberculin skin test (TST) and IFN-γ release assays (IGRAs). TST is the standard method to detect TBI via intradermal injection of tuberculin purified protein derivative (PPD). The diameter of the skin reaction is used to evaluate TBI. The benefit of this test is that it is inexpensive, simple, and suitable for resource-limited settings, and extensive published literature is available for interpretation in different settings and populations. However, TST may give false positive results because of its cross-reactivity with non-tuberculous mycobacterium infection or Bacillus Calmette-Guérin (BCG) vaccination. In addition, a second visit is required for diagnosis 48-72 hours (hrs) post-injection, and trained staff is required to interpret results accurately. On the other hand, IGRAs are *in vitro* tests that include QuantiFERON-TB Gold (QFT), QFT-Plus, and T-SPOT.TB. IGRAs use two or three TB antigens, predominantly early secreted antigenic target 6 kDa (ESAT-6), and culture filtrate protein-10 (CFP-10). Because these antigens are absent from BCG and most non-tuberculous mycobacterium, IGRAs do not have cross-reactivity and are thus more specific than TST. Furthermore, negative and positive internal controls in each assay improve the specificity of the results. Importantly, T-SPOT.TB tests use peripheral blood mononuclear cells (PBMCs) and can and have been used on cryopreserved samples [42]. A positive IGRA test indicates previous exposure to Mtb. However, it does not give evidence of active TB disease. Therefore, clinical, radiological, or microbiological methods are required to confirm active TB disease.

1.3. Vaccination for infants

Vaccination is regarded as one of the most significant public health achievements of the 20th century. The Expanded Programme of Immunization (EPI) was launched in 1974 to provide immunization against TB, diphtheria, tetanus, pertussis, measles, and polio to all children by 1990 [43,44]. Globally, vaccination prevents four to five million deaths yearly [45]. Each country adopts immunization programs based on the disease burden and economic resources status. BCG and tetanus toxoid (TT) vaccines are discussed in the following sections as these vaccines are relevant to this dissertation.

1.3.1. BCG vaccine

BCG is the only currently licensed vaccine against TB disease worldwide [46]. BCG is commonly given at birth in most countries, although it is contraindicated in symptomatic HIV infection, as the vaccination can lead to disseminated BCG [47]. When administered to newborn infants, BCG protects against childhood TB disease and disseminated forms of TB disease, including miliary TB and TB meningitis [48]. Since TB morbidity and mortality can be high in children under the age of five [49], BCG vaccine is invaluable in preventing TB disease among this vulnerable group.

A meta-analysis has indicated that the duration of protection afforded by BCG can last up to 10 years [50]. The efficacy of BCG appears to vary by country, lasting up to 15 years in the UK [51], 40 years in Norway [52], and even extending to 50-60 years among American Indians and Alaska Natives [53,54]. The underlying mechanisms for this variability in BCG efficacy may be (1) exposure to environmental mycobacteria, (2) skewed immune response towards Th2 type due to parasitic infections, and (3) immunization with different strains of BCG, (4) host genetics, and (5) gut microbiota [54–56], among others.

BCG is a live attenuated vaccine derived from *Mycobacterium bovis*, isolated in 1902. Due to the prolonged passage of bacterial strains in various conditions in different countries, there are several regions of difference (RD) that have been introduced in the bacterial genomic deoxyribonucleic acid (DNA) through insertion or tandem duplication (**Figure 1.3**) [57]. It is believed that the deletion of RD1 is responsible for the attenuation of BCG [58]. The RD1 encodes several proteins, including ESAT-6 and CFP-10, that are known to be essential for the pathogenicity of Mtb [59]. BCG strains can be divided into two types. BCG Japan, Birkhaug, Sweden, and Russia are considered as "early strains," and BCG Pasteur, Denmark, Glaxo, Connaught, and Tice are considered as "late strains" [57]. The major difference between the early and late strains is that the late strains have an absence of RD2. This variation of BCG strains may explain some of the variability in efficacy of BCG in human clinical trials and varying T-cell responses *in vitro* [60,61].

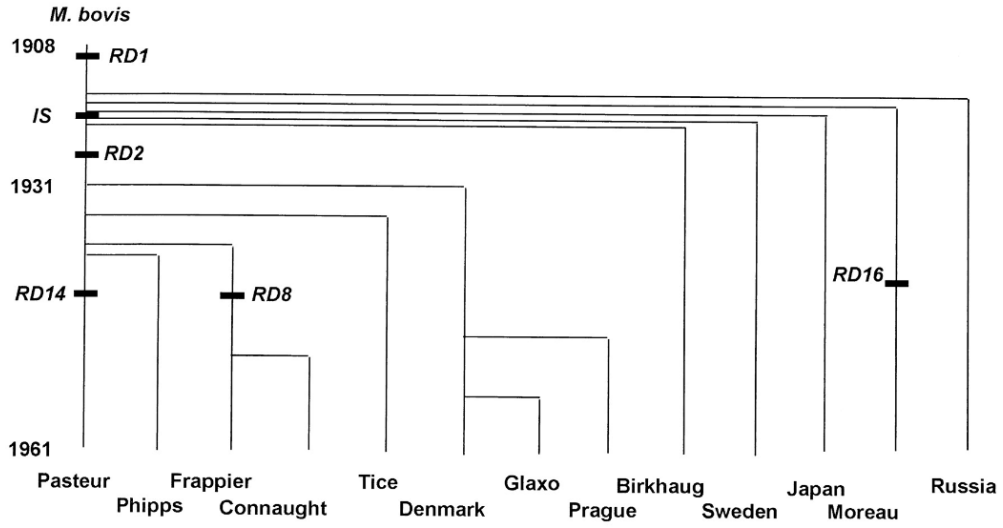

Figure 1.3. Genealogy of BCG sub-strains. BCG vaccine was developed from *M. bovis*, a bacterium closely related to *Mtb*. The bacterium was repeatedly cultured in different laboratories under different conditions, introducing several RD. The most significant factor in the attenuation of BCG was the loss of the RD1 region. This region is responsible for the secretion of the ESX-1 system, which includes the proteins ESAT-6 and CFP-10. These proteins are thought to be important for the virulence of TB. Based on the genomic difference, BCG sub-strains are grouped into "early strains" (BCG Birkhaug, Japan, Russia, and Sweden) and "late strains" (BCG Pasteur, Glaxo, Denmark, Tice, Connaught). Abbreviation: BCG, Bacillus Calmette-Guérin; CFP-10, culture filtrate protein-10; ESAT-6, early secreted antigenic target 6 kDa; RD, regions of difference; TB, tuberculosis (Adapted from Behr *et al*., 1999).

BCG is recognized by innate immune cells, such as neutrophils, macrophages, and DCs [54,62]. Pathogen-associated molecular patterns (PAMPs) from the bacterium cell wall, such as peptidoglycan, arabinogalactan, and mycolic acids, are recognized via different pattern recognition receptors (PRRs). In particular, TLR2 and TLR4 are involved in the recognition of BCG [54]. Another group of receptors involved in recognizing BCG are nucleotide-binding oligomerization domain (NOD)-like receptors. It is known that NOD2 receptors recognize peptidoglycan of bacterial cell walls [63]. In addition, C-type lectin receptors, such as DC-specific intercellular adhesion molecule-3-grabbing nonintegrin (DC-SIGN), are involved in the recognition of BCG [64]. Adaptive immune responses of both CD4+ and CD8+ cells are then induced by antigen-presenting cells (APCs), such as DCs and macrophages, presenting antigenic peptides on their major histocompatibility complex (MHC) molecules. It is important to note that BCG induces Th1 response in infants with skewed Th2 immunity [65]. Th1 cells secrete IFN-γ, which induces the anti-mycobacterial activity of macrophages [66], and TNF-α and interleukin (IL)-2 [67]. A longitudinal observational study in infants showed that the primary response to BCG involves IFN-

γ production from activated CD4+ T cells with predominant CD45RA-CCR7+ central memory phenotypes. The BCG-specific CD4+ T-cell response was the highest at the 10-weeks post-vaccination and had waned at 40 weeks [67]. Importantly, a growing body of evidence indicates that BCG protects against all-cause childhood mortality, besides protecting against TBI [68–70].

1.3.2. Tetanus toxoid (TT) vaccine

Tetanus is an infection caused by the bacterium *Clostridium tetani* spores, which can be found in various places, including in soils, ash, rusty tools, and animal excrement [71,72]. Spores of *Clostridium tetani* can enter the body through the skin, often due to injuries. Once the bacterium enters the body, it releases a toxin (tetanospasmin) into the bloodstream. The toxin affects the nervous system, including the brain or spinal cord, and interferes with the motor neurons that control muscle movement. Symptoms of tetanus appear 3-21 days after the infection. Common symptoms include jaw muscle cramps, seizures, headache, fever, sweating, and muscle spasms in the back, abdomen, and limbs. Although the disease is not spread between humans, an estimated 34,000 newborn infants died from neonatal tetanus in 2015 globally [71]. The main prevention of the disease is through immunization with TT-containing vaccines.

TT vaccines can be administered alone or in combinations to protect from other diseases [72], such as DTaP (diphtheria toxoid [DT]), TT, and acellular pertussis [aP]), DTwP (DT, TT, and whole-cell pertussis [wP]), DT (DT and TT), Tdap (TT, DT, and aP), and Td (TT and DT) [72]. In South Africa and Nigeria, infants receive TT vaccination at 6, 10, and 14 weeks of age (DTaP and DTwP, respectively). In Botswana, infants receive DTwP at 2, 3, and 4 months of age [73]. Importantly, TT response can depend on the formulation of the combination vaccine. It has been shown that the acellular DTaP vaccination induced a Th2-skewed immune response compared to the cellular DTwP formulation, indicating that the response to pertussis is dependent on the type of boost, but in addition, responses to TT boost can also be skewed by the pertussis formulation used at prime [74]. Neonatal tetanus can occur in newborn infants when the umbilical cord is cut using nonsterile instruments, or the umbilical stump is covered with nonsterile material [71]. However, if mothers are vaccinated and have sufficient circulating antibodies, infants can be protected from tetanus through the transplacental transfer of antibodies [72].

1.4. Epigenetic modifications

1.4.1. Chromatin structure

The human DNA genome usually consists of 23 pairs of chromosomes per cell that encode genetic information. Each chromosome varies in size from around 50 to 300 million base pairs, and they are tightly packaged within the nucleolus of a cell, which is only about 6 µm in diameter. Human DNA is wrapped around a complex of proteins called histones. The core histone complex gives structural support to form nucleosomes (**Figure 1.4**) [75], which serve as the primary unit of packing. The core histone complex comprises two units of H2A, H2B, H3, and H4 each, and 147 bp of DNA is wrapped around the octamer complex [76]. Each nucleosome is joined by a short fragment of linker DNA (10-100 bp), forming 11 nm chromatin fiber representing a "beads-on-a-string" structure (**Figure 1.4**). Chromatin is further folded to form chromosomes [75]. Based on the accessibility, chromatin fibers can be categorized as euchromatin (open chromatin) or heterochromatin (closed chromatin). Dynamic alternations of chromatin structure are achieved by epigenetic modifications.

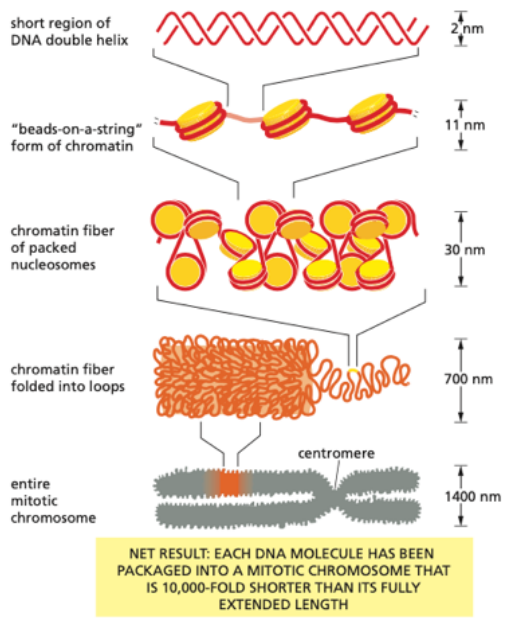

Figure 1.4. Chromatin structure. DNA is wrapped around histone proteins to form chromatin, a "beads-on-a-string" structure. Chromatin is a primary packing level and is folded into 30-nm chromatin fiber. The chromatin fiber further compacted to form higher-order structures called chromosomes (Adapted from Alberts *et al*., 2014).

Epigenetics is the heritable chemical changes in DNA, ribonucleic acid (RNA), or protein without alterations in the DNA sequence itself that thereby influence gene expression. There are three types of epigenetic modifications observed in mammalian systems: (1) DNA methylation, (2) histone modification, and (3) non-coding RNA (**Figure 1.5**) [77]. Various factors can induce epigenetic changes, including nutrition, behavior, stress, smoking and alcohol consumption, air pollution, and vaccines [78–80].

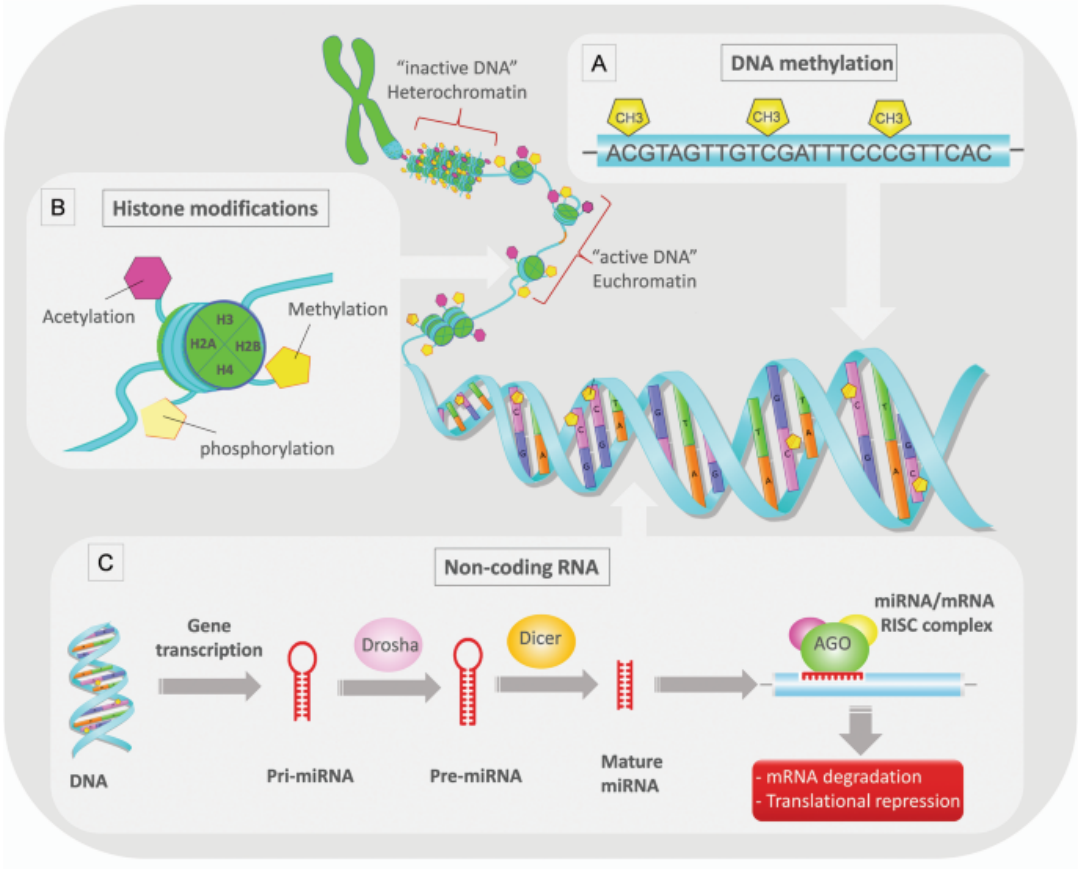

Figure 1.5. Types of epigenetic modification. (A) DNA methylation involves the enzymic addition of a methyl group onto the 5' region of a DNA cytosine. This modification is mediated by DNA methyltransferase. In general, cytosine hypermethylation at CpG sites in a gene promoter region often results in transcriptional silencing. (B) Histone modification occurs at the N-terminal of the histone tail. The modification can be methylation, acetylation, ubiquitylation, or phosphorylation. Specific histone modification is associated with alterations in chromatin structure, thereby influencing gene regulation. (C) Non-coding RNAs, including lncRNAs, miRNAs, and piRNAs, regulate gene transcription and translation. Abbreviation: lncRNAs, long non-coding RNAs; mRNA, messenger RNA; miRNAs, micro-RNAs; piRNAs, piwi-interacting RNAs; RISC, RNA-induced silencing complex (Adapted from Arif *et al*., 2019).

1.4.2. DNA methylation

DNA methylation is the enzymatic addition of a methyl (-CH_3) group onto the 5'-position of the pyrimidine ring in the cytosine to form 5-methylcytosine, mediated by DNA methyltransferase (DNMT). DNA methylation is associated with gene suppression, and these epigenetic patterns are maintained by DNMT1 during somatic cell division [81,82]. DNA methylation also maintains cellular identity and embryonic development [83,84]. Most DNA methylation occurs within the CG dinucleotide (CpG) sites. On the other hand, CpG islands, defined as clusters of CpG-rich DNA longer than 200 bp, are usually devoid of DNA methylation. CpG islands are highly conserved across vertebrate genomes, and about 60% of CpG islands in human genomes are located in promoters [85]. Supporting this, hypermethylation at the CpG island of tumor-suppressor genes is associated with cancer [86].

1.4.3. Non-coding RNA

Genes encoding mRNA that become proteins make up about 1% of the human genome, and the function of remaining non-coding transcripts was only uncovered over the past two decades [87]. Non-coding RNAs (ncRNAs) are classified into two categories based on size. Long non-coding RNAs (lncRNAs) are transcribed RNAs that are longer than 200 nt and represent 80% of the transcribed human genome [88]. lncRNAs are transcribed by RNA polymerase II and have a similar structure as mRNA, containing capped 5' ends and polyadenylated 3' ends [89]. Small non-coding RNAs, on the other hand, are highly conserved RNAs shorter than 200 nt in length. Small non-coding RNAs are further classified as micro-RNAs (miRNAs), piwi-interacting RNAs (piRNAs), and small interfering RNAs (siRNAs) based on their biological functions [90]. An increasing body of evidence indicates that non-coding RNAs have diverse roles in regulating gene expression [91].

1.4.4. Histone modification

The N-terminal tails of core histones (H2A, H2B, H3, and H4) and the C-terminal tails of H2A and H2B protrude from the surface of the nucleosome (**Figure 1.6**) [92]. These histone tails are more susceptible to post-transitional modifications compared to the regions around the core. Histone modification regulates chromatin structure and alters the accessibility for transcription factors (TFs), thereby regulating gene transcription. For this reason, histone modifications can be

considered markers of transcriptional status. Thus far, over 60 histone modification sites with different biological roles in transcriptional activity have been described [93]. Major histone modifications include methylation, acetylation, ubiquitylation, and phosphorylation. These modifications couple with various enzymes [94].

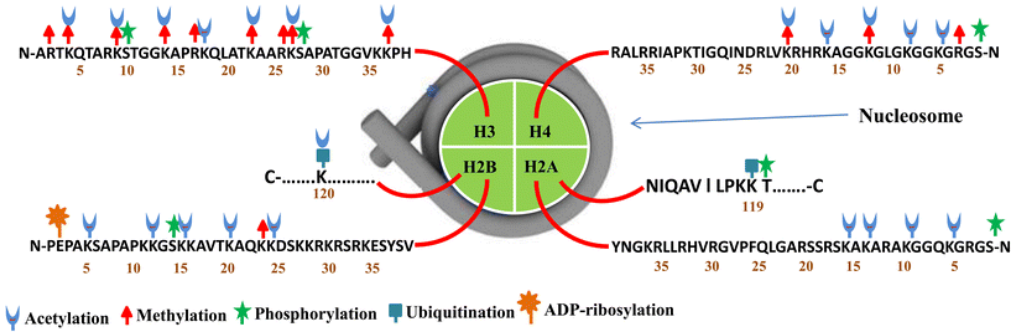

Figure 1.6. Post-translational modifications on histone tails. The N-terminal tails of the core histones (H3, H2A, H2B, and H4) and the C-terminal tails of H2A and H2B protrude from the nucleosome and are readily subjected to post-translational modifications. The major histone modifications include methylation, acetylation, ubiquitylation, and phosphorylation. The location and types of post-translational modifications are shown (Adapted from G. K. Azad & Tomar, 2014).

The location of histone markers depends on the types of modification. Some histone markers are enriched at DNA regulatory sequences, such as the promoter (a region where transcription is initiated) and enhancer regions (a short region of DNA that promotes gene expression). In contrast, other histone markers are found across the gene body (i.e., the whole gene region, including exon and intron regions) (**Figure 1.7**) [95,96].

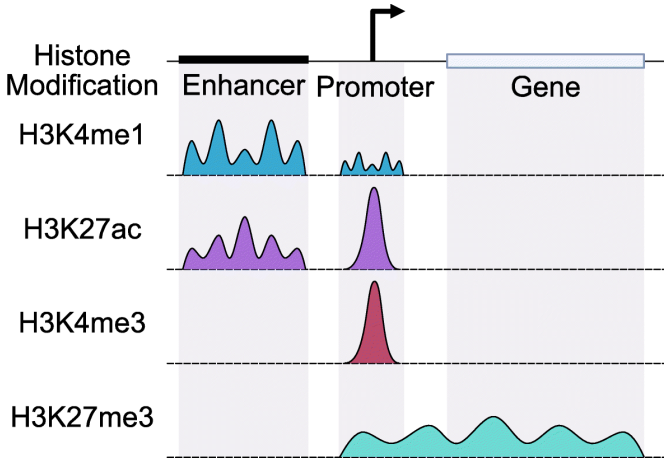

Figure 1.7. Peak profiles of representative histone modifications. Peak profiles of H3K4me1, H3K27Ac, H3K4me3, and H3K27me3 along the DNA regulatory sequences (such as enhancer and promoter) and gene body. Abbreviation: H3K27Ac, acetylation of histone H3 at lysine 27; H3K4me1, monomethylation of

histone H3 at lysine 4; H3K4me3, trimethylation of histone H3 at lysine 4; H3K27me3, trimethylation of histone H3 at lysine 27 (Adapted from Yashar WM, Kong G, VanCampen J, *et al*).

1.4.4.1. Histone modifications: Methylation

The common targets for methylation are lysine (K) and arginine (R) residues. Methylation mainly occurs on lysine residues on H3 and H4 histone tails. Histone methylation is a reversible process. The addition and removal of a methyl group (-CH3) occur via histone methyltransferases (HMTs) and histone demethylases (HDMs), respectively. The reversible process can modulate chromatin conformation. Histones can be either mono-, di-, or tri-methylated, and each modification serves different functions. For example, the trimethylation of histone H3 at lysine 27 (H3K27me3) is associated with gene repression, and mono-, di-, and trimethylation of histone H3 at lysine 4 (H3K4me1, H3K4me2, and H3K4me3) are associated with active transcription. Interestingly, while H3K4me2 can be found in active enhancers and promoters, H3K4me1 is enriched in active enhancers, and H3K4me3 is enriched in active promoters. In addition, H3K4me3 is considered a hallmark of active genes [97]. H3K4me3 is also found in CpG islands, and the level of H3K4me3 markers is inversely associated with DNA methylation levels [98].

1.4.4.2. Histone modifications: Acetylation

Acetylation involves the addition of an acetyl group (-COCH3) to a lysine residue on the histone tail. Lysine residues can be acetylated via histone acetyltransferase (HAT) and removed by histone deacetylases (HDACs). Adding an acetyl group to a histone neutralizes positively charged lysine residues, making the DNA more accessible to TFs. Conversely, removing an acetyl group from a histone restores the positive charge of lysine residues and promotes nucleosome interaction, leading to less accessibility to TFs [99]. Therefore, histone acetylation is typically associated with active transcription, while deacetylation is associated with transcriptional silencing. One of the most studied histone acetylation sites is lysine 27 of histone H3 (H3K27Ac). This modification is found in active enhancers. Since histone modification of H3K27Ac (active gene marker) and H3K27me3 (repressed gene marker) target the same lysine residue, studies have shown that switching between acetylation and methylation markers is mutually exclusive [100,101].

Table 1.1. Histone modifications and their association with gene expression.

Active promoters	H3K4me2, H3K4me3, H3 and H4 acetylation
Inactive promoters	H3K27me3, H3K9me3
Active enhancers	H3K4me1, H3K4me2, H3K27Ac
Inactive enhancers	H3K9me2, H3K9me3
Active gene bodies	H3K36me3, H3 and H4 acetylation, H3K79me3

1.4.4.3. Histone modifications: Ubiquitylation

Ubiquitin (Ub) is an 8.5 kDa protein expressed in all cells of eukaryotic organisms. Histone ubiquitination is mediated by histone ubiquitin ligase and removed by deubiquitinating enzymes (DUBs) [102,103]. Monoubiquitylation mainly occurs on histone H2A (H2Aub1) and H2B (H2Bub1). H2Aub1 is enriched in gene silencing coupled with Polycomb repressive complexes [104]. H2Bub1, on the other hand, is associated with transcription elongation and enriched in the gene body of active genes [105]. H2Bub1 is also involved in the regulation of chromatin conformation [106]. Other histone modifications also accompany histone ubiquitination. For example, ubiquitination on H2B (H2Bub) is associated with H3K4me3 [107] and with H3K79me3 [108,109].

1.4.4.4. Histone modification: Phosphorylation

The addition of the phosphate group to histones is mediated by kinases and removed by phosphatases [110]. Phosphorylation of histones occurs at tyrosine (Y), serine (S), and threonine (T) residues of the histone tails. Well-studied histone phosphorylation sites include histone H3 at threonine-3 (H3T3ph), serine-10 (H3S10ph), and histone H2A at threonine-120 (H2AT120ph). Similar to histone ubiquitination, histone phosphorylation is associated with other histone modifications. For example, H3S10ph is linked to histone acetylation, such as H4K16Ac, H3K9Ac, and H3K14Ac [111,112]. Histone phosphorylation has been associated with various cellular activities, including mitosis, DNA repair, and gene regulation [113–115]. As such, H3T3ph mediates the chromosomal passenger complex (CPC) positioning into the correct orientation during mitosis, which is critical for chromosome segregation [113].

1.4.5. Detection methods for histone modifications

The standard technique for detecting histone modification is chromatin immunoprecipitation (ChIP; **Figure 1.8a**) [116]. In this assay, proteins and DNA are cross-linked within cells, followed by fragmentation of chromatin and immunoprecipitation using antibodies to selectively pull down a protein of interest and the associated DNA fragments. Samples are then reverse cross-linked, and proteins are digested to release DNA. Purified DNA is analyzed using microarrays (ChIP-chip), quantitative real-time polymerase chain reaction (ChIP-qPCR), or sequencing (ChIP-seq) to identify the genomic regions with which the protein modification of interest is associated. The number of input cells required for ChIP assays varies depending on the downstream application. However, using 1-10 million cells per antibody as input is generally recommended to ensure reliable results [117].

Cleavage under targets & release using nuclease (CUT&RUN; **Figure 1.8b**) is an alternative approach to assess histone modifications [118,119]. It was first described in 2017 and became a more appealing method as it provides improved specificity and sensitivity compared to the ChIP-seq. CUT&RUN uses protein A that is conjugated with micrococcal nuclease (MNase-pA). This fusion protein complex binds to an antibody attached to the histone modification of interest and cleaves off adjacent DNA regions, releasing short DNA fragments, which can then be subjected to library preparation and sequencing. The advantage of CUT&RUN is that the cleavage and release of DNA fragments only occurs at specific sites of interest within the cells, without undergoing cross-linking and physical fragmentation of chromatins (as in ChIP-seq), which often causes epitope masking. Moreover, CUT&RUN requires fewer input cells, as low as 100 cells per antibody [119], allowing investigation of protein-DNA interactions using rare cell populations or limited samples. This *in situ* approach provides higher specificity and efficiency, resulting in improved resolution of sequencing data with significantly less background noise. As a result, the required sequencing depth for CUT&RUN is also considerably lower, around 3-5 million reads, which is 10% of the sequencing depth required for ChIP-seq. Cleavage under targets and tagmentation (CUT&Tag; **Figure 1.8c**) is a similar approach to the CUT&RUN assay proposed by the same group in 2019 [120,121]. Key differences between CUT&Tag and CUT&RUN are: (1) CUT&Tag utilizes protein A that is conjugated with Tn5 transposase-protein A (pA-Tn5) instead of MNase-pA, (2) no separate DNA library preparation step is required, (3) fewer input

cell numbers can be used compared to CUT&RUN, and (4) the protocol can be applied to the single-cell platform.

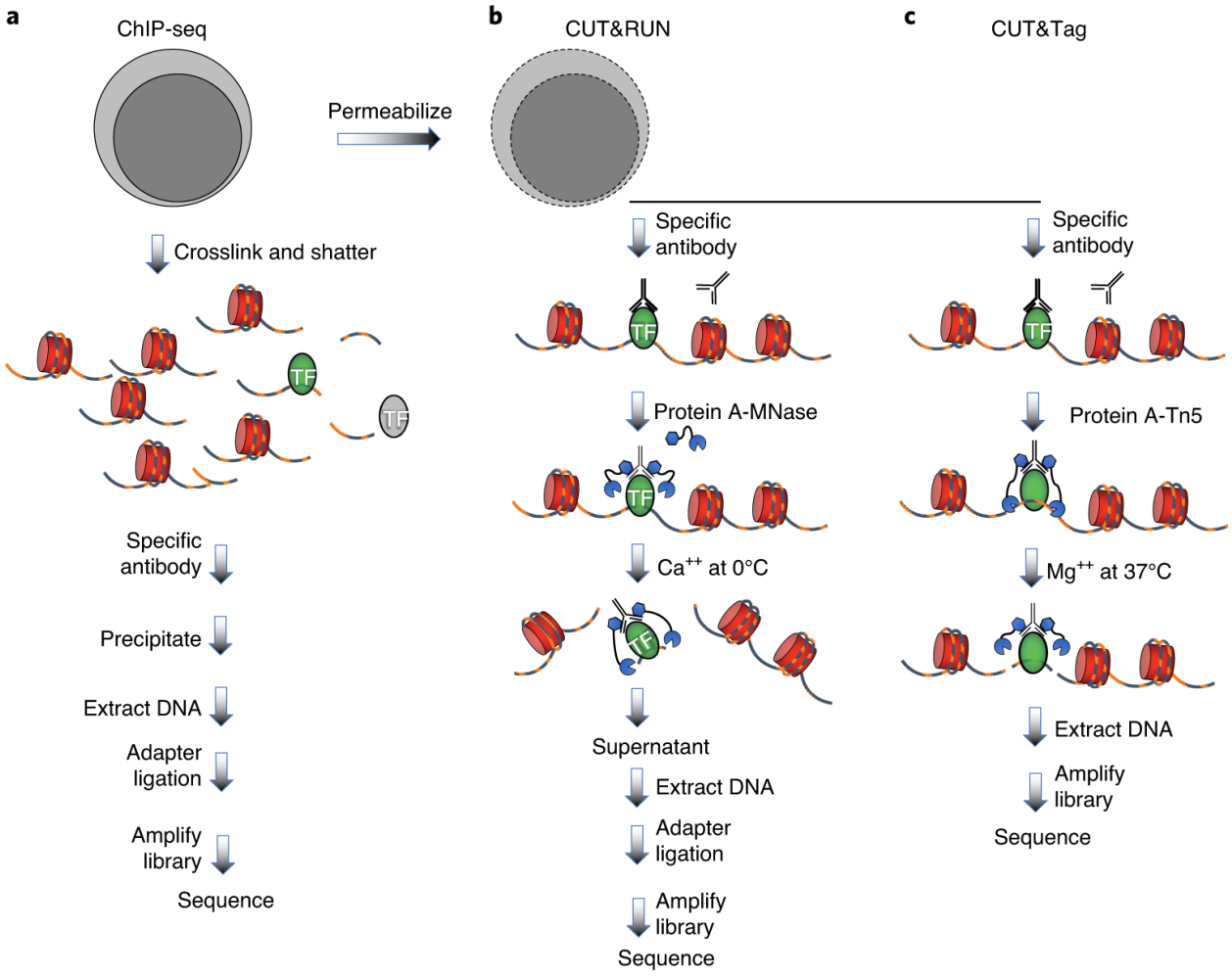

Figure 1.8. Histone modification profiling strategies. Experimental steps of ChIP-seq (a), CUT&RUN (b), and CUT&Tag (c). Cells and nuclei are indicated in grey, nucleosomes in red, and target protein in green. Unlike ChIP-seq, which involves cross-linking and fragmentation (*in vivo*), CUT&RUN and CUT&Tag experiments are carried out without these steps (*in situ*). During CUT&RUN and CUT&Tag experiments, only the nucleosomes close to the target protein are cleaved and released into the solution. This targeted cleavage approach reduces background noise compared to ChIP-seq. Abbreviation: ChIP-seq, chromatin immunoprecipitation and sequencing; CUT&RUN, Cleavage Under Targets and Release Using Nuclease; CUT&Tag, Cleavage Under Targets And Tagmentation (Adapted from Kaya-Okur, Janssens, Henikoff, Ahmad, & Henikoff, 2020).

1.5. The human immune system

1.5.1. Innate immunity

Innate immunity serves as a first line of defense against invading pathogens. Key cellular components involved in the innate immune response include natural killer (NK) cells, neutrophils, monocytes, macrophages, and DCs.

Monocytes are leukocytes derived from hematological precursors in the bone marrow. They are precursors of macrophages and DCs. Monocytes represent 5-10% of PBMCs and circulate in peripheral blood for several days [122,123]. Monocytes protect the host against pathogens through antigen presentation [124], phagocytosis [125], reactive oxygen species (ROS) production [126], as well as cytokine and chemokine release [127]. Monocytes display significant heterogeneity in both their functional and phenotype characteristics. Monocytes can be categorized into three major populations according to the CD14 and CD16 expression: classical (CD14++CD16−), intermediate (CD14+CD16+), and non-classical (CD14+CD16++) [128]. The classical monocytes, accounting for 80-95% of the total monocyte population, are the predominant subset [129]. They exhibit pro-inflammatory properties, high phagocytic activity, and scavenging capabilities. The intermediate monocytes constitute 2-8% of circulating monocytes and possess anti-inflammatory characteristics. They are involved in antigen presentation, ROS release, and T-cell activation. Non-classical monocytes comprise 2-11% of total circulating monocytes, and their primary functions are patrolling the bloodstream and clearing debris, apoptotic cells, and pathogens.

NK cells are large granular lymphocytes. In humans, NK cells express CD56 and CD16 in the absence of CD3. NK cells have cytotoxic ability and can induce cell death of target cells without requiring prior exposure [130]. There are multiple mechanisms for activating NK cells, including antibody-dependent cellular cytotoxicity (ADCC) and receptor-mediated pathways. ADCC happens when Fc receptors on NK cells recognize antibodies that bind to the surface of target cells. This binding activates NK cells and induces cytotoxic granules to release perforin and granzymes. Perforin punctures holes in the cell membrane of the target cells, which allows granzyme to enter the cell to induce cell apoptosis. NK cells also trigger cell death through activating or inhibitory receptor-mediated pathways [131]. This process is called “recognition of missing self.” NK cells recognize several self-ligands expressed on the surface of host cells. When host cells are healthy,

this recognition sends signals to NK cells not to attack the host cells. However, when host cells are infected or transformed, these self-ligands are often downregulated, which is recognized by NK cells, thereby allowing NK cells to exert their cytotoxic functions to kill the target cells [132].

Some innate immune cells recognize PAMPs of invading pathogens via PRRs. Cells that express PRRs include macrophages/ monocytes, DCs, neutrophils, and epithelial cells [133–135]. PRRs can be divided into two types: membrane-bound proteins and cytoplasmic proteins. Membrane-bound proteins include some of the TLR family, whereas cytoplasmic proteins include NOD-like receptors and retinoic acid-inducible gene I (RIG-I)-like receptors. The interaction of PAMPs and PRRs induces pro-inflammatory responses required to eliminate the invading pathogens [136–138]. For example, PAMP/PRR interaction triggers phagocytes (including macrophages, neutrophils, monocytes, and DCs) to engulf pathogens, a process called phagocytosis [139]. DCs serve as a cellular link between innate and adaptive immunity [140]. Upon activation, DCs migrate to the lymph nodes, which is crucial in initiating adaptive immune responses via antigen presentation to T cells [141]. Additionally, DCs interact with NK cells to protect against viral infections [142].

Although innate immune systems are historically considered short-lived and to provide uniform responses, recent observations have revealed the existence of immunological memory within the innate immune system, referred to as “trained innate immunity” [143]. Further details regarding trained innate immunity will be discussed in a dedicated section below.

1.5.2. Adaptive immunity

The adaptive immune system is the hallmark of the immune system in higher animals that have evolved to combat invading pathogens [144]. Adaptive immunity is an antigen-specific second-line of defense response typically mediated by B and T cells. Although adaptive immunity takes time to respond to the pathogen upon first encounter, it possesses immunological memory that enables it to mount a robust and more effective response upon second exposure to the same pathogen-derived antigens. Adaptive immunity comprises two arms of systems: cell-mediated and humoral immunity.

1.5.2.1. Cell-mediated immunity

Cell-mediated immunity is a highly specific immune response mediated by CD4+ and CD8+ T cells. T cells originate from the bone marrow and undergo maturation in the thymus during thymic development. In the thymus, T cells undergo differentiation and a selection process to ensure that only functional T cells circulate in the blood and secondary lymphatic tissues (i.e., lymph nodes). The high specificity of T cells is owing to the somatic recombination of T cell receptors (TCRs). TCRs possess variable (V) and constant (C) regions, which undergo recombination during T cell development upon antigen stimulation. Foreign antigens are recognized when presented by APCs, such as DCs, in the context of MHC I by conventional CD8+ T cells and MHC II by conventional CD4+ T cells. This recognition leads to the differentiation of naïve T cells into effector T cells. The differentiation of T cells is also directed by the cytokine environment [145]. Activated CD8+ T cells are crucial in eliminating the target cells via perforin/granzyme-induced apoptosis. On the other hand, activated CD4+ T cells regulate the activation of other immune cells, thereby controlling both humoral and cellular immune responses. Additionally, subsets of CD4+ and CD8+ T cells differentiate into memory cells. Upon subsequent exposure to the same antigen, these memory cells will differentiate into effector cells, enabling a rapid and effective immune response [146].

Depending on the types of cytokines they produce, CD4+ T cells can be classified into four major somewhat distinct subsets: Th1, Th2, Th17, and regulatory T cells (Tregs) (**Figure 1.9**) [147], although other subsets have been described, and in reality, there is some fluidity between the subsets. Th1 cells are characterized by their TNF-α and IFN-γ cytokine production. A Th1 response is associated with the activation of other immune cells, such as CD8+, macrophages, and NK cells. Th1-type immune responses are induced by intracellular organisms, such as viral and intracellular bacterial infections. Th2 cells are characterized by their production of IL-4, IL-5, and IL-13 cytokines. Th2 responses are involved in antibody-mediated immune responses and are typically induced by parasitic infections or allergic reactions. Th17 cells are characterized by their production of IL-17 and IL-22. Th17-type immune responses are induced by autoimmune disease and extracellular fungal and bacterial infections at mucosal sites. Lastly, some CD4+ T cell populations differentiate into Tregs, characterized by their production of IL-10 and transforming

growth factor (TGF)-β. Tregs play a crucial role in regulating immune responses to suppress inflammation.

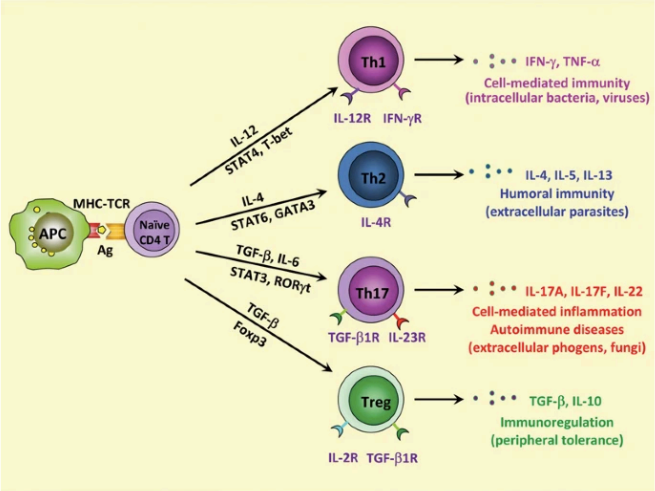

Figure 1.9. Differentiation of naive CD4+ T cells. Upon antigen presentation by APCs, naive CD4+ cells undergo differentiation into somewhat distinct subsets, namely Th1, Th2, Th17, or Treg cells, among others not discussed here. These subsets are characterized by their specific TFs and cytokine profiles. In the presence of IL-12, naive CD4+ T cells differentiate into Th1 cells. This process is mediated by the activation of the T-bet via STAT1 and STAT4 signaling. Th1 cells secrete IFN-γ and TNF-α, which are crucial in protection against intracellular pathogens. IL-4 induces Th2 differentiation. This differentiation requires the activation of STAT6 and GATA3. Th2 cells play an important role in humoral immunity against parasites via secretion of IL-4, IL-5, and IL-13. The combination of IL-6 and TGF-β promotes naive CD4+ T cells to differentiate into Th17 cells, mediated by activation of RORγt and STAT3. Th17 cells secrete IL-17A, IL-17F, and IL-22 and are involved in autoimmune disease and the clearance of extracellular pathogens. TGF-β alone induces naive CD4+ cells to differentiate into Treg cells through the activation of Foxp3+. Treg cells secrete IL-10 and TGF-β and are involved in immunoregulation. Abbreviation: APCs, antigen-presenting cells; Foxp3, forkhead box P3; GATA3, GATA binding protein 3; IFN-γ, interferon-gamma; IL, interleukin; RORγt, retinoic acid-related orphan receptor gamma; Treg, regulatory T cells; STAT, Signal transducer and activator of transcription; Th, T helper; TFs, transcription factors; TGF-β, transforming growth factor-beta; TNF-α, tumor necrosis factor-alpha (Adapted from Leung *et al*., 2010).

1.5.2.2. Humoral immunity

Humoral immunity involves the production of antibodies by plasma cells (effector B cells) in response to antigens. Immature B cells are released from the bone marrow and develop into naïve B cells. The optimal activation of B cells and subsequent clonal expansion relies on the involvement of antigen-activated T cells. After B cell clonal expansion, some B cells directly differentiate into short-lived plasma cells, while others migrate to the germinal center (**Figure 1.10**) [148]. These B cells further proliferate in the "dark zone" within the germinal center. The rapid proliferation of B cells induces somatic hypermutation (SHM), which allows the

modification of the immunoglobulin variable region (IgV). This step is crucial for the affinity maturation of B cells. Subsequently, B cells migrate to the "light zone" within the germinal center and undergo affinity selection in the presence of follicular dendritic cells (FDCs) and T follicular helper (TFH) cells. Further differentiation via class-switching occurs [149], allowing the heavy chain of antibodies to switch from IgM and IgD to IgG, IgA, or IgE, thereby providing different effector functions [150]. B cells that fail to produce appropriate antibodies undergo apoptosis, while selected B cells either re-enter the germinal cycles or exit from the germinal center to become memory B cells or long-lived plasma cells [148]. Importantly, the signal strength of the B-cell receptor (BCR) determines the fate of B-cell differentiation [151]. Memory B cells can be formed in a T-cell-independent manner via the synergetic interaction of B cell TLR and BCR [152,153]. These memory B cells exhibit a longer life span [154,155] and lower levels of SHM [156] than memory B cells generated in a T-cell-dependent manner.

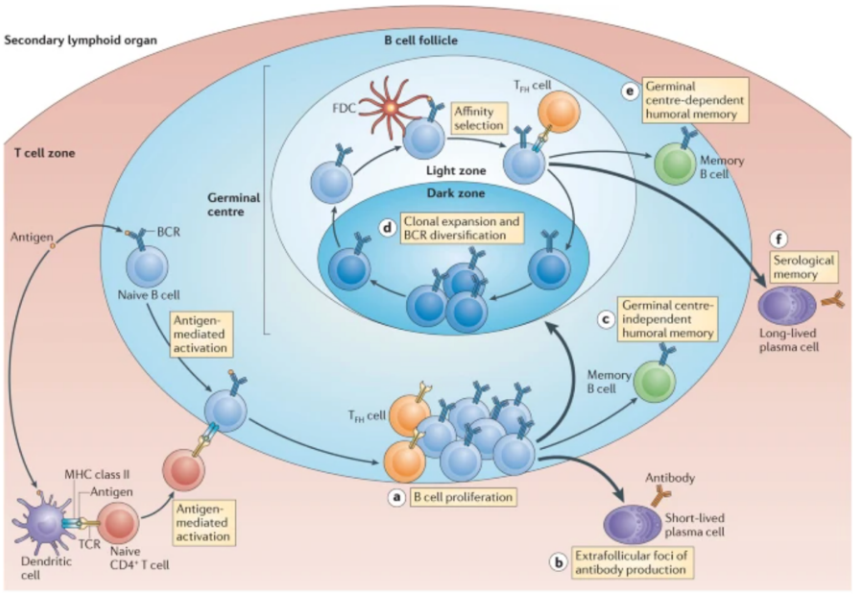

Figure 1.10. Memory B cell generation. Naïve CD4+ T cells and B cells are activated upon encountering an antigen in a secondary lymphoid organ. Following this activation, the CD4+ T cells and B cells migrate and interact at the border of the T cell and B cell zones. This interaction promotes the proliferation of B cells (a). The proliferating B cells have three possible fates. They can differentiate into short-lived plasma cells (b) or memory B cells (c) without migrating to the germinal center. Alternatively, B cells can migrate to the germinal center, where they undergo rapid clonal expansion and diversification of their BCRs in the "dark zone" within the germinal center (d). Subsequently, the B cells relocate to the "light zone" within the germinal center and interact with FDCs and antigen-specific TFH cells. Affinity-matured B cells can re-enter the cycles or exit from the germinal center to become memory B cells (e) or long-lived plasma cells (f). The fate of B cell differentiation depends on the signals they receive. Stronger signals (indicated as thick arrows) favor the development of plasma cells. In contrast, weaker signals (indicated as thin arrows)

favor the development of memory B cells. Abbreviation: BCRs, B cell receptors; FDCs, follicular dendritic cells; TFH cells, follicular helper T cells (Adapted from Kurosaki, Kometani, & Ise, 2015).

1.5.3. Infant immunity

Infant immune systems during the first months of life are dynamic and functionality different in many aspects from the adults. In general, infant immune systems are considered "immature" [157], such that younger infants are more susceptible to pathogens, including pertussis, enterovirus, respiratory syncytial virus, or influenza [158–161]. However, this vulnerability of the infant immune system is thought to result from tolerance mechanisms established during pregnancy to protect against human leukocyte antigen (HLA)-mismatched inflammatory responses between mothers and fetuses [162], since failure to establish immune tolerance is associated with a higher risk of miscarriage [163]. Therefore, rather than simply being immature, the infant's immune system is under active suppression.

Immunity in early life exhibits unique characteristics. For instance, infant NK cells, a key effector cell population at the initial phase of infection, are at higher frequency and have greater cytotoxic capability than those of adults [164,165]. TLR responses also differ in infants, with higher production of Th2 immune responses (including IL-6 and IL-10 production, respectively) and reduced Th1 immune responses (including IFN-γ and IL-12 production) compared to adults [166–168]. This Th2-skewed immunity is a hallmark of neonatal and infant immune systems, partially due to impaired TLR-mediated APC responses. Collectively, these data support that infant immune systems are phenotypically and functionally different compared to adults. Despite Th2-biased immunity, live attenuated vaccines, such as BCG, have been shown to induce robust Th1 response in infants [169–171].

To develop a vigilant immune system, the fetal immune system requires priming through several steps at the right time. Exposure to a diverse community of gut microbiota in early life is also essential for shaping infant immunity and is often referred to as the "neonatal window of opportunity" [172], as discussed further below.

Infants receive a wide range of protection from their mothers, which provides initial immunity during early life. Placental transfer of maternal antibodies starts in the first trimester of pregnancy and provides passive protective humoral immunity until infants can produce their own antibodies [173]. The transfer primarily occurs through the neonatal Fc receptor (FcRn) located in the placental syncytiotrophoblasts [174]. The amount of IgG that a fetus receives from their mother via the placenta depends on maternal antibody titers, the quantity of FcRn, and the length of gestation [175]. Maternal antibodies are also provided through breast milk, which contains antibodies such as igA, IgM, IgG, and secretory IgA (SIgA) [176]. SIgA comprises the highest proportion of antibodies in breast milk.

1.5.4. Trained innate immunity

1.5.4.1. Concept of trained innate immunity

Adaptive immunity is the ability to recognize specific pathogens based on prior exposures and elicit enhanced secondary immune responses upon re-exposure. Immunological memory is established by preserving receptors specific for a collection of epitopes in adaptive immune cells (i.e., T cells and B cells). Upon re-exposure to the same epitopes, memory cells are activated and expand to mount an immune response. In contrast, innate immunity has been considered a non-specific defense mechanism against invading pathogens. However, this notion of innate immunity being primitive and non-specific has been challenged. There is a growing body of evidence suggesting that organisms lacking adaptive immune responses, such as plants [177] and invertebrates [178,179], exhibit non-specific protection against secondary infection after the first exposure. Upon non-specific restimulation, this memory-like broad protection was also observed in vertebrates, including mice [180] and humans [69]. The enhanced non-specific immunological protection can last several months to a year in innate cells, including monocytes, macrophages, and NK cells [181–185]. This phenomenon has been termed “trained innate immunity” by Netea *et al*. in 2011 [143]. It is important to note that while adaptive immune responses confer long-term responses to the same or highly similar pathogens, trained innate immunity provides broad immune-enhancing effects [186].

1.5.4.2. Stimuli that are known to induce trained innate immunity

Infectious stimuli like bacterial or fungal antigens can induce trained innate immunity. For example, β-glucan, a *Candida albicans* cell wall component, has been shown to induce trained innate immunity in monocyte-derived macrophages [185]. BCG is one of the most extensively studied stimuli in the context of trained innate immunity and its corresponding mechanisms. Vaccination with BCG in severe combined immunodeficiency (SCID) mice (lacking T cells and B cells) has improved survival post-challenge with unrelated infections compared to the non-vaccinated mice, indicating that BCG induces non-specific protection against non-mycobacterial infection through functional reprogramming of innate immune cells [181]. Notably, proof-of-principle trials among BCG-vaccinated healthy adult volunteers showed elevated production of pro-inflammatory cytokines (TNF-α, IFN-γ, and IL-1β). This enhancement is accompanied by an altered functional state of circulating monocytes, characterized by increased expression of activation markers (CD11b and TLR4), which persist for at least three months post-vaccination [187]. Furthermore, a comparison of candida infection between SCID mice and NOD/SCID/IL2Ry (NGS) mice (lacking NK cells, T cells, and B cells) suggested that NK cells partially mediate the BCG-induced protection [182]. BCG-induced trained innate immunity has also been observed to influence responses not only in heterologous Th1 cells but also in Th17 cells, persisting up to a year post-vaccination [187]. Epidemiological evidence further supports the heterologous effects induced by BCG. A randomized control trial in Uganda showed that BCG vaccination at birth reduced all-cause infectious morbidity during the first six weeks of life [188]. Importantly, lower risk of sepsis was observed among BCG-vaccinated children aged under 15 years in Spain [189], and among low-birth-weight children aged under one year in Guinea-Bissau [190]. Similarly, reduced risk of lower respiratory tract infections was also observed among the same cohort in Spain [189], and children aged under five years in Guinea-Bissau where the protective effect was more prominent among girls [191].

1.5.4.3. Mechanisms of trained innate immunity

Trained innate immunity has been observed in many innate immune cells, including monocytes [181], macrophages [185], DCs [192], neutrophils [193], and NK cells [182]. Recent research has shown that self-renewing long-lived cells, such as hematopoietic stem and progenitor cells (HSPCs) in bone marrow, are associated with trained innate immunity [194–196]. This explains

how circulating monocytes, with an average lifespan of 5-7 days, exhibit "memory-like characteristics" for 3-12 months after BCG immunization [197].

Trained innate immunity is accompanied by genome-wide epigenetic histone modifications. These epigenetic modifications induce or repress gene expression, enhancing protection against subsequent infection. Studies have demonstrated that trained innate immunity accompanies changes in chromatin architecture, including increased levels of active histone modification markers, including H3K27Ac, H3K4me1, and H3K4me3, and decreased levels of repressive histone modification, including H3K9me3 (**Figure 1.11**) [197–200]. These changes in the histone markers are observed in the promoter or enhancer region of genes associated with inflammatory cytokine responses, such as IL-1β, TNF-α, and IL-6 [197,201].

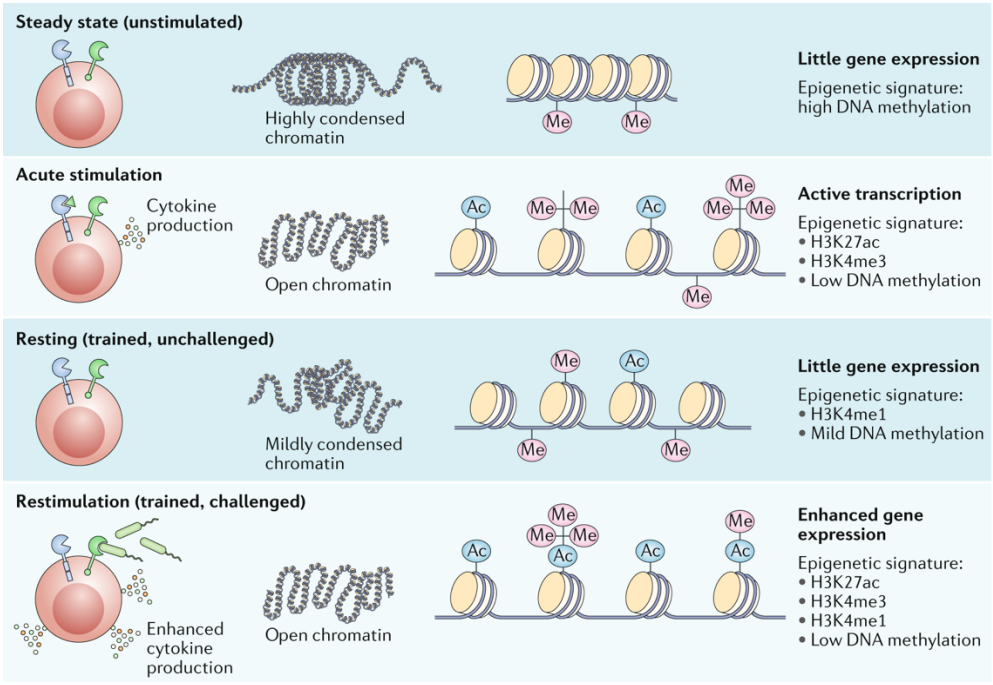

Figure 1.11. Epigenetic modifications associated with trained innate immunity. Epigenetic modifications and chromatin remodeling play an essential role in trained innate immunity. During the acute stimulation phase, there are changes in epigenetic signatures and DNA methylation patterns, leading to alterations in chromatin structure. These changes facilitate pro-inflammatory responses. Even after ceasing the stimuli, some of these epigenetic changes persist, enabling innate immune cells to mount a faster and more robust reaction with enhanced cytokine production upon restimulation. Key epigenetic changes accompanied by trained innate immunity include increased H3K27Ac, H3Kme1, and H3K4me3 markers and decreased DNA methylation levels. These epigenetic modifications collectively contribute to establishing and maintaining trained innate immunity. Abbreviation: H3K27Ac, acetylation of histone H3

at lysine 27; H3K4me1, monomethylation of histone H3 at lysine 4; H3K4me3, trimethylation of histone H3 at lysine 4 (Adapted from Netea *et al*., 2020).

Multiple signaling pathways are involved in the regulation of trained innate immunity. The BCG-induced trained innate immunity observed in monocytes affects the NOD2 signaling pathway [181]. In addition, recent work has revealed the interplay between epigenetics and metabolism involved in trained innate immunity (**Figure 1.12**) [202]. For example, BCG-trained monocytes showed a shift in glucose metabolism towards glycolysis through the PI3K/AKT/mTOR pathways, resulting in increased lactate production and glucose consumption (Warburg Effect) [199]. Similar phenomena have been observed in β-glucan-trained monocytes [203].

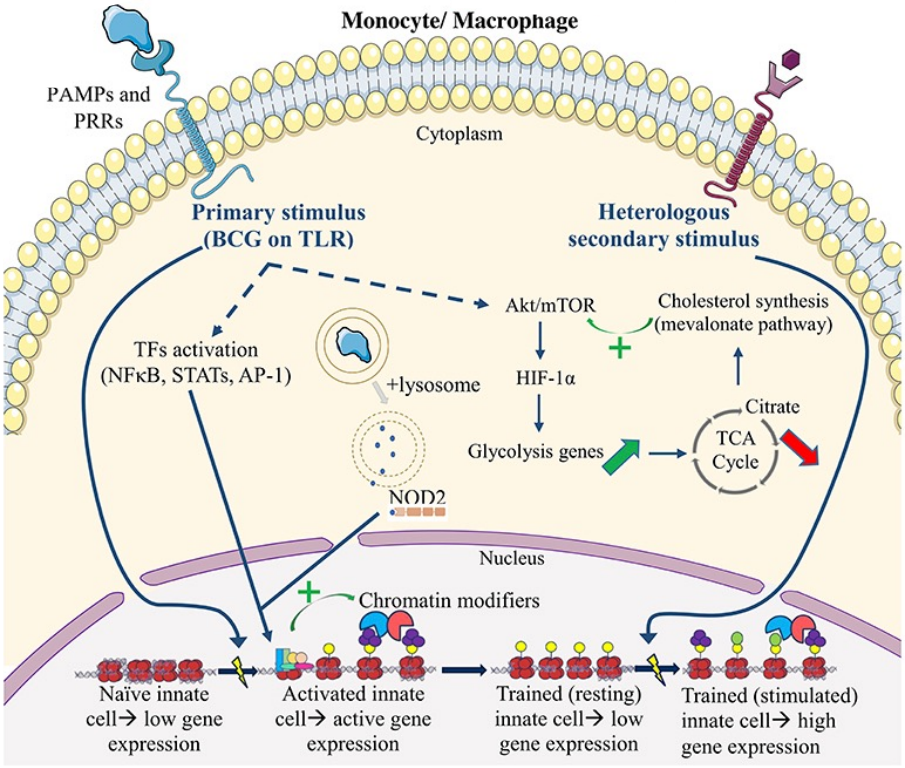

Figure 1.12. Mechanisms of non-specific protection induced by trained innate immunity. In monocytes or macrophages, BCG (as the primary stimulus) is recognized by TLR, initiating a cascade of events. This recognition triggers the activation of various TFs, including NFκB, STATs, and AP-1. The activation of the TFs leads to the transcription of pro-inflammatory cytokines, such as TNF-α, IL-6, and IL-1β. BCG stimulation also induces autophagy and activates the NOD2 signaling pathway, thereby further enhancing pro-inflammatory responses. In addition, BCG upregulates Akt/mTOR signaling and HIF-1α, resulting in the upregulation of gene expressions involved in glycolysis. The activated Akt/mTOR pathways alter metabolite levels associated with chromatin-modifying enzymes. Notably, these responses are heightened when the cells are challenged with heterologous secondary stimulus. Abbreviation: AP-1, activator protein 1; BCG, Bacillus Calmette-Guérin; HIF-1α, hypoxia-inducible factor-1α; IL, interleukin;

AKT, protein kinase B; TLR, Toll-like receptor; TFs, transcription factors; TNF-α, tumor necrosis factor-alpha; mTOR, mammalian target of rapamycin; NFκB, nuclear factor kappa B; NOD2, nucleotide-binding oligomerization domain 2; STATs, signal transducers and activators of transcription (Adapted from Uthayakumar *et al*., 2018).

1.6. Human gut microbiota

1.6.1. Bacterial distribution and abundance in the gut

The adult intestine harbors about 10^{13}-10^{14} bacterial cells in total, which outnumber human cells 10-fold [204]. The collective genomes of these bacteria consist of more than five million genes [205,206]. This vast array of bacterial gene products has a diverse impact on the human host's biomedical and metabolic activities. The bacterial population in the gastrointestinal (GI) tract increases in density and complexity from the proximal to the distal gut [207]. Per gram of intestinal content, the microbial density is 0-10^2 microbial cells/gram in the stomach, 10^2 microbial cells/gram in the jejunum, 10^7-10^8 microbial cells/gram in the distal ileum, and 10^{11}-10^{12} microbial cells/gram in the colon (**Figure 1.13**) [208]. Analysis of the 16S ribosomal RNA (rRNA) genes in infants and their mothers revealed that Firmicutes, Bacteroidetes, Actinobacteria, and Proteobacteria accounted for approximately 95% of bacterial cells in gut microbiota [209].

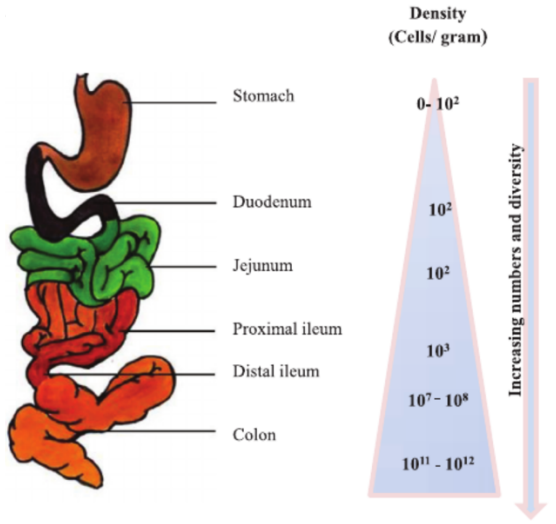

Figure 1.13. Bacterial distribution and abundance in GI tract. The human adult GI tract contains approximately 10^{13}-10^{14} bacterial cells in total. In the stomach, the density of bacteria is 0-10^2 cells per gram of intestinal content. The microbial cell density in the duodenum and jejunum is around 10^2 cells per gram. The count rises to approximately 10^3 cells per gram in the proximal ileum. In the distal ileum, the density further ranges to 10^7-10^8 cells per gram. Finally, the bacterial density in the colon peaks at 10^{11}-10^{12} microbial cells per gram. Abbreviation: GI, gastrointestinal (Adapted from Singh *et al*., 2019).

1.6.2. Establishment of the gut microbiota in infants

The mutualistic relationship between microbes and humans begins at birth. At the early stages of microbiota development, bacterial diversity is low, allowing newly incoming bacteria to colonize successfully without competition from existing ones [210]. The early stage of neonatal microbiota is characterized by low bacterial diversity and high variability between individuals.

An individual's age is an important driver of the gut microbiota development. Other bacterial species colonize over time and reach an "adult-like" gut microbial state after a few years, characterized as highly diverse with a high relative abundance of *Bacteroides* and *Clostridium* spp. [211,212]. Once the gut microbiota reaches an "adult-like" state, it remains relatively stable throughout life [213]. Several factors are associated with the initial seeding and establishment of the infant gut microbiota, described in the sections below (**Figure 1.14**) [214].

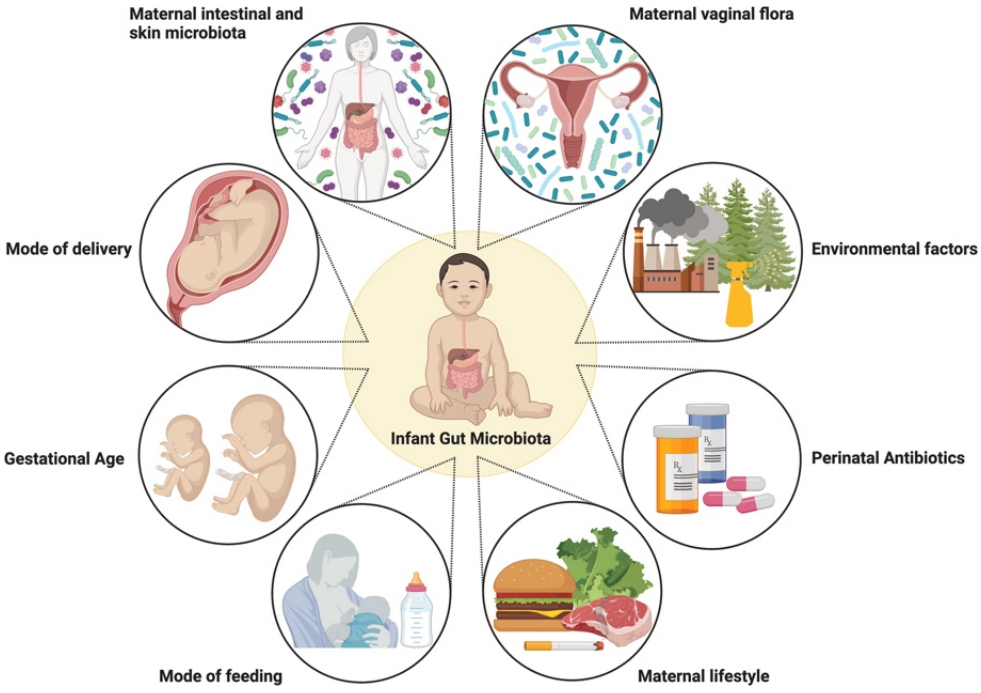

Figure 1.14. Factors influence infant gut microbiota development. The neonatal microbiota can be affected by several factors, including mode of delivery, mode of feeding, gestational age, antibiotics usage, maternal factors, and environmental conditions (Adapted from Hill *et al*., 2021).

1.6.2.1. Mode of delivery

Microbiota within the female reproductive tract is associated with maternal and infant health outcomes. The vaginal microbiota mainly comprises *Lactobacillus*, *Gardnerella, Prevotella*, or *Sneathia* spp. Among them, some *Lactobacillus* species (such as *L. gasseri*, *L. crispatus*, and *L. jensenii*) are known to have protective characteristics, including lowering pH in the vaginal canal through lactic acid production [215], while the role of *L. iners* is less clear [216]. Therefore, a non-*iners*-*Lactobacillus*-dominated vaginal microbiota is considered favorable and associated with positive health outcomes. When babies travel through the birth canal during labor, they are exposed to the maternal vaginal microbiota. As a result, neonates born through vaginal birth have a gut microbiota closely related to that of their mother's vaginal microbiota, which is dominated by *Escherichia*, *Lactobacillus*, *Bacteroides*, *Bifidobacterium* and *Prevotella* [217]. In contrast, infants delivered by Cesarean section (C-section) often have a microbiota similar to their mothers' skin or nosocomial environment, including *Staphylococcus*, *Streptococcus*, *Klebsiella*, *Enterococcus,* and *Clostridium* [218]. Canadian infants delivered by C-section demonstrated lower bacterial diversity and richness at four months of life than vaginally delivered infants [219]. In addition, a systematic analysis suggested that this effect may last up to six months [220]. Whereas some studies have shown this effect is either minimum or short-lived [221–223], other studies have suggested that this effect may persist much longer, up to two to seven years [224–226].

Although it has been believed that the fetal environment is devoid of bacteria and bacterial colonization only begins after birth (the "sterile womb paradigm"), a number of studies suggest the presence of bacteria in the amniotic fluid, placenta, and meconium. However, this "*in utero* colonization hypothesis" is still under debate [227–234]. The result can be heavily interfered with by contamination in samples with low biomass when next-generation sequencing (NGS) is applied for analysis. In addition, NGS techniques merely amplify bacterial DNA isolated from samples and do not indicate whether the bacterial DNA was obtained from viable organisms [227].

1.6.2.2. Mode of feeding

Breastfeeding is considered the ideal mode of feeding for infants as human milk contains all the necessary nutrients required for the first half-year of life [235]. In addition, breast milk is rich in other bioactive molecules, including immunoglobulins, fatty acids, human milk oligosaccharides

(HMOs), lysozyme, and other antimicrobial peptides [236]. Colostrum (the breast milk secreted during the initial days after birth) possesses unique properties, rich in minerals, proteins, and fat-soluble vitamins compared to milk produced later [235].

Breastfeeding plays an important role in shaping infants' gut microbiota composition by transmitting the microbial community from breast milk to the gut. The breast milk microbiota is composed of facultative anaerobes (such as *Staphylococcus*, *Streptococcus*, *Propionibacterium*, *Enterococcus*, and *Lactobacillus*) and obligate anaerobes (such as *Bifidobacterium* and *Veillonella*) [237]. This partially explains why breastfed infants have a higher absolute abundance of *Lactobacillus*, *Enterococcus*, and *Bifidobacterium* in their gut [238–241]. Some microbial strains in breast milk samples have beneficial properties, particularly *Lactobacillus gasseri* and *Enterococcus faecium*, which can potentially prevent infections in breastfed infants [238,242,243]. In addition, a follow-on formula containing *Lactobacillus* has been shown to reduce the incidence of infections in infants between 6 and 12 months of age [244]. Lastly, studies have demonstrated that commensal lactic acid bacteria (LAB) found in breast milk can inhibit HIV transmission, indicating LAB have protective properties against HIV infection in gut mucosa in breastfed infants [245,246].

HMOs are the third most abundant solid component in human breast milk [247]. Although HMOs are non-digestible to the host, they serve as carbon sources for bacterial growth in the gut. For example, HMOs promote the colonization of *Bifidobacterium* spp. in breastfed infants while preventing the colonization of pathogenic bacteria [248]. Moreover, the SIgA in human breast milk, especially in colostrum, facilitates the establishment of healthy infant gut microbiota [249]. On the other hand, formula feeding has been associated with higher microbial diversity compared to breastfed infants, resembling the microbial composition of older children with increased taxa from the phyla *Bacteroidetes*, *Clostridium*, *Streptococcus*, *Veillonella*, *Atopobium*, and Enterobacteriaceae [250,251].

1.6.2.3. Introduction of complementary foods

Breast milk is important for developing and maturing infant gut microbiota, but introducing solid food is essential for stabilizing microbial composition. For instance, introducing solid food

increases the relative abundance of the phyla Bacteroidetes and Firmicutes [252]. Introduction of complementary foods introduces a broader range of substrates and non-digestible carbohydrates, which leads to increased bacterial proliferation and diversity in the gut. As a result, the gut microbiota of infants transitions towards an "adult-like" state, typically dominated by phyla Bacteroidetes and Firmicutes. Conversely, the relative abundance of bacteria, such as Lactobacillaceae, Bifidobacteriaceae, Enterococcaceae, and Enterobacteriaceae, which are commonly found during the breastfeeding period, starts to decrease during with complementary feeding practices [253].

1.6.2.4. Gestational age

The gut microbiota of preterm infants (< 37 completed weeks gestational age) exhibits delayed bacterial colonization and lower diversity compared to term infants. For example, among preterm infants, there is a notable decrease in the relative abundance of *Bifidobacterium,* while *Enterobacter*, *Enterococcus*, and *Staphylococcus* tend to be more abundant [210,254]. Similarly, higher gestational age is positively associated with the relative abundance of *Bifidobacterium*-dominated gut microbiota and negatively associated with the colonization of facultative anaerobes [255]. Moreover, several studies report that potentially pathogenic bacteria, such as Clostridia, *Bacteroides*, *E. coli,* and *Klebsiella*, are also increased in preterm infants' gut microbiota. This altered gut microbiota composition in preterm infants is often associated with a higher risk of pathogenic infection, such as necrotizing enterocolitis (NEC) and sepsis [256,257].

1.6.2.5. Use of antibiotics

Often, antibiotics target both pathogens and commensal bacteria in the gut, leading to significant alterations in the gut microbiota. This disruption includes reducing microbial diversity, richness, and evenness and suppressing dominant bacterial growth, subsequently impacting microbial succession [258–260]. A study investigating infants with suspected early-onset neonatal sepsis demonstrated that antibiotic treatment led to the overgrowth of potentially pathogenic bacteria, including *Klebsiella* and *Enterococcus* spp. In contrast, beneficial *Bifidobacterium* spp. were profoundly negatively affected by the treatment [261]. Moreover, early exposure to antibiotics has been linked to non-optimal gut microbiota composition and associated with an increased risk of various immune disorders, such as asthma, allergy, or autoimmune diseases [262].

1.6.2.6. Maternal factors

Maternal diet during pre- and postnatal periods significantly impacts the acquisition and development of the infant gut microbiota. For example, a study by Chu *et al*. revealed that maternal high-fat diet during pregnancy was negatively associated with the relative abundance of *Bacteroides* in their infants' gut microbiota during the first six weeks of life [263]. In addition, Lundgren *et al*. showed that the association between maternal food intake and infant gut microbiota was influenced by mode of delivery. For example, maternal fruit consumption was positively correlated with the relative abundance of *Streptococcus*/*Clostridium* group among infants delivered by vaginal birth, and maternal dairy consumption was positively correlated with the relative abundance of *Clostridium* group among infants delivered by C-section [264].

Maternal diet can also affect the gut microbiota of infants through breastfeeding. A cross-over dietary intervention study revealed that maternal diet influenced the composition of HMOs, specifically sialic acid and fucose, thereby shaping the metagenomic function of breast milk microbiota [265]. Furthermore, maternal administration of antibiotics can profoundly affect the colonization of infant gut microbiota and may lead to non-optimal infant gut microbiota composition [266]. Additionally, accumulating evidence suggests that maternal obesity can influence their infant gut microbiota [267,268].

1.6.2.7. Geography, ethnicity, and genetics

Geographical location and ethnicity have been found to significantly impact the establishment of infant gut microbiota, likely influenced by lifestyle and dietary patterns. Studies have demonstrated variations in gut microbiota profiles across countries. For example, Falony *et al*. identified a 17-genera core gut microbiota among Western countries (Flemish and Dutch populations as well as the US and UK), which reduced to 14 genera when compared to data from cohorts in Papua New Guinea, Peru, and Tanzania [269]. Similarly, children living in rural areas of Burkina Faso showed significant enrichment of Bacteroidetes and depletion of Firmicutes compared to children living in urban areas in Italy. This study also suggested that diet can influence the total short-chain fatty acid levels and the growth of potentially pathogenic bacteria in the infant's gut, especially Enterobacteriaceae (such as *E. shigella* and *E. coli*) [270].

Emerging evidence indicates that geographical location and genetics are associated with acquiring and maintaining specific bacterial taxa in the gut. Accumulating studies have revealed associations between specific genetic loci and the colonization of particular bacteria [271–274]. To understand the interaction between genetics and microbiota, well-controlled and unbiased approaches are required. Due to the genetic and environmental resemblance, twins provide an appropriate model for such studies. For instance, a study of monozygotic and dizygotic twin pairs demonstrated a higher concordance rate for the carriage of methanogens (methane-producing bacterium) in monozygotic twin pairs than in dizygotic twin pairs, indicating that host genetics influence the composition of gut microbiota [275]. Furthermore, microbial communities and HMOs in human milk also differ by genetic factors, contributing to variations among breastfed infants across countries [276].

1.6.3. Relationship between gut microbiota and immunity

1.6.3.1. Structure and function of intestinal mucosa

The human intestinal mucosa serves crucial roles in the body by facilitating nutrient absorption and creating physical barriers between the external nonsterile environment and the internal host milieu. Additionally, it plays a vital role in immune sensing and regulation of the immune response. Defense mechanisms against invading pathogens can be categorized into mechanical and biological barriers (**Figure 1.15**) [277,278].

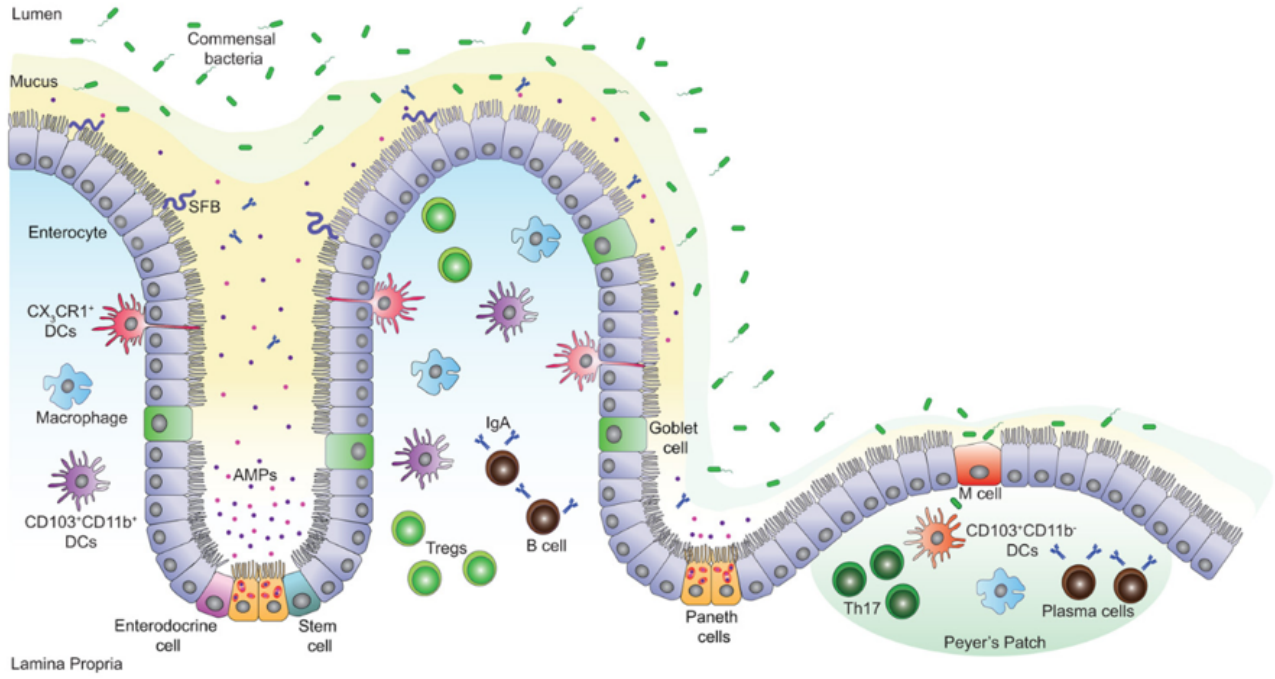

Figure 1.15. The architecture of the intestinal barrier. The intestinal epithelium is composed of a monolayer of IECs interconnected by TJs. The intestinal epithelium is covered by a protective mucus layer, which can be divided into inner and outer layers. The inner mucus layer is abundant in IgA and AMPs, which help to prevent bacterial growth within the region. However, certain opportunistic bacteria, like segmented filamentous bacteria, can reside in the inner area. Subsets of IECs include Paneth cells, goblet cells, enterocytes, enteroendocrine cells, and M cells. Paneth cells are located in the crypt bases and are responsible for producing AMPs. The M cells in the PPs play a key role in antigen sampling in the gut. Various immune cells reside in lamina propria, including plasma cells, IgA-producing B, macrophages, DCs, mast cells, and effector T cells. Abbreviation: AMPs, antimicrobial peptides; DCs, dendritic cells; IECs, intestinal epithelial cells; M cells, microfold cells; PPs, Peyer's patches; TJs, tight junctions (Adapted from Muniz, Knosp, & Yeretssian, 2012).

Mechanical barrier

Mucus membranes play a crucial role as a mechanical barrier against luminal antigens. These membranes comprise two main layers: the epithelium layer and the mucus layer (**Figure 1.15**) [278]. The intestinal epithelium layer is composed of a monolayer of intestinal epithelial cells (IECs) connected by tight junctions (TJs) [279]. TJs are multiprotein complexes and act as selectively permeable seals between the adjacent intestinal epithelial cells. They also set a boundary between the apical and basolateral membrane domains. While TJs serve as an intestinal barrier, they also allow the paracellular movements of ions and nutrients across the intestinal epithelium [279]. Various IECs exist, including goblet cells, enteroendocrine cells, enterocytes, microfold cells (M cells), and Paneth cells [278].

The intestinal mucus layer is primarily composed of glycosylated proteins (known as mucins). Over 20 different mucins have been reported in humans, with MUC2 being the predominant mucin secreted by goblet cells [280–282]. The heavy glycosylation of mucins contributes to their viscous nature, which helps to prevent direct contact between microorganisms and host epithelial cells [283]. Notably, the absence of MUC2 leads to bacterial contact with the epithelium and can result in colitis, highlighting the important role of MUC2 in segregating bacteria from epithelium [284,285].

In the small intestine, a single mucus layer is closely attached to the intestinal epithelium [286]. In contrast, the colon, which has a higher bacterial diversity, features two distinct mucus layers: a dense inner layer tightly attached to the intestinal epithelium and a looser outer layer that lies above the inner layer [284]. While the inner layer remains devoid of bacteria, the looser layer allows colonization of commensal bacteria in the colon [278,286].

Biological barrier

The immune barrier in the intestine consists of effector T cells, Tregs, antigen-producing plasma cells, innate lymphoid cells (ILCs), and gut-associated lymphoid tissue (GALT) (**Figure 1.15**) [249]. In addition, antimicrobial proteins (AMPs) are secreted by Paneth cells in response to enteric pathogen exposure. AMPs are a wide range of small peptide antibiotics that are important to innate immunity. A diverse array of AMPs provides different inhibitory effects against microorganisms [287,288].

The largest proportion of the immune system resides in the GALT, which mainly consists of T cells, B cells, and DCs. The GALT can be classified into two types according to the anatomic and functional properties: inductive sites and effector sites (**Figure 1.15**). Inductive sites include draining mesenteric lymph nodes, isolated lymphoid follicles, Peyer's patches (PPs), and cryptopatches [289]. Within PPs, M cells are highly specialized in phagocytosis and provide a major pathway for transporting luminal antigens [290]. M cells engulf and exocytose luminal antigens into the subepithelial dome in PPs (the process is known as transcytosis). DCs and macrophages then capture antigens for antigen presentation.

Following the sampling and processing of antigens at inductive sites, effector cells modulate immune responses in effector sites, primarily located in the epithelium and lamina propria. Intraepithelial lymphocytes (IELs) are long-lived effector cells expressing a significant proportion of TCRγδ+ markers and possessing cytotoxic properties [291–294]. Activated B cells migrate into lamina propria and differentiate into IgA-secreting plasma cells (**Figure 1.16**) [295]. Epithelial cells expressing polymeric immunoglobulin receptors (pIgR) capture the IgA dimers. The dimeric IgA-plgR is then cleaved in epithelial cells, releasing SIgA into the intestinal lumen [296,297]. Released SIgA protects the host from pathogens by antigen-pathogen cross-linking, known as "immune exclusion" [298].

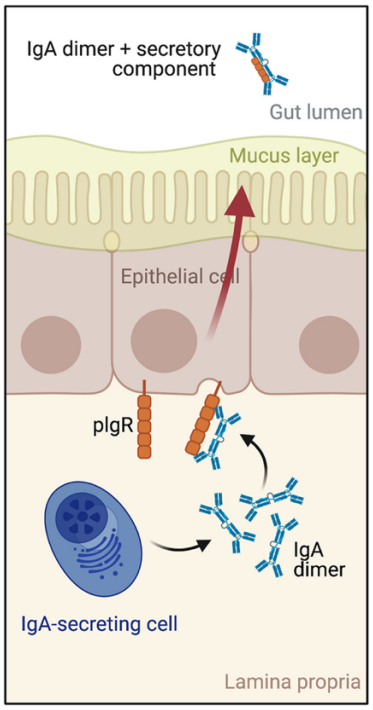

Figure 1.16. Formation of SIgA. IgA-secreting plasma cells in the lamina propria produce IgA dimer. The pIgR expressed on the basolateral surfaces of intestinal epithelial cells binds to the IgA dimer and facilitates its release into the intestinal lumen. Abbreviation: pIgR, polymeric immunoglobulin receptor; SIgA, secretory IgA (Adapted from Costello *et al*., 2022).

Commensal bacteria colonizing the intestine also play a crucial role in preventing the colonization of pathogens by producing antimicrobial compounds and competing for limited resources. Numerous studies have shown the important role of beneficial bacteria, including *Lactobacillus* and *Bifidobacterium*, in stabilizing the microbiota and enhancing the integrity of the intestinal

mucosal barrier [299–301]. In addition, Tan *et al*. showed that serum IL-6, an inflammatory cytokine, was positively associated with the bacterial load of potentially pathogenic bacteria (including Enterobacteriaceae and *Enterococcus*) in the gut microbiota of adults. Conversely, a negative association was observed with beneficial bacteria (such as *Bifidobacterium*) [302]. These findings suggest that dysbiosis of the gut can lead to systemic inflammation.

1.6.3.2. Antigen passage in the intestinal lumen

In order to protect the host from invading pathogens, multiple pathways exist to sample antigens in the intestinal lumen [303]. As described in the previous section, M cells in the PPs sample antigens and actively transport them into the subepithelial dome where DCs and lymphocytes are located. This induces T-cell differentiation and secretion of SIgA into the intestinal lumen [290,304]. In addition, DCs can extend their dendritic extensions across paracellular junctions and sample luminal antigens. Upon activation, DCs migrate into lymphoid structures to activate lymphocytes [305]. Another method of antigen sampling involves the recognition of PAMPs or microbe-associated molecular patterns (MAMPs) via PRRs (including TLRs and NOD-like receptors). Activated PRRs trigger inflammatory responses, including the production of cytokines, chemokines, and antimicrobial peptides, to effectively eliminate the invading pathogen [306]. For instance, lipopolysaccharides (LPS), a major component of the surface membrane of gram-negative bacteria, is recognized by TLR4, followed by increased IL-6 expression.

1.6.3.3. Mechanisms of intestinal mucosal tolerance

Gut microbiota and host immune systems are balanced in a dynamic equilibrium. Interaction with diverse microorganisms enables intestinal development and maturation of the innate and adaptive immune systems [307]. Cross-talk between the host and microbiota is vital in regulating gut homeostasis during infancy and later life [308–310]. In order to maintain a balanced symbiotic relationship between the host immune system and gut microbiota, the immune system must develop tolerogenic responses towards commensal bacteria while mounting an effective response against invading pathogens [311]. Several immune cell populations contribute to immune tolerance within the intestinal mucosal immune system.

Forkhead box P3+ (Foxp3+) Tregs play a crucial role in regulating and suppressing other immune cells. Tregs are located in various tissues, including the intestinal mucosa [312]. Gut-resident Tregs, characterized by co-expression of retinoic acid-related orphan receptor gamma (RORγt) and FoxP3, are crucial for immune tolerance to the commensal bacteria in the gut. These RORγt+ Tregs express higher levels of immune suppressive molecules (such as inducible co-stimulator [ICOS], lymphocyte activation gene 3 [LAG-3], and cytotoxic T-lymphocyte-associated protein 4 [CTLA-4]) than Tregs in lymph nodes [313]. The RORγt+ Tregs are differentiated and maintained locally in response to microbiota-derived antigens, including bacterial fermentation products of dietary fibers, short-chain fatty acids (SCFAs), and microbial secondary bile acids [314–316]. Studies have shown that Tregs residing in the intestine have a distinct TCR repertoire compared to Tregs in other locations, suggesting that gut microbiota antigens influence the Treg population in the intestine [317,318]. These commensal-specific Tregs also promote the production of IgA in PPs, contributing to the immune homeostasis between the host and microbiota [319,320]. Importantly, the proportion of Tregs in tissue is higher in neonates compared to adults (30-40% vs. 1-10%) with greater suppressive capacities, supporting the role of Tregs in establishing an environment favorable for colonization of bacteria without excessive inflammation [321].

ILCs are another type of innate immune cells that share developmental and functional characteristics with CD4+ T cells [322]. ILCs are subdivided into ILC1s, ILC2s, and ILC3s, characterized by T-bet+, GATA3+, and RORγt+ expression, respectively (**Figure 1.17**) [322]. Accumulating evidence suggests that group three ILCs (ILC3s) play a key role in establishing immune tolerance to commensal microbes in the gut [323–326]. ILC3s are found in the mesenteric lymph nodes and the lamina propria of the colon [325]. They are regulated by various cytokines and microbial factors [322,327] and are involved in maintaining the integrity of the intestinal mucosal barrier [328]. A study by Hepworth *et al*. showed that deletion of MHCII from ILC3s in mice led to dysregulation of CD4+ T cell responses against commensal bacteria, leading to intestinal inflammation [324]. The subsequent study showed that MHCII-expressing ILC3s induced apoptosis of commensal-bacteria-specific T cells, thereby maintaining intestinal homeostasis without causing systemic inflammation, a process referred to as “intestinal selection” [325]. These findings also correlated with the dysregulation of ILC3-intrinsic MHCII (HLA-DR) expression in patients with inflammatory bowel disease (IBD), supporting the notion that ILC3s

regulate the immune response to commensal intestinal bacteria. Moreover, a recent study using a mouse model has demonstrated that ILC3s closely work with RORγt+ Tregs to establish immune tolerance to commensal microbes in the gut [326].

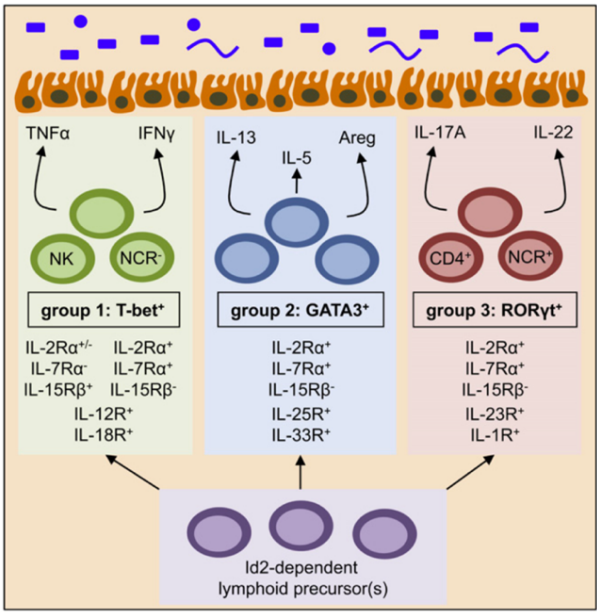

Figure 1.17. Subsets of ILCs. ILCs are categorized into three subsets: ILC1s (group one), ILC2s (group two), and ILC3s (group three). Each subset is classified according to the expression levels of TFs: T bet+, GATA3+, and RORγt+, respectively. ILCs are derived from lymphoid progenitors, and their development relies on the transcription factor ID2. ILC1s, which include NK cells, are regulated by various cytokines, such as IL-2, IL-7, IL-15, IL-12, and IL-18. ILC1s produce TNF-α and IFN-γ. ILC2s are regulated by cytokines IL-2, IL-7, IL-25, and IL-33. ILC2s produce IL-5, IL-13, and Areg. ILC3s express CD4+ and NCRs+ and are regulated by cytokines such as IL-2, IL-7, IL-15, IL-23, and IL-1β. ILC3s produce IL-17A and IL-22. Abbreviation: Areg, amphiregulin; GATA3, GATA binding protein 3; ILCs, innate lymphoid cells; ID2, inhibitor of DNA Binding 2; IL, interleukin; IFN-γ, interferon-gamma; NCRs, natural cytotoxicity receptors; NK cells, natural killer cells; RORγt, retinoic acid-related orphan receptor gamma; TFs, transcription factors; TNF-α, tumor necrosis factor-alpha (Adapted from Sonnenberg & Artis, 2012).

DCs also play an essential role in immunotolerance towards commensal intestinal bacteria. DCs actively sample commensal bacteria-derived antigens in the intestinal lumen. Cross-talk between DCs and Tregs is a key determinant of whether a systemic inflammatory reaction or a tolerogenic/local protective immune response is induced [329,330]. For instance, cyclooxygenase-2 (COX2)-expressing DCs in the mesenteric lymph nodes have been associated with the differentiation of Tregs, which in turn helps to maintain the mucosal tolerogenic response in the intestine [330].

1.6.3.4. Microbiota and human immune system development

The microbiota is closely linked with immune and metabolic development. Therefore, the development of microbiota during early life has long-term implications for human health. Studies using germ-free mice demonstrated that gut microbiota is critical for development of lymphoid structures. For instance, germ-free mice had smaller PPs and lower proportions of CD4+ T cells and IgA-producing plasma cells [331]. Supporting this, exposure to commensals induces lymphoid tissue development and maintains intestinal homeostasis. This regulation is partly mediated via NOD1, an important receptor recognizing microbial components [332]. Moreover, TLR4, a key PRR for LPS recognition [333], is involved in immune tolerance, B cell recruitment, and IgA production [334,335].

In addition, accumulating evidence suggests that microbial metabolites are essential for maintaining the immune system. SCFAs are well-known microbial metabolites. These SCFAs enhance immunity and modulate inflammatory responses through various mechanisms, such as G-protein-coupled receptor (GPR) signaling and inhibition of HDAC [336]. SCFAs have been reported to play a pivotal role in maintaining intestinal integrity [337] and regulating the function and size of colonic Tregs [316,338,339]. The induction of Tregs by SCFAs occurs via DCs through activation of cell surface receptors, such as GPR109a and GPR43 [340,341].

Induction of Foxp3+ Tregs has also been observed with various bacteria in mouse models, such as *Bacteroides fragilis* [342], *Helicobacter hepaticus* [343], *Clostridium* species [344], *Lactobacillus* species [345,346], and many other *Bifidobacterium* species [347–351]. However, the mechanisms underlying this induction vary between bacterial taxa. For example, *B. fragilis* promotes Treg development through TLR2 signaling in the intestine [342], while *Clostridium* species induce Treg development in epithelial cells independent of PRR signaling pathways [344]. These findings suggest that the microbiota shapes the repertoire of Foxp3+ Tregs to maintain the host-microbe relationship through several mechanisms.

Infants with non-optimal gut microbiota are more likely to develop immune disorders, such as atopy, IBD, and metabolic disorders [352–354]. Allergies, particularly atopic eczema and asthma

have been linked to gut microbiota dysbiosis. An increased relative abundance of *Clostridium* and reduced relative abundance of *Lachnospira*, *Veillonella*, *Faecalibacterium*, *Rothia*, *Bifidobacterium*, *Akkermansia,* and *Faecalibacterium* during the first year of life have been linked to the development of asthma later in life [352,355,356]. Similarly, a higher absolute abundance of *E. coli* and *C. difficile* or reduced microbial diversity during early life are risk factors for atopic eczema in young children [357,358]. Importantly, studies have shown that SCFA-producing bacteria during early life potentially reduce the risk of developing such allergic diseases [359–361].

1.6.4. Analysis methods for the microbiota

The investigation of the human gut microbiota has traditionally relied on culture-based methods, which are labor-intensive and often challenging to optimize for each bacterium. However, with the emergence of NGS technology, massive sequencing of universal phylogenetic marker genes can be carried out. This culture-independent approach allows the identification and characterization of microbial communities in a high-throughput manner [362,363]. One commonly used marker gene for microbiota analysis is the 16S rRNA gene, a conserved region spanning about 1,500 bp. This gene has minimal variation among bacterial species with nine “hypervariable regions” (V1-V9), which can be utilized for identifying organisms at the genus or species level (**Figure 1.18**) [364–366]. Each hypervariable region is flanked by highly conserved sequences that serve as ideal binding sites for PCR primers [366]. Amplified 16S rRNA gene regions, typically targeting two to three hypervariable regions, are sequenced and clustered into nearly identical tags according to the sequence homology.

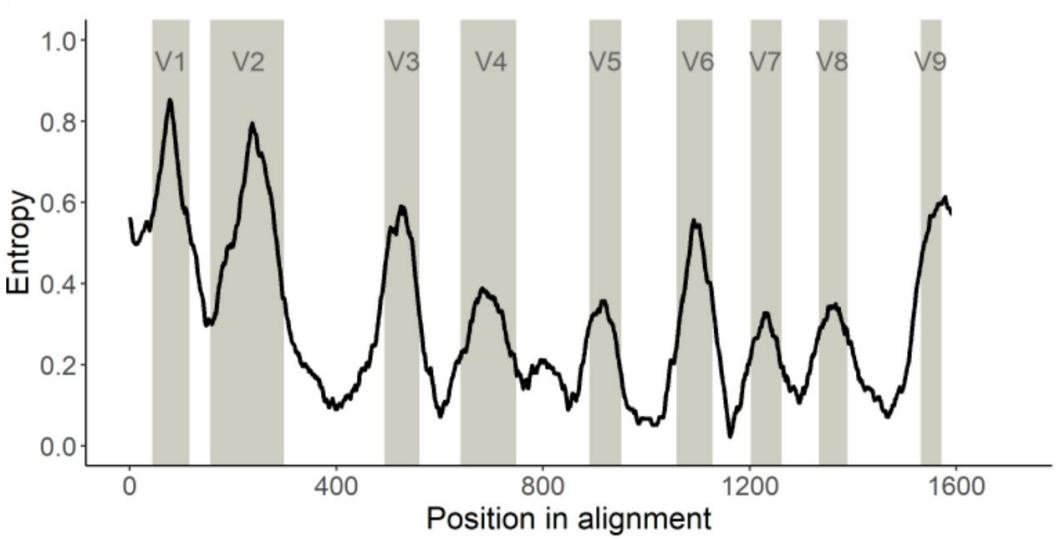

Figure 1.18. Hypervariable regions of 16S rRNA gene. The entropy of the 16S rRNA gene and its position in the alignment provides information about the extent of variability. A higher entropy value indicates that the region has more variation across bacterial species, while a lower entropy value suggests that the region is more conserved. Locations of hypervariable regions (labeled V1-V9), based on the *E. coli* sequence, are shown in grey (Adapted from Hoffman *et al*., 2021).

Other culture-independent methods used for microbial analysis include shotgun metagenomic sequencing and DNA microarrays. Whole-genome shotgun metagenomics sequencing provides a comprehensive view of all the genes of the microorganisms present in a sample, offering information on their genomic, functional, and metabolic potential in an untargeted manner [367,368]. Unlike 16S rRNA gene sequencing, whole-genome shotgun metagenomics sequencing does not specifically target a marker gene, allowing species identification across all three taxonomic domains (Bacteria, Archaea, and Eukarya) [368]. However, this is a highly computationally-intensive approach. On the other hand, DNA microarrays involve the hybridization of labeled samples with DNA arrays, providing robust wide-range detection at a low cost [369,370]. However, a limitation of this method is that species lacking complementary sequences on the array will not be detected.

1.7. Infants who are HIV-exposed but uninfected (iHEU)

1.7.1. Epidemiology of iHEU

With the success of prevention programs, vertical transmission has been considerably reduced from 25-30% to approximately 2-5% [371]. As a result, there is an emerging, increasing population of iHEU in sub-Saharan African regions. These infants are born to mothers with HIV, but they do not have HIV themselves. The estimated number of children who are HIV-exposed uninfected (aged under 14 years) was 14.8 million globally in 2018, with 90% of these children concentrated in sub-Saharan Africa [372]. Among the global estimate of the children, South Africa accounted for 3.5 million (23.8%), Nigeria accounted for 0.9 million (6.0%), and Botswana accounted for 0.2 million (1.4%).

1.7.2. Clinical outcomes of iHEU

Thus far, numerous studies have compared the immunological and clinical aspects of iHEU. Despite being born free of HIV, accumulating studies show that iHEU are at a higher risk of mortality and morbidity during their first year of life than infants who are HIV-unexposed uninfected (iHUU) [373–377]. This is predominantly due to infectious causes, such as diarrhea, pneumonia, sepsis, and respiratory disease [373,378–381]. The prevalence of TBI among South African iHEU was 41 per 1,000 child years (95% confidence interval (CI): 31-52 per 1,000 child years) for the period between 2004 and 2008 [382]. Another study conducted in South Africa between 2008 and 2009 showed a higher incidence of TBI, with 11 per 100 child-year for infants with HIV and 15 per 100 child-year for iHEU [383].

1.7.3. Epigenetics of iHEU

Although studies have shown that HIV infection is associated with alterations in DNA methylation [384], only a limited number of studies have explored the impact of *in utero* HIV exposure on epigenetics in offspring. Among those, one study looked at transcriptomic profiling and showed that genes associated with chromatin remodeling were downregulated among iHEU [385]. Another study showed that iHEU who are exposed to ART *in utero* showed lower DNA methylation in small interspersed nuclear element (SINE) repetitive elements and long interspersed nuclear element (LINE) compared to iHEU who are unexposed to ART [386].

1.7.4. Immunology of iHEU

iHEU experience many biomedical/biological adversities. For example, exposure to HIV and/or ART *in utero* can affect fetal growth, T-cell subsets, antigen-specific immune responses, and cellular production of IFN-γ [387–389]. Moreover, maternal immunity also can influence the iHEU immune system. It has been shown that both pregnancy and HIV infection are associated with changes in Th1, Th2, and Th17 cytokine profiles [390,391]. In addition, HIV infection may induce a shift in cytotoxic T cell cytokine production towards type 1 [392]. These differences can affect neonatal antigen responses and immune maturation in iHEU [393–395]. In fact, some studies have shown that iHEU tend to have an altered cell-mediated immunity, T-cell maturation, and cell function during the first year of life [396,397]. Dysfunction of NK cells in iHEU is also reported [398]. iHEU show altered transplacental antibody transfer from their mothers [399]. Moreover, iHEU display sub-optimal responses to vaccines such as BCG, oral polio, and TT [400,401].

1.7.5. Microbiota of iHEU

Establishing a healthy gut microbiota in infants is important for their immune development and overall health. PLHIV often experience non-optimal microbiota compared to people without [402,403]. In addition, the composition of HMOs in breast milk of mothers living with HIV differs from their counterparts [404]. Since infant microbiota is determined largely from maternal influences, it is plausible that the microbiota of iHEU is altered due to maternal HIV infection, which may account for their increased risk of morbidity and mortality compared to iHUU. However, there is conflicting evidence regarding gut microbiota in iHEU. While clear associations between maternal HIV infection and infant gut microbiota were observed in some studies [404,405], marginal differences were reported in other studies [406–409]. A study that enrolled over 120 children in Canada, Belgium, and South Africa suggested that the alternation in gut microbiota in iHEU could be country-specific [406]. Thus, further investigation is required to elucidate the influence of *in utero* exposure to HIV on infant microbiota and subsequent health outcomes.

1.8. Aims and objective of the dissertation

The primary objective of this dissertation was to investigate the mechanisms behind the increased risk of morbidity in iHEU compared to iHUU in sub-Saharan Africa. The objectives of the specific aims and rationales of the study were as follows:

Aim 1: To investigate the prevalence of TBI in BCG-vaccinated iHEU and iHUU.

Rationale: Children under five years are at high risk of progressing to severe forms of TB disease [410]. BCG vaccination induces IFN-γ production in T cells, an important component for protecting against TBI [411]. Since TBI prevalence is higher in mothers with HIV than those without [412] and iHEU have shown to have lower BCG-specific CD4+ T cells than iHUU [389], we investigated whether BCG-vaccinated iHEU have a higher TBI prevalence than iHUU. We performed T-SPOT.TB assay on PBMCs obtained from 418 BCG-vaccinated infants/children under two years in Botswana and South Africa. The TBI prevalence was compared by HIV exposure status.

This will be discussed in Chapter 2 and has been published as:

Saori C. Iwase, Paul T. Edlefsen, Lynnette Bhebhe, Kesego Motsumi, Sikhulile Moyo, Anna-Ursula Happel, Danica Shao, Nicholas Mmasa, Sara Schenkel, Melanie A. Gasper, Melanie Dubois, Megan A. Files, Chetan Seshadri, Fergal Duffy, John Aitchison, Mihai G. Netea, Jennifer Jao, Donald W. Cameron, Clive M. Gray, Heather B. Jaspan, Kathleen M. Powis. (2023). **T-SPOT.TB reactivity in Southern African children with and without *in utero* HIV exposure**. Clinical Infectious Diseases, 8–11. http://doi.org/10.1093/cid/ciad356

Aim 2: To explore the association between infant gut microbiota, HIV exposure, and immunity to vaccination.

Rationale: Bacterial colonization in the gut facilitates the development of the immune system in infants. Conversely, an alteration of the gut microbiota is associated with a higher risk of morbidity [413]. We investigated the potential association between *in utero* HIV exposure, gut microbiota, and TT vaccine response in infants. 16S rRNA gene sequencing was conducted using stool samples from 278 infants (202 iHEU and 76 iHUU) in Nigeria and South Africa at 1 and 15 weeks of age. Plasma anti-tetanus IgG titers were measured by enzyme-linked immunosorbent assay (ELISA) in

mother-infant pairs. Finally, the association between gut microbiota structure and TT vaccine responses was evaluated.

This will be discussed in Chapter 3 and has been published as:
***Saori C. Iwase**, *Sophia Osawe, Anna-Ursula Happel, Clive M. Gray, Jonathan Blackburn, Susan P. Holmes, *Alash'le Abimiku, *Heather B. Jaspan. **Longitudinal gut microbiota composition of South African and Nigerian infants in relation to tetanus vaccine responses**. Microbiology Spectrum, 12:e03190-23. https://doi.org/10.1128/spectrum.03190-23
*Contributed equally

Aim 3: To establish an assay assessing epigenetic changes associated with BCG-induced trained innate immunity using ultra-low input samples in iHEU and iHUU.
Rationale: Whether BCG-induced trained innate immunity offers iHEU equal immune protection as iHUU are unknown. However, conducting an epigenetic assay on infant cells, particularly targeting low-abundant cell populations, is challenging. Often, the maximum blood volume obtainable in infants is 3-5 ml (i.e., < 2.5% of total blood volume), and this blood is often used for multiple assays, therefore allowing fewer than 10 million cells after PBMC isolation. Given that the proportion of NK cells and monocytes in PBMCs ranges between 2-4% in infants, it is challenging to conduct ChIP-seq, the golden standard method for assessing the histone modifications, as this assay requires at least 1 million cells as a starting material [117]. For this reason, optimization of an epigenetic assay that allows evaluation of histone modification with ultra-low input cell numbers was carried out. A cell sorting strategy was established to isolate monocytes and NK cells from infant PBMCs using fluorescence-activated cell sorting (FACS). The protocol of CUT&Tag, a recently developed cutting-edge technique [121], was adapted in order to achieve the sufficient data quality required for the downstream analysis of infant samples. The optimized assay strategy was applied to 14 PBMCs obtained from infants at six to seven weeks of age, and histone modifications of NK cells and monocytes were compared.

This will be discussed in Chapter 4.

Chapter 2. T-SPOT.TB reactivity in Southern African children with and without *in utero* HIV exposure

2.1.Abstract

Background: Children under the age of five years are at risk for tuberculosis (TB). Bacillus Calmette-Guérin (BCG) vaccination may prevent TB infection (TBI) and prevents severe forms of TB disease in children. Although infants who are HIV-exposed but uninfected (iHEU) experience a higher risk of infectious morbidity than infants who are HIV-unexposed and uninfected (iHUU), it is unknown whether iHEU receive equal protection from BCG vaccination as iHUU.

Methods: Leveraging ongoing parent studies, women living with and without HIV and their HIV-uninfected newborn infants were enrolled in Botswana and South Africa. T-SPOT.TB assays (Oxford Immunotec) were performed on infant cryopreserved peripheral mononuclear cells (PBMCs) collected at 9-18 months of age in Botswana and at 9-12-months in South Africa. Sensitivity analysis was conducted by simulating all outcomes at 12 months of age while considering the conversion and reversion rates between the time points.

Results: Of the 418 infants tested, 293 (70%) were iHEU and 125 (30%) were iHUU. Mothers with HIV were older with higher gravidity compared to those without HIV. No infant presented with TB disease. Overall, 10 (3.4%) iHEU and 4 (3.2%) iHUU tested T-SPOT.TB positive. Two seroreversions occurred in Botswanan iHEU. Sensitivity analysis suggested that the T-SPOT.TB results were robust, irrespective of variance in test timing between the sites.

Conclusions: The prevalence of TBI was similar between iHEU and iHUU in two Southern African infant cohorts, contrary to previous reports where overall prevalence was higher, suggesting that iHEU may receive equal protection from BCG vaccination as iHUU. Future studies with larger cohorts are required to verify this finding.

2.2. Introduction

Children under five years of age experience a high risk of progression from tuberculosis (TB) infection to disease if untreated [410]. About 47% of women of childbearing potential account for new HIV infections [414]. Successful antiretroviral treatment (ART) scale-up for pregnant persons living with HIV has resulted in an increasing number of infants born HIV-exposed but uninfected (iHEU). iHEU experience a greater risk of infectious morbidity than infants born HIV-unexposed uninfected (iHUU) [415].

Bacillus Calmette-Guérin (BCG) vaccine prevents severe TB disease in children. BCG vaccination induces T cell interferon-gamma (IFN-γ) production, an important component of protection against TB [411]. We previously found a significantly lower proportion of BCG-specific IFN-γ producing CD4+ T cells among iHEU, suggesting that iHEU may not achieve equivalent BCG immune protection compared to iHUU [389]. Therefore, we investigated the TBI prevalence by HIV exposure status among BCG-vaccinated infants in Botswana and South Africa, two high burden HIV and TB settings.

2.3. Material and methods

2.3.1. Study design

The study was nested within two prospective observational cohort studies enrolling pregnant women with and without HIV and their infants. The Tshilo Dikotla study (Gaborone, Botswana) and the Innate Factors Associated with Nursing Transmission (InFANT) study (Khayelitsha Site B, Cape Town, South Africa) recruited participants from government antenatal clinics between 2013 and 2020 [416,417]. Inclusion and exclusion criteria of each study are indicated in **Appendix A-B**. Infants with severe birth complications, or born to mothers with active TB or TB symptoms at the time of enrolment were excluded. All infants received BCG vaccination within 72 hours (hrs) of birth. Participants were followed over 36 months in Botswana and 12 months in South Africa. Peripheral blood mononuclear cells were collected at 9-12 and 18 months in Botswana, and at 9 and 12 months in South Africa, and stored in liquid nitrogen.

2.3.2. Ethics

This study was approved by the Health Research Development Committee in Botswana (protocol HRDC 00850), Massachusetts General Hospital's Institutional Review Board, and University of Cape Town's Human Research Ethics Committee (protocol 285/2012). Women provided written informed consent for their participation and that of their infant.

2.3.3. T-SPOT.TB assay

T-SPOT.TB assays (Oxford Immunotec) were performed and interpreted according to manufacturer's instructions. Briefly, $2.5x10^5$ rested PBMCs were incubated overnight with phytohaemagglutinin (PHA; positive control), TB antigens Early Secretory Antigenic Target 6 (ESAT-6) and culture filtrate protein-10 kDa (CFP-10), or AIM-V™ medium (ThermoFisher; Nil control). Spot-forming cells (SFCs) were enumerated using ImmunoSpot3 software (Cellular Technology). Samples containing below the recommended cell number were normalized as previously described [418]. As per manufacturers' instructions, the test result was considered positive if at least one TB antigen had ≥ 8 SFCs more than the Nil control, borderline if the difference between the Nil control and at least one TB antigen was 5-7 SFCs, or invalid if PHA < 20 SFCs or Nil control > 10 SFCs. If the result did not meet the described criteria, it was interpreted as negative. For invalid or borderline results, re-testing was performed using an aliquot collected at the same visit or a follow-up visit. If the re-tested result was valid, the valid result was assigned to the initial visit. Infants testing T-SPOT.TB positive were referred to government clinics. We defined "TBI" as T-SPOT.TB positive without TB disease symptoms at the time of specimen draw.

2.3.4. Sensitivity analysis

Due to timing variation of testing between sites, we simulated results as if all testing was performed at 12 months. For South African infants, we assumed a positive test at month nine would have a negative at month 12 with probability R (reversion), and infants with a negative or invalid result at month nine would have a positive at month 12 with probability C (conversion). These probabilities were applied to 12- to 18-months results in the Botswana cohort. We assumed a baseline P (prevalence) at 12 months to calculate the probability of a positive (or negative/invalid) test at 18 months having been negative (or positive) at month 12. For each combination of R, C, and P, ranging from 0% to 20% based on published studies [383,418], we randomly generated

5,000 datasets and performed Fisher's exact tests on the pooled month 12 data, comparing the proportion of positive results by infant HIV exposure status.

2.3.5. Statistical analysis

Data analysis was performed using R (version 4.0.4). Normally distributed continuous variables were compared by t-test using means with standard deviations (SDs). Continuous variables with skewed distributions were compared by Wilcoxon rank-sum test using medians with interquartile ranges (IQRs). Categorical variables were compared by Chi-square test. Proportions of TBI were compared by infant HIV exposure status using Fisher's exact test.

2.3.6. Power calculations

Previous sub-Saharan data reported a TBI prevalence of 10.9% (95% confidence interval (CI), 6.1-17.7%) in six-month-old iHEU [418]. Thus, we expected that at least 18% of iHEU would test positive by 12 months. Given our study's sample size (125 iHUU and 293 iHEU), we had at least 80% power to detect a 57.5% difference in TBI at 12 months, assuming a prevalence of ≤ 7.65% among iHUU.

2.4. Results

2.4.1. Cohort Characteristics

The study included 418 mother-infant pairs, of which 293 were iHEU (**Table 2.1**). The proportion of iHEU was higher in Botswana compared to South Africa. Infant sex and gestational age at birth were similar between HIV exposure groups. Women with HIV were older and had higher gravidity than women without HIV. Among women with HIV, 63.0% were on ART at conception with median CD4 count of 463 cells/mm^3 at enrollment. Fifteen (3.6%) infants had a household TB exposure during follow-up (n = 5 in Botswana; n = 10 in South Africa), including six from South Africa whose mothers developed active TB disease during the course of the study. Household exposure did not differ by HIV exposure status.

Table 2.1. Comparison of overall cohort characteristics by HIV exposure status.

		iHUU N = 125	iHEU N = 293	*P*
Study site, n (%)	Botswana	33 (26.4)	135 (46.1)	<0.001
	South Africa	92 (73.6)	158 (53.9)	
Household water accessibility, n (%)[b]		85 (70.8)	206 (71.0)	1
Maternal characteristics				
Age at delivery, years (mean (SD))[a]		26.05 (4.60)	29.67 (5.45)	<0.001
Marital status, n (%)[c]	Married	25 (21.0)	37 (12.8)	0.038
	Living together	15 (12.6)	65 (22.4)	
	Separated	0 (0.0)	1 (0.3)	
	Single	79 (66.4)	187 (64.5)	
Completed at least secondary education, n (%)[d]		111 (92.5)	208 (73.2)	<0.001
Employed, n (%)[a]		59 (47.2)	128 (43.7)	0.41
Number of prior pregnancies (median [IQR])[e]		1.00 [0.00, 2.00]	2.00 [1.00, 2.00]	<0.001
On ART at conception, n (%)[f]		-	184 (63.0)	-
CD4 count at enrollment, cells /mm^3 (median [IQR])[h]		-	463 [323, 622]	-
Proportion with HIV viral suppression (<40 copies/ml), n (%)[i]			177 (93.2)	-
Developed active TB during study, n (%)		1 (0.8)	5 (1.7)	0.79
Infant characteristics				
Male sex, n (%)[j]		58 (48.7)	142 (49.0)	1
Gestational age at birth, weeks (median [IQR])[k]		39.64 [38.61, 40.57]	39.29 [38.00, 40.29]	0.17
Household TB contact, n (%)		3 (2.4)	12 (4.1)	0.57

Abbreviations: HIV, human immunodeficiency virus; iHUU, HIV-unexposed uninfected infants; iHEU, HIV-exposed uninfected infants; IQR, interquartile range; SD, standard deviation; ART, antiretroviral treatment; TB, tuberculosis. [a]Missing data from 8 infants (iHUU, n = 5; iHEU, n = 3). [b]Missing data from 15 infants (iHUU, n = 6; iHEU, n = 9). [c]Missing data from 9 infants (iHUU, n = 6; iHEU, n = 3). [d]Missing data from 14 infants (iHUU, n = 5; iHEU, n = 9). [e]Missing data from 13 infants (iHUU, n = 7; iHEU, n = 6). [f]Missing data from 1 iHEU infant. [g]Missing data from 5 iHEU infants. [h]Missing data from 19 iHEU infants. [i]Missing data from 102 iHEU infants. [j]Missing data from 9 infants (iHUU, n = 6; iHEU, n = 3). [k]Missing data from 10 infants (iHUU, n = 7; iHEU, n = 3).

2.4.2. Prevalence of TBI

Out of 418 infants, 14 (3.3%) tested T-SPOT.TB positive, 1 (0.24%) borderline, 15 (3.6%) invalid, and 388 (92.8%) negative (**Table 2.2**). T-SPOT.TB reactivity did not differ by infant HIV exposure status (iHUU n = 4 (3.2%) and iHEU n = 10 (3.4%); 95% CI 0.30- 4.76; **Table 2.2**) or by study site (**Table 2.3**). No infants who tested TBI positive and were referred for clinical evaluation were diagnosed with TB disease. Two reversions (0.48%) occurred among Botswana iHEU, one of which had a household TB contact (**Table 2.1**). Although SFCs for TB antigens did not differ pre-reversion, SFCs for PHA (positive control) were significantly lower than other positive cases when they reverted (median 165 vs. 724, $P = 0.003$).

Table 2.2. T-SPOT.TB reactivity by HIV exposure status.

		iHUU N = 125	**iHEU N = 293**
Study site, n (%)	Botswana	33 (26.4)	135 (46.1)
	South Africa	92 (73.6)	158 (53.9)
Testing time point, n (%)	Month 9	44 (35.2)	117 (39.9)
	Month 12	48 (38.4)	46 (15.7)
	Month 18	33 (26.4)	130 (44.4)
T-SPOT.TB result, n (%)	Positive[a]	4 (3.2)	10 (3.4)
	Negative[b]	115 (92.0)	273 (93.2)
	Borderline[c]	0 (0.0)	1 (0.3)
	Invalid[d, e]	6 (4.8)	9 (3.1)

Abbreviations: iHUU, HIV-unexposed uninfected infants; iHEU, HIV-exposed uninfected infants; SFCs, spot-forming cells; PHA, phytohemagglutinin. [a]Positive if there were ≥ 8 SFCs above Nil control for at least one of TB antigens. [b]Negative if a test did not fall into any of the interpretations. [c]Borderline if the difference to Nil control was between 5-7 SFCs for at least one of TB antigens. [d]Invalid if there were PHA < 20 SFCs or Nil control > 10 SFCs. [e]Reason for invalid results: contamination of kits or assay (n = 2); PHA < 20 SFCs (n = 7) and Nil control > 10 SFCs (n = 6).

Table 2.3. T-SPOT.TB results by study sites.

		South Africa		Botswana	
		iHUU N = 92	**iHEU N = 158**	**iHUU N = 33**	**iHEU N =135**
Testing time point, n (%)	Month 9	44 (47.8)	117 (74.1)	-	-
	Month 12	48 (52.2)	41 (25.9)	0 (0.0)	5 (3.7)
	Month 18	-	-	33 (100.0)	130 (96.3)
T-SPOT.TB result (%)	Positive[a]	3 (3.3)	4 (2.5)	1 (3.0)	6 (4.4)
	Negative[b]	85 (92.4)	146 (92.4)	30 (90.9)	127 (94.1)
	Borderline[c]	0 (0.0)	0 (0.0)	0 (0.0)	1 (0.7)
	Invalid[d, e]	4 (4.3)	8 (5.1)	2 (6.1)	1 (0.7)

Abbreviations: iHUU, HIV-unexposed uninfected infants; iHEU, HIV-exposed uninfected infants; SFCs, spot-forming cells; PHA, phytohemagglutinin. [a]Positive if there were ≥ 8 SFCs above Nil control for at least one of TB antigens. [b]Negative if a test did not fall into any of the interpretations. [c]Borderline if the difference to Nil controls was between 5-7 SFCs for at least one of TB antigens. [d]Invalid if there was PHA < 20 SFCs or Nil control >10 SFCs. [e]Reason for invalid results: PHA < 20 SFCs (n = 6) and Nil control >10 SFCs (n = 6) in South Africa; PHA < 20 SFCs (n = 1) and contamination of kits or assay (n = 2) in Botswana.

We conducted a sensitivity analysis to impute T-SPOT.TB results at 12 months of age across study sites, considering potential conversion and reversion rates over time (**Appendix C**). No combination of assumptions gave a statistically significant difference between HIV-exposure groups in T-SPOT.TB positivity more than 5% of the time.

2.5. Discussion

In our Southern African cohorts, we found a low overall risk of TBI among infants BCG-vaccinated at birth, with no influence of HIV exposure status. The lack of difference is important, as iHEU have been reported to be at high risk of infectious morbidity [415]. Although testing was performed between nine and 18 months of life, with some infants having a longer window of risk for TB exposure, the sensitivity analysis suggests that the prevalence of T-SPOT.TB positivity was robust to conversion and reversion between the observed time points. Literature investigating TBI in iHEU using IFN-γ release assays (IGRAs) like the QuantiFERON-TB or T-SPOT.TB is limited

[42], and studies including iHUU as a comparison group are scarce. To our knowledge, this is the largest study comparing TBI prevalence between Southern African iHEU and iHUU using T-SPOT.TB.

The prevalence of TBI was lower among infants in this study compared to other studies using IGRA-based approaches [383]. Differences in cohort characteristics likely account for lower IGRA positivity in our study. We excluded mothers with active TB disease at baseline. Further, the previously published South African study assessed TBI in children with a mean age of 3.5 years [383], evaluating a longer exposure window. It was also conducted during a period when South Africa recorded its highest TB incidence in the last two decades [419]. Thus, household TB contacts were more common than in our study (13.2% vs. 3.6%).

We found no difference in T-SPOT.TB reactivity by HIV exposure status. This differs from a Ugandan study where children who were HEU up to five years of age had higher IGRA positivity prevalence than children who were HUU [42]. Differences in maternal inclusion criteria and longer follow-up period likely explain the higher prevalence reported in Ugandan children who were HEU.

The strengths of this study include a large sample size, with cohorts recruited in neighboring countries, both with high HIV and TB burden, using a common protocol. Pooling of data increased study power. Although timing of testing varied between sites, we employed a sensitivity analysis to assess for robustness of findings. Given the lower than anticipated T-SPOT.TB positivity prevalence, we did not have sufficient power to conclusively evaluate the association between HIV exposure and TBI. Since the prevalence of a T-SPOT.TB reactivity in iHEU was 3.4% in our cohort, prevalence among iHUU would had to have been ≤ 0.175%, a 94.9% reduction, to detect a significant difference. Adequately powered studies would be needed to definitively exclude a higher risk of TBI in iHEU.

We employed IGRA-based testing, similar to previous studies [42,383]. Infant T cells have lower IFN-γ producing capacity than adult T cells [420], and perinatal HIV exposure has been associated with altered immunity [398]. Thus, it is unclear whether iHEU and iHUU have similar immune response against TB antigens. Furthermore, IGRA testing is not recommended for children under

two years of age, but tuberculin skin testing can result in false positive tests in BCG-vaccinated individuals. Assays targeting non-IFN-γ markers have been proposed as alternatives in BCG-vaccinated children under two years of age [421] and may be beneficial to inclusion in future studies. Further, it is possible that co-trimoxazole prophylaxis recommended to iHEU at six weeks of age contributed to the low prevalence of TBI among this population [422].

In summary, we showed that the TBI prevalence among BCG-vaccinated infants from two Southern African countries with high HIV and TB prevalence was low and did not vary by HIV exposure status.

2.6. Contribution, acknowledgments and financial support

Contribution: Saori C. Iwase, Investigation (T-SPOT.TB assays on South African cohort), Data curation, Formal analysis, Visualization, Writing – original draft | Paul T. Edlefsen, Methodology, Supervision, Writing – review and editing | Lynnette Bhebhe, Investigation (T-SPOT.TB assays on Botswana cohort), Writing – review and editing | Kesego Motsumi, Investigation (T-SPOT.TB assays on Botswana cohort), Writing – review and editing | Sikhulile Moyo, Conceptualization, Writing – review and editing | Anna-Ursula Happel, Supervision, Writing – review and editing | Danica Shao, Methodology, Supervision, Writing – review and editing | Nicholas Mmasa, Data curation, Writing – review and editing | Sara Schenkel, Data curation, Writing – review and editing | Melanie A. Gasper, Supervision, Writing – review and editing | Melanie Dubois, Supervision, Writing – review and editing | Megan A. Files, Supervision, Writing – review and editing | Chetan Seshadri, Conceptualization, Supervision, Writing – review and editing | Fergal Duffy, Supervision, Writing – review and editing | John Aitchison, Conceptualization, Writing – review and editing | Mihai G. Netea, Methodology, Writing – review and editing | Jennifer Jao, Conceptualization, Writing – review and editing | Donald W. Cameron, Conceptualization, Writing – review and editing | Clive M. Gray, Conceptualization, Supervision, Writing – review and editing | Heather B. Jaspan, Conceptualization, Supervision, Writing – review and editing | Kathleen M. Powis, Conceptualization, Funding acquisition, Supervision, Writing – review and editing. All authors approved the final manuscript.

Acknowledgments: We thank the mothers and infants who participated in this study, the research and lab staff at Botswana Harvard AIDS Institute Partnership in Gaborone, Botswana, and the clinic Maternal Obstetric Unit in Cape Town, South Africa. We also would like to thank Western Cape Department of Health (DOH) for use of their space and an infrastructure award from the University of Washington/Fred Hutch Center for AIDS Research, National Institutes of Health (NIH)-funded program under award number AI027757 which is supported by the following NIH Institutes and Centers: National Institute of Allergies and Infectious Disease (NIAID), National Cancer Institute (NCI), National Institute of Mental Health (NIMH), National Institute on Drug Abuse (NIDA), National Institute of Child Health and Human Development (NICHD), National Heart, Lung, and Blood Institute (NHLBI), National Intelligence Authority (NIA), National Institute of General Medical Sciences (NIGMS), and National Institute of Diabetes and Digestive and Kidney Diseases (NIDDK).

Financial support: This work was supported by the NIAID (grant number R01AI142670 awarded to K. M. P.). The Tshilo Dikotla study was funded by the National Institute of Diabetes and Digestive and Kidney Diseases (grant number R01DK109881 awarded to J. J.). The InFANT study was supported in part by the Global Health Research Initiative (GHRI), a research funding partnership composed of the Canadian Institutes of Health Research, the Canadian International Development Agency, and the International Development Research Centre (grant number THA-118568 awarded to H. B. J. and C. M G.), as well as the NIAID (grant number R01AI120714-01A1 awarded to H. B. J.) and NICHD (grant number R21HD083344 awarded to H. B. J. and C. M. G.). M. D. was supported by NIAID (grant number T32AI007433). S. C. I. was funded by Yoshida Scholarship Foundation.

Chapter 3. Longitudinal gut microbiota composition of South African and Nigerian infants in relation to tetanus vaccine responses

3.1. Abstract

Background: Infants who are exposed to HIV but uninfected (iHEU) have a higher risk of infectious morbidity than infants who are HIV-unexposed and uninfected (iHUU), possibly due to altered immunity. As infant gut microbiota may influence immune development, we evaluated the effects of HIV exposure on infant gut microbiota and its association with tetanus toxoid (TT) vaccine responses.

Methods: We evaluated the gut microbiota of 82 South African (61 iHEU and 21 iHUU) and 196 Nigerian (141 iHEU and 55 iHUU) infants at < 1 and 15 weeks of life by 16S ribosomal ribonucleic acid (rRNA) gene sequencing. Anti-tetanus antibodies were measured by enzyme-linked immunosorbent assay (ELISA) at matched time points.

Results: Gut microbiota in the 278 included infants and its succession were more strongly influenced by geographical location and age than by HIV exposure. Microbiota of Nigerian infants, who were exclusively breastfed, drastically changed over 15 weeks, becoming dominated by *Bifidobacterium longum* subspecies *infantis*. This change was not observed among South African infants, even when limiting the analysis to exclusively breastfed infants. The Least Absolute Shrinkage and Selection Operator (LASSO) regression suggested that HIV exposure and gut microbiota were independently associated with tetanus titres at week 15, and that high passively transferred maternal antibody levels, as seen in the Nigerian cohort, may mitigate these effects.

Conclusions: In two African cohorts, HIV exposure minimally altered the infant gut microbiota compared to age and setting, but both specific gut microbes and HIV exposure independently predicted humoral tetanus vaccine responses.

3.2. Introduction

The mutualistic relationship between microbes and humans begins in early life. Emerging evidence suggests that the colonization of microbes in the gut facilitates the development of the immune system and growth trajectories [413,423]. Due to the successful prevention of vertical transmission programs, the number of infants who are HIV-exposed yet uninfected (iHEU) has been increasing, particularly in sub-Saharan Africa [424]. Compared to infants who are HIV-unexposed and uninfected (iHUU), iHEU are at higher risk of morbidity and mortality, predominantly due to infectious diseases [425]. This is thought to be linked to their altered immunity [426,427], which may be secondary to altered gut microbiota. To our knowledge, there are limited longitudinal studies comparing gut microbiota between iHEU and iHUU, and most of them were conducted in a single country [404,405, 407,409]. Some studies have found few differences [407–409], whereas clear differences in microbiota profile were observed in Haitian [404] and Nigerian iHEU [405]. Thus far, only one cross-sectional study compared the gut microbiota between iHEU and iHUU in multiple countries, including Belgium, Canada, and South Africa, and suggested that the difference in microbiota by HIV exposure status may be population-specific [406]. Therefore, the effect of geography and HIV exposure on infant gut microbiota requires further investigation.

Vaccines are critical for protecting infants from infectious diseases and consequent morbidity and mortality. However, multiple factors can influence vaccine immunogenicity, including genetics, nutritional status, and pre-existing immunity [428]. In addition, emerging evidence points to a possible role of the gut microbiota in influencing vaccine response [429]. In Bangladeshi infants, CD4+ T-cell proliferation and IgG against tetanus toxoid (TT) vaccination were positively associated with abundance of Actinobacteria, particularly *Bifidobacterium longum*, until at least two years of age [56,430]. Conversely, vaccine-induced CD4+ T-cell proliferation against TT vaccine was negatively associated with the abundance of *Enterobacteriales* and *Pseudomonadales* [430].

To evaluate the contribution of gut microbiota to observed differences in immunity between iHEU and iHUU, we longitudinally compared the gut microbiota of South African and Nigerian infants exposed and unexposed to HIV, and correlated these with TT vaccine responses.

3.3. Material and methods

3.3.1. Study participants

Mothers with and without HIV and their neonates were recruited into a multicenter longitudinal study between September 2013 and November 2017 [417]. Mother-infant pairs were enrolled during the first week post-delivery at the Khayelitsha Site B Midwife Obstetric Unit in Cape Town, South Africa, and the Plateau State Specialist Hospital in Jos, Nigeria. Clinical and demographic data and samples (including stool and blood) were collected. All mothers with HIV received antiretroviral therapy according to local guidelines, and their infants were confirmed as HIV-negative by polymerase chain reaction (PCR) at birth and later time points [431,432]. In addition, all iHEU received nevirapine post-exposure prophylaxis (PEP) after birth, and co-trimoxazole was recommended at six weeks of age as per country-specific guidelines [431,433]. Exclusive breastfeeding was advised to all mothers for six months. Feeding data were collected using a structured questionnaire validated in similar settings [434]. Feeding practices were categorized as "exclusive breastfeeding," defined as receiving only breastmilk or prescribed medicines since birth, or "mixed feeding," defined as receiving breastmilk supplemented with other liquids or food or receiving formula. In this analysis, we included stool and plasma collected from term infants during the first and at 15 weeks of life born to mothers without complications during pregnancy or delivery.

3.3.2. Immunization

Routine childhood vaccinations were given to all infants according to the World Health Organization (WHO) Expanded Program on Immunization [43]. In both countries, infants were vaccinated against tetanus at 6, 10, and 14 weeks. South African infants received DTaP (diphtheria toxoid [DT], TT, and acellular pertussis [aP]), while Nigerian infants received DTwP (DT, TT, and whole-cell pertussis [wP]). Pregnant mothers were given booster TT vaccination (Serum Institute of India Pvt. Ltd.) in Nigeria.

3.3.3. Sample collection, deoxyribonucleic acid (DNA) extraction and 16S rRNA gene sequencing

Fecal samples were collected from diapers, avoiding the surface. Samples were placed on ice immediately, transferred to the lab within 6 hours (hrs), and stored at -40 to -20°C until analysis. Samples were thawed and treated with a cocktail of mutanolysin (300 U/ml, Sigma Aldrich), lysozyme (45,000 U/ml, Sigma Aldrich), and lysostaphin (24 U/ml, Sigma Aldrich) in 300 µl phosphate-buffered saline (PBS) for 1 hr at 37°C. Samples were then mechanically disrupted by bead-beating at 50 Hertz (Hz) for 10 minutes (mins) using the Qiagen TissueLyser LT [435]. Genomic DNA was extracted using the PowerSoil DNA extraction kit (Qiagen), following the manufacturer's protocol. For cross-contamination filtering, genomic DNA was extracted from mock bacterial community cells with equal colony-forming units from each of the 22 known species (HM-280, BEI). Extracted genomic DNA was subjected to PCR amplification in triplicates using primers targeting the V3-V4 region (357F/806R primers) of the 16S rRNA gene, as described previously [436]. Negative controls for DNA extraction and PCR were included. Amplified libraries were purified using AMPure XP beads (Beckman Coulter), quantitated using Quant-iT dsDNA High Sensitivity Assay Kits (ThermoFisher), pooled in equal molar amounts, and paired-end sequenced using a MiSeq Reagent Kit V3 (600-cycle, Illumina). Following demultiplexing, barcode primers were removed using Cutadapt (version 3.4) [437], and reads were processed using DADA2 (version 1.19.2) [438] within the R framework (R version 4.0.4) [439]. Taxonomic classification of amplicon sequence variants (ASVs) was done using an updated SILVA training set (version 132) [440], available at https://github.com/itsmisterbrown/updated_16S_dbs [441]. Contaminant ASVs were identified and removed using the decontam package (version 1.16.0) [442]. Samples with less than 2,000 filtered reads were excluded from the downstream analysis.

3.3.4. Plasma IgG anti-tetanus antibodies

Blood samples were obtained from infants at 1 and 15 weeks and from Nigerian mothers at 1 week postpartum. All blood samples were collected in heparinized tubes and transported to the lab within 6 hours for sample processing. Plasma was removed prior to cell isolation using Ficoll density-gradient separation medium (Sigma Aldrich) and stored at -80°C until analysis. Plasma anti-tetanus IgG was measured by enzyme-linked immunosorbent assay (ELISA) following the

manufacturer's protocol (TECAN, IBL International GmbH). The optical density at 450 nm was measured using an ELISA microplate reader (BioTek ELx808 absorbance plate reader), and a standard curve was generated using the readings from the calibrators included on each plate and used to calculate the individual titers (IU/ml). To validate each assay, we considered only calibration curves for each plate that had a coefficient of determination (r^2) above 0.95. Calibration curves that had an r^2 below 0.95 were repeated. The manufacturer provided the intra-assay and inter-assay coefficient of variation (CV%) as 6.9 and 10.4, respectively. Samples on each plate were run in duplicate and averaged. Previously tested positive samples were incorporated into subsequent runs as in-house controls.

3.3.5. Data analysis

Differences in study cohort characteristics were assessed using the Student's t-test (parametric continuous variables), Wilcoxon signed-rank test (non-parametric continuous variables), and Chi-squared test (parametric categorical variables). Spearman's rank correlation coefficient (R) was used to analyze associations between groups. Bacterial community analysis was done using the phyloseq (version 1.40.0) [443] and vegan (version 2.4.6) [444] packages. The ASV table was normalized (i.e., transformed to relative abundance * median sample read depth) and filtered so that each ASV had at least 10 counts in at least 20% of the samples or had a total relative abundance of at least 0.1%. Shannon index was calculated as a measure of α-diversity. Comparison of microbial community composition between groups was evaluated by principal coordinate analysis (PCoA) and permutational multivariate analysis of variance (PERMANOVA) using the adonis2 function in the vegan package [444], based on the Bray-Curtis dissimilarity and 999 permutations. Partitioning around medoids (PAM) clustering was applied to determine the optimal *k* using the cluster package (version 2.1.4) [445]. Analysis of Compositions of Microbiomes with Bias Correction (ANCOM-BC; version 1.6.4) [446] was used to identify significantly differentially abundant ASVs through pair-wise comparisons with an adjusted *P*-value of < 0.05, and $\log_e$ fold change of > 0.5 or < -0.5. *P*-values of anti-tetanus IgG titers were compared by Wilcoxon signed-rank tests and adjusted for multiple comparisons using the Benjamini-Hochberg method. To identify factors associated with infant anti-tetanus IgG titers at 15 weeks of age, we applied the Least Absolute Shrinkage and Selection Operator (LASSO) regression using the glmnet package (version 4.1.4) [447]. Since microbiota compositional data are often highly skewed, we employed

rank-based transformation [448] for the regression analysis using the top 50 ASVs among infants who had microbiota data available at both week 1 and week 15. After the transformation, the most abundant bacterial taxon within the sample was given the highest score of 50, and the least abundant bacterial taxon was given a score of 1. The rank-transformed ASVs, infant anti-tetanus IgG titers at one week of age (indicative of passive maternal antibody transfer), and HIV exposure status were used as explanatory variables. Models were created according to the infant's age and geographical location separately. The predictive models were validated by 10-fold cross-validation using the cv.glmnet() function in the glmnet package [447]. Lambda value that gave the lowest model error was used as a tuning parameter. Variables that fitted within the regression model were considered to be predictor variables for the TT vaccine response. *P*-values < 0.05 and 95% confidence intervals were used to assess statistical significance.

3.4.Results

3.4.1. Cohort characteristics

Overall, there were 278 mother-infant pairs included in this analysis; 82 were from South Africa, and 196 were Nigerian. Several demographic and socioeconomic characteristics differed by study site (**Table 3.1**). At enrolment, Nigerian mothers were older (mean age 31 (standard deviation (SD) ± 5.31) vs. 28 (SD ± 5.38) years, $P = 0.001$) with higher gravidity (median 2 [interquartile range (IQR): 1-4] vs. 1 [IQR: 1-2], $P < 0.001$) and lower body weight (mean 62.87 (SD ± 11.51) vs. 72.69 (SD ± 13.86) kg, $P < 0.001$) than South African mothers. While electricity was equally available for participants from both countries, significantly more mothers in South Africa had a refrigerator and running water at home, and significantly more Nigerian mothers lived in formal housing made of bricks or concrete structure (all $P < 0.001$). The weight-for-length z score (wflz) of Nigerian infants was significantly lower than that of South African infants at 15 weeks of age (0.54 vs. 0.86, $P = 0.023$). All Nigerian infants were exclusively breastfed (EBF) until 15 weeks of life, whereas only 58.5% of South African mothers still reported EBF at 15 weeks postpartum ($P < 0.001$). Among the South African mothers who reported "mixed feeding," 58.8% (n = 19) introduced formula feeding or solid food while continuing breastfeeding, and 41.2% (n = 14) completely switched to formula feeding during the course of the study (median breastfeeding duration: 32 days). Mmothers of iHUU had higher formal education than mothers of iHEU (*P* =

0.002; **Table 3.2**). History of antibiotic use was higher among iHEU due to co-trimoxazole prophylaxis (86.6% iHEU vs. 6.6% iHUU, $P < 0.001$). Significantly fewer South African iHEU reported co-trimoxazole prophylaxis than Nigerian iHEU (55.7% vs. 100%, $P < 0.001$).

Table 3.1. Cohort characteristics.

		South Africa (N = 82)	Nigeria (N = 196)	*P*
Maternal characteristics				
Mother's age at delivery (years; mean (SD))		28 (5.38)	31 (5.31)	0.001
Education (n; %)	None	0 (0.0)	2 (1.0)	<0.001
	Elementary	5 (6.1)	65 (33.2)	
	Secondary	72 (87.8)	73 (37.2)	
	Higher	5 (6.1)	56 (28.6)	
Unemployed (n; %)		59 (72.0)	6 (3.1)	<0.001
Formal housing (n; %)		33 (40.2)	185 (94.4)	<0.001
Electricity (n; %)		78 (95.1)	178 (90.8)	0.332
Refrigerator (n; %)		70 (85.4)	96 (49.0)	<0.001
Running water (n; %)		38 (46.3)	48 (24.5)	0.001
Marital status (n; %)	Married/ living together	25 (30.5)	186 (94.9)	<0.001
	Single	57 (69.5)	10 (5.1)	
Gravidity (n; median [IQR])		1 [1, 2]	2 [1, 4]	<0.001
Mother's weight at enrollment (kg; mean (SD))[a]		72.69 (13.86)	62.87 (11.51)	<0.001
Infant characteristics				
iHEU (n; %)		61 (74.4)	141 (71.9)	0.787
Male (n; %)		41 (50.0)	94 (48.0)	0.858
Gestational age at delivery (weeks; median [IQR])		39.30 [38.02, 40.38]	39.95 [38.98, 40.62]	0.011
Vaginal delivery (n; %)		82 (100.0)	167 (85.2)	0.001
Wflz at W15 (median [IQR])[b]		0.86 [0.32, 1.90]	0.54 [-0.64, 1.42]	0.023
Mode of feeding at W15 (n; %)	Exclusive breastfeeding	48 (58.5)	196 (100.0)	<0.001
	Mixed feeding	34 (41.5)	0 (0.0)	
Reported antibiotic use (n; %)	Co-trimoxazole	34 (41.5)	141 (71.9)	<0.001
	Other	2 (2.4)	3 (1.5)	

Abbreviations: IQR, interquartile range; SD, standard deviation; iHEU, infants who are HIV-exposed uninfected; Wflz, weight-for-length z score; W15, 15 weeks of age. [a]Missing data from 5 participants in Nigeria; [b]Missing data from 41 participants (South Africa, n = 16; Nigeria, n = 25).

Table 3.2. Comparison of overall cohort characteristics by HIV exposure status.

		iHUU (N = 76)	iHEU (N = 202)	*P*
Maternal characteristics				
Study site (n; %)	South Africa	21 (27.6)	61 (30.2)	0.787
	Nigeria	55 (72.4)	141 (69.8)	
Mother's age at delivery (years; mean (SD))		29 (5.00)	30 (5.57)	0.098
Education (n; %)	None	0 (0.0)	2 (1.0)	0.002
	Elementary	11 (14.5)	59 (29.2)	
	Secondary	38 (50.0)	107 (53.0)	
	Higher	27 (35.5)	34 (16.8)	
Unemployed (n; %)		16 (21.1)	49 (24.3)	0.911
Formal housing (n; %)		61 (80.3)	157 (77.7)	0.548
Electricity (n; %)		70 (92.1)	186 (92.1)	1
Refrigerator (n; %)		48 (63.2)	118 (58.4)	0.561
Running water (n; %)		28 (36.8)	58 (28.7)	0.245
Marital status (n; %)	Married/ living together	63 (82.9)	148 (73.3)	0.130
	Single	13 (17.1)	54 (26.7)	
Gravidity (n; median [IQR])		2 [1, 3]	2 [1, 3]	0.071
Mother's weight at enrollment (kg; mean (SD))[a]		66.82 (13.56)	65.45 (12.86)	0.443
Mother on ART at delivery (n; %)		-	199 (98.5)	-
CD4 count > 250 cells/mm^3 (n; %)[b]		-	158 (81.0)	-
Viral load below detection limit (n; %)[c,d]		-	93 (58.1)	-
Infant characteristics				
Male (n; %)		38 (50.0)	97 (48.0)	0.873
Gestational age at delivery (weeks; median [IQR])		40.00 [39.00, 40.70]	39.60 [38.40, 40.40]	0.086
Vaginal delivery (n; %)		67 (88.2)	182 (90.1)	0.801
Wflz at W15 (median [IQR])[e]		0.70 [-0.20, 1.47]	0.61 [-0.52, 1.50]	0.302
Mode of feeding at W15 (n; %)	Exclusive breastfeeding	62 (81.6)	182 (90.1)	0.084
	Mixed feeding	14 (18.4)	20 (9.9)	
Reported antibiotics use (n; %)	Co-trimoxazole	0 (0.0)	175 (86.6)	<0.001
	Other	5 (6.6)	0 (0.0)	

Abbreviations: ART, antiretroviral treatment; iHUU, HIV-unexposed uninfected infants; iHEU, HIV-exposed uninfected infants; IQR, interquartile range; SD, standard deviation; Wflz, weight-for-length z score; W15, 15 weeks of age. [a]Missing data from 5 participants (mothers of iHUU, n = 2; mothers of iHEU, n =3); [b]Missing data from 7 participants ; [c]Viral load < 20 copies/ml; [d]Missing data from 42 participants; [e]Missing data from 41 participants (iHUU, n = 18; iHEU, n = 23).

3.4.2. Gut microbiota differs substantially between South African and Nigerian infants in the first week of life

Of the 524 samples sequenced, 442 samples passed the quality filtering of requiring at least 2,000 filtered reads. Of the samples that were filtered out, majority were week 1 samples due to low biomass at early stages of life (week 1 n = 63 vs. week 15 n = 19, $P < 0.0001$). Among 278 infants who were included in the downstream analysis, 164 (47 South African and 117 Nigerian) had gut microbiota data available at both weeks 1 and 15 of life, and the rest of infants had data available for one of the time points. Gut microbiota composition differed significantly by study site during the first week of life (**Figure 3.1A**). Within-sample microbial diversity (Shannon index) was higher among South African than Nigerian infants (median 2.23 [IQR: 1.96-2.62] vs. 1.13 [IQR: 0.77-1.68], $P < 0.0001$; **Figure 3.1B**). In addition, microbial community composition was significantly different by geographical location, although the site only explained 6% of the community composition (**Figure 3.1C**; PERMANOVA $P < 0.001$).

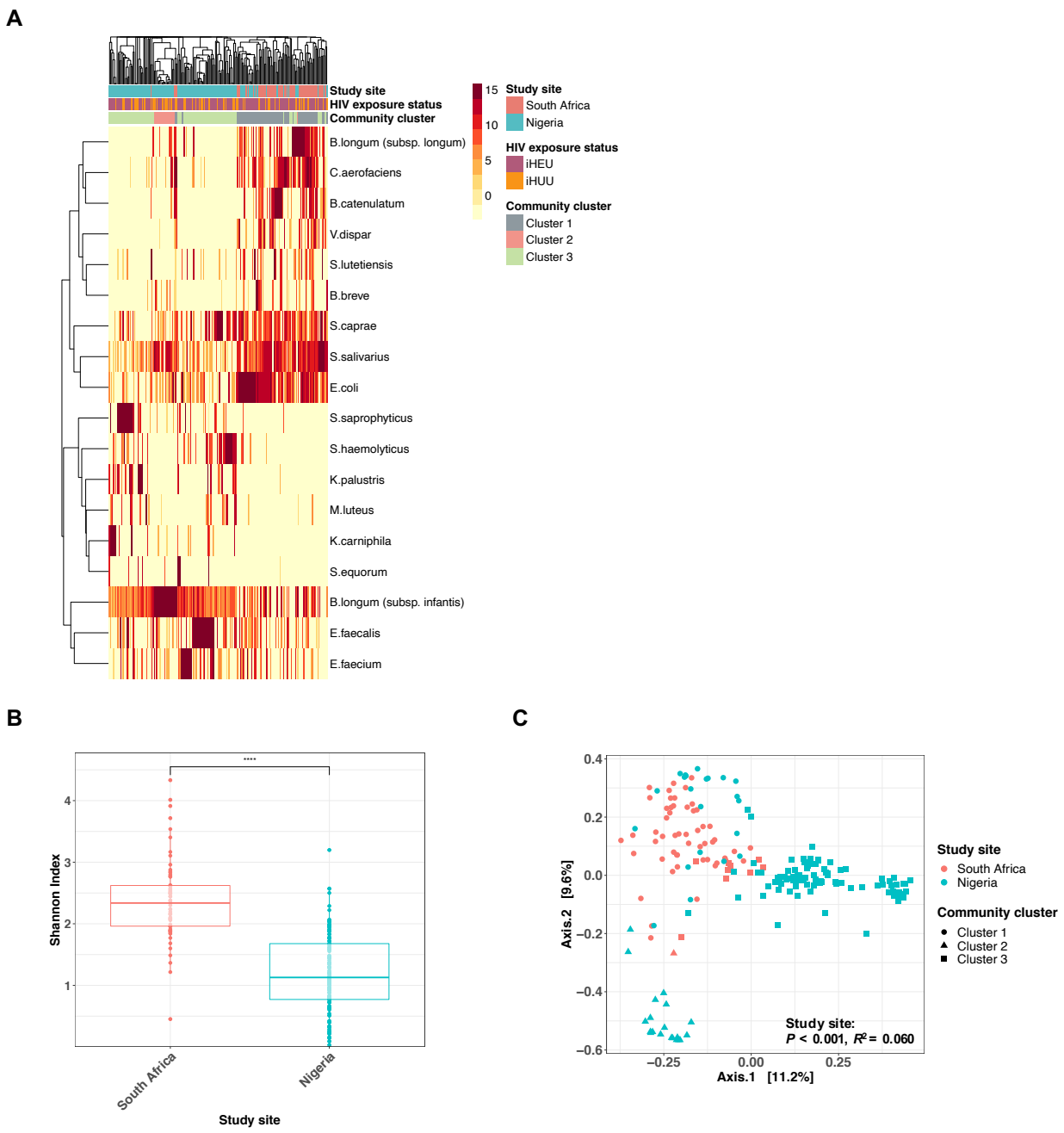

Figure 3.1. Geographical location strongly affects gut microbiota among African infants in the first week of life. (A) Heatmap of the top 20 taxa in the gut microbiota of South African and Nigerian infants in the first week of age. Study site, HIV exposure status, and community cluster types (based on PAM clustering; $k = 3$) are shown in annotation bars. (B) Comparison of α-diversity (Shannon index) between South African (n = 63) and Nigerian (n = 141) infants during the first week of life. (C) PCoA and PERMANOVA (Bray-Curtis dissimilarity) of gut microbiota during the first week of age (South African, n = 63; Nigerian, n = 141), colored by study site and shaped by community groups, based on PAM clustering ($k = 3$). Abbreviations: iHEU, infants who are HIV-exposed uninfected; iHUU, infants who are HIV-unexposed uninfected; PCoA, principal coordinate analysis; PERMANOVA, permutational multivariate analysis of variance; PAM, partitioning around medoids. **** $P < 0.0001$.

Geographical location remained significantly associated with α- and β- diversity after adjusting for sequencing batch or in separate models adjusting for demographic factors that significantly differed between countries, namely maternal marital status, weight, age, gravidity, education level, occupation, type of house, access to a refrigerator or running water, mode of delivery or infant gestational age ($P < 0.001$ for both α- and β-diversity). Moreover, α- and β- diversity remained significantly different by the geographic location when the comparison was made strictly among samples collected on the first day of life (n = 147; **Figure 3.2**).

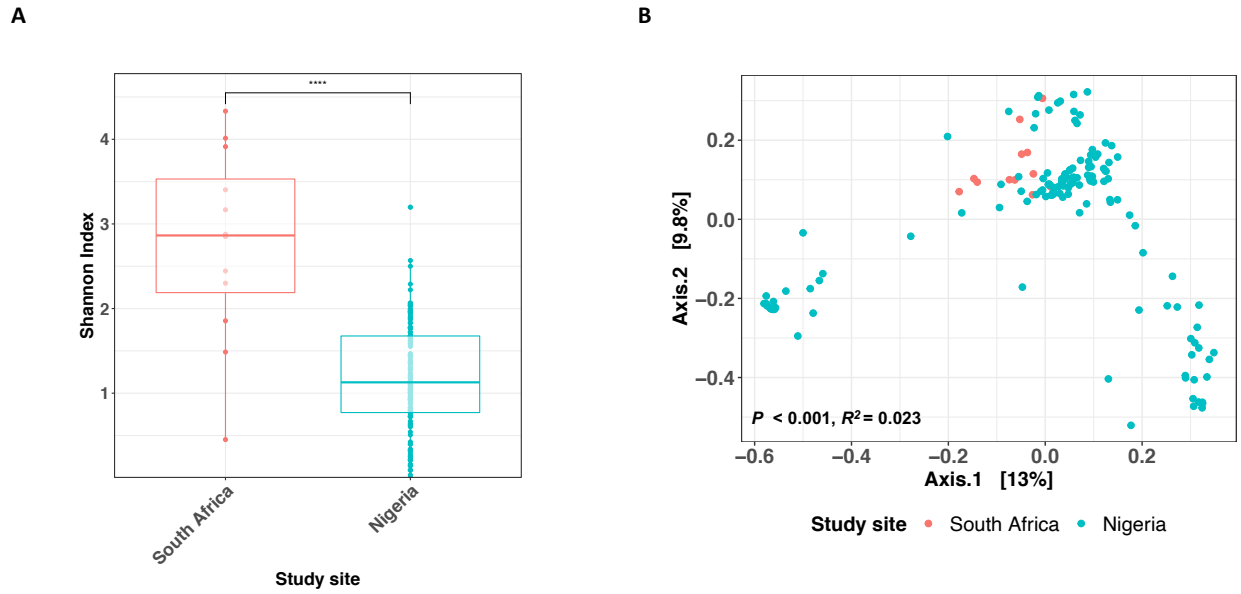

Figure 3.2. α-diversity of meconium samples differs significantly by study site. (A) Comparison of α-diversity (Shannon index) of meconium samples collected at day one of life between South African (n = 12) and Nigerian infants (n = 135). (B) PCoA and PERMANOVA (Bray-Curtis dissimilarity) of gut microbiota of meconium samples at day one of life (n = 147), colored by study site. Abbreviations: PCoA, principal coordinate analysis; PERMANOVA, permutational multivariate analysis of variance. **** $P < 0.0001$.

At baseline, most South African infants had gut microbiota consisting of (1) Actinobacteriota, including several *Bifidobacterium* species (such as *B. longum* subspecies *longum*, *B. catenulatum,* and *B. breve*) and *Collinsella aerofaciens*, (2) Firmicutes, including *Streptococcus* species (such as *S. salivarius*, *S. caprae*, and *S. lutetiensis*) and *Veillonella dispar* and (3) Proteobacteria which mainly consist of *E. coli*, which was named "cluster 1" identified by PAM clustering (**Figure 3.1A**). On the other hand, the majority of Nigerian infants' microbiota was classified as community cluster 3, dominated by (1) Actinobacteriota, mainly *B. longum* subspecies *infantis* and (2)

Firmicutes, including *Staphylococcus* species (such as *S. haemolyticus* and *S. saprophyticus*) and *Enterococcus* species (such as *E. faecalis* and *E. faecium*). The remaining Nigerian infants had microbiota in cluster 2, which was a low-diversity population dominated by *B. longum* subspecies *infantis*.

3.4.3. Age is a major driver of microbiota development, but microbial succession differs between sites

We next assessed gut microbiota longitudinally. The α-diversity in South African infants increased significantly from week 1 to week 15 (median 2.33 [IQR: 1.96-2.62] vs. 2.54 [IQR: 2.26-2.77], $P = 0.036$), while α-diversity in Nigerian infants significantly decreased (median 1.13 [IQR: 0.77-1.68] vs. 0.87 [IQR: 0.51-1.166], $P < 0.0001$) (**Figure 3.3A**), further exacerbating the differences in α-diversity between sites. There was distinct microbial community composition among Nigerian samples by age, which was less evident for South African infants (**Figure 3.3B**). In agreement, the dominant bacteria changed only marginally from week 1 to week 15 among South African infants, while Nigerian infants experienced a shift from a Firmicutes-dominated microbiota (cluster 3) to one dominated by *Bifidobacterium infantis* and *Streptococcus salivarius* (cluster 2) at 15 weeks of age (**Figure 3.3C**; **Figure 3.4**).

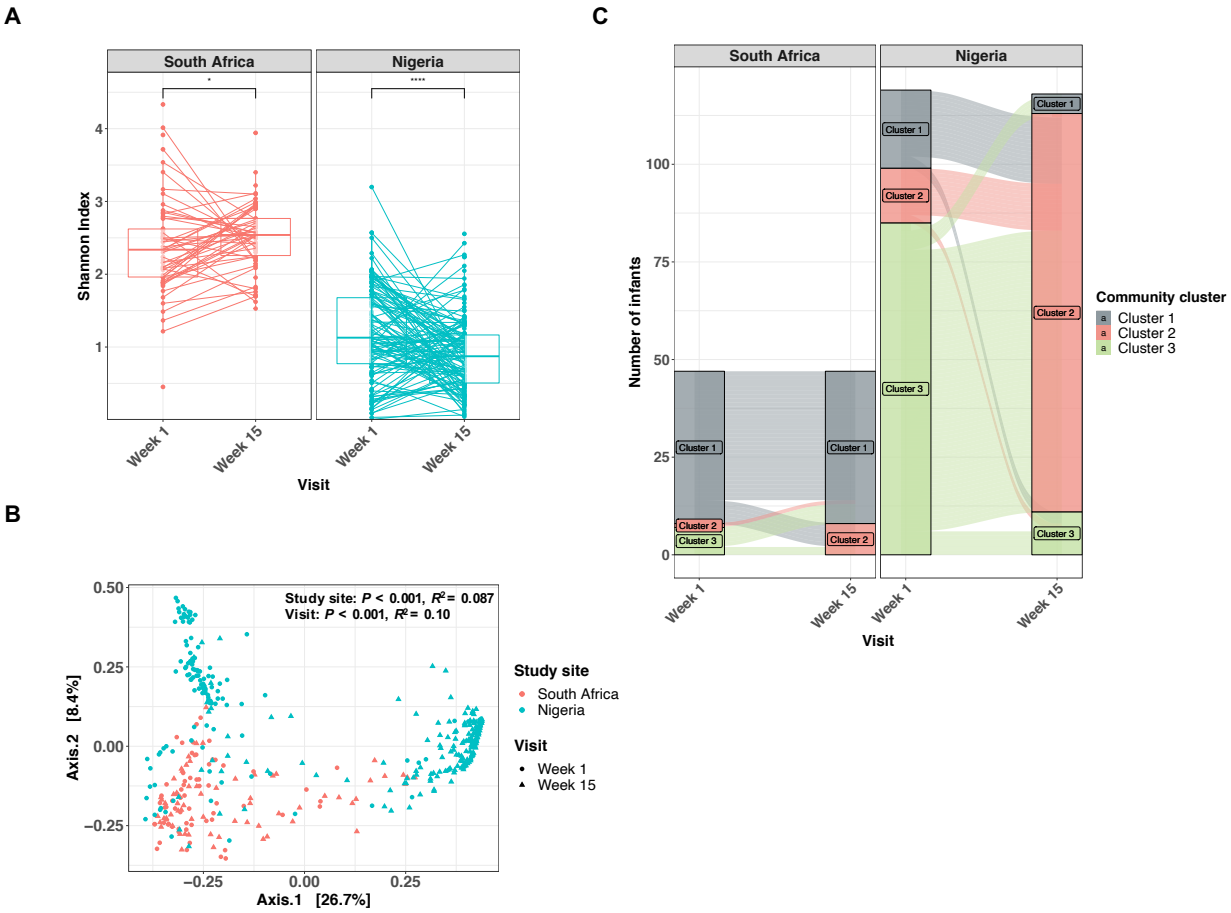

Figure 3.3. Longitudinal transition of gut microbiota is distinct among infants in South Africa and Nigeria. (A) The transition of α-diversity (Shannon index) of infant gut microbiota over the first 15 weeks of age in South Africa (n = 82) and Nigeria (n = 196). (B) PCoA and PERMANOVA (Bray-Curtis dissimilarity) of gut microbiota at 1 week and 15 weeks of age, colored by study site and shaped by visit (South African, n = 82; Nigerian, n = 196). (C) Alluvial plot showing the transition of cluster groups from week 1 to week 15 at each study site (South African, n = 82; Nigerian, n = 196). Samples were grouped according to PAM clustering (k = 3), indicated by color. Abbreviations: PCoA, principal coordinate analysis; PERMANOVA, permutational multivariate analysis of variance; PAM, partitioning around medoids. * $P < 0.05$; **** $P < 0.0001$.

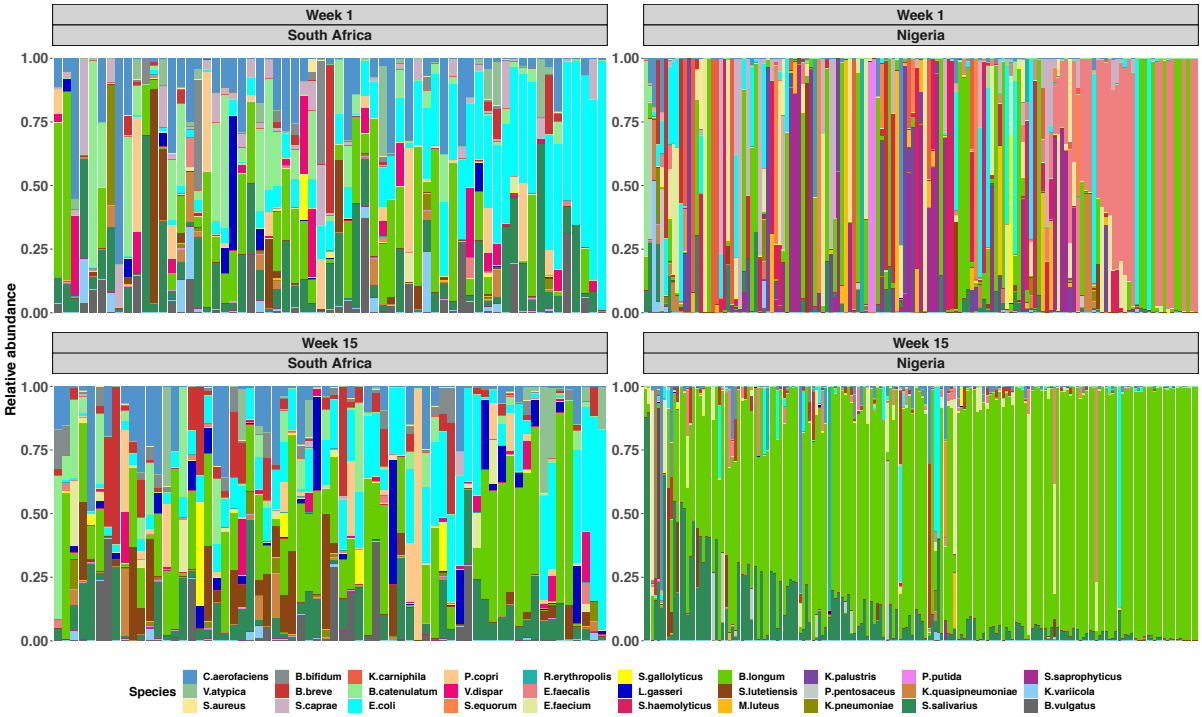

Figure 3.4. Infants' gut microbial succession over the first 15 weeks differs substantially between the study sites. Relative abundance plot of most abundant 30 taxa of South African (n = 82) and Nigerian (n = 196) infants at the 1 week and 15 weeks of age. Each column represents individual participants. *B. longum* subspecies *infantis* and *B. longum* subspecies *longum* are indicated as the same color (green).

Given the differences in delivery mode and proportion of exclusively breastfed infants between sites, we also performed the analysis restricting to EBF (n = 212) or vaginally delivered (n = 249) infants. The significant differences observed between countries in α- and β-diversity remained over the 15 weeks when the comparison was strictly among EBF infants (**Figure 3.5**) or vaginally delivered infants (**Figure 3.6**).

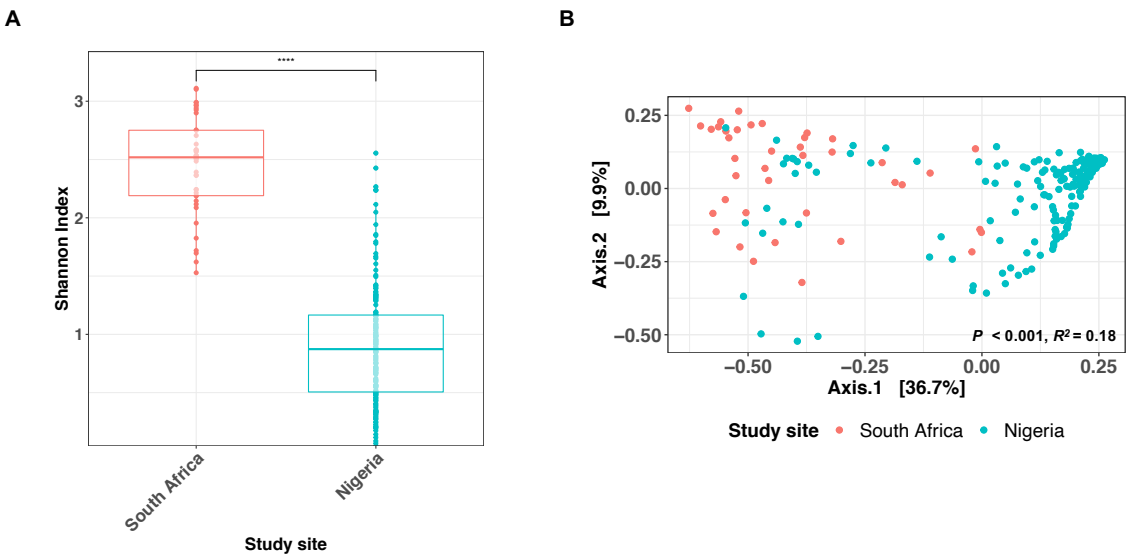

Figure 3.5. α- and β-diversity significantly differ between the countries in exclusively breastfed infants. (A) Comparison of α-diversity (Shannon index) between EBF South African (n = 40) and Nigerian (n = 172) infants at 15 weeks of age. (B) PCoA and PERMANOVA (Bray-Curtis dissimilarity) of gut microbiota among EBF infants at 15 weeks of age (n = 212), colored by study site. Abbreviations: EBF, exclusively breastfed; PCoA, principal coordinate analysis; PERMANOVA, permutational multivariate analysis of variance. **** $P < 0.0001$.

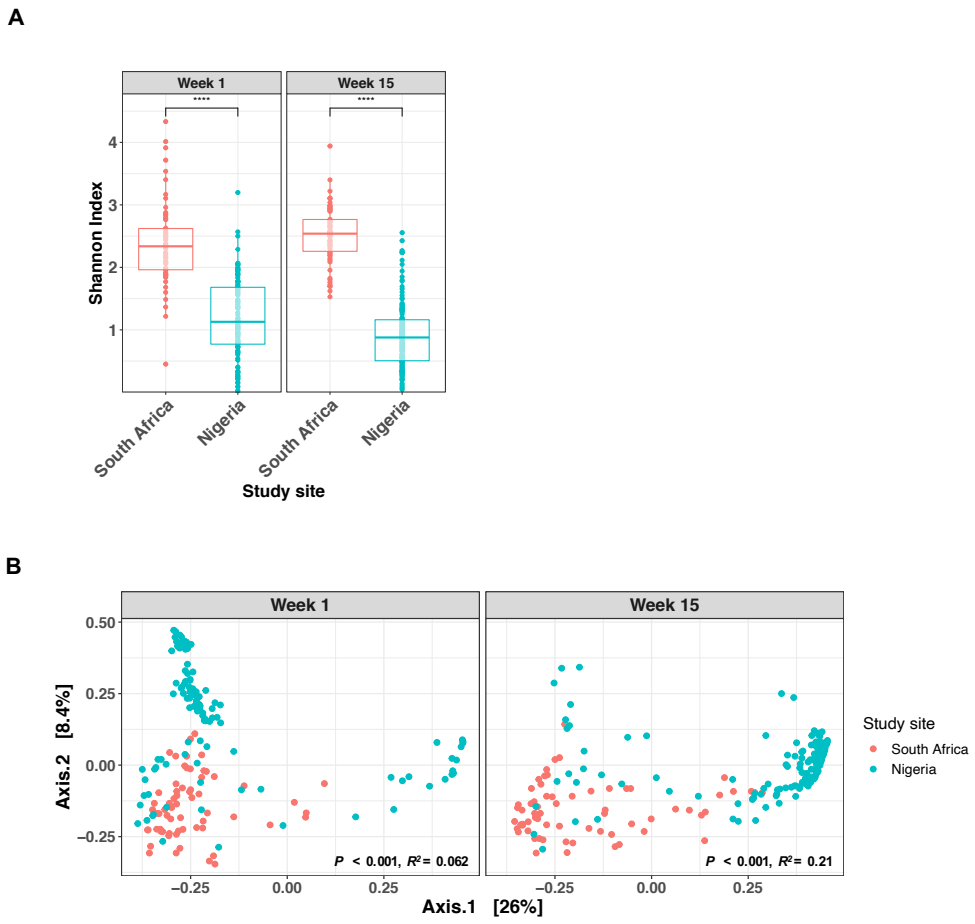

Figure 3.6. α- and β-diversity significantly differ between the countries in vaginally delivered infants. (A) Comparison of α-diversity (Shannon index) between vaginally delivered South African (n = 82) and Nigerian (n = 167) infants at week 1 and week 15. (B) PCoA and PERMANOVA (Bray-Curtis dissimilarity) of gut microbiota among vaginally delivered infants (n = 249) at week 1 and week 15, colored by study site. Abbreviations: PCoA, principal coordinate analysis; PERMANOVA, permutational multivariate analysis of variance. **** $P < 0.0001$.

3.4.4. HIV exposure has a subtle effect on the gut microbiota regardless of the geographical location

There were no significant differences in α-diversity (**Figure 3.7A**), β-diversity (**Figure 3.7B**), or PAM cluster transition **Figure 3.7C-D**) by HIV exposure status in either country.

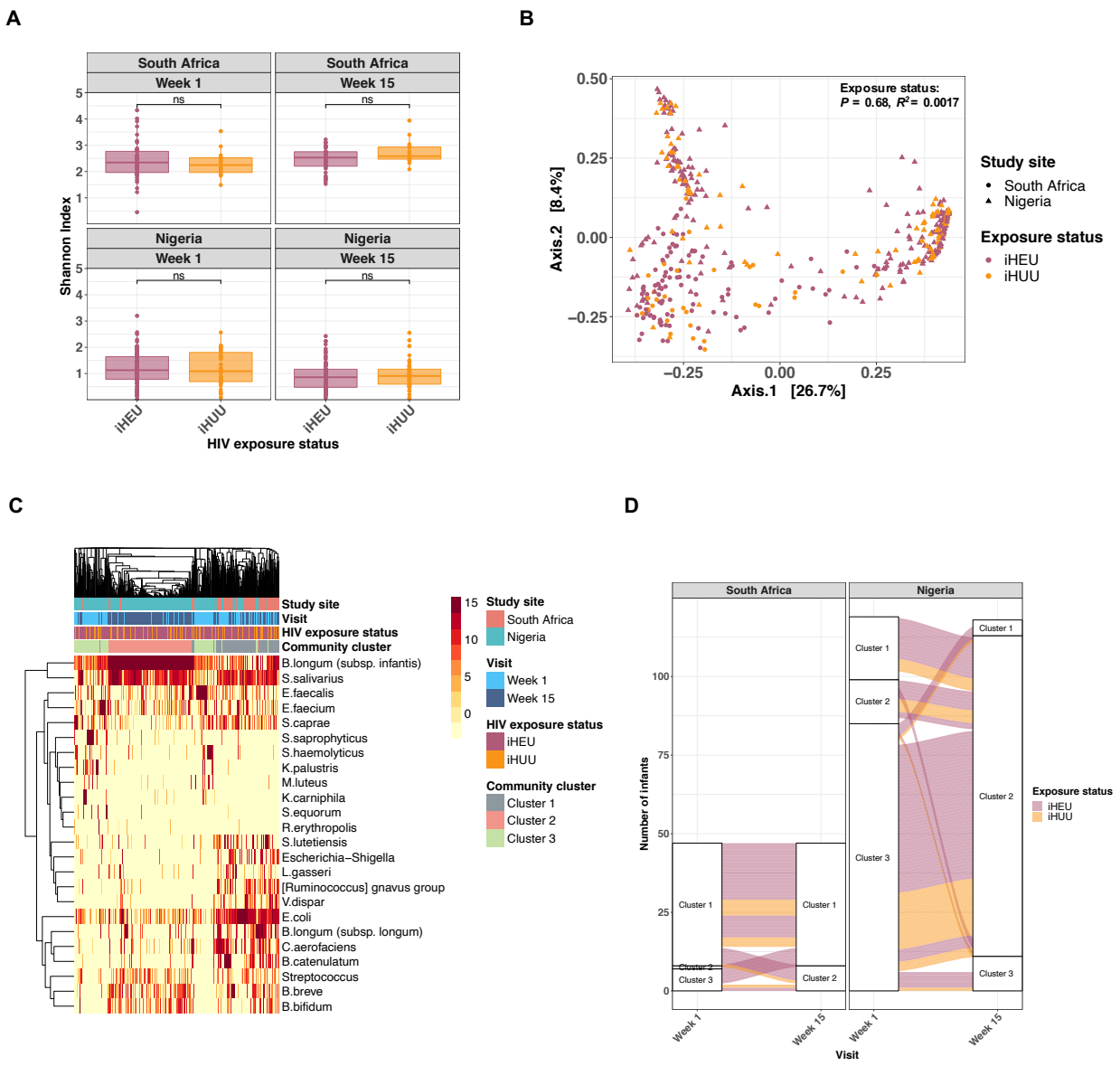

Figure 3.7. HIV exposure has a subtle effect on gut microbiota across two African countries. (A) Comparison of α-diversity (Shannon index) between iHEU (n = 202) and iHUU (n = 76) at each time point by study sites. (B) PCoA and PERMANOVA (Bray-Curtis dissimilarity) of gut microbiota at 1 week and 15 weeks of age, colored by HIV exposure status (iHEU, n = 202; iHUU, n = 76) and shaped by the study site. (C) Heatmap of the top 25 taxa in the gut microbiota of South African (n = 82) and Nigerian (n = 196) infants at 1 week and 15 weeks of age. Study site, study visit, HIV exposure status, and community cluster types (based on PAM clustering; $k = 3$) are annotated. Different ASV IDs with identical bacterial taxa are merged. (D) Alluvial plot showing the transition of cluster groups from week 1 to week 15 at each study site (South African, n = 82; Nigerian, n = 196). Samples are grouped by PAM clustering ($k = 3$). HIV exposure status is indicated by color. Abbreviations: iHEU, infants who are HIV-exposed uninfected; iHUU, infants who are HIV-unexposed uninfected; PCoA, principal coordinate analysis; PERMANOVA, permutational multivariate analysis of variance; PAM, partitioning around medoids; ASVs, amplicon sequence variants. ns, not significant.

Differential abundance testing using ANCOM-BC was performed, adjusting for feeding mode at week 15 [446]. Several bacterial taxa were significantly associated with HIV exposure status in South Africa (**Table 3.3**). Several *Enterococcus* species were significantly more abundant in iHEU than iHUU at week 1 (*E. faecium*; Log_e fold change (LFC): 0.57) and week 15 (*E. faecalis*, *E. gilvus,* and *E. raffinosus*; LFC: 0.61, 1.02, and 0.76, respectively). Moreover, *Collinsella aerofaciens* (LFC: 0.72 at week 1 and 1.18 at week 15) and *Klebsiella quasipneumoniae* (LFC: 0.84 at both week 1 and week 15), which are known to be pathobionts [449,450], were consistently more abundant in iHEU during the first 15 weeks of life. In contrast, no bacterial taxa were differentially abundant by HIV exposure in the Nigerian cohort.

Table 3.3. ANCOM-BC analysis of iHEU and iHUU living in South Africa.

Taxonomy (Genus, Species)	Taxon ID	LFC[a]
At 1 week of age		
Klebsiella variicola	ASV46	1.22
Sutterella (unclassified)	ASV150	1.02
Holdemanella (unclassified)	ASV53	1.00
Parabacteroides merdae	ASV101	0.98
Catenibacterium (unclassified)	ASV218	0.96
Blautia obeum	ASV59	0.93
Senegalimassilia (unclassified)	ASV145	0.87
Bifidobacterium breve	ASV10	0.84
Klebsiella quasipneumoniae	ASV36	0.84
Libanicoccus (unclassified)	ASV153	0.81
Blautia (unclassified)	ASV225	0.80
Ruminococcus torques group (unclassified)	ASV75	0.72
Collinsella aerofaciens	ASV25	0.72
Subdoligranulum (unclassified)	ASV251	0.70
Bacteroides vulgatus	ASV83	0.70
Sutterella (unclassified)	ASV496	0.67
Klebsiella pneumoniae	ASV39	0.66
Megamonas (unclassified)	ASV169	0.65
Romboutsia ilealis	ASV93	0.64
Senegalimassilia (unclassified)	ASV171	0.64
Faecalibacterium (unclassified)	ASV505	0.58
Fusobacterium mortiferum	ASV278	0.57
Enterococcus faecium	ASV7	0.57
Parabacteroides distasonis	ASV138	0.54
Actinomyces (unclassified)	ASV668	-0.54
Parabacteroides distasonis	ASV203	-0.57

At 15 weeks of age		
Streptococcus gallolyticus	ASV44	1.33
Collinsella aerofaciens	ASV25	1.18
Clostridium innocuum group (unclassified)	ASV336	1.13
Enterococcus gilvus	ASV157	1.02
Klebsiella quasipneumoniae	ASV42	0.84
Veillonella atypica	ASV163	0.83
Enterococcus raffinosus	ASV338	0.76
Enterococcus (unclassified)	ASV40	0.71
Bifidobacterium adolescentis	ASV296	0.71
Enterococcus raffinosus	ASV51	0.71
Lactococcus lactis	ASV206	0.66
Enterococcus faecalis	ASV5	0.61
Granulicatella (unclassified)	ASV681	0.59
Dorea formicigenerans	ASV229	0.59
Faecalibacterium prausnitzii	ASV103	0.52
Staphylococcus (unclassified)	ASV41	0.51
Lactobacillus rhamnosus	ASV191	-0.51
Klebsiella michiganensis	ASV266	-0.51
Lactobacillus gasseri	ASV161	-0.53
Prevotella copri	ASV405	-0.55
Megasphaera elsdenii	ASV167	-0.58
Olsenella (unclassified)	ASV97	-0.58
Prevotella (unclassified)	ASV176	-0.83
Bacteroides caccae	ASV552	-0.93
Olsenella (unclassified)	ASV120	-1.89
Ruminococcus torques group (unclassified)	ASV75	-2.43

Differentially abundant ASVs (adj $P < 0.05$) among iHEU relative to iHUU at 1 week or 15 weeks of age in South Africa (n = 82). Data at week 15 were adjusted by mode of feeding. Positive LFC values indicate higher abundance among iHEU, whereas negative LFC values indicate higher abundance among iHUU. [a]Abundance in iHEU in relation to iHUU. Abbreviations: ANCOM-BC, Analysis of Compositions of Microbiomes with Bias Correction; LFC, Log_e fold change; ASV, amplicon sequence variant; iHEU, infants who are HIV-exposed uninfected; iHUU, infants who are HIV-unexposed uninfected.

To attempt to disentangle the effects of co-trimoxazole and HIV exposure on infant gut microbiota, we assessed the gut microbiota based on reported co-trimoxazole prophylaxis history. We did not see any effects of co-trimoxazole on α- and β-diversity among South African iHEU at 15 weeks of age (**Figure 3.8**).

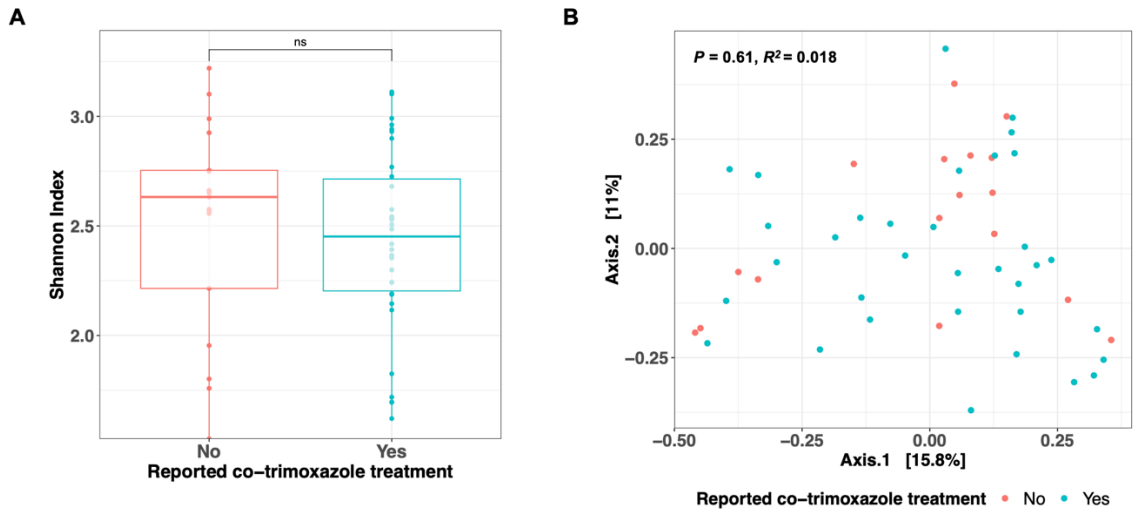

Figure 3.8. The effect of α- and β-diversity of co-trimoxazole on gut microbiota is marginal. (A) Comparison of α-diversity (Shannon index) based on record of reported co-trimoxazole treatment among South African iHEU at 15 weeks of age (n = 51). (B) PCoA and PERMANOVA (Bray-Curtis dissimilarity) of gut microbiota among South African iHEU at 15 weeks of age (n = 51), coloured reported co-trimoxazole treatment history. PCoA, principal coordinate analysis; PERMANOVA, permutational multivariate analysis of variance.

We further explored whether co-trimoxazole partially contributed to the differentially enriched bacterial taxa that were identified in South African iHEU. When adjusting the ANCOM-BC for reported co-trimoxazole prophylaxis, several bacterial taxa were no longer enriched in iHEU (**Table 3.4**), including *Enterococcus* species (*E. faecalis* and unclassified species), *Veillonella atypica*, and *Staphylococcus* (unclassified species).

Table 3.4. ANCOM-BC analysis of iHEU and iHUU living in South Africa at 15 weeks of age, adjusted for mode of feeding and reported antibiotic history.

Taxonomy (Genus, Species)	Taxon ID	LFC[a]
At 15 weeks of age		
Collinsella aerofaciens	ASV25	1.15
Klebsiella quasipneumoniae	ASV42	1.13
Bifidobacterium adolescentis	ASV296	1.08
Streptococcus gallolyticus	ASV44	1.08
Enterococcus gilvus	ASV157	1.07
Lactococcus lactis	ASV206	1.01
Enterococcus raffinosus	ASV51	0.98
Clostridium innocuum group (unclassified)	ASV336	0.93
Enterococcus raffinosus	ASV338	0.89
Dorea formicigenerans	ASV229	0.82
Corynebacterium propinquum	ASV479	0.73
Faecalibacterium prausnitzii	ASV103	0.61
Leuconostoc lactis	ASV324	0.60
Granulicatella (unclassified)	ASV681	0.56
Rothia mucilaginosa	ASV264	0.52
Streptococcus salivarius	ASV104	0.50
Streptococcus peroris	ASV250	0.50
Lactobacillus vaginalis	ASV170	-0.51
Lactobacillus fermentum	ASV141	-0.52
Parabacteroides distasonis	ASV216	-0.52
Lactobacillus rhamnosus	ASV191	-0.55
Veillonella (unclassified)	ASV258	-0.55
Enterococcus gilvus	ASV472	-0.65
Megasphaera elsdenii	ASV167	-0.70
Olsenella (unclassified)	ASV97	-0.73
Senegalimassilia (unclassified)	ASV171	-0.75
Klebsiella michiganensis	ASV266	-0.81
Bacteroides caccae	ASV552	-0.82
Prevotella (unclassified)	ASV176	-0.93
Veillonella parvula	ASV503	-0.95
Olsenella (unclassified)	ASV120	-2.07
Ruminococcus torques group (unclassified)	ASV75	-2.37

Differentially abundant ASVs (adj $P < 0.05$) among iHEU relative to iHUU at the first week or 15 weeks of age in South Africa (n = 82). Data at week 15 were adjusted by mode of feeding and reported antibiotics history. Positive LFC values indicate higher abundance among iHEU, whereas negative LFC values indicate higher abundance among iHUU. [a]Abundance in iHEU in relation to iHUU. ANCOM-BC: Analysis of Compositions of Microbiomes with Bias Correction; LFC, loge fold change; ASV, amplicon sequence variants; iHEU, infants who are HIV-exposed uninfected; iHUU, infants who are HIV-unexposed uninfected.

3.4.5. Maternal HIV status and infant gut microbes are associated with infant TT vaccine response

In Nigeria, it is recommended that pregnant women receive TT booster vaccinations, whereas this policy was only introduced in 2020 in the Western Cape, South Africa, and was therefore not in effect during the study period: September 2013 and November 2017 [451]. Therefore, not surprisingly, infant anti-tetanus titers in the first week of life, representing maternally transferred antibodies, were significantly lower among South African infants than Nigerian infants (median 1.0 [IQR: 0.55-2.2] vs. 1.5 [IQR: 0.9-4.1] IU/ml, adj $P = 0.002$; **Figure 3.9A**). In contrast, titers did not differ between South African and Nigerian infants at 15 weeks of age (median 1.9 [IQR: 0.65-2.5] vs. 1.6 [IQR: 1.0-3.9] IU/ml, adj $P = 0.280$). We investigated the correlation of TT vaccine response between mother and infant pairs living in Nigeria. Anti-tetanus titers were strongly correlated at week 1. However, iHEU mother-infant anti-tetanus titers showed a lower Pearson's correlation coefficient compared to iHUU (R: 0.72 ($P < 0.001$) vs. 0.95 ($P < 0.001$)) (**Figure 3.9B**). The correlation between maternal and infant anti-tetanus IgG titers was no longer evident by 15 weeks of age in either iHEU or iHUU (**Figure 3.9C**). We did not see any difference in anti-tetanus titers among Nigerian mothers by their HIV status (**Figure 3.9D**). However, iHEU had significantly lower anti-tetanus IgG concentrations than iHUU at 15 weeks of life ($P = 0.016$), and this remained significant after adjusting for multiple comparisons (adj $P = 0.031$; **Figure 3.9E**). However, the difference between iHEU and iHUU at week 15 was no longer statistically significant when infants were compared separately by study site (adj $P = 0.290$ in South Africa and adj $P = 0.180$ in Nigeria**; Figure 3.9F**). Further investigation on the health status of mothers with HIV (CD4 count, HIV viral load and ART treatment status) and its correlation with impaired passive maternal antibody transfer to their infants did not uncover specific contributing factors (**Figure 3.10**).

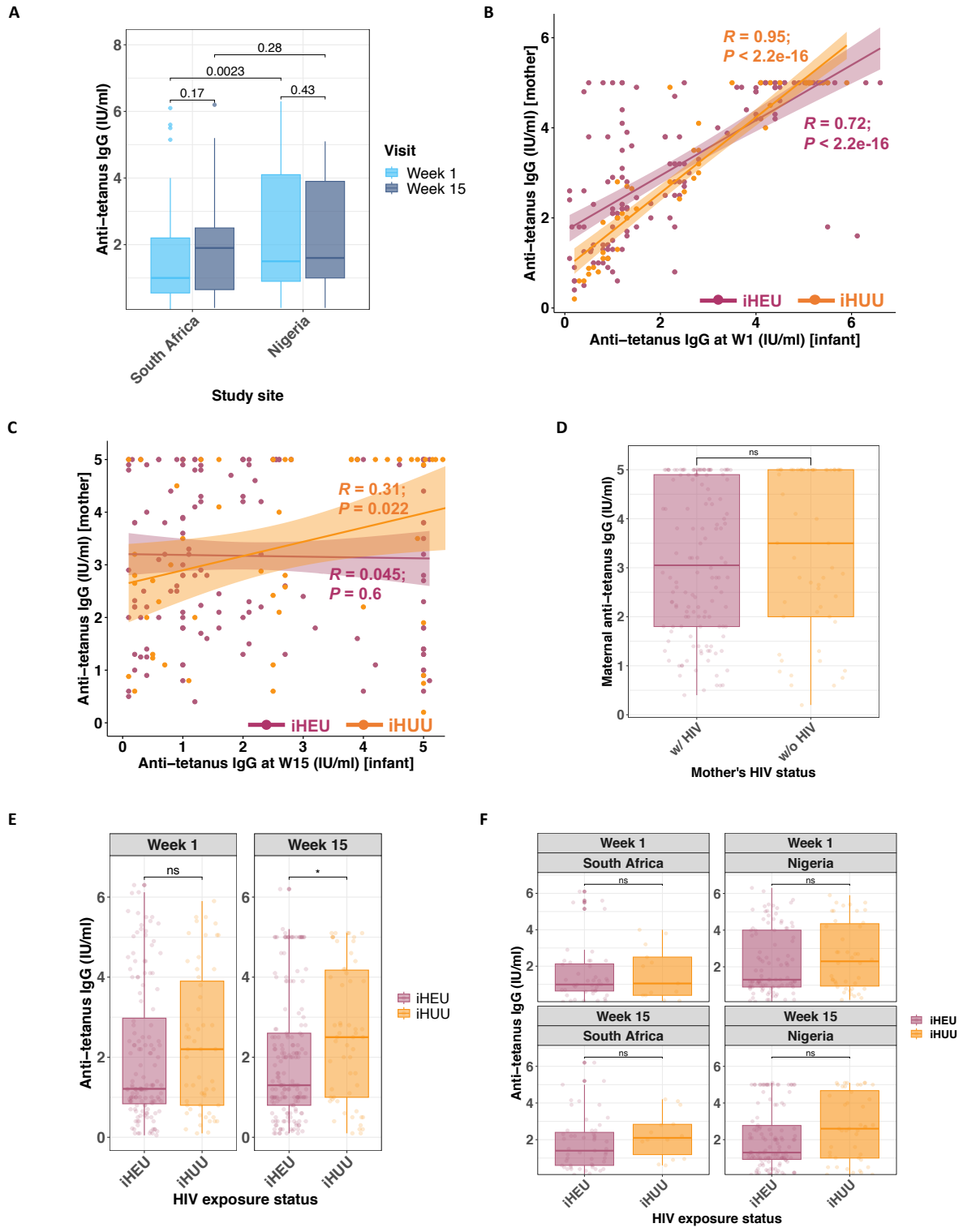

Figure 3.9. Passive maternal antibody and HIV exposure are both associated with infant TT vaccine response. (A) Comparison of infant anti-tetanus titers (IU/ml) between week 1 and week 15 in South Africa (n = 77) and Nigeria (n = 192). (B) Scatter plot and Spearman's rank correlation coefficients (R) of anti-tetanus IgG titers (IU/ml) between Nigerian mothers (y-axis; n = 191) and their infants at week 1 (x-axis; n = 191). Dots and lines of best fit are colored by HIV exposure status. (C) Scatter plots and Spearman's

rank correlation coefficients (R) of anti-tetanus IgG titers between Nigerian mothers (y-axis; n = 191) and their infants at week 15 (x-axis; n = 191). Dots and lines of best fit were colored by HIV exposure status. (D) Box plot comparing maternal anti-tetanus IgG titers by HIV status (HIV positive, n = 138; HIV negative, n = 53). (E) Comparison of anti-tetanus titers between iHEU (n = 197) and iHUU (n = 72) at week 1 and week 15. *P*-values comparing anti-tetanus IgG titres were adjusted for multiple comparisons using the Benjamini-Hochberg method. (F) Comparison of anti-tetanus IgG titers between iHEU (n = 197) and iHUU (n = 72) at each time point by study sites. *P*-values comparing anti-tetanus IgG titers were adjusted for multiple comparisons using the Benjamini-Hochberg method. Abbreviations: W1, 1 week of age; W15, 15 weeks of age; iHEU, infants who are HIV-exposed uninfected; iHUU, infants who are HIV-unexposed uninfected; TT, tetanus toxoid; ns, not significant; w/, with; w/o, without. * $P < 0.05$.

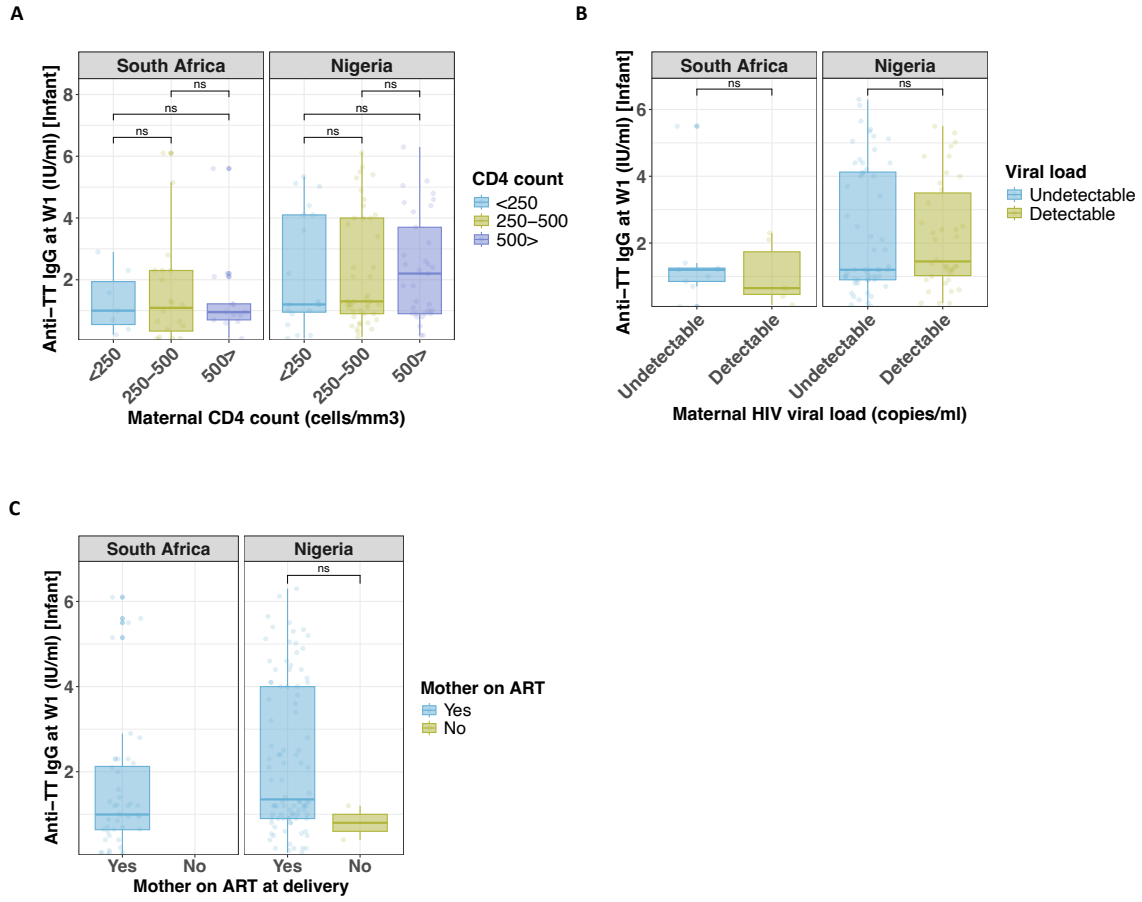

Figure 3.10. Maternal health status and passive maternal antibody transfer among iHEU. (A) Comparison of anti-tetanus IgG titers of iHEU (n = 136) at week 1 and maternal CD4 count (cells/mm^3) at enrollment. Maternal CD4 count was categorized into below 250 cells/mm^3 (South African, n = 7; Nigerian, n = 19), between 250-500 cells/mm^3 (South African, n = 20; Nigerian, n = 44), and more than 500 cells/mm^3 (South African, n = 13; Nigerian, n = 33). (B) Comparison of anti-tetanus IgG titers of iHEU (n = 109) at week 1 and maternal HIV viral load (copies/ml) at enrollment. Maternal HIV viral load was categorized into undetectable level with < 20 copies/ml (South African, n = 9; Nigerian, n = 56) and detectable level (South African, n = 6; Nigerian, n = 38). (C) Comparison of anti-tetanus IgG titers of iHEU (n = 140) at week 1 and maternal antiretroviral therapy status. Samples were categorized into wither mothers were on ART at delivery (South African, n = 44; Nigerian, n = 94) or not on ART at delivery (South African, n = 0; Nigerian, n = 2).

Since gut microbiota is thought to modulate the development of the immune system [430], we intended to investigate the relationship between infant gut microbiota and TT vaccine response at week 15, a week after infants receive their primary TT series. We did not see consistent correlations between 15-week anti-tetanus IgG titers and Shannon diversity at 1 or 15 weeks (**Figure 3.11A**). To further explore factors associated with infant TT vaccine response at week 15, we conducted a LASSO regression. Rank-transformed top 50 ASVs at either week 1 or week 15, HIV exposure status, and anti-tetanus IgG titers at week 1 were included as explanatory variables to investigate the predictor, TT vaccine response at 15 weeks of age. In South Africa, infant HIV exposure status showed a strong negative association with 15-week TT vaccine response (β-coefficient = -0.44), and the rank-transformed taxon abundance at week 1 of some bacterial species, including *Streptococcus salivarius* (β-coefficient = 0.038), *Bacteroides dorei* (β-coefficient = 0.016), *Collinsella aerofaciens* (β-coefficient = 0.015), and *Sutterella wadsworthensis* (β-coefficient = -0.011) were independently associated with vaccine response, albeit with weaker β-coefficients than HIV-exposure (**Figure 3.11B**; **Appendix D**). In contrast, no variables were selected as predictors of the TT vaccine response in the Nigerian cohort.

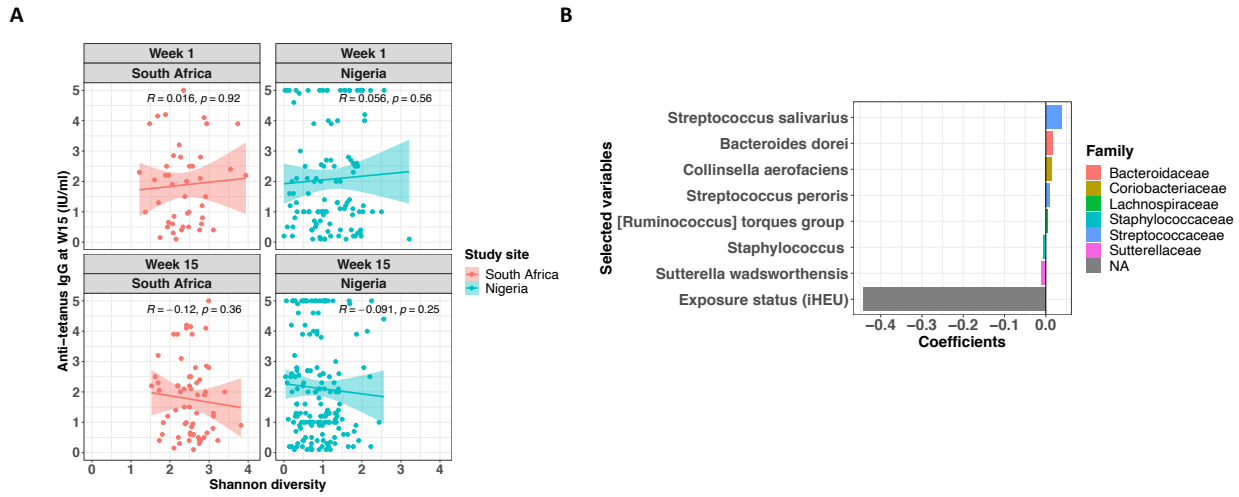

Figure 3.11. HIV exposure status and gut microbiota are independently associated with TT vaccine response. (A) Correlation analysis of infants' anti-tetanus titers (IU/ml) measured at 15 weeks of age and α-diversity (Shannon index) at each study site and visit (South African, n = 65; Nigerian, n = 170). Spearman's rank correlation coefficients (R) are indicated on each panel. (B) Rank-transformed top 50 ASVs (at either week 1 or week 15), HIV exposure status, and anti-tetanus IgG titer data at week 1 were used as explanatory variables for the LASSO regression to assess the association with TT vaccine response at 15 weeks of age. Each model was constructed separately based on geographical location and time point. The optimal coefficient tuning parameter (lambda.min) was chosen using 10-fold cross-validation. Selected variables and their glmnet coefficients were plotted. Color of the bars represents taxonomy at the family level. Week 1 ASVs and HIV exposure status were associated with week 15 TT vaccine response among South African infants. No variables were selected for the Nigerian cohort. Abbreviations: ASVs, amplicon sequence variants; iHEU, infants who are HIV-exposed uninfected; LASSO, Least Absolute Shrinkage and Selection Operator; TT, tetanus toxoid; W15, 15 weeks of age.

Previously, it has been shown that passively transferred maternal antibody interferes with infant TT vaccination response [452]. Since Nigerian infants showed significantly higher maternal antibodies than South African infants at week 1 (**Figure 3.9A**), we speculated that these maternal tetanus antibodies may have masked any associations underlying the infant TT vaccine response at week 15 of life. For this reason, we re-assessed the LASSO regression without including week 1 anti-tetanus IgG data in the explanatory variables (**Figure 3.12**; **Appendix E**). Although there was no change in the result for the South African infants (**Figure 3.12A**), HIV exposure and several bacteria present at 15 weeks of age, including *S. salivarius*, were independently associated with the TT vaccine response in Nigerian infants (**Figure 3.12B**). However, the β-coefficients for all selected predictors were small, including HIV exposure status.

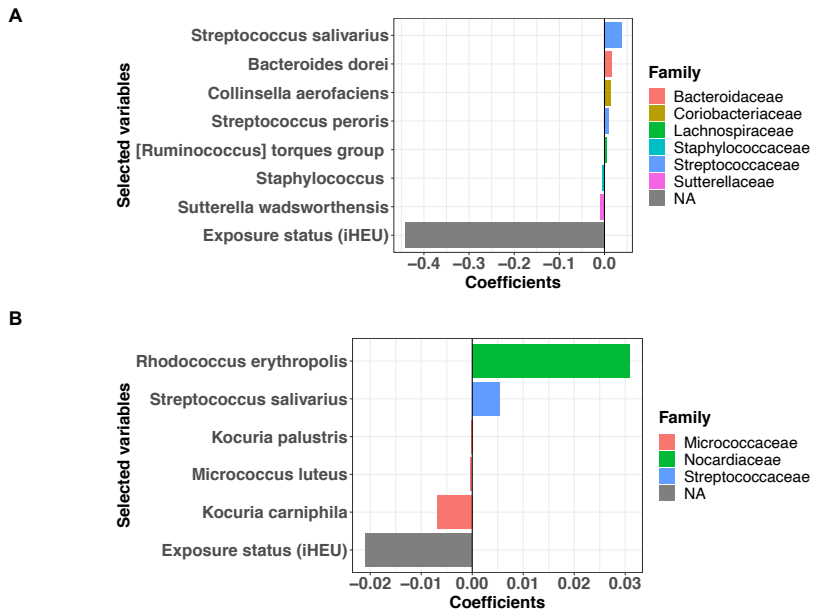

Figure 3.12. Maternal antibodies may mask the effect of HIV exposure and microbiota on infant vaccine response. Rank-transformed top 50 ASVs (at either week 1 or week 15) and HIV exposure status were used as explanatory variables for the LASSO regression to assess the association with TT vaccine response at 15 weeks of age. To explore the masking effect of passively transferred maternal antibodies on the regression model, anti-tetanus IgG at week 1 data were not included in the model. Each model was constructed separately based on geographical location and time point. The optimal coefficient tuning parameter (lambda.min) was chosen using 10-fold cross-validation. Selected variables and their glmnet coefficients were plotted. Color of the bars represents taxonomy at the family level. Week 1 ASVs and HIV exposure were associated with week 15 TT vaccine response among South African infants (A), and week 15 ASVs and HIV exposure were associated with the vaccine response among Nigerian infants (B). Abbreviations: ASVs, amplicon sequence variants; iHEU, infants who are HIV-exposed uninfected; LASSO, Least Absolute Shrinkage and Selection Operator; TT, tetanus toxoid.

3.5. Discussion

This is one of the largest studies that longitudinally compared the gut microbiota between iHEU and iHUU in two settings and investigated the association with their vaccine responses. Our findings suggest that the country of origin was the most influential factor in the infants' gut microbiota at week 1, which also strongly affected its succession over the first 15 weeks of life. Both feeding and delivery modes have been shown to influence infant gut microbiota [453]. Since these demographic characteristics significantly differed between our South African and Nigerian cohorts, we explored their potential effects on the infant gut microbiota. A comparison restricted to infants still EBF at 15 weeks showed that α- and β-diversity at that time point remained

significantly different between the countries. Similarly, the difference was independent of mode of delivery. Analysis of stool samples collected shortly after birth suggested that the difference in gut microbiota profile was already prominent before feeding was established. Collectively, these data indicate that geographical location strongly influences the initial seeding of gut microbes, and this affects the trajectory of microbiota regardless of feeding practices [454]. Notably, the term "geography" includes not only the physical location (rural vs. urban) but also extends to socioeconomics, genetics, diet, climate, and ethnicity, among others [210,454].

Microbiota among Nigerian infants transitioned drastically over the first 15 weeks of life, such that at 15 weeks, *B. infantis* was the dominant taxon, with some *S. salivarius*. Both are commonly found in breast milk and gut microbiota among breastfed infants [455]. *Bifidobacteria* benefit human health and are often used as probiotics [456]. Moreover, *Streptococcus salivarius*, classified as a lactic acid bacterium (LAB), has been shown to have probiotic properties [457]. However, the drastic changes in microbiota over the 15 weeks occurred mostly among the Nigerian infants and far less in the South African infants. Plausible explanations for this may be the difference in profiles of maternal gut and breastmilk microbiota and human milk oligosaccharides (HMOs) influenced by genetics, ethnicity, diet, and body mass index (BMI) [458]. For instance, a higher maternal BMI is associated with reduced *Bifidobacterium* in breastmilk [459], which might suggest that South African mothers, who had higher mean weight, had less *Bifidobacterium* in their breastmilk than Nigerian mothers, leading to less *Bifidobacterium* in their infants' gut. An additional explanation is that Nigerian mothers in this setting have a diet rich in fermented foods, whereas South African mothers may have a more Westernized diet [460,461]. South African infants also had higher relative abundance of *B. longum* but lower relative abundance of *B. infantis* at baseline.

Nigerian infants had significantly higher anti-tetanus titers at week 1, likely due to maternal immunization and consequent high passive maternal antibody transfer compared to South African infants [462]. In contrast, in the Western Cape region where our South African cohort was recruited, there was no routine TT booster vaccination for pregnant women due to the prolonged absence of neonatal tetanus cases in the province [451]. Notably, anti-tetanus IgG levels post-vaccination among Nigerian infants remained similar to those at week 1 and were comparable with South

African infants. This inferior induction of anti-tetanus titers observed in Nigerian infants may be explained by the inhibition of TT vaccine response by passively transferred high maternal antibodies, as previously described [452].

We identified several bacterial taxa that exhibited differential abundance in iHEU compared to iHUU, including several pathobionts. Whether these identified bacterial taxa contribute to increased risk of infectious morbidity in iHEU is unknown. Moreover, several bacterial enrichments in iHEU may, in part, be attributed to co-trimoxazole prophylaxis recommended for this population. For example, *E. faecalis* is frequently co-trimoxazole resistant [463]. Supporting this, our differential abundance analysis showed that the enrichment of *E. faecalis* was no longer evident in 15-week-old iHEU after adjusting for reported co-trimoxazole prophylaxis use. Of note, there was a significant difference in reported co-trimoxazole use among iHEU between the countries in our study. Since the record of co-trimoxazole treatment was sorely relied on mothers' recall at each follow-up visit, it is possible that the accuracy of reported antibiotics records among iHEU may be underestimated.

LASSO regression models also suggested that *in utero* HIV exposure and relative abundance of several bacterial taxa at week 1 were independently associated with later TT vaccine response in South Africa, but not Nigeria. The higher passive antibody levels observed in Nigerian infants may have mitigated the effects of HIV exposure and microbiota on the infant vaccine response. In fact, excluding the week 1 titer data from the regression model indicated that the HIV exposure and several microbes found at 15 weeks of age were independently associated with the infant TT vaccine response among Nigerian infants. In line with our assumption, removing week 1 titer data from the regression model did not change the LASSO regression result in South African infants, who showed much lower passive maternal antibody transfer. Interestingly, *S. salivarius* relative abundance was predictive of improved anti-tetanus titers in both cohorts. Since the microbiota at week 1 among South African infants was associated with TT vaccine response at week 15, this suggests that in some settings, vaccine responses could potentially be modified using an early-life microbiota intervention where maternal vaccination is not possible.

There are several limitations in our study. Firstly, we did not have comprehensive records of maternal lifestyle and dietary information, which are known to have an impact on gut microbiota composition. In addition, co-trimoxazole adherence among iHEU was not extensively captured. All iHEU received nevirapine post-exposure prophylaxis, therefore the effects of HIV exposure versus antiretroviral exposure cannot be disentangled. Lastly, additional data, both maternal (such as vaginal and breastmilk microbiota) and infant (such as gut metabolomics, metatranscriptomics, and metagenomics), could have provided more insights into our study.

In summary, this study showed that the transition of infant gut microbiota was strongly dependent on geographical location and age, while the effect of *in utero* HIV exposure was modest. However, maternal HIV status was negatively associated with the passive maternal anti-tetanus antibody transfer, and the negative effect of HIV exposure on TT vaccine response persisted over the first 15 weeks of life among iHEU. In addition, there were independent associations of specific gut microbes and HIV exposure with infant humoral response to TT vaccine at 15 weeks of age.

3.6. Contribution, acknowledgments and financial support

Contribution: Saori C. Iwase, Investigation (DNA extraction and 16S rRNA gene sequencing), Data curation, Formal analysis, Visualization, Writing – original draft | Sophia Osawe, Investigation (acquisition of anti-tetanus IgG data), Data curation, Writing – review and editing | Anna-Ursula Happel, Data curation, Formal analysis, Supervision, Writing – review and editing | Clive M. Gray, Conceptualization, Writing – review and editing | Susan P. Holmes, Methodology, Supervision, Writing – review and editing | Jonathan M. Blackburn, Conceptualization, Writing – review and editing | Alash'le Abimiku, Conceptualization, Funding acquisition, Supervision, Writing – review and editing. Heather B. Jaspan, Conceptualization, Formal analysis, Investigation, Supervision, Writing – review and editing. All authors approved the final manuscript.

Acknowledgments: We would like to thank the mothers and infants who participated in this study, the clinic staff at the Plateau State Specialist Hospital, Jos, Nigeria, and the Khayelitsha Site B Clinic in Cape Town, South Africa, and the InFANT study lab technologists. We also would like to thank Western Cape Department of Health (DOH) for use of their space and an infrastructure

award from the University of Washington/Fred Hutch Center for AIDS Research, National Institutes of Health (NIH)-funded program under award number AI027757 which is supported by the following NIH Institutes and Centers: National Institute of Allergies and Infectious Disease (NIAID), National Cancer Institute (NCI), National Institute of Mental Health (NIMH), National Institute on Drug Abuse (NIDA), National Institute of Child Health and Human Development (NICHD), National Heart, Lung, and Blood Institute (NHLBI), National Intelligence Authority (NIA), National Institute of General Medical Sciences (NIGMS), and National Institute of Diabetes and Digestive and Kidney Diseases (NIDDK).

Financial support: This work was funded by the Canadian Institutes of Health Research (CIHR) (01044000 awarded to C.M.G.) and the NICHD, and the National Human Genome Research Institute (NHGRI) (U01HD094658 to A.A.). S.C.I. was funded by the Yoshida Scholarship Foundation.

Chapter 4. Optimization of an epigenetic assay to investigate histone modifications in ultra-low cell input infant innate immune cells

4.1. Abstract

Background: Beyond its primary protection, Bacillus Calmette-Guérin (BCG) vaccination offers non-specific protection thought to be mediated via trained innate immunity, which is facilitated through histone modifications. Infants who are HIV-exposed but uninfected (iHEU) are at higher risk of infectious morbidity than infants who are HIV-unexposed and uninfected (iHUU). However, thus far, no studies have investigated the effects of *in utero* HIV exposure on trained innate immunity. The gold standard to investigate histone modifications requires more peripheral mononuclear cells (PBMCs) than feasibly obtained from infant samples. To establish a workflow for a future ongoing study assessing trained immunity induced by BCG amongst iHEU and iHUU, optimization of Cleavage Under Targets and Tagmentation (CUT&Tag) and downstream analysis were conducted.

Methods: CUT&Tag was optimized using monocytes and natural killer (NK) cells isolated from PBMCs by fluorescence-activated cell sorting (FACS). An antibody targeting trimethylation of histone 3 at lysine 27 (H3K27me3) was used as an assay control. The optimized assay using antibodies targeting H3K27me3, trimethylation of histone 3 at lysine 4 (H3K4me3), acetylation of histone 3 at lysine 27 (H3K27Ac), and IgG (negative control) were applied to 14 infant PBMC samples. Libraries were sequenced on the Illumina NextSeq platform. Peak calling was performed using Model-based Analysis for ChIP-Seq 2 (MACS2) and Sparse Enrichment Analysis for CUT&RUN (SEACR). Peak distribution, differential binding analysis, and pathway enrichment analysis were performed using Bioconductor packages.

Results: Optimal cell numbers, polymerase chain reaction (PCR) cycles, and sequencing depth to apply CUT&Tag to infant samples were determined. Libraries showed nucleosome ladder patterns, indicating a successful assay. Using SEACR with a numeric threshold was the most suited approach for peak calling. CUT&Tag data clustered by cell type and histone marker, thus validating the success of the assay. As another means of validation, pathway enrichment analysis

on differentially bound sites between monocytes and NK cells was conducted and showed that these were in line with their cellular functions.

Conclusions: The CUT&Tag protocol was optimized successfully and showed its capability of identifying multiple histone modifications using ultra-low infant cell numbers, supporting the application for future studies on the effect of *in utero* HIV exposure on BCG-induced trained immunity.

4.2. Introduction

Bacillus Calmette-Guérin (BCG) is a live-attenuated vaccine against tuberculosis (TB) infection and disease. It is routinely administered to neonates, especially in countries with high TB burdens. Emerging research indicates that beyond its specific effects, BCG may offer non-specific enhancement of protection against other infections, thereby contributing to reduced mortality rates [188]. This non-specific protection is thought to be facilitated by "trained innate immunity" [464,465].

Histone modifications involve adding or removing chemical groups on histone tails, exerting a profound influence on chromatin structure and thereby regulating gene transcription. In the context of trained innate immunity, a number of reports have highlighted the involvement of histone modifications in the upregulation of immune gene transcription, such as pro-inflammatory cytokines (e.g., interleukin-1 beta [IL-1β], interferon-gamma [IFN-γ], and tumor necrosis factor-alpha [TNF-α]) [464]. Additionally, BCG-induced trained innate immunity was correlated with increased nucleotide-binding oligomerization domain 2 (NOD2) signaling and trimethylation of histone H3 at lysine 4 (H3K4me3) marks in circulating monocytes [464]. In addition, the histone modifications monomethylation of histone H3 at lysine 4 (H3K4me1), H3K4me3, and acetylation of histone H3 at lysine 27 (H3K27Ac) have been observed in β-glucan-trained macrophages [185,466]. On the other hand, while some reports have indicated the role of deoxyribonucleic acid (DNA) methylation in the development of "memory-like" natural killer (NK) cells [467,468], the involvement of histone modifications in NK cells remains significantly understudied.

To our knowledge, only one study has examined whether epigenetic changes occur after BCG vaccination in infants [188]. This study, which recruited infants who were HIV-unexposed uninfected (iHUU) living in Uganda, found BCG vaccination given on the first day of life was associated with changes in H3K4me3 and trimethylation of histone H3 at lysine 9 (H3K9me3) at the TNF promoter region in peripheral blood mononuclear cells (PBMCs), albeit in a different manner than that of adults [464]. These epigenetic changes were associated with lower physician-diagnosed infection episodes in the first six months of life. Of note, there were no infants who were HIV-exposed and uninfected (iHEU) included in this study [188]. All other studies on trained innate immunity have been conducted in adults, or those in children have only explored cytokine

responses [185, 193, 199, 201, 203,469–471], and none has included iHEU. Therefore, BCG-induced epigenetic changes among iHEU are thus far unexplored. Given that iHEU exhibit altered immune activation and responses to BCG vaccination [389, 401,472], verifying whether BCG induces epigenetic changes in iHEU, and thus potentially also confers equal non-specific protective effects as in iHUU, is highly important. Moreover, identifying pathways to optimize BCG vaccine-induced non-specific immunological benefits in iHEU could reduce the disparity in all-cause infectious morbidity risk between iHEU and iHUU [415,425].

The most common method to investigate histone modifications associated with trained innate immunity is chromatin immunoprecipitation and sequencing (ChIP-seq). However, this technique often requires at least 1 million input cells per antibody [117], while blood draws from young infants are typically < 3 ml. Further, ChIP-seq needs > 20 million reads for narrow histone marks (such as H3K27Ac and H3K4me3) and > 40 million reads for broad histone markers (such as H3K27me3) to be able to differentiate true signals from background noise [473,474]. These factors pose a challenge, especially when investigating epigenetic modifications using infant samples, as cell yield from small-volume specimens is often limited [182]. For this reason, we optimized Cleavage Under Targets and Tagmentation (CUT&Tag) [120,121] as an alternative approach. CUT&Tag is a recently described cutting-edge technique for investigating histone modifications. This approach involves immobilizing cells onto concanavalin A (ConA) conjugated paramagnetic beads and utilizing a fusion complex of protein A (pA) and prokaryotic transposase 5 (Tn5). This pA-Tn5 complex selectively cleaves chromatin regions bound to antibodies and inserts sequencing adapters into the cleaved DNA, allowing for high-throughput polymerase chain reaction (PCR) amplification and sequencing. One of the key strengths of CUT&Tag compared to the traditional ChIP-seq technique is its ability to achieve reliable results with significantly lower cell inputs [120,121], making it more feasible to apply this method to clinical samples with limited cell numbers or rare cell populations.

In this study, we optimized a panel to sort NK and monocyte cell populations, as well as the CUT&Tag protocol. The optimized protocol was then applied to low-input infant samples obtained from ongoing or completed parent studies. Further, downstream data analysis pipelines were optimized.

4.3. Material and methods

4.3.1. Participants

For the initial optimization of the CUT&Tag assay, cryopreserved PBMCs from adult donors were used. Then, the established CUT&Tag protocol was applied to 14 cryopreserved infant PBMCs obtained from parent studies, namely the InFANT and BCG studies. The InFANT study, an ongoing observational study [416,417], involves the recruitment of both iHEU and iHUU who have received BCG vaccination within 72 hours (hrs) of birth as per the standard of care. On the other hand, the BCG study, a randomized trial conducted between June 2010 and December 2011 [475–477], involved the recruitment of iHEU who were randomly assigned to either an early arm, receiving BCG vaccination within 72 hrs after delivery, or a delayed arm, receiving BCG vaccination at 8 weeks of age after confirmation of negative HIV DNA PCR tests. For both studies, participants were enrolled at the Midwife Obstetric Unit at Site B in Khayelitsha, Cape Town, where the antenatal HIV prevalence was 34.3% in 2012 [478]. Each study's inclusion and exclusion criteria are outlined in **Appendix A and F**. Physical examinations were conducted at every visit, and extensive health histories were collected from medical records and maternal interviews. For the purposes of this chapter, samples from six- to seven-week-old infants were used from both studies, which was before BCG vaccination in the delayed arm of the BCG study, which will allow for the comparison of BCG on epigenetic changes. This study was approved by the University of Cape Town's Human Research Ethics Committee (HREC) with HREC REF: 319/2021. Parent studies were also approved by the HREC with reference numbers 285/2012 (InFANT study) and 405/2009 (BCG study). Written informed consent was obtained from the infants' mothers prior to their participation.

Since additional CUT&Tag assays and data analysis are planned for a future study using the samples from the same cohort, the information regarding the allocation of samples (iHEU vs. iHUU and early vs. delayed BCG vaccination) has not been unblinded at the time of dissertation submission. Consequently, the data analysis in this chapter is focused on comparisons between the cell types.

4.3.2. Cell staining

Cryopreserved PBMCs were thawed at 37°C and washed in 10 ml Roswell Park Memorial Institute (RPMI) medium (Sigma Aldrich) supplemented with 10% fetal calf serum (FCS) and Benzonase (Sigma Aldrich; 25 U/µl). Cells were washed again with 10 ml phosphate-buffered saline (PBS), and cell concentration and viability were measured by TC20 Automated Cell Counter (Bio-Rad). Cells were then resuspended in PBS at $2x10^6$ cells/ml. Cells were then aliquoted into a 96-well V-bottom plate (Greiner) at 50 µl per well. Two additional washes with 150 µl PBS followed by centrifugation were performed. Cells were stained in PBS with Staining Panel 1 (**Table 4.1**), containing live/dead dye and Fc block. Cells were incubated in the dark at room temperature (RT) for 20 minutes (mins). Cells were then washed twice with 150 µl fluorescence-activated cell sorting (FACS) buffer (2% FCS in PBS) and stained in FACS buffer with Staining Panel 2 (**Table 4.2**), containing APC-H7-CD3, PE-CD14, APC-CD56, and AF488-CD16. Cells were incubated in the dark at RT for 20 mins, followed by two washes with 150 µl FACS buffer (2% FCS in PBS). Cells were resuspended at a concentration of $1x10^6$ cells/100 µl FACS buffer and transferred to a FACS tube (Falcon).

Table 4.1. Staining Panel 1.

Fluorochrome/ Reagent	Antigen	Marker	Clone/ Lot	Supplier	Volume (µl) in 50 µl
Aqua	Amine	Live/Dead cells	-	Thermofisher	0.2
Fc block	-	-	564219	BD Pharmingen	2
PBS	-	-	-	-	47.8

Table 4.2. Staining Panel 2.

Fluorochrome	Antigen	Marker	Clone	Supplier	Volume (µl) in 50 µl
APC-H7	CD3	T-lymphocytes	SK7	BD Pharmingen	2

PE	CD14	Myelomonocytes lineage	M5E2	BD Pharmingen	15
APC	CD56	NK cells	HCD56	Biolegend	0.3
AF488	CD16	Monocyte subsets	3G8	Biolegend	2
FACS buffer	-	-	-	-	30.7

4.3.3. Cell sorting and gating strategy

Acquisition and cell sorting were performed using FACSAria Fusion Flow Cytometer with a 100-micron nozzle (BD Biosciences). Monocytes and NK cells were sorted using the gating strategy shown in **Figure 4.1**. Data were analyzed using FlowJo (version 10.8.2; FlowJo, LLC).

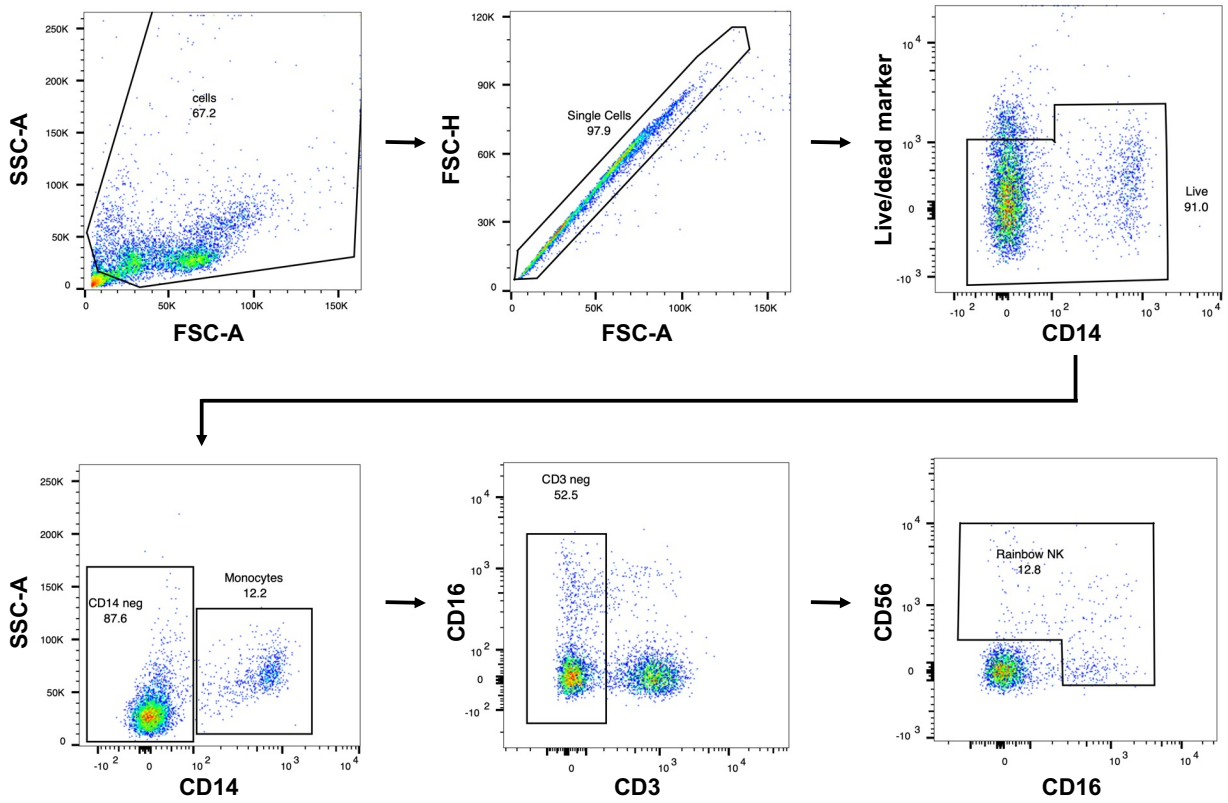

Figure 4.1. Gating strategy for sorting monocytes and NK cells.

4.3.4. CUT&Tag assay workflow

CUT&Tag was performed according to the previously described protocol [121,479] with some modifications (**Figure 4.2**). Briefly, 5 µl ConA beads (Polysciences) were aliquoted into 8-strip PCR tubes (SSIbio) and washed three times with 200 µl binding buffer (20 mM HEPES pH 7.5, 10 mM KCl, 1 mM $CaCl_2$, 1 mM $MnCl_2$). Throughout the assay, ConA-binding cells were mixed by gently flicking the tubes instead of mixing by pipetting to avoid potential sample loss. Sorted monocytes and NK cells were resuspended in wash buffer (20 mM HEPES pH 7.5, 150 mM NaCl, 0.5 mM spermidine, 1xRoche complete EDTA-free protease cocktail), and the desired number of cells was added into the PCR tubes. Additional wash buffer was added to bring the total volume to 200 µl. Samples were placed on a nutator (Nutating Mixers, Fisherbrand) and incubated for 10 mins at RT at 12 rpm. This step facilitates the ConA bead binding to the mannosyl- and glucosyl-containing extracellular glycoproteins on the cell surface.

Samples were then resuspended in 50 µl dig-wash buffer (20 mM HEPES pH 7.5, 150 mM NaCl, 0.5 mM spermidine, 1xRoche complete EDTA-free protease cocktail, 0.05% digitonin), supplemented with 2 mM EDTA and a 1:100 dilution of the primary antibody that targets the histone marker of interest (**Table 4.3**). Samples were incubated for 2 hrs at RT on a nutator at 12 rpm, followed by overnight incubation on a magnetic stand at 4°C.

Table 4.3. Antibodies used for CUT&Tag assay.

Histone Marker	Antibody Target	Catalog No. (Clone/ lot)	Antibody Types	Conc. (mg/ml)	Supplier
H3K27me3	Tri-Methyl-Histone H3 (Lys27)	9733 (C36B11)	Rabbit monoclonal IgG	0.1	Cell Signaling Technology
H3K27Ac	Acetyl-Histone H3 (Lys27)	ab4729 (GR3374555-1)	Rabbit polyclonal IgG	1.0	Abcam
H3K4me3	Tri-Methyl-Histone H4 (Lys4)	C15410003-50 (A8034D)	Rabbit polyclonal IgG	1.3	Diagnostech

IgG	Rabbit IgG (Heavy & Light Chain)	ABIN101961 (NE-200-121900)	Guinea Pig polyclonal IgG	1.21	antibodies online

The following day, the liquid was removed from the tube while the samples were on a magnetic stand. Samples were then resuspended in 50 µl dig-wash buffer containing the secondary antibody at a dilution of 1:100 (guinea pig anti-rabbit IgG; **Table 4.3**), followed by incubation on a nutator at 12 rpm for 45 mins at RT. During this step, the secondary antibody binds to the primary antibody, creating more binding sites for the pA-Tn5 complex.

To remove any unbound antibodies, samples were washed three times with 200 µl dig-wash buffer. Samples were then incubated with 50 µl dig-300 buffer (20 mM HEPES pH 7.5, 300 mM NaCl, 0.5 mM spermidine, 1xRoche complete EDTA-free protease cocktail, 0.01% digitonin), containing pA-Tn5 (Diagenode) at a dilution of 1:250. Samples were incubated for 1 hr at RT on a nutator at 12 rpm, then washed three times with 200 µl dig-300 buffer. Samples were resuspended in 250 µl tagmentation buffer (20 mM HEPES pH 7.5, 300 mM NaCl, 0.5 mM spermidine, 1xRoche complete EDTA-free protease cocktail, 0.01% digitonin, 10 mM $MgCl_2$) and placed in an incubator for 1 hr at 37°C. In this step, the presence of magnesium ions facilitates the Tn5 transposome to cleave nearby DNA by integrating adapters, generating amplifiable sequencing libraries. To stop the tagmentation process and solubilize DNA fragments, 10 µl 0.5 M EDTA, 3 µl 10% SDS, and 2.5 µl 20 mg/ml Proteinase K (Thermofisher) were added to the sample and incubated for 1 hr at 55°C using a thermal cycler (SimpliAmp Thermal Cycler, Thermofisher).

To extract the tagmented DNA, the samples were transferred into microcentrifuge tubes containing 250 µl phenol:chloroform:isoamyl alcohol (PCI; 25:24:1, v/v; Thermofisher). Samples were mixed by vortexing, transferred to phase-lock tubes (Qiagen), and centrifuged for 3 mins at 16,000 g at RT. Then 250 µl chloroform was added to each tube and mixed by inverting 10 times, followed by centrifugation for 3 mins at 16,000 g at RT. The aqueous layer was transferred into a new microcentrifuge tube containing 750 µl 100% ethanol. Samples were centrifuged for 15 mins at 16,000 g at 4°C. The liquid was carefully removed by decanting. Samples were washed with 1 ml 100% ethanol and centrifuged for 1 min at 16,000 g at 4°C. The supernatant was carefully removed

by decanting, and samples were left with the cap open for 5-10 mins at RT to air dry the pellet. Samples were resuspended in 21 µl 0.1x TE buffer (1 mM Tris-HCl, 0.1 mM EDTA, pH 8.0) and mixed with 2 µl each of 10 µM i5 primers i7 primers [480], and 25 µl NEBNext HiFi 2xPCR master mix (New England Biolabs). Samples were amplified by PCR with the following cycling conditions: 72°C for 5 mins (gap filling); 98°C for 30 s; 18 vs. 20 cycles (see section on optimization) of 98°C for 10 s and 63°C for 30 s; 72°C for 1 min (final extension) and hold at 4°C. The resulting libraries were purified with 65 µl (i.e., 1:1.3 ratio) AMPure XP beads (Beckman Counter) for 15 mins, washed with 80% ethanol twice, and eluted in 25 µl EB buffer (10 mM Tris-HCl, pH 8.0). Libraries were quantified by the 4200 TapeStation system using D1000 Screen Tapes (Agilent). Libraries were pooled at equimolar concentrations. For samples with low concentrations, the total volumes were added to the pool, as recommended by the original protocol [479]. CUT&Tag libraries during optimization were sent to Seattle Children's Research Institute, Seattle, USA, and sequenced on an Illumina MiSeq 50-cycle flow cell (pair-end, 25 bp). CUT&Tag libraries derived from infant PBMCs were sent to Northwest Genomics Center, Seattle, USA, and sequenced for pair-end 37 bp on an Illumina NextSeq High Output 75-cycle flow cell.

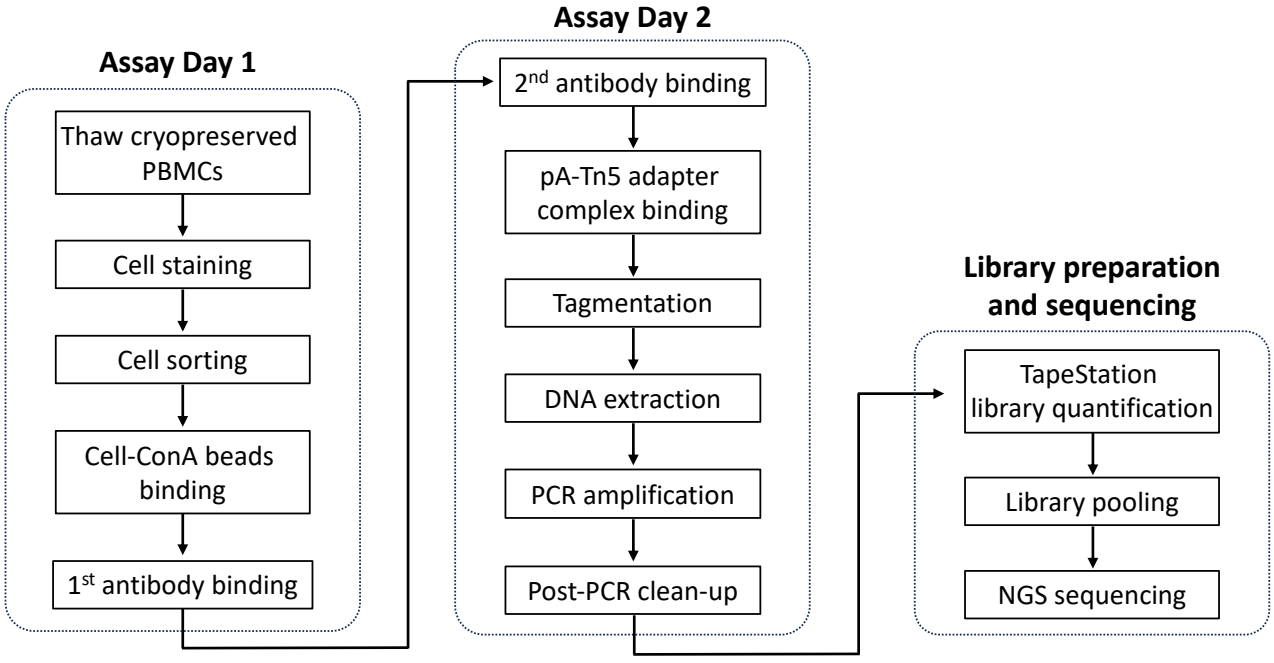

Figure 4.2. CUT&Tag assay flow. Schematic diagram of the CUT&Tag assay protocol. The CUT&Tag procedure spans two consecutive days, followed by library preparation and NGS sequencing. Abbreviations: ConA, concanavalin A conjugated paramagnetic beads; CUT&Tag, Cleavage Under

Targets And Tagmentation; pA-Tn5, fusion protein of protein A and Tn5 transposase; PBMCs, peripheral blood mononuclear cells; PCR, polymerase chain reaction; NGS, next-generation sequencing.

4.3.5. Experiment strategies for handling infant samples with limited cell number

Each histone marker of interest was evaluated using 5,000 monocytes or NK cells isolated from infant PBMCs. When the isolated cell count was insufficient to assess all three histone markers, assays were prioritized according to the rules illustrated in **Appendix G**. Briefly, when the total sorted cell yield was below 15,000, the assessment of histone markers was prioritized in the following order: H3K4me3 > H3K27Ac > H3K27me3. While both H3K4me3 and H3K27Ac are involved in trained innate immunity [185,466], our preliminary data showed that CUT&Tag targeting H3K4me3 tended to yield a higher library concentration than H3K27Ac (data not shown). This could be due to its higher abundance or better antibody performance. As a result, H3K4me3 was selected as the primary marker when cell numbers were limited. The H3K27me3, on the other hand, was the least prioritized histone marker, as it was chosen as a pilot histone marker for a future study to investigate BCG-induced trained innate immunity, and at least one H3K27me3 sample was required per assay to serve as a positive control [121,479]. If there were fewer than 5,000 cells, an assay was still performed to include as many samples as possible. When the sorted cell yield was more than 15,000, the remaining cells not utilized for the assay were homogenized in 500 µl Trizol (Invitrogen) and stored at -20°C for future research.

4.3.6. CUT&Tag assay data processing and analysis

Steps from quality control until peak calling were conducted following the CUT&Tag tutorial [481] with some modifications (**Appendix H**). Thereafter, the processed data were used for downstream analysis, such as visualization of signals, peak calling, peak annotation, differential binding analysis, and pathway enrichment analysis. **Figure 4.3** illustrates the flow of downstream analysis used in the study.

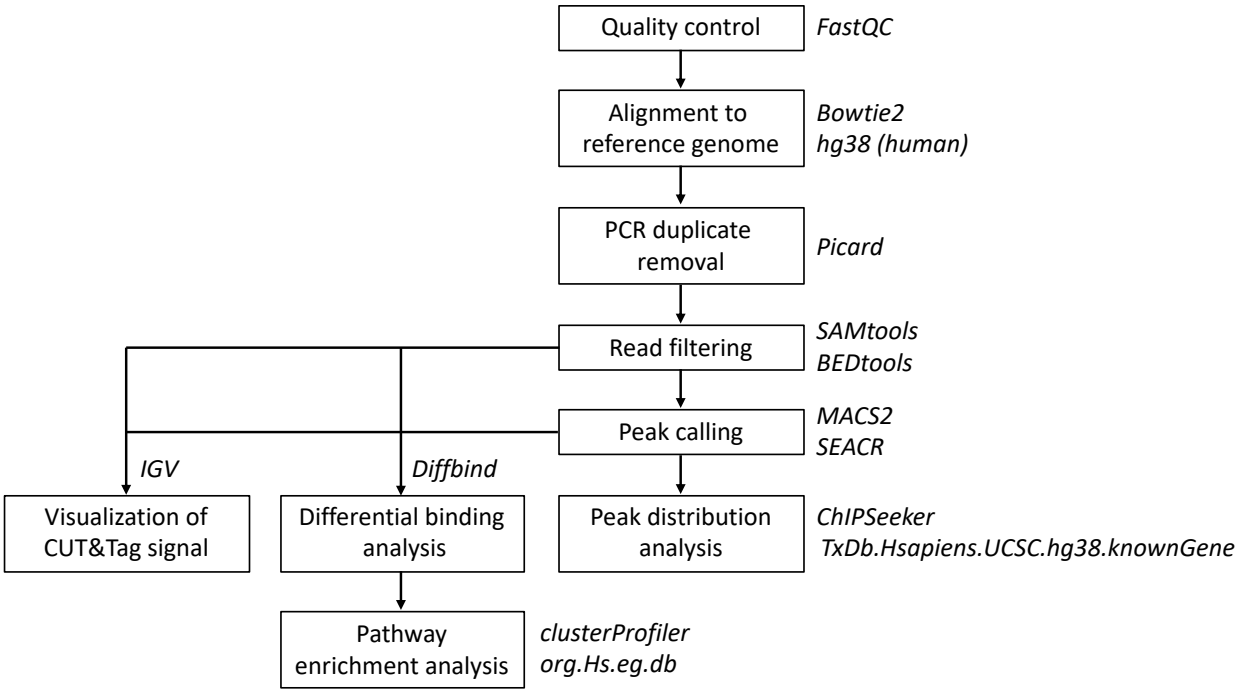

Figure 4.3. CUT&Tag downstream analysis. Schematic diagram of downstream analysis steps employed in the CUT&Tag data analysis. Abbreviations: CUT&Tag, Cleavage Under Targets and Tagmentation; hg38, Genome Reference Consortium Human Build 38; PCR, polymerase chain reaction; MACS2, Model-based Analysis for ChIP-Seq 2; SEACR, Sparse Enrichment Analysis for CUT&RUN; IGV, Integrative Genomics Viewer.

4.3.6.1. Quality control

Sequencing data were subjected to FastQC (version 0.11.9) [482] to validate the sequencing data quality and to identify any major issues, such as adapter contamination or poor read qualities. **Appendix I** illustrates the sequencing results. Given the short read length, trimming the adapter sequence was not necessary [481].

4.3.6.2. Alignment to the reference genome

The human genome reference sequence (GRCh38; hg38) was obtained from the University of California Santa Cruz (UCSC) database [483], and the index was generated using the "bowtie2-build" function within Bowtie2 (version 2.5.1) [484]. The CUT&Tag FASTQ files were aligned to hg38 using Bowtie2. The phred quality threshold was set to 33. The size range of the insert was set to between 10-700 bp. SAM files were produced as output with alignment reports in text files.

4.3.6.3. PCR duplicate removal

PCR duplicates were identified and removed using Picard (version 2.25.1) [485]. Using SortSam, aligned data were sorted by coordinate. The duplicates were marked and removed by MarkDuplicates.

4.3.6.4. Fragment size check

Using SAMtools (version 1.12) [486], fragment length information was extracted from the SAM files, and the output was saved in a text format. The parameter "-F 0x04" was set to specify not to include unmapped reads in an output file.

4.3.6.5. Read filtering

Mapped reads were filtered by alignment score using SAMtools (version 1.12) [486]. The minimum mapping quality was set to 2 with the parameter "-q 2." Filtered data were produced as a SAM file. The parameter "-h" was set to include the output header.

4.3.6.6. File conversion

Using SAMtools (version 1.12) [486], filtered SAM files were converted to BAM files with parameters "-bS" and "-F 0x04" to filter only mapped reads. BAM files were then sorted by the read names with the parameter "-n." For downstream analysis, files were indexed and converted to BED files using BEDtools (version 2.30.0) [487]. The parameter "-bedpe" was set to produce BAM files in BEDPE format. Only alignments from pair-end reads on the same chromosome with fragment lengths < 1,000 bp were filtered.

4.3.6.7. Peak calling with MACS2

Model-based Analysis for ChIP-Seq 2 (MACS2; version 2.2.7.1) is a widely employed peak calling tool for ChIP-seq analysis [488]. Sorted BAM files were used as input data. Both narrow and broad peak calling were employed. For the broad peaks, additional parameters ("--broad" and "--broad-cutoff 0.1") were included. The parameter "-g hs" was set to specify the genome size as "human" and "--nomodel" to skip the step of calculating fragment size.

4.3.6.8. Peak calling with SEACR

Sparse Enrichment Analysis for CUT&RUN (SEACR) [489] is a peak calling tool suited for assays with low background noise, such as CUT&RUN [118,119] and CUT&Tag [118,119, 121,479]. As BedGraph files were required for SEACR analysis, BED files were converted to a BedGraph format using the BEDtools command "genomecov." For the peak calling with SEACR, several parameters are required to be specified:

1) The choice between "relaxed" or "stringent" mode for peak calling.
2) The option to employ IgG as a normalization control or to define a numeric threshold (*n*) for selecting the top n fraction of peaks.
3) The selection of "norm" or "non" for normalization.

In this study, SEACR (version 1.3) was performed with different parameter settings (conditions #1-4; **Table 4.4**), as described below. For the negative control (i.e., CUT&Tag with anti-IgG antibody [481]), sample "E27-S1-Mono-IgG" was used for normalization, as this sample had higher sequencing depth (386,781 reads) than the other IgG sample ("E30-S4-Mono-IgG"; 24,100 reads) (**Appendix I**).

Table 4.4. SEACR peak calling conditions.

SEACR Condition	Peak Calling Mode (1)	Normalization Control (2)	Normalization Parameter (3)*
#1	Relaxed	IgG sample	"norm"
#2	Relaxed	Numeric threshold (Top 1% peaks)	"non"
#3	Stringent	IgG sample	"norm"
#4	Stringent	Numeric threshold (Top 1% peaks)	"non"

*norm, normalized; non, non-normalized.

4.3.6.9. Visualization of peaks

To visualize the CUT&Tag peaks, BAM files and peak call output files were loaded onto Integrative Genomics Viewer (IGV) software (version 2.9.4) [490].

4.3.6.10. Peak distribution analysis

CUT&Tag peaks obtained from the peak calling step were annotated using the ChIPSeeker package (version 1.32.1) with default settings [491]. This tool reports the closest genomic features to the peaks. Annotation was based on the TxDb.Hsapiens.UCSC.hg38.knownGene package (version 3.15.0) [492]. Genomic features were annotated as promoter, 5' untranslated region (UTR), 3' UTR, exon, intron, and intergenic. Based on the report, bar charts of the genomic features were produced using the "plotAnnoBar" function in the ChIPSeeker package.

4.3.6.11. Differential binding analysis

Differential bindings between groups were identified by DESeq2 (differential analysis of count data) in the DiffBind package (version 3.6.5) [493]. The default setting "minOverlap=2" was used in the "dba.count" function to select only a peak that exists at least in two samples among all samples. Data were normalized by library size (read depth) using the "dba.normalize" function. DESeq2 analysis was performed using the "dba.contrast" function with design formula "~ cell type + histone marker" and the "dba.analyze" function to execute the differential analysis. Blacklist regions [494] were automatically removed in the process. Differential binding sites were selected based on an adjusted *P*-value threshold of 0.05. A correlation heatmap was created using the "dba.plotHeatmap" function. Principal component analysis (PCA) plots were created using the "dba.plotPCA" function.

4.3.6.12. Pathway enrichment analysis

Kyoto Encyclopedia of Genes and Genomes (KEGG) pathway enrichment analysis was performed using the clusterProfiler package (version 4.9.0.2) [495,496]. Data of active gene markers (H3K27Ac and H3K4me3) were used. Prior to the analysis, differentially bound sites between monocytes and NK cells were annotated using the org.Hs.eg.db package (version 3.15.0) [497]. The identified enriched pathways with adjusted *P*-value (Benjamini-Hochberg) less than 0.05 were chosen for the display. Using the "dotplot" function, the top 10 enriched pathways were visualized for each histone modification based on the gene count. The gene-concept network was plotted using the "cnetplot" function.

4.4. Results

4.4.1. CUT&Tag optimization

Adult PBMCs were used for initial optimization. Monocytes and NK cells were isolated using the established gating strategy illustrated in **Figure 4.1**. The original CUT&Tag protocol recommends including an antibody targeting a ubiquitously abundant histone marker in a cell (such as H3K27me3) as an assay control [121,479]. To determine the optimal number of input cells, number of PCR cycles, and sequencing depth suited for low-input cell number conditions, CUT&Tag was conducted using an anti-H3K27me3 antibody with different experimental conditions, as described below (**Table 4.5**):

Table 4.5. CUT&Tag optimization conditions.

Sample ID	Input Cell Number (cells)	Cell Type	Target Histone Marker	PCR Cycles
#1	5,000	Monocytes	H3K27me3	18
#2	1,500	Monocytes	H3K27me3	18
#3	30,000	NK cells	H3K27me3	18
#4	5,000	NK cells	H3K27me3	20
#5	1,500	NK cells	H3K27me3	20

Abbreviations: NK cells, natural killer cells; PCR, polymerase chain reaction; H3K27me3, trimethylation of histone H3 at lysine 27.

Preliminary CUT&Tag assays with < 17 PCR cycles using ultra-low input cells yield extremely low DNA library concentration, which led to sequencing failure (data not shown). While the original protocol advises maintaining PCR cycles between 12 and 14 to sustain the library complexity [121], in the case of the ultra-low input samples, PCR cycles can be increased to meet the required concentration for sequencing and bioinformatic removal of PCR duplicates can be performed [479,498]. All the conditions (sample ID #1-5; **Table 4.5**) yielded nucleosome ladder patterns (**Figure 4.4A-B**), indicating a successful CUT&Tag assay [479]. The band at 350 bp represents a mononucleosome (~200 bp) with sequencing adapters (~130 bp), and the bands positioned above represent oligonucleosomes with sequencing adapters (i.e., 550 bp, 750 bp, 950

bp). The 200 bp band represents DNA fragments released from nucleosome-depleted regions adjacent to the antibody-tethered nucleosome [479].

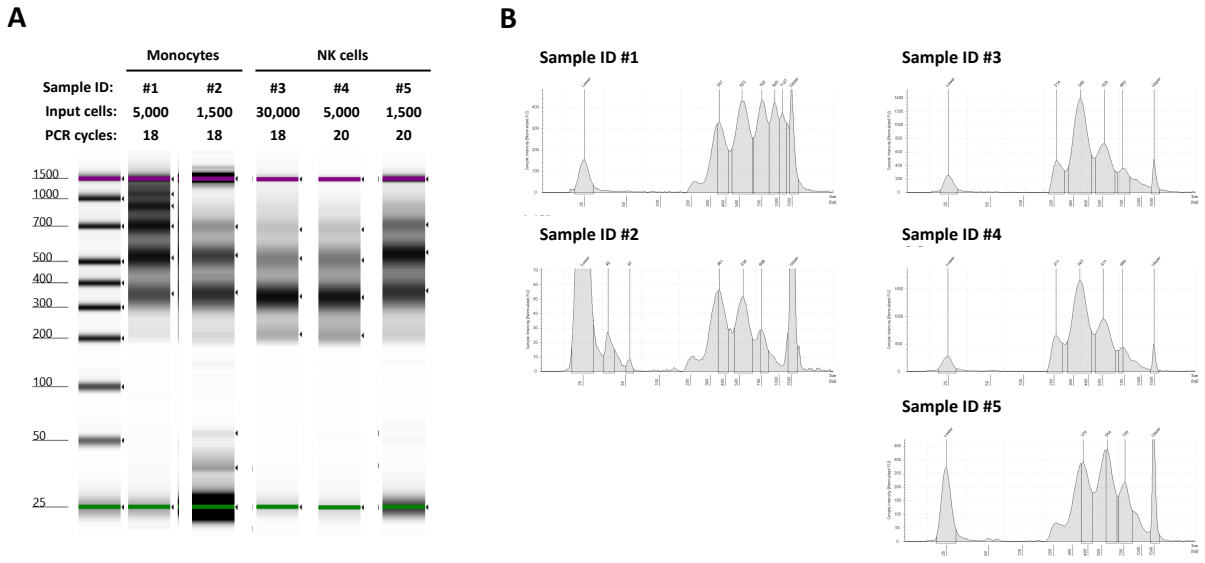

Figure 4.4. TapeStation results of CUT&Tag libraries with different experiment conditions. CUT&Tag was performed on adult monocytes and NK cells using an anti-H3K27me3 antibody as a positive control. The resulting libraries were analyzed by TapeStation. The capillary electrophoretic gel images (A) and electropherograms (B) are shown. For an optimization, different input cell numbers and PCR cycle conditions were applied (sample ID #1-5): (#1) 5,000 monocytes and 18 PCR cycles, (#2) 1,500 monocytes and 18 PCR cycles, (#3) 30,000 NK cells and 18 PCR cycles, (#4) 5,000 NK cells and 20 PCR cycles, and (#5) 1,500 NK cells and 20 PCR cycles. Abbreviations: CUT&Tag, Cleavage Under Targets and Tagmentation; NK cells, natural killer cells; PCR, polymerase chain reaction; H3K27me3, trimethylation of histone H3 at lysine 27.

The resulting CUT&Tag libraries were pooled and sequenced on an Illumina MiSeq using a 50-cycle flow cell (pair-end, 25 bp). The average sequencing depth was 3.0 million reads per sample (IQR: 2.6-3.3), meeting the required sequencing depth (2-3 million reads per sample) described in the original protocol [121,479]. Sequencing reads were processed, and the output BAM files were loaded on IGV to visualize the signals (**Figure 4.5**). Although the CUT&Tag assay with 1,500 input cells successfully produced nucleosome ladder patterns (**Figure 4.4A-B**; sample ID #2 and #5), the peaks observed on IGV suggested that the sequencing data may not be sufficient for downstream analysis with the given sequencing depth (**Figure 4.5**; sample ID #2 and #5). To determine the minimum input cells required for the assay while ensuring the ability to assess multiple histone markers on infant samples, several factors were carefully considered:

1) Based on the experience from parent studies, infant PBMCs are typically divided and stored in multiple vials, each containing 2-3 million PBMCs. However, since PBMC vials need to be shared between assays, only one vial was available for epigenetics.
2) Based on preliminary experiments, the abundance of target cell populations (monocytes and NK cells) in infant PBMCs is generally 2-4% (data not shown).
3) Three histone modifications (H3K4me3, H3K27Ac, and H3K27me3) were planned to be analyzed on each target cell population.

Considering these factors and results from the optimization experiments, we concluded that performing the CUT&Tag assay using 5,000 cells per histone modification would be the optimal approach for this study.

In addition, although we had ensured the required sequencing depth stated in the original protocol [121,479], the results from the optimization experiment suggested that conducting the CUT&Tag assay with low input samples would require higher sequencing depth to obtain sufficient data. Given that sample ID #1 yielded the highest sequencing depth with 4.3 million reads and the clearest CUT&Tag peak pattern among the samples assessed (**Figure 4.5**), we decided that targeting 5 million sequencing reads per sample would be ideal. PCR cycles were set at 20 to ensure a sufficiently high library concentration, regardless of the histone marker or cell types being analyzed.

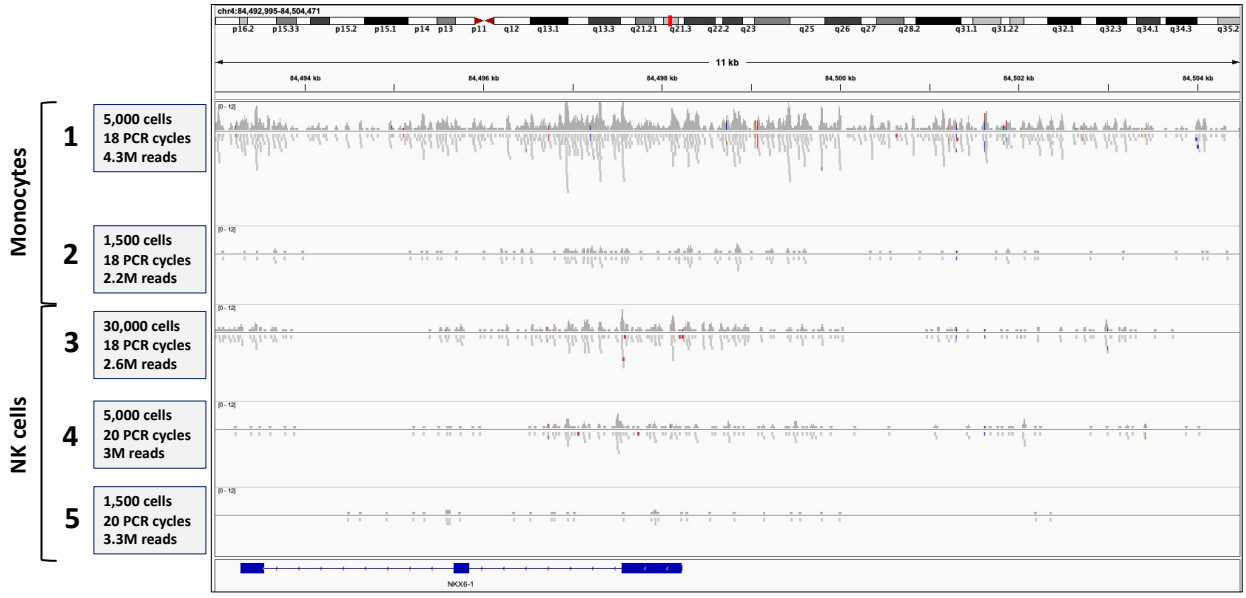

Figure 4.5. Visualization of CUT&Tag peaks. Sequenced CUT&Tag data were processed and visualized on the IGV. A snapshot of CUT&Tag peaks on an arbitrary gene (NKX6-1) located on chromosome 4 is shown. The track height (horizontal range) is set at 12 for comparison. The read coverage track (top) and the alignment track (squashed setting; bottom) are displayed for each sample. The sample IDs with experiment conditions are indicated on the left, corresponding to **Table 4.5** and **Figure 4.4**. Abbreviations: CUT&Tag, Cleavage Under Targets and Tagmentation; IGV, Integrative Genomics Viewer; kbp, kilobase pair; NK cells, natural killer cells; PCR, polymerase chain reaction.

4.4.2. Application of CUT&Tag to infant samples

4.4.2.1. Sample characteristics

To apply the optimized CUT&Tag assay protocol to infant samples, PBMCs obtained from 14 infants enrolled in the InFANT or BCG study were randomly selected (**Table 4.6**). In addition, a sample obtained from an adult donor was included as a control. Monocytes and NK cells were isolated using the gating strategy illustrated in **Figure 4.1**. The median total PBMC count of infant samples immediately after thawing was 1.9 million cells per vial (IQR: 1.4-2.4), with a median viability of 74.0% (IQR: 62.9-85.0). The median monocyte abundance was 2.0% (IQR: 1.1-2.6), and the median NK cell abundance was 3.9% (IQR: 3.2-5.9). Therefore, the median live cell count was 19,743 cells (IQR: 8,768-31,632) and 44,573 cells (IQR: 20,876-85,720) for monocytes and NK cells, respectively (**Table 4.6**).

Table 4.6. Sample information and sorting results.

Assay Batch	PBMCs ID	Study Name	PBMC Count (million)	Viability (%)	Monocyte Count	Monocyte Abundance (%)	NK cell Count	NK cell Abundance (%)
E27	E27-S1	InFANT	2.1	85	111,721	4.9	64,501	2.8
E27	E27-S2	InFANT	2.4	86	39,227	2.0	75,033	3.8
E28	E28-S1	InFANT	2.3	85	4,505	0.9	13,018	2.6
E28	E28-S2	BCG	1.0	36	4,448	2.5	1,318	0.7
E30	E30-S1	BCG	1.1	73	23,865	2.5	35,183	3.7
E30	E30-S2	BCG	3.0	93	100,150	3.0	186,710	5.6
E30	E30-S3	BCG	na*	na*	5,129	1.0	18,869	3.9
E30	E30-S4	na (adult)	1.0	95	19,050	2.3	96,407	11.7
E31	E31-S1	InFANT	5.9	80	90,105	1.8	172,282	3.5
E31	E31-S2	BCG	1.3	37	1,302	0.5	21,256	7.6
E31	E31-S3	BCG	1.0	75	24,036	5.8	20,496	4.9
E33	E33-S1	InFANT	2.8	58	19,743	1.0	118,035	6.2
E33	E33-S2	InFANT	1.8	66	18,460	1.1	44,573	2.7
E33	E33-S3	BCG	1.7	62	21,520	2.7	54,096	6.7
E33	E33-S4	BCG	2.0	69	12,406	1.5	42,914	5.3

PBMC count and cell viability were counted by TC20 Automated Cell Counter immediately after thawing. Monocytes and NK cell count and abundance are based on the record obtained during the sorting. Abbreviations: na, not applicable; NK cells, natural killer cells; PBMC, peripheral blood mononuclear cell. *Too low cell concentration. Information regarding the allocation of samples (iHEU vs. iHUU and early vs. delayed BCG vaccination) was unavailable as unblinding has not occurred yet.

4.4.2.2. CUT&Tag sequencing statistics

The optimized CUT&Tag assay protocol was applied to the isolated infant monocytes and NK cells. Three histone markers (H3K27me3, H3K27Ac, and H3K4me3) were assessed with a negative control antibody (IgG). A total of 77 CUT&Tag libraries were made. Among them, 37 libraries (48.1%) were derived from monocytes (11 H3K27me3, 10 H3K27Ac, 14 H3K4me3, and 2 IgG), and 40 libraries (51.9%) were derived from NK cells (13 H3K27me3, 13 H3K27Ac, and 14 H3K4me3). These libraries were pooled for sequencing. The median sequencing depth per sample was 6.0 million reads (IQR: 4.9-6.8) (**Figure 4.6A**). The sequencing metrics are shown in

Appendix I. The median alignment rate for monocytes and NK cells combined against the human reference genome (hg38) was generally high but showed variation depending on the specific histone marker: H3K27me3 at 98.3%, H3K27Ac at 97.1%, H3K4me3 at 92.3%, and IgG at 87.5% (**Figure 4.6B**). Most fragments corresponded to mononucleosomes, with a peak at approximately 200 bp. Some fragments derived from dinucleosomes (peak at around 400 bp) were also observed (**Figure 4.7A-B**).

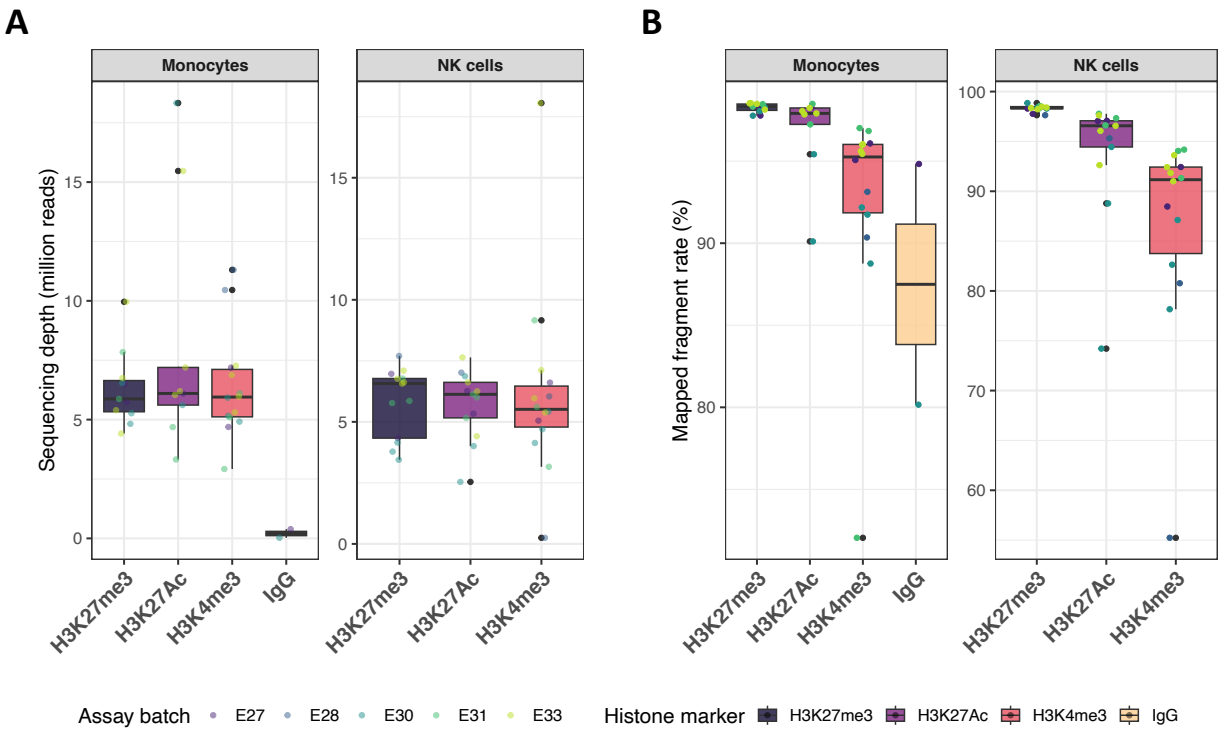

Figure 4.6. Sequencing depth and alignment rates. (A) Sequencing depth (million reads) for each target histone marker of interest (H3K27me3, H3K27Ac, H3K4me3, and IgG). (B) Alignment rate (%) for each target histone marker of interest, calculated by "sequencing reads mapped to the human reference genome (hg38) / total sequencing reads x100." The target histone marker is indicated by the color of the box plot, and the assay batch is indicated by the color of the dot. Abbreviations: H3K27Ac, acetylation of histone H3 at lysine 27; hg38, Genome Reference Consortium Human Build 38; NK cells, natural killer cells; H3K4me3, trimethylation of histone H3 at lysine 4; H3K27me3, trimethylation of histone H3 at lysine 27.

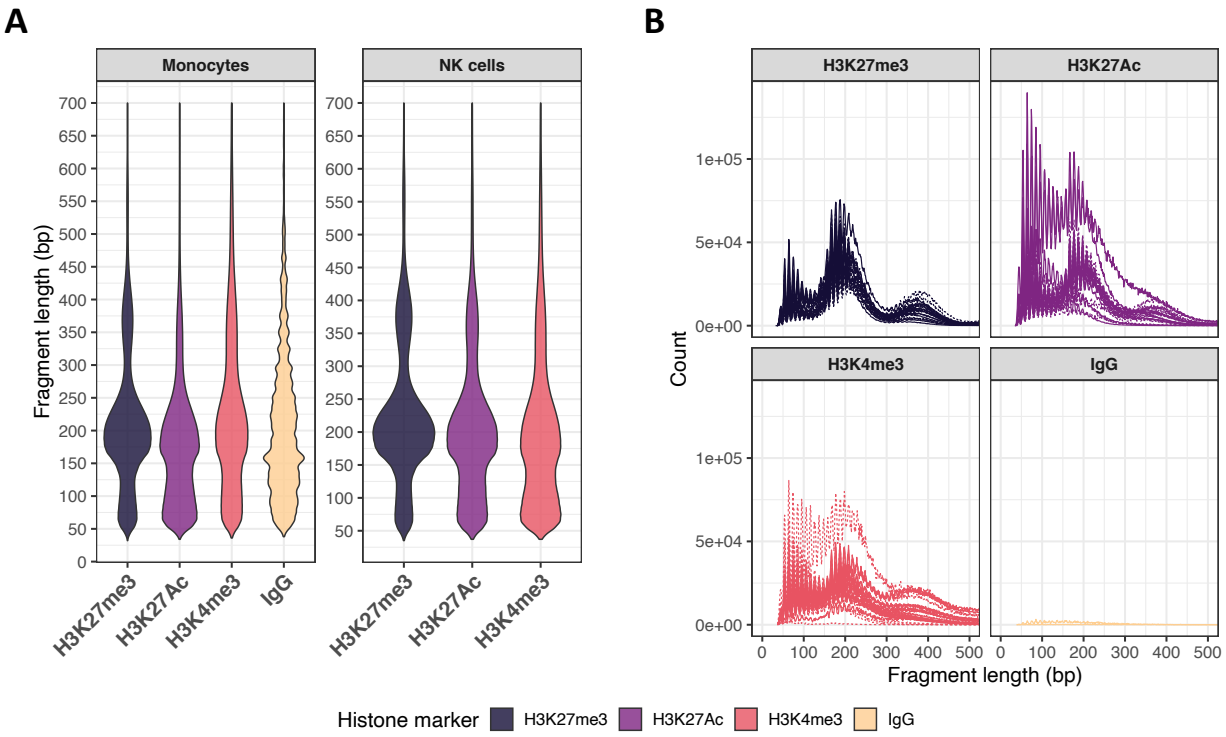

Figure 4.7. Distribution of library fragment sizes. (A) Violin plots of fragment length (bp) for each histone marker (H3K27me3, H3K27Ac, H3K4me3, and IgG) and cell type (monocytes and NK cells). (B) Distribution of fragment size (bp) for each histone marker. Abbreviations: H3K27Ac, acetylation of histone H3 at lysine 27; bp, base pair; NK cells, natural killer cells; H3K4me3, trimethylation of histone H3 at lysine 4; H3K27me3, trimethylation of histone H3 at lysine 27.

As expected, due to the high number of PCR cycles, PCR duplication rates were high across the samples (**Figure 4.8A**). The duplication rate was inversely correlated with the abundance of histone markers, where H3K27me3, a highly abundant histone marker, showed an average duplication rate of 79.6%. On the other hand, the other less abundant histone markers, H3K27Ac and H3K4me3, showed higher duplication rates of 88.5% and 89.1%, respectively. Lastly, the PCR duplication rates of IgG samples (negative control) were the highest at 95.5%. The estimated library size and unique fragment count inversely correlated with the duplication rates (**Figure 4.8B-C**). The PCR duplicates were removed by Picard before downstream analyses to ensure data quality.

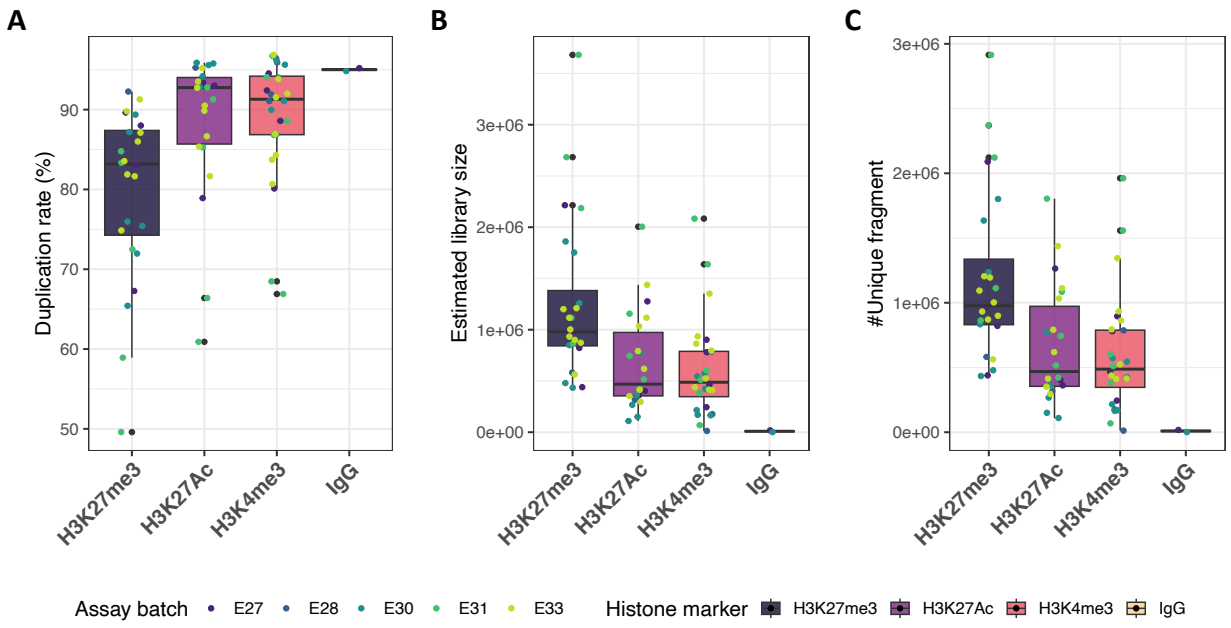

Figure 4.8. Picard summary. (A) Duplication rate (%) of samples for each target histone marker of interest (H3K27me3, H3K27Ac and H3K4me3, and IgG). (B) Estimated library sizes (reads). (C) The number of unique fragments. The target histone marker is represented by the color of the box plot, and the assay batch is indicated by the color of the dot. Abbreviations: H3K27Ac, acetylation of histone H3 at lysine 27; H3K4me3, trimethylation of histone H3 at lysine 4; H3K27me3, trimethylation of histone H3 at lysine 27.

4.4.2.3. Peak calling consideration

Next, peak calling was conducted using two different peak callers, MACS2 and SEACR. While MACS2 is a widely used tool to identify significantly enriched peaks for ChIP-seq [488], SEACR was developed by the same team that established the CUT&Tag technique. SEACR specializes in assays with low background noise, such as CUT&Tag and CUT&RUN [489].

The peak calling results of MACS2 and SEACR were compared with different parameter settings (**Figure 4.9**). Peak calling with MACS2 generated fewer peaks with wider variation across the samples. This was the same regardless of the peak call settings: a median of 60 peaks (IQR: 1-1,920) was obtained for narrow peak calling and a median of 157 peaks (IQR: 2-4,041) for broad peak calling. On the other hand, peak calling with SEACR resulted in a higher number of peaks with smaller variation across the samples: a median of 5,160 peaks (IQR: 2,752-17,986) when using IgG for normalization with the relaxed peak calling mode, a median of 281,638 peaks (IQR: 178,177-458,863) when selecting the top 1% with the relaxed peak calling mode, a median of 3,258 peaks (IQR: 1,231-17,986) when using IgG for normalization with the stringent peak calling

mode, and a median of 2,738 peaks (IQR: 1,774-4,584) when selecting the top 1% with the stringent peak calling mode. These results underscored that SEACR was better suited as a peak caller for analysis of CUT&Tag assay using infant samples as compared to MACS2.

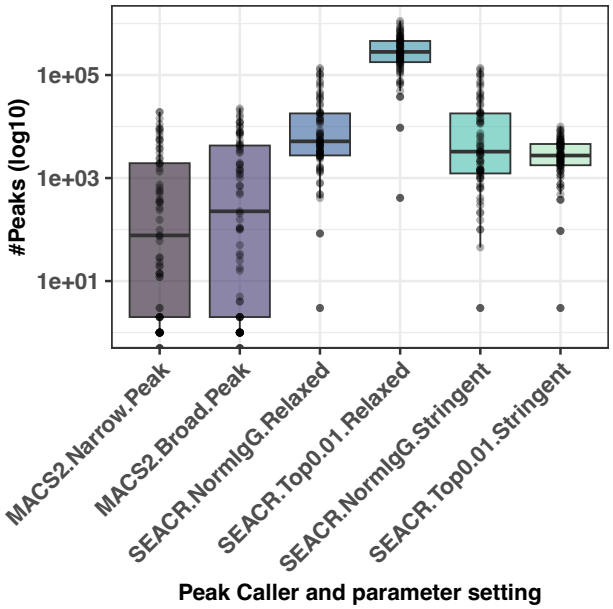

Figure 4.9. Peak calling results. Peak calling was conducted using MACS2 and SEACR. For the MACS2, both narrow peak and broad peak settings were assessed. For the SEACR, combinations of peak calling modes (relaxed or stringent) and normalization methods (using IgG as normalization control or selecting the top 1% of peaks) were assessed. The resulting number of peaks (log10) is plotted. Abbreviations: MACS2, Model-based Analysis for ChIP-Seq 2; SEACR, Sparse Enrichment Analysis for CUT&RUN.

The number of peaks identified varied depending on the parameter settings for SEACR. Selecting the top 1% with the relaxed peak calling mode resulted in the highest number of peaks (median 281,638; IQR: 178,177-458,863). Peak distribution patterns were investigated for each setting to explore the optimal peak calling settings with SEACR (**Figure 4.10**). The results suggested that the peak distribution pattern was strongly influenced by the peak calling parameter setting used. Specifically, when IgG was used as the normalization control, the peak distribution patterns were similar regardless of peak calling modes (i.e., relaxed vs. stringent). In contrast, selecting the top 1% using the relaxed peak calling mode with SEACR led to an increased percentage of peaks within intron and distal intragenic regions. In addition, with this parameter setting, the peak distribution pattern became more similar across the samples, regardless of the histone marker. As this setting exhibited the highest number of peaks, we speculated that significant "false positive" peaks might be included in the peak calling output.

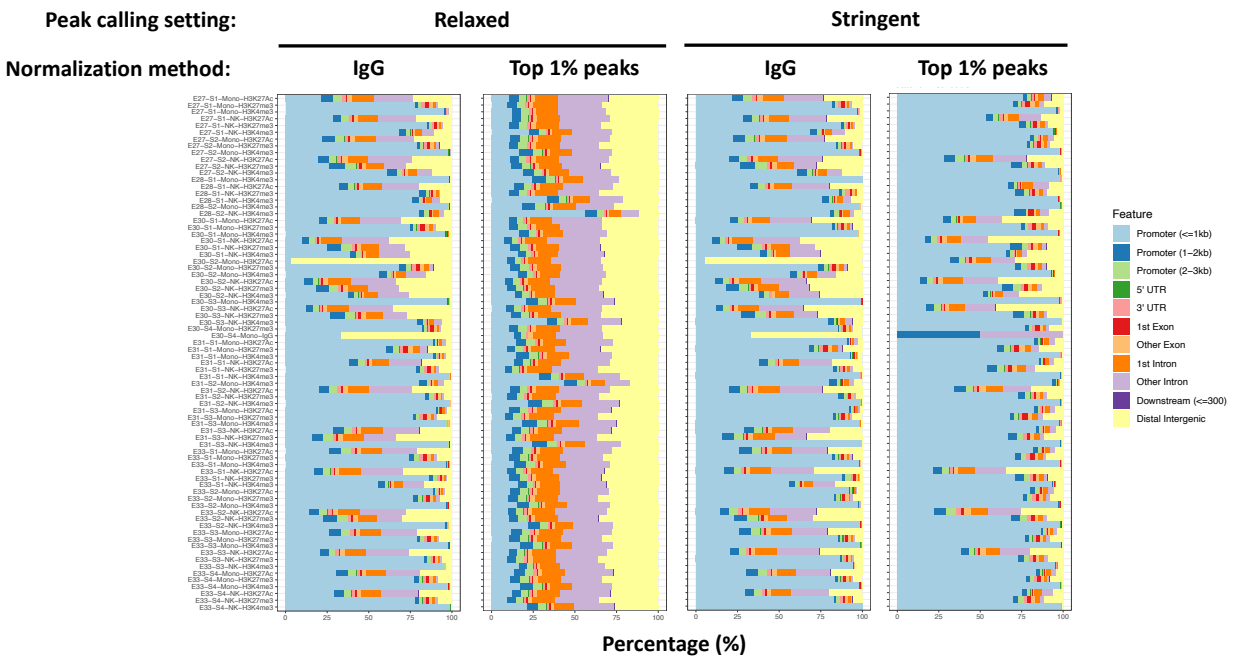

Figure 4.10. Peak distribution of SEACR peak calling output with different parameter settings. Bar plots indicating the peak distributions (%) of histone markers and control (namely, H3K27me3, H3K27Ac, H3K4m3, and IgG). Peak calling settings of SEACR (relaxed or stringent) and normalization methods (using IgG as a normalization control or selecting the top 1% of peaks) are annotated on the top. Annotation of the genomic feature includes promoter (≤ 1 kbp), promoter (1-2 kbp), promoter (2-3 kbp), 5'UTR, 3'UTR, 1st exon, other exon, 1st intron, other intron, downstream (≤ 300 bp) and distal intergenic, indicated by color. Abbreviations: H3K27Ac, acetylation of histone H3 at lysine 27; bp, base pair; kbp, kilobase pair; NK cells, natural killer cells; SEACR, Sparse Enrichment Analysis for CUT&RUN; H3K4me3, trimethylation of histone H3 at lysine 4; H3K27me3, trimethylation of histone H3 at lysine 27; UTR, untranslated region.

To further explore the optimal parameter settings for SEACR, peak calling was reassessed using the "stringent" mode to minimize the false positive peaks with a varied range of threshold settings. We hypothesized that more false positive peaks would be included in the output as the cut-off threshold is increased. The results were then compared to the analysis where IgG was used as a normalization control (**Figure 4.11**). With the lowest threshold cut-off (top 0.1%), the H3K27me3 markers were predominantly enriched at promoter regions. The proportion of other regions, such as intron and downstream regions, was uniformly increased by lowering the threshold. On the other hand, the peak calling using IgG as a normalization control showed that some of the samples were strongly enriched in intron and downstream regions, suggesting unsuccessful normalization. As this issue can occur when the read depth of the IgG sample is low, as reported by the SEACR

developer [499], the parameter combination of "selecting the top 1% peaks" and "stringent peak calling mode" was selected as optimal settings for this study.

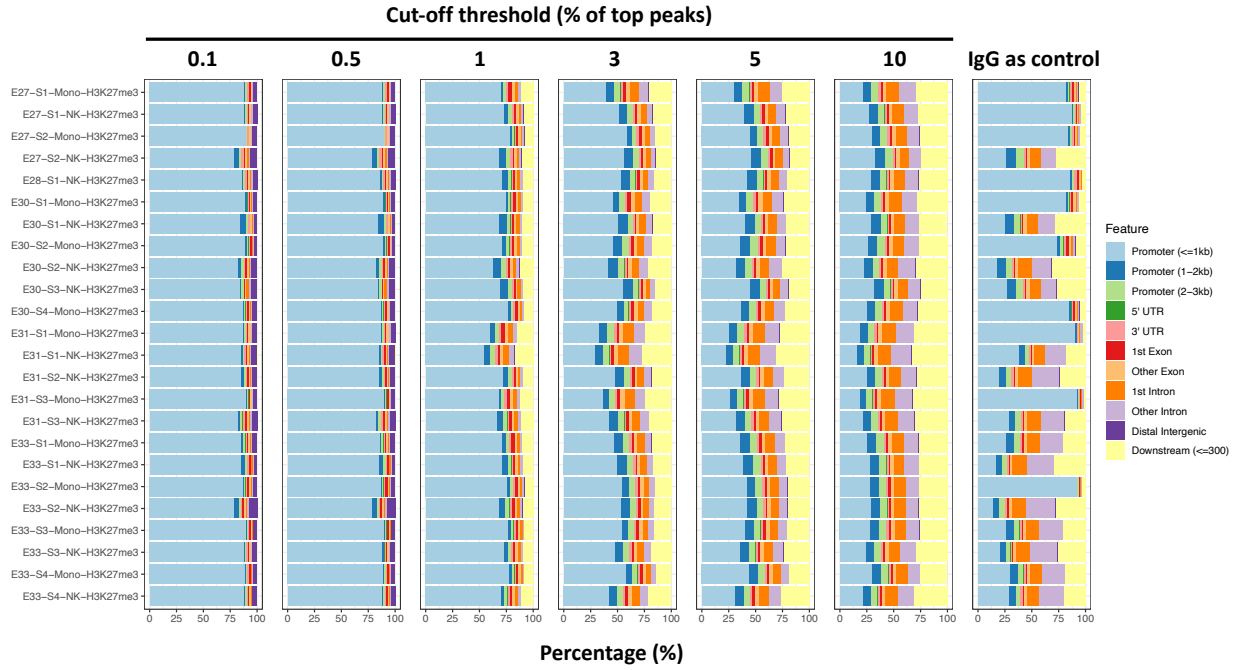

Figure 4.11. Peak distribution of SEACR peak calling with different threshold settings. Peak calling with SEACR (stringent setting) was conducted with different cut-off thresholds for peaks, ranging between the top 0.1-10%, indicated on the top. SEACR (stringent setting) using IgG as a normalization control is included as a comparison (rightmost panel). Peak distributions (%) of H3K27me3 samples are indicated by bar plots. Annotation of genomic features includes promoter (≤ 1 kbp), promoter (1-2 kbp), promoter (2-3 kbp), 5'UTR, 3'UTR, 1st exon, other exon, 1st intron, other intron, downstream (≤ 300 bp) and distal intergenic, indicated by color. Abbreviations: UTR, untranslated region. Abbreviations: bp, base pair; kbp, kilobase pair; NK cells, natural killer cells; SEACR, Sparse Enrichment Analysis for CUT&RUN; H3K27me3, trimethylation of histone H3 at lysine 27; UTR, untranslated region.

4.4.2.4. Peak distribution by cell types

Next, the peak distribution pattern was assessed by cell type, monocytes vs. NK cells (**Figure 4.12**). As anticipated, the H3K4me3 marks were enriched at the promoter regions of both cell types [500]. However, some NK samples exhibited higher enrichment at distal intragenic and intron regions. The H3K27Ac marks were mainly enriched at promoter regions in monocytes, except two samples showed high enrichment at intron and distal intergenic regions. Interestingly, the distribution profiles of H3K27Ac in NK cells were strikingly different from monocytes with a higher proportion of intron or other intergenic regions, suggesting that peaks were more enriched

at enhancers than promoters. Both monocytes and NK cells exhibited enrichment of H3K27me3 marks at promoter regions, followed by uniform distribution at other regions, such as intron or intergenic regions. These peak distribution profiles validate not only the success of the CUT&Tag assay but also the capability of the assay to explore the characteristics of histone modifications using ultra-low cells obtained from clinical samples.

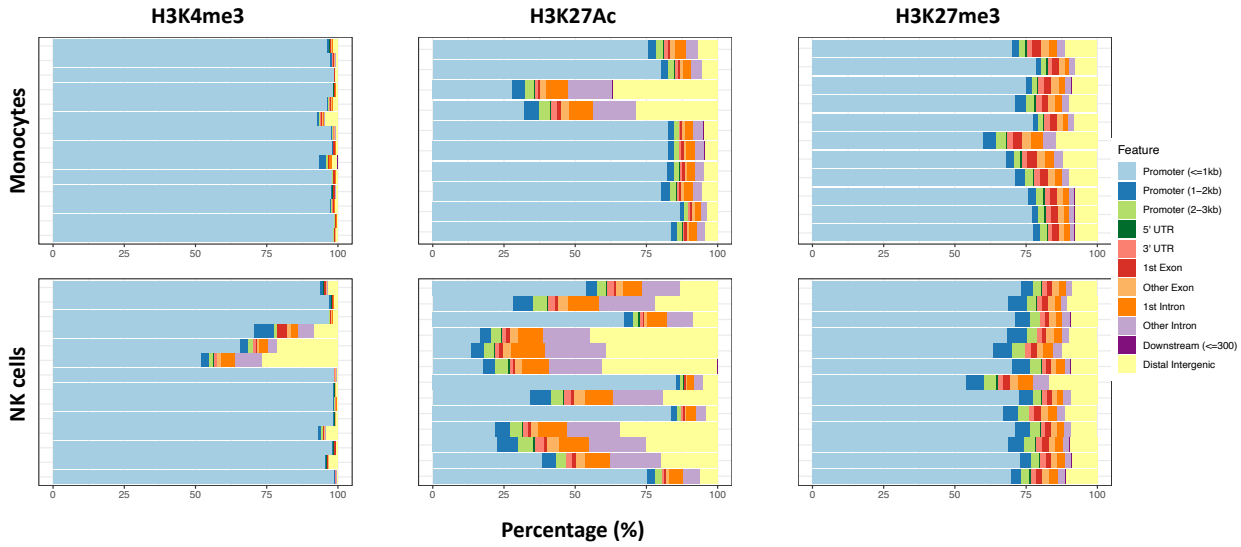

Figure 4.12. Peak distribution by cell type and histone modification. SEACR peak calling was conducted with the stringent setting, and the top 1% of peaks were selected. Peak distributions (%) of each histone marker (H3K27me3, H3K27Ac, and H3K4me3) are displayed by bar plots based on the cell type (monocytes or NK cells). Annotation of genomic features includes promoter (≤ 1 kbp), promoter (1-2 kbp), promoter (2-3 kbp), 5'UTR, 3'UTR, 1st exon, other exon, 1st intron, other intron, distal intergenic and downstream (≤ 300 bp), indicated by color. Abbreviations: H3K27Ac, acetylation of histone H3 at lysine 27; bp, base pair; kbp, kilobase pair; NK cells, natural killer cells; SEACR, Sparse Enrichment Analysis for CUT&RUN; H3K4me3, trimethylation of histone H3 at lysine 4; H3K27me3, trimethylation of histone H3 at lysine 27; UTR, untranslated region.

4.4.2.5. Relationship and differentially bound sites between cell types

Next, the relationship between samples was assessed. A PCA plot of differentially bound regions showed clustering by histone mark but also by cell type (**Figure 4.13**). A correlation matrix based on the cell type and histone marker confirmed this (**Figure 4.14**). In particular, histone markers of inactive genes (H3K27me3) and active genes (H3K27Ac and H3K27me3) clustered completely separately (**Figure 4.14**). These results highlighted that the relevant histone modification characteristics were captured by CUT&Tag. Using DESeq2, a total of 5,201 sites (based on

H3K27me3), 1,538 sites (based on H3K27Ac), and 1,372 sites (based on H3K4me3) were differentially bound between monocytes and NK cells.

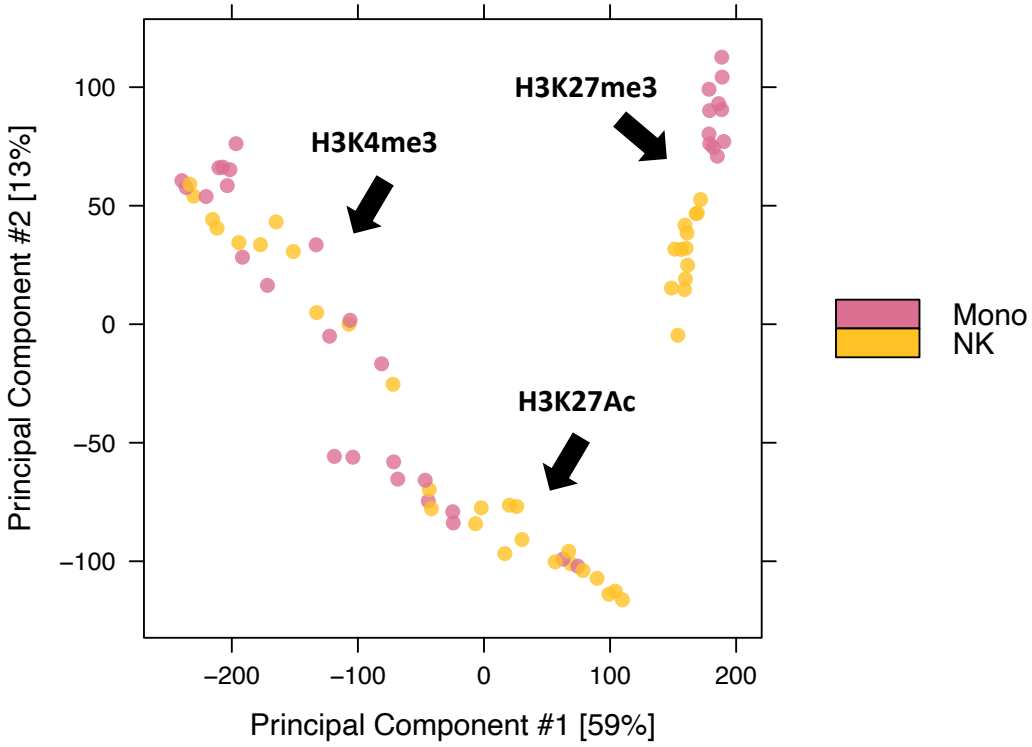

Figure 4.13. PCA of differentially bound regions. PCA plots showing the distance between differentially bound regions based on the histone markers (H3K27me3, H3K27Ac, and H3K4me3). The color indicates cell types. Abbreviations: H3K27Ac, acetylation of histone H3 at lysine 27; Mono, monocytes; NK cells, natural killer cells; PCA, principal component analysis; H3K4me3, trimethylation of histone H3 at lysine 4; H3K27me3, trimethylation of histone H3 at lysine 27.

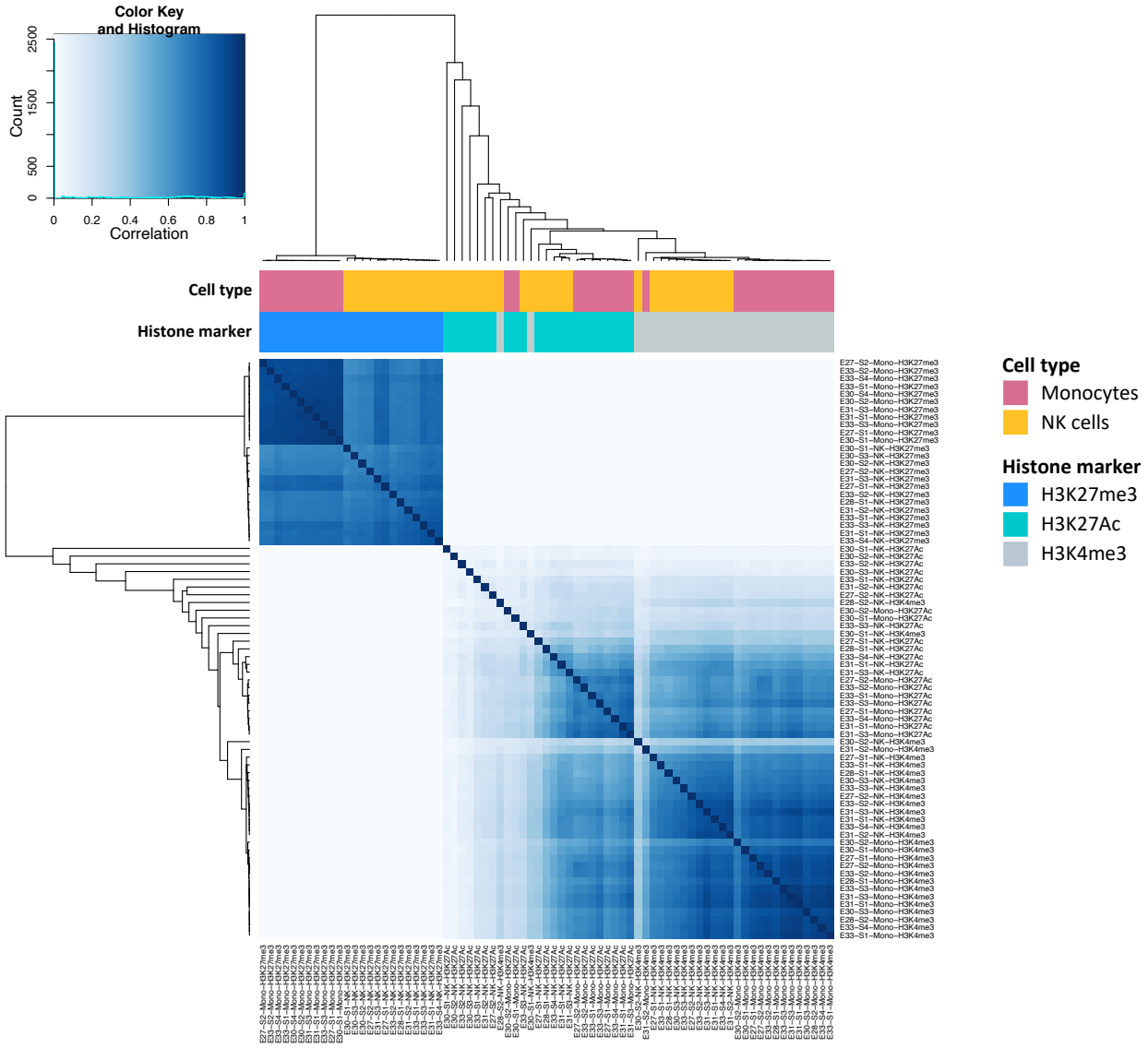

Figure 4.14. Correlation heatmap of CUT&Tag samples. Correlation values between each pair of columns in the binding matrix are plotted as a correlation heatmap. Annotation of cell type (monocytes and NK cells) and histone marker (H3K27me3, H3K27Ac, and H3K4me3) are annotated on the top bars. Abbreviations: H3K27Ac, acetylation of histone H3 at lysine 27; CUT&Tag, Cleavage Under Targets and Tagmentation; NK cells, natural killer cells; H3K4me3, trimethylation of histone H3 at lysine 4; H3K27me3, trimethylation of histone H3 at lysine 27.

4.4.2.6. Pathway enrichment analysis

Lastly, KEGG pathway enrichment analysis was performed using the differentially bound sites of active gene markers (i.e., H3K27Ac and H3K4me3) between monocytes and NK cells, identified by DESeq2 (**Figure 4.15-4.16**). Although a few shared pathways were identified, the comparison

between the cell types highlighted the characteristic functions of each innate immune cell. For example, enriched pathway terms in monocytes included "*Lysosome*" and "*Fc gamma R-mediated phagocytosis*," indicating that genes associated with phagocytosis were marked as active gene regions in monocytes compared to NK cells, in line with their described function [125,501]. In contrast, the enriched pathways terms in NK cells included "*Natural killer cell mediated cytotoxicity*" and "*Calcium signaling pathways*," indicating the genes associated with their cytotoxicity functions were active [502].

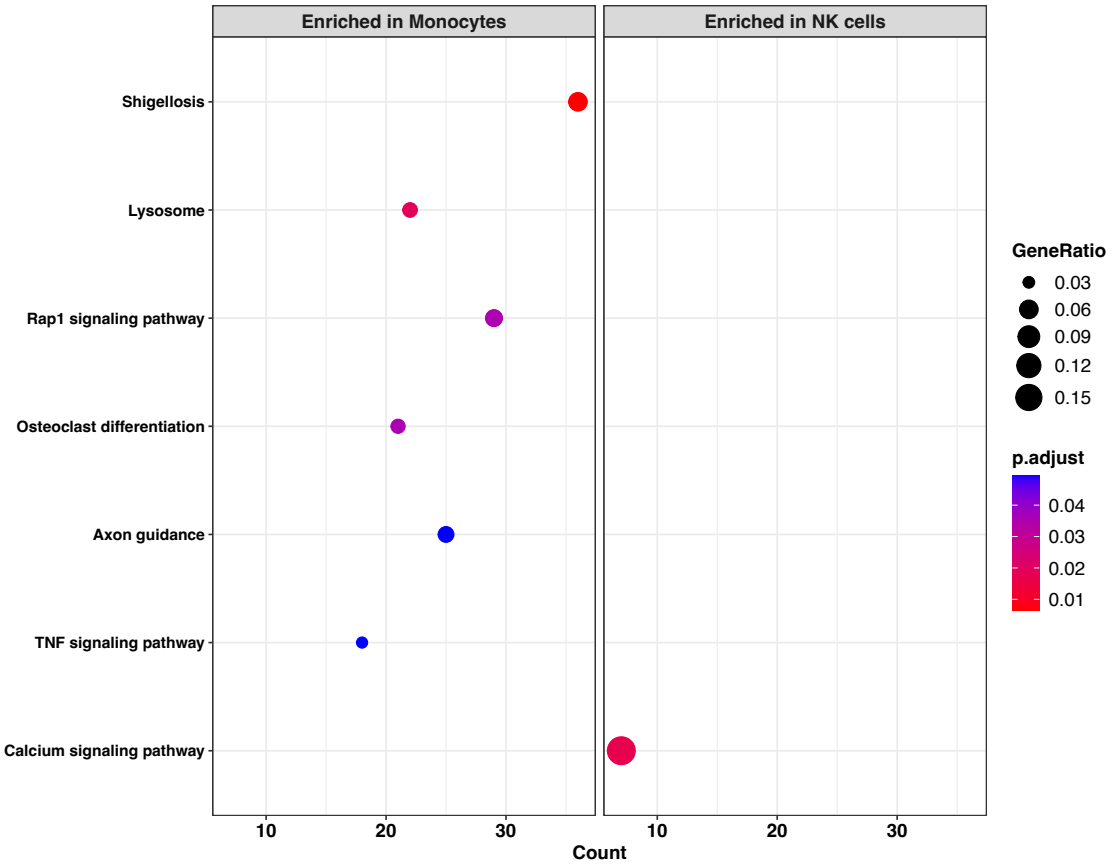

Figure 4.15. Pathway enrichment analysis of H3K27Ac between cell types. Differentially bound regions of H3K27Ac between monocytes and NK cells were assessed for pathway enrichment analysis using the KEGG database. Gene ratios (the proportion of enriched genes in each group) were calculated by dividing the "count of core enrichment genes" by the "count of pathway genes." Gene ratios of the top pathway categories are plotted based on gene count. The dot size represents gene ratios, and the color indicates the adjusted *P*-value. Abbreviations: H3K27Ac, acetylation of histone H3 at lysine 27; KEGG, Kyoto Encyclopedia of Genes and Genomes; NK cells, natural killer cells; Rap1, Ras-related protein 1; TNF, tumor necrosis factor.

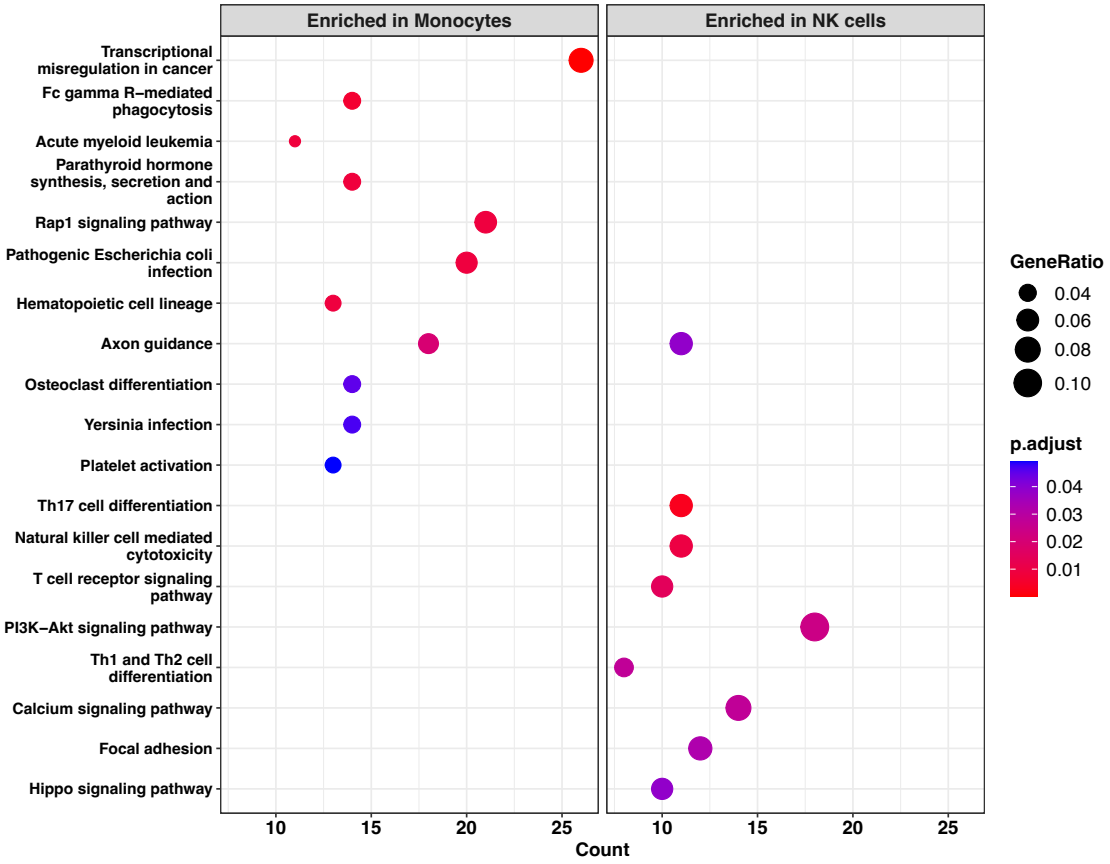

Figure 4.16. Pathway enrichment analysis of H3K4me3 between cell types. Differentially bound regions of H3K4me3 between monocytes and NK cells were assessed for pathway enrichment analysis using the KEGG database. Gene ratios (the proportion of enriched genes in each group) were calculated by dividing the "count of core enrichment genes" by the "count of pathway genes." Gene ratios of the top pathway categories are plotted based on gene count. The dot size represents gene ratios, and the color indicates the adjusted *P*-value. Abbreviations: H3K4me3, trimethylation of histone H3 at lysine 4; KEGG, Kyoto Encyclopedia of Genes and Genomes; NK cells, natural killer cells; PI3K, phosphoinositide 3-kinases; Akt, protein kinase B; Rap1, Ras-related protein 1; Th, T helper cell.

In NK cells, several pathway terms linked to the activation and differentiation of T cells were also highly marked with H3K4me3. These terms include "*Th17 cell differentiation*," "*Th1 and Th2 cell differentiation*," and "*T cell receptor signaling pathway*" (**Figure 4.16**). Further analysis using a gene-concept network revealed many of the genes involved in the T cell activation/differentiation pathways were also involved in the "*Natural killer cell mediated cytotoxicity*" pathway, including CD247, linker for activation of T cells (LAT), lymphocyte cell-specific protein tyrosine kinase (LCK), nuclear factor of activated T cells 2 (NFATC2), and zeta-chain-associated protein kinase 70 (ZAP-70) (**Figure 4.17**).

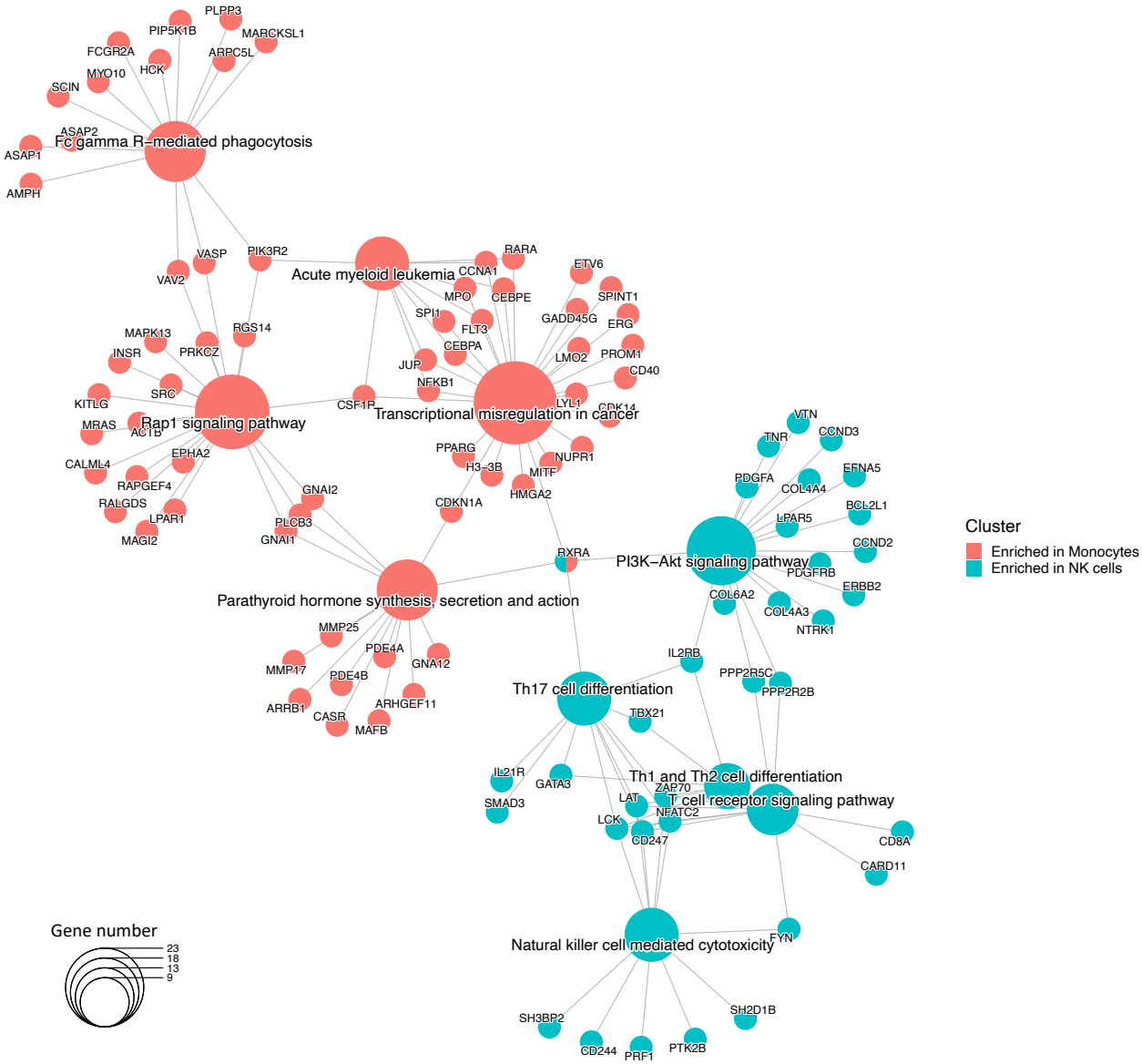

Figure 4.17. Gene-concept network analysis on enriched KEGG pathways (H3K4me3) between cell types. Enriched pathways (represented by nodes), obtained from KEGG pathway analysis of differentially bound regions between monocytes and NK cells based on the H3K4me3 marker, were linked with genes involved in the pathways. Pathways and genes were colored by the cluster type (either enriched in Monocytes or NK cells). Abbreviations: KEGG, Kyoto Encyclopedia of Genes and Genomes; NK cells, natural killer cells; H3K4me3, trimethylation of histone H3 at lysine 4.

Overall, as the enriched signaling pathways matched the canonical functions of monocytes or NK cells, these results serve as another indication that CUT&Tag can successfully identify the binding sites of a histone marker within a specific cell type of interest.

4.5. Discussion

The literature on BCG-induced trained innate immunity and its associated epigenetic modifications among infants is scarce. In particular, to our knowledge, no studies have examined whether iHEU, who are at a higher risk of infectious morbidity [415,425], receive similar levels of protection through trained innate immunity as iHUU. One of the reasons so few infant studies exist is that the widely used method for investigating epigenetic modifications, ChIP-seq, requires more than 1 million cells per target protein of interest [24–26]. This poses challenges when the sample availability and cell number are limited. To address this issue, we applied a recently established CUT&Tag assay [118,119, 121,479]. The assay protocol was optimized for the ideal experimental conditions to evaluate three histone modifications using limited cells that could be obtained from six- to seven-week-old South African infants. Optimization included consideration of the minimum number of input cells, number of PCR cycles, and sequencing depth to ensure the feasibility of the assay while maintaining high data quality for the downstream analysis. In addition, optimization of bioinformatic analysis steps, such as choice of peak caller and option for peak calling parameters, was performed.

Utilizing the IgG control sample for normalization in SEACR led to conflicting outcomes. This discrepancy could be attributed to the notably lower sequencing depth observed in the IgG sample (386,781 reads) compared to the other samples (6,324,145 reads on average). In fact, the developer of SEACR reports that low sequencing depth or substantial depth variation between the control and samples may impact the precision of peak calling [499]. This supports our rationale for opting to use a numerical threshold approach, which will likely ensure more reliable peak calling results.

The CUT&Tag peaks showed characteristic distribution patterns based on the histone modifications. For instance, the H3K4me3 marker, an active gene marker often found at gene promoter regions and CpG islands [500], displayed significant enrichment within a 1 kbp proximity to the promoter regions. It is worth noting that while the pattern aligned with that of a previous study [95], the proportion of peaks assigned to promoter regions was slightly higher in our study. This disparity could be due to the difference in the SEACR peak calling mode used in the analysis (relaxed vs. stringent mode) or sample types analyzed [95]. The H3K27Ac marker, an active gene marker that marks distal promoter and enhancer regions [503,504], exhibited a

different enrichment pattern. H3K27Ac was not only enriched in promoter regions (within 1 kbp) but also enriched in intron and distal intergenic regions. Interestingly, contrasting patterns of H3K27Ac marks were observed between monocytes and NK cells, though the implication of this difference on their immune functions remains unexplored. Lastly, the H3K27me3 marker, indicative of repressed gene regions, displayed prominent enrichment at promoter regions and more evenly enriched peaks at other locations than the other two histone markers. This distinctive characteristic may be because H3K27me3 broadly marks genomic regions [505].

The pathway enrichment analysis of differentially bound sites between monocytes and NK cells identified activating histone marks according to the distinct functional profiles of each cell type. These include pathway terms related to phagocytosis in monocytes [125,501] and cytotoxic function in NK cells [502], highlighting the accuracy of CUT&Tag assay outcomes. Interestingly, several pathway terms related to T cell activation and differentiation were also identified in NK cells, including "*Th17 cell differentiation*," "*Th1 and Th2 cell differentiation*," and "*T cell receptor signaling pathway*." Since the CD3+ cell population was excluded during the cell sorting process, it is unlikely that these pathways were attributed to natural killer T (NKT) cells, which are known to possess characteristics of both NK cells (CD56+) and T cells (CD3+ and TCR+) [506]. Although secretion of IFN-γ in NK cells can directly promote Th1 cell differentiation without prior priming by antigen-presenting cells (APCs) [507,508], identification of broad aspects related to T cell activation and differentiation suggests that genes commonly active in both NK cells and T cells were marked as enriched pathways. Supporting this, the gene-concept network analysis identified several genes that are involved with both NK cell-mediated cytotoxicity and T cell activation and differentiation pathways.

The limitation of this study includes a small sample size, as only a subset of samples was used for this initial optimization. This was intentional, aligning with the primary objectives of Aim 3, which was to optimize the CUT&Tag assay protocol and validate data accuracy to meet the parent project's specific requirements, which is currently still blinded. Blinding also limited the capacity to evaluate epigenetic changes induced by BCG vaccination and HIV exposure. Another limitation of this study is that the cells were not stimulated prior to the assay to avoid potential sample loss. This approach might have limited our ability to detect changes in histone modifications and

associated immune responses. Nevertheless, it is worth noting that during the CUT&Tag assay, cells were bound to beads conjugated with ConA, which has been reported to induce stimulation in innate immune cells, including monocytes and NK cells [509,510]. Consequently, incubation with ConA beads might have sufficiently stimulated the cells.

In summary, the optimized CUT&Tag assay successfully demonstrated its capability to analyze multiple histone modifications in infant monocytes and NK cells, utilizing only 5,000 cells as input. In contrast to the conventional ChIP-seq technique, this approach allows us to investigate histone modifications using precious samples or rare cell populations. This is particularly relevant in the realm of clinical studies, where sample availability is often limited [182]. Although the primary focus of this study was histone modifications, this optimized approach can be extended to chromatin-protein interactions (such as transcriptional factors). The findings of the peak distribution patterns, sample correlation, and pathway enrichment analysis collectively indicate the successful assay outcome. This supports implementing our optimized CUT&Tag assay protocol on a bigger sample scale in the future study to explore the effects of *in utero* HIV exposure in the context of BCG-induced trained innate immunity. The findings we gain from this future investigation would be valuable, as the existing literature has thus far only investigated the epigenetic changes associated with trained innate immunity in infants using ChIP-qPCR [188], which limits the assessment to specific gene regions. In contrast, our approach offers an unbiased global view, allowing us to uncover other gene regions involved in trained innate immunity.

Chapter 5. Discussion

Since 2013, prevention of vertical HIV transmission has been shifting towards Option B+, an approach in which all pregnant women living with HIV receive lifelong ART irrespective of their CD4 count [4]. Consequently, there has been a substantial reduction in vertical HIV transmissions, leading to the growing population of iHEU, especially in sub-Saharan Africa [372]. Globally, including in low- or middle-income settings, all mothers, including those with HIV, are advised to exclusively breastfeed their infants for the first six months of life. This is followed by a combination of complementary feeding and breastfeeding for up to 24 months of age. This recommendation is based on the understanding that the benefits of breastfeeding outweigh the risk of HIV transmission [13]. Furthermore, since 2000, co-trimoxazole prophylaxis has been strongly advised for iHEU, starting at six weeks of age until infants test negative for HIV after the cessation of breastfeeding, albeit its necessity was under debate for some years [511]. It is important to note that this guideline has been revised in South Africa in 2023, and iHEU became no longer eligible for the co-trimoxazole prophylaxis [512]. Accumulating studies indicate that iHEU face an elevated risk of hospitalization, primarily due to infectious diseases such as diarrhea and respiratory infections during the first two years of life, and especially during the first three to six months of life [373,374, 378, 380,513–520]. Factors contributing to this vulnerability appear to be maternal health parameters (such as viral load, CD4 count, and the timing of ART initiation), feeding practices, infants' gestational age at birth, and vaccination timing [373, 378, 380, 514,516–518]. The majority of these increased hospitalization risks were reported before Option B+ was recommended by the WHO [373,374, 378, 380, 514,515, 517,519,520]. While universal use of ART during pregnancy may improve some of the maternal health parameters associated with increased morbidity risk in their infants, adverse health outcomes may nonetheless persist among iHEU in the Option B+ era [513,518]. Mechanisms underlying this increased vulnerability are considered to be altered immunity and/or gut microbiota [396,397, 404,405,521,522], though the exact mechanisms remain unclear.

In this dissertation, the primary focus was investigating possible mechanisms responsible for this increased infectious morbidity risk among iHEU. The specific objectives were: (1) to investigate whether BCG provides comparable protection against TBI and disease in iHEU and iHUU (Aim

1; described in Chapter 2); (2) to examine the effect of HIV exposure on longitudinal gut microbiota composition and association with TT vaccine response (Aim 2; described in Chapter 3); and (3) to optimize an epigenetic assay protocol, intended for future investigation of BCG-induced histone modifications in iHEU (Aim 3; described in Chapter 4). Using ongoing and completed parent studies, these aspects were explored in sub-Saharan African infants born between 2013 and 2019.

In Chapter 2, we report that the overall TBI prevalence in 9-18 months-old infants living in South Africa and Botswana (293 iHEU and 125 iHUU) was low (3.3%), and no infants were diagnosed with TB disease. Notably, this prevalence was similar between HIV exposure groups, and the trend was consistent across both countries. Our finding contradicts previous reports, which showed a higher TBI prevalence among iHEU in sub-Saharan African regions [418,523,524] and Botswana/ South Africa settings [382,383]. In addition, a study conducted in Uganda reported that iHEU were at a greater risk of TBI than iHUU [42]. These disparities between our findings and previous studies are likely due to differences in study cohort characteristics: (1) some previous studies assessed TBI prevalence prior to the introduction of universal ART and during the period with a higher occurrence of TBI compared to recent years compared to our study [382,383,418]; (2) a previous study included participants with previous TB disease in their cohort [383]; (3) several studies measured TBI prevalence in older participants than our study, potentially resulting in a longer window of TB exposure [42,383]; (4) some studies used TST, a standard method for measuring TBI in the pediatric population [523,524], though this method is less specific than IGRAs due to a tendency to produce false positives because of cross-reactivity with BCG and environmental mycobacteria [525].

Specifically, few studies have investigated the prevalence of TBI using IGRA-based approaches among iHEU under two years of age who were born after Option B+ has been recommended [523,524]. Among these studies, research conducted on Kenyan infants by LaCourse *et al*. revealed that while the TBI prevalence in iHEU was 10.1% at one year of age, this result was primarily influenced by TST, and the IGRA positivity rate tested on the same cohort was only 1.2% [523]. Similarly, a follow-up study by Warr *et al*. reported that the TBI prevalence of iHEU at 18 months of age was 9.6% using TST and 1.1% using IGRA [524]. Additionally, Warr *et al*. noted that the

iHEU born to virally suppressed mothers during pregnancy had a higher BCG-induced CD4+ IFN-γ+ responses (but not IL-2, TNF, and IL-17 responses) at 6-10 weeks of age compared to iHEU born from mothers who are newly diagnosed with HIV during pregnancy with measurable HIV viral loads. Moreover, cytokine responses of infants of mothers who are diagnosed with HIV before pregnancy and had measurable HIV viral loads during pregnancy were not different from infants of mothers with suppressed viral load or who are newly diagnosed with HIV during pregnancy [524]. In our study, 93.2% of mothers with HIV were virally suppressed at enrollment, which may explain why iHEU had comparable protection from BCG vaccination against TBI as iHUU. Nevertheless, given that iHEU tend to have altered immunity [396,397,521,522], and about 20% of young children with TBI develop TB disease within two years [526], it remains unclear whether iHEU with TBI are at a higher risk of developing TB disease at a later stage. A multi-country longitudinal study with an extended follow-up period is essential to address this question. Lastly, testing non-IFN-γ markers (such as IP-10, IL-2, MCP-2, and TNF-α) has been proposed as an alternative approach for detecting TBI [524,527–529]. Notably, Warr *et al.* demonstrated that TST results were imprecise, while the non-IFN-γ cytokine detection approach proved to be a more suitable method for identifying TBI in infants [524]. Considering that the pediatric population, especially iHEU, often exhibit reduced IFN-γ responses to antigens [389, 401, 420,472], utilizing these non-IFN-γ markers for TBI testing may hold significant importance for future research for a better TBI prevalence estimation.

In Chapter 3, we investigated the impact of HIV exposure on humoral response to the TT vaccine and its relationship with infant gut microbiota. Our study is one of the largest to date that longitudinally investigated the gut microbiota composition in multiple countries: Nigeria and South Africa (total n = 278; 202 iHEU and 76 iHUU). In our study, all Nigerian infants were exclusively breastfed, whereas feeding practice among South African infants comprised exclusive breastfeeding and mixed feeding. This difference between the countries was due to the sample selection process in the parent study and not a reflection of mothers' preferences in each country. In Nigeria, infants were selected based on their feeding status of being exclusively breastfed during the first 15 weeks of age, whereas in South Africa, the selection criteria focused on infants who were breastfed during the study. For this reason, we assessed the impact of feeding practice on infants' gut microbiota to investigate any potential bias this may have caused. However, we did

not find any significant effects. The crosstalk between gut microbiota and immune cells during early life is critical for developing mucosal and systemic immune systems, and gut microbiota perturbations are associated with a higher risk of infectious morbidity [530–532]. Our study indicated that HIV exposure did not influence the alpha- and beta-diversity during the first 15 weeks of life, even among exclusively breastfed infants. This suggests that, despite altered HMO composition often observed in women living with HIV [404,533], there were no stark differences in the gut microbiota of iHEU. This also implies that the impact of co-trimoxazole prophylaxis treatment for iHEU was likely marginal, which contradicts other studies that have found that co-trimoxazole may perturb infant gut microbiota [534,535]. Nonetheless, we identified some bacterial taxa that were differentially enriched in iHEU compared to iHUU. These bacteria included several *Klebsiella* species (such as *K. quasipneumoniae*, *K. pneumoniae*, and *K. variicola*). While *K. pneumoniae* has been identified in immunocompromised patients with diarrhea [536,537] and can be an invasive pathogen, whether this contributes to the increased morbidity in iHEU is yet to be explored. Although some studies have previously shown evidence of altered gut microbiota among iHEU [404,405], our results support the notion that the effect of HIV exposure on gut microbiota is likely dependent on geographical location or cohort-specific characteristics [406].

Regarding humoral immunity in the infants, we observed some evidence of the effects of HIV exposure. Consistent with other studies [400,538–540], maternal HIV infection impaired passive maternal antibody transfer, and iHEU exhibited lower anti-tetanus titers at birth. At 15 weeks of age, iHEU had significantly lower anti-tetanus titers than iHUU. Of note, most infants still reached protective levels of anti-tetanus titers (> 0.1 IU/ml). The effects of this noted antibody response should be explored for other vaccines for which protective titers are not universally achieved after the primary series, such as pertussis. In contrast to the altered immune responses in iHEU, we did not observe any differences in maternal anti-tetanus titers based on their HIV infection status. Previous research has shown that anti-tetanus IgG titers are influenced by CD4+ count [400]. In our study, the majority (98.5%) of our mothers with HIV were on ART at delivery and 81% had a CD4+ count > 250 cells/mm^3. Yet despite this, transplacental IgG transfer was altered.

The LASSO regression models indicated that gut microbiota and *in utero* HIV exposure were independently associated with TT vaccine responses at 15 weeks of age. However, this was more the case in South Africa than in Nigeria. Nigerian mothers were encouraged to receive TT vaccination during pregnancy, whereas South African mothers were not. This resulted in significantly higher maternal IgG titers among Nigerian infants at week 1 of age, which may have interfered with vaccine responses among the infants, although this phenomenon is more striking with live vaccines [452,541]. Indeed, the elevated baseline anti-tetanus titers stayed very similar post-vaccination in Nigerian infants. It has been documented that maternal HIV alters transplacental IgG transfer [542]. Yet, despite lower passive antibodies, iHEU mounted a lower response to vaccination, suggesting this was not due to inhibition by maternal antibody. Whether this is due to B cell functional abnormalities is unknown, but certain gut microbes can modulate adaptive responses through immune priming, thereby possibly influencing the TT vaccine response. The role of bacterial antigens and/or SCFAs produced by bacteria in this association is an area that warrants further exploration [543–545]. Collecting additional data, both on the maternal side (such as vaginal or breastmilk microbiota) and on the infant side (such as gut metabolomics, metatranscriptomics, and metagenomics), could have provided further insights into the mechanisms of microbiota influence on TT vaccine responses.

In Chapter 4, the primary objective was to develop an assay to investigate a potential contributing factor for the increased infectious morbidity observed in iHEU from the perspective of innate immunity. There is a significant knowledge gap in relation to the potential association between HIV exposure and trained innate immunity. This gap is partially because the standard methodology typically requires a large number of cells, which limits the ability to globally investigate histone modification markers of trained innate immunity using infant samples [117]. To address this challenge, we optimized the recently established CUT&Tag protocol and its downstream analysis for infant samples. We successfully characterized multiple histone modifications in infant monocytes and NK cells by applying the optimized protocol to infant samples, even with ultra-low cell input. The investigation of the effect of HIV exposure on trained innate immunity will be undertaken in the near future. Importantly, a previous study has shown that the time of maternal ART initiation, whether during pregnancy or before conception, can affect monocyte activation

and hospitalization rate in iHEU [546]. This may be mediated by differing degrees of trained innate immunity induced by BCG.

Throughout this dissertation, we focused on infants living in sub-Saharan Africa, a region where 90% of iHEU reside [372]. To capture a comprehensive perspective, we included infants from three countries: South Africa, Botswana, and Nigeria. We explored the mechanisms underlying the increased vulnerability often observed in iHEU and addressed this question broadly (Aims 1-3). Overall, our findings indicated that iHEU exhibited reduced passive maternal tetanus antibody levels at one week of age and lower plasma IgG anti-tetanus antibody titers after receiving three doses of TT vaccinations by 15 weeks of age, suggesting that iHEU have impaired humoral responses, possibly related to certain gut microbes. On the other hand, the prevalence of TBI, based on the T cell IFN-γ release in response to TB antigens, was similar between the HIV exposure groups in infants aged 9-18 months. Whether iHEU receive BCG-induced non-specific immune protection remains to be investigated in the near future. With the implementation of improved health care programs (such as the universal maternal ART, good vaccine coverage, exclusive breastfeeding, and co-trimoxazole prophylaxis), the health risks associated with the iHEU population have declined in recent years at least during the first two years of life. Supporting this, studies investigated hospitalization rates during the first year of life among infants born in South Africa during Option B+ era were similar between HIV exposure groups [417], or the effect of exposure was only temporary (up to the first three months) [518]. Similarly, a study in Botswana showed a reduction in infectious morbidity cases among iHEU following the introduction of the Rotavirus vaccine and the pneumococcal conjugate vaccine in 2012 [547]. Furthermore, our cohort of iHEU may represent a relatively "healthier" group by benefitting from timely vaccination and access to extensive counseling and health care throughout the study.

It is important to acknowledge certain limitations. We did not assess the same mother-infant pairs across the projects within this dissertation, which may have limited a comprehensive evaluation. Although all three study sites investigated in this dissertation face challenges related to HIV and TB infections [2,419], differences in cohort demographics may had an impact on the results. For example, Khayelitsha Site B is a heavily populated informal settlement (10,120 persons/km^2) in South Africa with inadequate sanitation and high unemployment and crime rates [548,549]. Jos is

the capital of Plateau State in Nigeria and is a densely populated area (2,489 persons/km^2) [550]. Although Nigeria faces vast economic disparities as a nation [551], mothers recruited in the study showed a high employment rate compared to South African mothers. Compared to the other two sites, malaria infection cases are significantly higher in Nigeria, accounting for 27% of malaria cases in the world [552]. Gaborone is a capital city of Botswana with better sanitation and less density populated (1,444 persons/km^2) compared to the other two study sites [553]. Moreover, because women with HIV experience a higher risk of preterm birth [554–557] and premature babies are often at risk of infectious disease [558,559], we may have missed assessing the most vulnerable group by excluding them from the parent studies. In summary, the results from this dissertation uncovered some immunological differences that remain between iHEU and iHUU in the B+ era, but mechanisms for increased risk of infectious morbidity deserve further investigation.

REFERENCES

1. Joint United Nations Programme on HIV/AIDS. UNAIDS Global AIDS Update 2022 [Internet]. 2022 [cited 2023 Mar 7]. Available from: https://www.unaids.org/sites/default/files/media_asset/2022-global-aids-update_en.pdf
2. UNICEF. Children, HIV and AIDS, Regional snapshot: Sub-Saharan Africa [Internet]. 2019 [cited 2023 Mar 7]. Available from: https://data.unicef.org/resources/children-hiv-and-aids-global-and-regional-snapshots-2019/
3. Kore G. Review article HIV in pregnancy. International Journal of Reproduction, Contraception, Obstetrics and Gynecology. **2021**; 10(3):1241–1246.
4. WHO. Programmatic Update: Use of Antiretroviral Drugs for Treating Pregnant Women and Preventing Hiv Infection in Infants: Executive Summary [Internet]. 2012 [cited 2023 Mar 7]. Available from: https://iris.who.int/handle/10665/70892?&locale-attribute=fr
5. WHO GHO. Estimated percentage of pregnant women living with HIV who received antiretrovirals for preventing mother-to-child transmission [Internet]. 2022 [cited 2023 Aug 21]. Available from: https://www.who.int/data/gho/data/indicators/indicator-details/GHO/estimated-percentage-of-pregnant-women-living-with-hiv-who-received-antiretrovirals-for-preventing-mother-to-child-transmission#:~:text=Globally%2C
6. Tweya H, Gugsa S, Hosseinipour M, Speight C, Ng'ambi W, Bokosi M, Chikonda J, Chauma A, Khomani P, Phoso M, Mtande T, Phiri S. Understanding factors, outcomes and reasons for loss to follow-up among women in Option B+ PMTCT programme in Lilongwe, Malawi. Tropical Medicine and International Health. **2014**; 19(11):1360–1366.
7. Chadambuka A, Katirayi L, Muchedzi A, Tumbare E, Musarandega R, Mahomva AI, Woelk G. Acceptability of lifelong treatment among HIV-positive pregnant and breastfeeding women (Option B+) in selected health facilities in Zimbabwe: A qualitative study. BMC Public Health. **2017**; 18:57.
8. Kieffer MP, Mattingly M, Giphart A, Ven R Van De, Chouraya C, Walakira M, Boon A, Mikusova S, Simonds RJ. Lessons learned from early implementation of option B+: The elizabeth glaser pediatric aids foundation experience in 11 African countries. Journal of Acquired Immune Deficiency Syndromes. **2014**; 67(Suppl 4):S188–S194.
9. Zijenah LS, Bandason T, Bara W, Chipiti MM, Katzenstein DA. Mother-to-child transmission of HIV-1 and infant mortality in the first six months of life, in the era of Option B Plus combination antiretroviral therapy. International Journal of Infectious Diseases. **2021**; 109:92–98.
10. Kalua T, Barr BAT, Oosterhout JJ Van, Mbori-Ngacha D, Schouten EJ, Gupta S, Sande A, Zomba G, Tweya H, Lungu E, Kajoka D, Tih P, Jahn A. Lessons learned from option B+ in the evolution toward test and start from Malawi, Cameroon, and the United Republic of Tanzania. Journal of Acquired Immune Deficiency Syndromes. **2017**; 75(Suppl 1):S43–S50.
11. UNAIDS. Countdown to zero: Global plan towards the elimination of new HIV infections among children by 2015 and keeping their mothers alive, 2011-2015 [Internet]. 2011 [cited 2023 Mar 7]. Available from: https://www.unaids.org/sites/default/files/media_asset/20110609_JC2137_Global-Plan-Elimination-HIV-Children_en_1.pdf
12. UNAIDS. Start Free, Stay Free, AIDS Free Final report on 2020 targets [Internet]. 2021 [cited 2023 Mar 7]. Available from: https://www.unaids.org/sites/default/files/media_asset/2021_start-free-stay-free-aids-free-

final-report-on-2020-targets_en.pdf
13. WHO and UNICEF. Updates on HIV and Infant Feeding: the duration of breastfeeding, and support from health services to improve feeding practices among mothers living with HIV. [Internet]. 2016 [cited 2023 Mar 7]. Available from: https://www.who.int/publications/i/item/9789241549707
14. CDC. HIV Treatment as Prevention [Internet]. 2023 [cited 2023 Mar 7]. Available from: https://www.cdc.gov/hiv/risk/art/index.html
15. Penazzato M, Kasirye I, Ruel T, Mukui I, Bekker A, Archary M, Musoke P, Essajee S, Siberry GK, Mahy M, Simnoue D, Simione B, Zech JM, Mushavi A, Abrams EJ. Antiretroviral postnatal prophylaxis to prevent HIV vertical transmission: present and future strategies. Journal of the International AIDS Society. **2023**; 26(2):e26032.
16. WHO. Global Tuberculosis Report 2019 [Internet]. 2019 [cited 2023 Mar 7]. Available from: https://www.who.int/publications/i/item/9789241565714
17. MacNeil A, Glaziou P, Sismanidis C, Date A, Maloney S, Floyd K. Global Epidemiology of Tuberculosis and Progress Toward Meeting Global Targets — Worldwide, 2018. MMWR Morbidity and Mortality Weekly Report. **2020**; 69(11):281–285.
18. Rao VG, Gopi PG, Bhat J, Selvakumar N, Yadav R, Tiwari B, Gadge V, Bhondeley MK, Wares F. Pulmonary tuberculosis: A public health problem amongst the Saharia, a primitive tribe of Madhya Pradesh, Central India. International Journal of Infectious Diseases. International Society for Infectious Diseases; **2010**; 14(8):e713–e716.
19. Rie A Van, Beyers N, Gie RP, Kunneke M, Zietsman L, Donald PR. Childhood tuberculosis in an urban population in South Africa: burden and risk factor. Archives of Disease in Childhood. **1999**; 80(5):433–437.
20. Jenkins HE, Tolman AW, Yuen CM, Parr JB, Keshavjee S, Pérez-Vélez CM, Pagano M, Becerra MC, Cohen T. Incidence of multidrug-resistant tuberculosis disease in children: Systematic review and global estimates. The Lancet. **2014**; 383(9928):1572–1579.
21. Dodd PJ, Gardiner E, Coghlan R, Seddon JA. Burden of childhood tuberculosis in 22 high-burden countries: A mathematical modelling study. The Lancet Global Health. **2014**; 2(8):e453-9.
22. Martinez L, Roux DM le, Barnett W, Stadler A, Nicol MP, Zar HJ. Tuberculin skin test conversion and primary progressive tuberculosis disease in the first 5 years of life: a birth cohort study from Cape Town, South Africa. The Lancet Child and Adolescent Health. **2018**; 2(1):46–55.
23. Agyeman AA, Ofori-Asenso R. Tuberculosis—an overview. Journal of Public Health and Emergency. **2017**; 1:7–7.
24. Frieden TR, Sterling TR, Munsiff SS, Watt CJ, Dye C. Tuberculosis. The Lancet. **2003**; 362:887–899.
25. Liu CH, Liu H, Ge B. Innate immunity in tuberculosis: host defense vs pathogen evasion. Cellular and Molecular Immunology. **2017**; 14(12):963–975.
26. Ramakrishnan L. Revisiting the role of the granuloma in tuberculosis. Nature Reviews Immunology. **2012**; 12(5):352–366.
27. Silva Miranda M, Breiman A, Allain S, Deknuydt F, Altare F. The tuberculous granuloma: An unsuccessful host defence mechanism providing a safety shelter for the bacteria? Clinical and Developmental Immunology. **2012**; 2012:139127.
28. Green AM, DiFazio R, Flynn JL. IFN-γ from CD4 T Cells Is Essential for Host Survival and Enhances CD8 T Cell Function during Mycobacterium tuberculosis Infection. The

Journal of Immunology. **2013**; 190(1):270–277.
29. Roca FJ, Whitworth LJ, Redmond S, Jones AA, Ramakrishnan L. TNF Induces Pathogenic Programmed Macrophage Necrosis in Tuberculosis through a Mitochondrial-Lysosomal-Endoplasmic Reticulum Circuit. Cell. **2019**; 178(6):1344–1361.e11.
30. Esmail H, Macpherson L, Coussens AK, Houben RMGJ. Mind the gap – Managing tuberculosis across the disease spectrum. eBioMedicine. **2022**; 78:103928.
31. Furin J, Cox H, Pai M. Tuberculosis. The Lancet. **2019**; 393(10181):1642–1656.
32. Drain PK, Bajema KL, Dowdy D, Dheda K, Naidoo K, Schumacher SG, Ma S, Meermeier E, Lewinsohn DM, Sherman DR. Incipient and subclinical tuberculosis: A clinical review of early stages and progression of infection. Clinical Microbiology Reviews. **2018**; 31(4):e00021-18.
33. Agbota G, Bonnet M, Lienhardt C. Management of Tuberculosis Infection: Current Situation, Recent Developments and Operational Challenges. Pathogens. **2023**; 12(3):362.
34. Nolt D, Starke JR. Tuberculosis Infection in Children and Adolescents: Testing and Treatment. Pediatrics. **2021**; 148(6):e2021054663.
35. Mathad JS, Yadav S, Vaidyanathan A, Gupta A, LaCourse SM. Tuberculosis Infection in Pregnant People: Current Practices and Research Priorities. Pathogens. **2022**; 11(12):1481.
36. Zhao A, Butala N, Luc CM, Feinn R, Murray TS. Telehealth Reduces Missed Appointments in Pediatric Patients with Tuberculosis Infection. Tropical Medicine and Infectious Disease. **2022**; 7(2):26.
37. Shammari B Al, Shiomi T, Tezera L, Bielecka MK, Workman V, Sathyamoorthy T, Mauri F, Jayasinghe SN, Robertson BD, D'Armiento J, Friedland JS, Elkington PT. The Extracellular Matrix Regulates Granuloma Necrosis in Tuberculosis. Journal of Infectious Diseases. **2015**; 212(3):463–473.
38. Clemens DL, Horwitz MA. The Mycobacterium tuberculosis phagosome interacts with early endosomes and is accessible to exogenously administered transferrin. Journal of Experimental Medicine. **1996**; 184(4):1349–1355.
39. Saini NK, Baena A, Ng TW, Venkataswamy MM, Kennedy SC, Kunnath-Velayudhan S, Carreño LJ, Xu J, Chan J, Larsen MH, Jacobs WR, Porcelli SA. Suppression of autophagy and antigen presentation by Mycobacterium tuberculosis PE-PGRS47. Nature Microbiology. **2016**; 1(9):16133.
40. Portal-Celhay C, Tufariello JM, Srivastava S, Zahra A, Klevorn T, Grace PS, Mehra A, Park HS, Ernst JD, Jacobs WR, Philips JA. Mycobacterium tuberculosis EsxH inhibits ESCRT-dependent CD4+ T-cell activation. Nature Microbiology. **2016**; 2:16232.
41. Pinto R, Nambiar JK, Leotta L, Counoupas C, Britton WJ, Triccas JA. Influence of phthiocerol dimycocerosate on CD4+ T cell priming and persistence during Mycobacterium tuberculosis infection. Tuberculosis. **2016**; 99:25–30.
42. Marquez C, Chamie G, Achan J, Luetkemeyer AF, Kyohere M, Okiring J, Dorsey G, Kamya MR, Charlebois ED, Havlir D V. Tuberculosis Infection in Early Childhood and the Association with HIV-exposure in HIV-uninfected Children in Rural Uganda. Pediatric Infectious Disease Journal. **2016**; 35(5):524–529.
43. Machingaidze S, Wiysonge CS, Hussey GD. Strengthening the Expanded Programme on Immunization in Africa: Looking beyond 2015. PLoS Medicine. **2013**; 10(3):e1001405.
44. Bland J, Clements J. Protecting the world's children: The story of WHO's immunization programme. World Health Forum. **1998**; 19(2):162–173.
45. WHO. Newsroom: Immunization [Internet]. 2019 [cited 2023 Jan 8]. Available from:

https://www.who.int/news-room/facts-in-pictures/detail/immunization
46. Fine PE. Variation in protection by BCG: implications of and for heterologous immunity. The Lancet. **1995**; 346(8986):1339–1345.
47. Hesseling AC, Rabie H, Marais BJ, Manders M, Lips M, Shaaf HS, Gie RP, Cotton MF, Helden PD Van, Warren RM, Beyers N. Bacille Calmette-Guérin Vaccine-Induced Disease in HIV-Infected and HIV-Unifected Children. Clinical Infectious Diseases. **2006**; 42(4):548–558.
48. Mangtani P, Abubakar I, Ariti C, Beynon R, Pimpin L, Fine PEM, Rodrigues LC, Smith PG, Lipman M, Whiting PF, Sterne JA. Protection by BCG vaccine against tuberculosis: A systematic review of randomized controlled trials. Clinical Infectious Diseases. **2014**; 58(4):470–480.
49. Dodd PJ, Yuen CM, Sismanidis C, Seddon JA, Jenkins HE. The global burden of tuberculosis mortality in children: a mathematical modelling study. The Lancet Global Health. **2017**; 5(9):e898–e906.
50. Abubakar I, Pimpin L, Ariti C, Beynon R, Mangtani P, Sterne J, Fine P, Smith P, Lipman M, Elliman D, Watson J, Drumright L, Whiting P, Vynnycky E. Systematic review and meta-analysis of the current evidence on the duration of protection by bacillus Calmette-Guérin vaccination against tuberculosis. Health Technology Assessment. **2013**; 17(37):1–4.
51. Sterne JAC, Rodrigues LC, Guedes IN. Does the efficacy of BCG decline with time since vaccination? International Journal of Tuberculosis and Lung Disease. **1998**; 2(3):200–207.
52. Nguipdop-Djomo P, Heldal E, Rodrigues LC, Abubakar I, Mangtani P. Duration of BCG protection against tuberculosis and change in effectiveness with time since vaccination in Norway: A retrospective population-based cohort study. The Lancet Infectious Diseases. **2016**; 16(2):219–226.
53. Aronson NE, Santosham M, Comstock GW, Howard RS, Moulton LH, Rhoades ER, Harrison LH. Long-term Efficacy of BCG Vaccine in American Indians and Alaska Natives: A 60-Year Follow-up Study. Jama. **2004**; 291(17):2086–2091.
54. Dockrell HM, Smith SG. What Have We Learnt about BCG Vaccination in the Last 20 Years? Frontiers in Immunology. **2017**; 8:1134.
55. Marinova D, Gonzalo-Asensio J, Aguilo N, Martin C. Recent developments in tuberculosis vaccines. Expert Review of Vaccines. **2013**; 12(12):1431–1448.
56. Huda MN, Ahmad SM, Alam MJ, Khanam A, Kalanetra KM, Taft DH, Raqib R, Underwood MA, Mills DA, Stephensen CB. Bifidobacterium abundance in early infancy and vaccine response at 2 years of age. Pediatrics. **2019**; 143(2):e20181489.
57. Behr MA, Wilson MA, Gill WP, Salamon H, Schoolnik GK, Rane S, Small PM. Comparative genomics of BCG vaccines by whole-genome DNA microarray. Science. **1999**; 284(5419):1520–1523.
58. Zhang W, Zhang Y, Zheng H, Pan Y, Liu H, Du P, Wan L, Liu J, Zhu B, Zhao G, Chen C, Wan K. Genome Sequencing and Analysis of BCG Vaccine Strains. PloS one. **2013**; 8(8):e71243.
59. Ingen J Van, Zwaan R De, Dekhuijzen R, Boeree M, Soolingen D Van. Region of difference 1 in nontuberculous Mycobacterium species adds a phylogenetic and taxonomical character. Journal of Bacteriology. **2009**; 191(18):5865–5867.
60. Andersen P, Doherty TM. The success and failure of BCG - Implications for a novel tuberculosis vaccine. Nature Reviews Microbiology. **2005**; 3(8):656–662.

61. Ritz N, Dutta B, Donath S, Casalaz D, Connell TG, Tebruegge M, Robins-Browne R, Hanekom WA, Britton WJ, Curtis N. The influence of bacille Calmette-Guérin vaccine strain on the immune response against tuberculosis: A randomized trial. American Journal of Respiratory and Critical Care Medicine. **2012**; 185(2):213–222.
62. Moliva JI, Turner J, Torrelles JB. Immune responses to Bacillus Calmette-Guérin vaccination: Why do they fail to protect against mycobacterium tuberculosis? Frontiers in Immunology. **2017**; 8:407.
63. Brooks MN, Rajaram MVS, Azad AK, Amer AO, Valdivia-Arenas MA, Park JH, Núñez G, Schlesinger LS. NOD2 controls the nature of the inflammatory response and subsequent fate of Mycobacterium tuberculosis and M. bovis BCG in human macrophages. Cellular Microbiology. **2011**; 13(3):402–418.
64. Gagliardi MC, Teloni R, Giannoni F, Pardini M, Sargentini V, Brunori L, Fattorini L, Nisini R. Mycobacterium bovis Bacillus Calmette-Guérin infects DC-SIGN– dendritic cell and causes the inhibition of IL-12 and the enhancement of IL-10 production . Journal of Leukocyte Biology. **2005**; 78(1):106–113.
65. Marchant A, Goetghebuer T, Ota MO, Wolfe I, Ceesay SJ, Groote D De, Corrah T, Bennett S, Wheeler J, Huygen K, Aaby P, McAdam KPWJ, Newport MJ. Newborns Develop a Th1-Type Immune Response to Mycobacterium bovis Bacillus Calmette-Guérin Vaccination. The Journal of Immunology. **1999**; 163(4):2249–2255.
66. Covián C, Fernández-Fierro A, Retamal-Díaz A, Díaz FE, Vasquez AE, Lay MK, Riedel CA, González PA, Bueno SM, Kalergis AM. BCG-Induced Cross-Protection and Development of Trained Immunity: Implication for Vaccine Design. Frontiers in Immunology. **2019**; 10:2806.
67. Soares AP, Kwong Chung CKC, Choice T, et al. Longitudinal changes in CD4+ T-cell memory responses induced by BCG vaccination of newborns. Journal of Infectious Diseases. **2013**; 207(7):1084–1094.
68. Kristensen I, Aaby P, Jensen H. Routine vaccinations and child survival: Follow up study in Guinea-Bissau, West Africa. British Medical Journal. **2000**; 321(7274):1435–1439.
69. Garly ML, Martins CL, Balé C, Baldé MA, Hedegaard KL, Gustafson P, Lisse IM, Whittle HC, Aaby P. BCG scar and positive tuberculin reaction associated with reduced child mortality in West Africa: A non-specific beneficial effect of BCG? Vaccine. **2003**; 21(21–22):2782–2790.
70. Vaugelade J, Pinchinat S, Guiella G, Elguero E, Simondon F. Non-specific effects of vaccination on child survival: Prospective cohort study in Burkina Faso. British Medical Journal. **2004**; 329(7478):1309–1311.
71. WHO. Fact sheets, Tetanus [Internet]. 2018 [cited 2022 Dec 6]. Available from: https://www.who.int/news-room/fact-sheets/detail/tetanus
72. CDC. About Tetanus [Internet]. [cited 2022 Dec 6]. Available from: https://www.cdc.gov/tetanus/about/index.html
73. WHO. Immunization data [Internet]. [cited 2023 Jul 11]. Available from: https://immunizationdata.who.int/listing.html?topic=coverage&location=Global
74. Silva Antunes R Da, Paul S, Sidney J, Weiskopf D, Dan JM, Phillips E, Mallal S, Crotty S, Sette A, Arlehamn CSL. Definition of human epitopes recognized in tetanus toxoid and development of an assay strategy to detect Ex vivo tetanus CD4+ T cell responses. PLoS ONE. **2017**; 12(1):e0169086.
75. Wilson J, Hunt T. Molecular Biology of the Cell, 6th edition. Garland Science; 2014.

76. Luger K, Mäder AW, Richmond RK, Sargent DF, Richmond TJ. Crystal structure of the nucleosome core particle at 2.8 Å resolution. Nature. **1997**; 389(6648):251–260.
77. Arif M, Sadayappan S, Becker RC, Martin LJ, Urbina EM. Epigenetic modification: a regulatory mechanism in essential hypertension. Hypertension Research. **2019**; 42(8):1099–1113.
78. Alegría-Torres JA, Baccarelli A, Bollati V. Epigenetics and lifestyle. Epigenomics. **2011**; 3(3):267–277.
79. Keil KP, Lein PJ. DNA methylation: A mechanism linking environmental chemical exposures to risk of autism spectrum disorders? Environmental Epigenetics. **2016**; 2(1):dvv012.
80. Bannister S, Kim B, Dominguez-Andres J, Kilic G, Ansell BRE, Neeland MR, Moorlag SJCFM, Matzaraki V, Vlahos A, Shepherd R, Germano S, Bahlo M, Messina NL, Saffery R, Netea MG, Curtis N, Novakovic B. Neonatal BCG vaccination is associated with a long-term DNA methylation signature in circulating monocytes. Science Advances. **2022**; 8(31):eabn4002.
81. Sharif J, Muto M, Takebayashi SI, Suetake I, Iwamatsu A, Endo TA, Shinga J, Mizutani-Koseki Y, Toyoda T, Okamura K, Tajima S, Mitsuya K, Okano M, Koseki H. The SRA protein Np95 mediates epigenetic inheritance by recruiting Dnmt1 to methylated DNA. Nature. **2007**; 450(7171):908–912.
82. Song J, Teplova M, Ishibe-Murakami S, Patel DJ. Structure-based mechanistic insights into DNMT1-mediated maintenance DNA methylation. Science. **2012**; 335(6069):709–712.
83. Hon GC, Rajagopal N, Shen Y, McCleary DF, Yue F, Dang MD, Ren B. Epigenetic memory at embryonic enhancers identified in DNA methylation maps from adult mouse tissues. Nature Genetics. **2013**; 45(10):1198–1206.
84. Li E, Beard C, Jaenisch R. Role for DNA methylation in genomic imprinting. Nature. **1993**; 366(6453):362–365.
85. Illingworth RS, Gruenewald-Schneider U, Webb S, Kerr ARW, James KD, Turner DJ, Smith C, Harrison DJ, Andrews R, Bird AP. Orphan CpG Islands Identify numerous conserved promoters in the mammalian genome. PLoS Genetics. **2010**; 6(9):e1001134.
86. Kim MS, Chang X, Yamashita K, Nagpal JK, Baek JH, Wu G, Trink B, Ratovitski EA, Mori M, Sidransky D. Aberrant promoter methylation and tumor suppressive activity of the DFNA5 gene in colorectal carcinoma. Oncogene. **2008**; 27(25):3624–3634.
87. Birney E, Stamatoyannopoulos JA, Dutta A, et al. Identification and analysis of functional elements in 1% of the human genome by the ENCODE pilot project. Nature. **2007**; 447(7146):799–816.
88. Cui P, Lin Q, Ding F, Xin C, Gong W, Zhang L, Geng J, Zhang B, Yu X, Yang J, Hu S, Yu J. A comparison between ribo-minus RNA-sequencing and polyA-selected RNA-sequencing. Genomics. **2010**; 96(5):259–265.
89. Ma L, Bajic VB, Zhang Z. On the classification of long non-coding RNAs. RNA Biology. **2013**; 10(6):924–933.
90. Kung JTY, Colognori D, Lee JT. Long noncoding RNAs: Past, present, and future. Genetics. **2013**; 193(3):651–669.
91. Kaikkonen MU, Lam MTY, Glass CK. Non-coding RNAs as regulators of gene expression and epigenetics. Cardiovascular Research. **2011**; 90(3):430–440.
92. Azad GK, Tomar RS. Proteolytic clipping of histone tails: The emerging role of histone proteases in regulation of various biological processes. Molecular Biology Reports. **2014**;

41(5):2717–2730.
93. Kouzarides T. Chromatin Modifications and Their Function. Cell. **2007**; 128(4):693–705.
94. Keppler BR, Archer TK. Chromatin-modifying enzymes as therapeutic targets - Part 1. Expert Opinion on Therapeutic Targets. **2008**; 12(10):1301–1312.
95. Yashar WM, Kong G, VanCampen J, Curtiss BM, Coleman DJ, Carbone L, Yardimci GG, Maxson JE, Braun TP. GoPeaks: histone modification peak calling for CUT&Tag. Genome Biology. **2022**; 23(1):144.
96. Dambacher S, Hahn M, Schotta G. Epigenetic regulation of development by histone lysine methylation. Heredity. **2010**; 105(1):24–37.
97. Santos-Rosa H, Schneider R, Bannister AJ, Sherriff J, Bernstein BE, Emre NCT, Schreiber SL, Mellor J, Kouzarides T. Active genes are tri-methylated at K4 of histone H3. Nature. **2002**; 419(6905):407–411.
98. Balasubramanian D, Akhtar-Zaidi B, Song L, Bartels CF, Veigl M, Beard L, Myeroff L, Guda K, Lutterbaugh J, Willis J, Crawford GE, Markowitz SD, Scacheri PC. H3K4me3 inversely correlates with DNA methylation at a large class of non-CpG-island-containing start sites. Genome Medicine. **2012**; 4(5):47.
99. Watanabe S, Resch M, Lilyestrom W, Clark N, Hansen JC, Peterson C, Luger K. Structural characterization of H3K56Q nucleosomes and nucleosomal arrays. Biochimica et Biophysica Acta. **2010**; 1799(5–6):480–486.
100. Katoh N, Kuroda K, Tomikawa J, Ogata-Kawata H, Ozaki R, Ochiai A, Kitade M, Takeda S, Nakabayashi K, Hata K. Reciprocal changes of H3K27ac and H3K27me3 at the promoter regions of the critical genes for endometrial decidualization. Epigenomics. **2018**; 10(9):1243–1257.
101. Pasini D, Malatesta M, Jung HR, Walfridsson J, Willer A, Olsson L, Skotte J, Wutz A, Porse B, Jensen ON, Helin K. Characterization of an antagonistic switch between histone H3 lysine 27 methylation and acetylation in the transcriptional regulation of Polycomb group target genes. Nucleic Acids Research. **2010**; 38(15):4958–4969.
102. Atanassov BS, Koutelou E, Dent SY. The role of deubiquitinating enzymes in chromatin regulation. FEBS Letters. **2011**; 585(13):2016–2023.
103. Mattiroli F, Penengo L. Histone Ubiquitination: An Integrative Signaling Platform in Genome Stability. Trends in Genetics. **2021**; 37(6):566–581.
104. Kralemann LEM, Liu S, Trejo-Arellano MS, Muñoz-Viana R, Köhler C, Hennig L. Removal of H2Aub1 by ubiquitin-specific proteases 12 and 13 is required for stable Polycomb-mediated gene repression in Arabidopsis. Genome Biology. **2020**; 21(1):144.
105. Pavri R, Zhu B, Li G, Trojer P, Mandal S, Shilatifard A, Reinberg D. Histone H2B Monoubiquitination Functions Cooperatively with FACT to Regulate Elongation by RNA Polymerase II. Cell. **2006**; 125(4):703–717.
106. Chandrasekharan MB, Huang F, Sun ZW. Ubiquitination of histone H2B regulates chromatin dynamics by enhancing nucleosome stability. Proceedings of the National Academy of Sciences of the United States of America. **2009**; 106(39):16686–16691.
107. Kim J, Guermah M, McGinty RK, Lee JS, Tang Z, Milne TA, Shilatifard A, Muir TW, Roeder RG. RAD6-Mediated Transcription-Coupled H2B Ubiquitylation Directly Stimulates H3K4 Methylation in Human Cells. Cell. **2009**; 137(3):459–471.
108. Briggs SD, Xiao T, Sun ZW, Caldwell JA, Shabanowitz J, Hunt DF, Allis CD, Strahl BD. Trans-histone regulatory pathway in chromatin. Nature. **2002**; 418(6897):498.
109. Lee JS, Shukla A, Schneider J, Swanson SK, Washburn MP, Florens L, Bhaumik SR,

Shilatifard A. Histone Crosstalk between H2B Monoubiquitination and H3 Methylation Mediated by COMPASS. Cell. **2007**; 131(6):1084–1096.
110. Rossetto D, Avvakumov N, Côté J. Histone phosphorylation: A chromatin modification involved in diverse nuclear events. Epigenetics. **2012**; 7(10):1098–1108.
111. Zippo A, Serafini R, Rocchigiani M, Pennacchini S, Krepelova A, Oliviero S. Histone Crosstalk between H3S10ph and H4K16ac Generates a Histone Code that Mediates Transcription Elongation. Cell. **2009**; 138(6):1122–1136.
112. Lo WS, Trievel RC, Rojas JR, Duggan L, Hsu JY, Allis CD, Marmorstein R, Berger SL. Phosphorylation of serine 10 in histone H3 is functionally linked in vitro and in vivo to Gcn5-mediated acetylation at lysine 14. Molecular Cell. **2000**; 5(6):917–926.
113. Yamagishi Y, Honda T, Tanno Y, Watanabe Y. Two histone marks establish the inner centromere and chromosome bi-orientation. Science. **2010**; 330(6001):239–243.
114. Collins PL, Purman C, Porter SI, Nganga V, Saini A, Hayer KE, Gurewitz GL, Sleckman BP, Bednarski JJ, Bassing CH, Oltz EM. DNA double-strand breaks induce H2Ax phosphorylation domains in a contact-dependent manner. Nature Communications. **2020**; 11(1):3158.
115. Aihara H, Nakagawa T, Mizusaki H, et al. Histone H2A T120 Phosphorylation Promotes Oncogenic Transformation via Upregulation of Cyclin D1. Molecular Cell. **2016**; 64(1):176–188.
116. Milne TA, Zhao K, Hess JL. Chromatin immunoprecipitation (ChIP) for analysis of histone modifications and chromatin-associated proteins. Methods in Molecular Biology. **2009**; 538:409–423.
117. Kidder BL, Hu G, Zhao K. ChIP-Seq: Technical considerations for obtaining high-quality data. Nature Immunology. **2011**; 12(10):918–922.
118. Skene PJ, Henikoff S. An efficient targeted nuclease strategy for high-resolution mapping of DNA binding sites. eLife. **2017**; 6:e21856.
119. Skene PJ, Henikoff JG, Henikoff S. Targeted in situ genome-wide profiling with high efficiency for low cell numbers. Nature Protocols. **2018**; 13(5):1006–1019.
120. Kaya-Okur HS, Janssens DH, Henikoff JG, Ahmad K, Henikoff S. Efficient low-cost chromatin profiling with CUT&Tag. Nature Protocols. **2020**; 15(10):3264–3283.
121. Kaya-Okur HS, Wu SJ, Codomo CA, Pledger ES, Bryson TD, Henikoff JG, Ahmad K, Henikoff S. CUT&Tag for efficient epigenomic profiling of small samples and single cells. Nature Communications. **2019**; 10(1):1930.
122. Gordon S, Taylor PR. Monocyte and macrophage heterogeneity. Nature Reviews Immunology. **2005**; 5(12):953–964.
123. Patel AA, Zhang Y, Fullerton JN, Boelen L, Rongvaux A, Maini AA, Bigley V, Flavell RA, Gilroy DW, Asquith B, Macallan D, Yona S. The fate and lifespan of human monocyte subsets in steady state and systemic inflammation. Journal of Experimental Medicine. **2017**; 214(7):1913–1923.
124. Lee J, Tam H, Adler L, Ilstad-Minnihan A, Macaubas C, Mellins ED. The MHC class II antigen presentation pathway in human monocytes differs by subset and is regulated by cytokines. PLoS ONE. **2017**; 12(8):e0183594.
125. Guilliams M, Laar L van de. A hitchhiker's guide to myeloid cell subsets: Practical implementation of a novel mononuclear phagocyte classification system. Frontiers in Immunology. **2015**; 6:406.
126. Wang L, Kuang Z, Zhang D, Gao Y, Ying M, Wang T. Reactive oxygen species in immune

cells: A new antitumor target. Biomedicine and Pharmacotherapy. **2021**; 133:110978.
127. Kaufmann A, Mühlradt PF, Gemsa D, Sprenger H. Induction of cytokines and chemokines in human monocytes by mycoplasma fermentans-derived lipoprotein MALP-2. Infection and Immunity. **1999**; 67(12):6303–6308.
128. Wong KL, Yeap WH, Tai JJY, Ong SM, Dang TM, Wong SC. The three human monocyte subsets: Implications for health and disease. Immunologic Research. **2012**; 53(1–3):41–57.
129. Sampath P, Moideen K, Ranganathan UD, Bethunaickan R. Monocyte Subsets: Phenotypes and Function in Tuberculosis Infection. Frontiers in Immunology. **2018**; 9:1726.
130. Herberman RB, Nunn ME, Lavrin DH. Natural cytotoxic reactivity of mouse lymphoid cells against syngeneic and allogeneic tumors. I. Distribution of reactivity and specificity. International Journal of Cancer. **1975**; 16(2):216–229.
131. Raulet DH, Vance RE. Self-tolerance of natural killer cells. Nature Reviews Immunology. **2006**; 6(7):520–531.
132. Ljunggren HG, Kärre K. In search of the "missing self": MHC molecules and NK cell recognition. Immunology Today. **1990**; 11(7):237–244.
133. Li D, Wu M. Pattern recognition receptors in health and diseases. Signal Transduction and Targeted Therapy. **2021**; 6(1):291.
134. Fukata M, Arditi M. The role of pattern recognition receptors in intestinal inflammation. Mucosal Immunology. **2013**; 6(3):451–463.
135. Thomas CJ, Schroder K. Pattern recognition receptor function in neutrophils. Trends in Immunology. **2013**; 34(7):317–328.
136. Patten DA, Collett A. Exploring the immunomodulatory potential of microbial-associated molecular patterns derived from the enteric bacterial microbiota. Microbiology. **2013**; 159(8):1535–1544.
137. Brubaker SW, Bonham KS, Zanoni I, Kagan JC. Innate immune pattern recognition: A cell biological perspective. Annual Review of Immunology. **2015**; 33:257–290.
138. Thaiss CA, Levy M, Itav S, Elinav E. Integration of Innate Immune Signaling. Trends in Immunology. **2016**; 37(2):84–101.
139. Moretti J, Blander JM. Insights into phagocytosis-coupled activation of pattern recognition receptors and inflammasomes. Current Opinion in Immunology. **2014**; 26(1):100–110.
140. Vatner RE, Janssen EM. STING, DCs and the link between innate and adaptive tumor immunity. Molecular Immunology. **2019**; 110:13–23.
141. Ingulli E, Mondino A, Khoruts A, Jenkins MK. In vivo detection of dendritic cell antigen presentation to CD4+ T cells. Journal of Experimental Medicine. **1997**; 185(12):2133–2141.
142. Thomas R, Yang X. NK-DC Crosstalk in Immunity to Microbial Infection. Journal of Immunology Research. **2016**; 2016:6374379.
143. Netea MG, Quintin J, Meer JWM Van Der. Trained immunity: A memory for innate host defense. Cell Host and Microbe. **2011**; 9(5):355–361.
144. Flajnik MF, Kasahara M. Origin and evolution of the adaptive immune system: Genetic events and selective pressures. Nature Reviews Genetics. **2010**; 11(1):47–59.
145. Williams MA, Bevan MJ. Effector and memory CTL differentiation. Annual Review of Immunology. **2007**; 25:171–192.
146. Seder RA, Ahmed R. Similarities and differences in CD4+ and CD8+ effector and memory T cell generation. Nature Immunology. **2003**; 4(9):835–842.
147. Leung S, Liu X, Fang L, Chen X, Guo T, Zhang J. The cytokine milieu in the interplay of pathogenic Th1/Th17 cells and regulatory T cells in autoimmune disease. Cellular and

Molecular Immunology. **2010**; 7(3):182–189.
148. Kurosaki T, Kometani K, Ise W. Memory B cells. Nature Reviews Immunology. Nature Publishing Group; **2015**; 15(3):149–159.
149. Liu YJ, Malisan F, Bouteiller O De, Guret C, Lebecque S, Banchereau J, Mills FC, Max EE, Martinez-Valdez H. Within germinal centers, isotype switching of immunoglobulin genes occurs after the onset of somatic mutation. Immunity. **1996**; 4(3):241–250.
150. Schroeder HW, Cavacini L. Structure and function of immunoglobulins. Journal of Allergy and Clinical Immunology. **2010**; 125(2 SUPPL. 2):S41-52.
151. Lechouane F, Bonaud A, Delpy L, Casola S, Oruc Z, Chemin G, Cogné M, Sirac C. B-cell receptor signal strength influences terminal differentiation. European Journal of Immunology. **2013**; 43(3):619–628.
152. Pone EJ, Zan H, Zhang J, Al-Qahtani A, Xu Z, Casali P. Toll-like receptors and B-cell receptors synergize to induce immunoglobulin class-switch dna recombination: Relevance to microbial antibody responses. Critical Reviews in Immunology. **2010**; 30(1):1–29.
153. Rivera CE, Zhou Y, Chupp DP, Yan H, Fisher AD, Simon R, Zan H, Xu Z, Casali P. Intrinsic B cell TLR-BCR linked coengagement induces class-switched, hypermutated, neutralizing antibody responses in absence of T cells. Science Advances. **2023**; 9(17):eade8928.
154. Bortnick A, Chernova I, Quinn WJ, Mugnier M, Cancro MP, Allman D. Long-Lived Bone Marrow Plasma Cells Are Induced Early in Response to T Cell-Independent or T Cell-Dependent Antigens. The Journal of Immunology. **2012**; 188(11):5389–5396.
155. Obukhanych T V., Nussenzweig MC. T-independent type II immune responses generate memory B cells. Journal of Experimental Medicine. **2006**; 203(2):305–310.
156. Toellner KM, Jenkinson WE, Taylor DR, Khan M, Sze DMY, Sansom DM, Vinuesa CG, MacLennan ICM. Low-level hypermutation in T cell-independent germinal centers compared with high mutation rates associated with T cell-dependent germinal centers. Journal of Experimental Medicine. **2002**; 195(3):383–389.
157. Basha S, Surendran N, Pichichero M. Immune responses in neonates. Expert Review of Clinical Immunology. **2014**; 10(9):1171–1184.
158. McIntyre P, Wood N. Pertussis in early infancy: Disease burden and preventive strategies. Current Opinion in Infectious Diseases. **2009**; 22(3):215–223.
159. Gantt S, Yao L, Kollmann TR, Casper C, Zhang J, Self SG. Implications of age-dependent immune responses to enterovirus 71 infection for disease pathogenesis and vaccine design. Journal of the Pediatric Infectious Diseases Society. **2013**; 2(2):163–170.
160. Castilow EM, Olson MR, Varga SM. Understanding respiratory syncytial virus (RSV) vaccine-enhanced disease. Immunologic Research. **2007**; 39(1–3):225–239.
161. Izurieta HS, Thompson WW, Kramarz P, Shay DK, Davis RL, DeStefano F, Black S, Shinefield H, Fukuda K. Influenza and the Rates of Hospitalization for Respiratory Disease among Infants and Young Children. New England Journal of Medicine. **2000**; 342(4):232–239.
162. Sasaki Y, Sakai M, Miyazaki S, Higuma S, Shiozaki A, Saito S. Decidual and peripheral blood CD4+CD25 + regulatory T cells in early pregnancy subjects and spontaneous abortion cases. Molecular Human Reproduction. **2004**; 10(5):347–353.
163. Inada K, Shima T, Nakashima A, Aoki K, Ito M, Saito S. Characterization of regulatory T cells in decidua of miscarriage cases with abnormal or normal fetal chromosomal content. Journal of Reproductive Immunology. **2013**; 97(1):104–111.

164. Peoples JD, Cheung S, Nesin M, Lin H, Francesca Tatad AM, Hoang D, Perlman JM, Cunningham-Rundles S. Neonatal cord blood subsets and cytokine response to bacterial antigens. American Journal of Perinatology. **2009**; 26(9):647–657.
165. Dalle JH, Menezes J, Wagner É, Blagdon M, Champagne J, Champagne MA, Duval M. Characterization of cord blood natural killer cells: Implications for transplantation and neonatal infections. Pediatric Research. **2005**; 57(5 I):649–655.
166. Kollmann TR, Crabtree J, Rein-Weston A, Blimkie D, Thommai F, Wang XY, Lavoie PM, Furlong J, Fortuno ES, Hajjar AM, Hawkins NR, Self SG, Wilson CB. Neonatal Innate TLR-Mediated Responses Are Distinct from Those of Adults. The Journal of Immunology. **2009**; 183(11):7150–7160.
167. Kollmann TR, Levy O, Montgomery RR, Goriely S. Innate Immune Function by Toll-like Receptors: Distinct Responses in Newborns and the Elderly. Immunity. **2012**; 37(5):771–783.
168. Lee HH, Hoeman CM, Hardaway JC, Guloglu FB, Ellis JS, Jain R, Divekar R, Tartar DM, Haymaker CL, Zaghouani H. Delayed maturation of an IL-12-producing dendritic cell subset explains the early Th2 bias in neonatal immunity. Journal of Experimental Medicine. **2008**; 205(10):2269–2280.
169. Lalor MK, Smith SG, Floyd S, Gorak-Stolinska P, Weir RE, Blitz R, Branson K, Fine PE, Dockrell HM. Complex cytokine profiles induced by BCG vaccination in UK infants. Vaccine. **2010**; 28(6):1635–1641.
170. Ota MOC, Vekemans J, Schlegel-Haueter SE, Fielding K, Sanneh M, Kidd M, Newport MJ, Aaby P, Whittle H, Lambert P-H, McAdam KPWJ, Siegrist C-A, Marchant A. Influence of Mycobacterium bovis Bacillus Calmette-Guérin on Antibody and Cytokine Responses to Human Neonatal Vaccination . The Journal of Immunology. **2002**; 168(2):919–925.
171. Vekemans J, Amedei A, Ota MO, D'Elios MM, Goetghebuer T, Ismaili J, Newport MJ, Prete G Del, Goldman M, McAdam KPWJ, Marchant A. Neonatal bacillus Calmette-Guérin vaccination induces adult-like IFN-γ production by CD4+ T lymphocytes. European Journal of Immunology. **2001**; 31(5):1531–1535.
172. Hornef MW, Torow N. 'Layered immunity' and the 'neonatal window of opportunity' – timed succession of non-redundant phases to establish mucosal host–microbial homeostasis after birth. Immunology. **2020**; 159(1):15–25.
173. Jauniaux E, Jurkovic D, Gulbis B, Liesnard C, Lees C, Campbell S. Materno-fetal immunoglobulin transfer and passive immunity during the first trimester of human pregnancy. Human Reproduction. **1995**; 10(12):3297–3300.
174. Story CM, Mikulska JE, Simister NE. A major histocompatibility complex class I-like Fc receptor cloned from human placenta: Possible role in transfer of immunoglobulin G from mother to fetus. Journal of Experimental Medicine. **1994**; 180(6):2377–2381.
175. Palmeira P, Quinello C, Silveira-Lessa AL, Zago CA, Carneiro-Sampaio M. IgG placental transfer in healthy and pathological pregnancies. Clinical and Developmental Immunology. **2012**; 2012:985646.
176. Rio-Aige K, Azagra-Boronat I, Castell M, Selma-Royo M, Collado MC, Rodríguez-Lagunas MJ, Pérez-Cano FJ. The breast milk immunoglobulinome. Nutrients. **2021**; 13(6):1810.
177. Ryals JA, Neuenschwander UH, Willits MG, Molina A, Steiner HY, Hunt MD. Systemic acquired resistance. Plant Cell. **1996**; 8(10):1809–1819.
178. Pham LN, Dionne MS, Shirasu-Hiza M, Schneider DS. A specific primed immune response

in Drosophila is dependent on phagocytes. PLoS Pathogens. **2007**; 3(3):e26.
179. Rodrigues J, Brayner FA, Alves LC, Dixit R, Barillas-Mury C. Hemocyte differentiation mediates innate immune memory in anopheles gambiae mosquitoes. Science. **2010**; 329(5997):1353–1355.
180. Sun JC, Beilke JN, Lanier LL. Adaptive immune features of natural killer cells. Nature. **2009**; 457(7229):557–561.
181. Kleinnijenhuis J, Quintin J, Preijers F, Joosten LAB, Ifrim DC, Saeed S, Jacobs C, Loenhout J Van, Jong D De, Hendrik S, Xavier RJ, Meer JWM Van Der, Crevel R Van, Netea MG. Bacille Calmette-Guérin induces NOD2-dependent nonspecific protection from reinfection via epigenetic reprogramming of monocytes. Proceedings of the National Academy of Sciences of the United States of America. **2012**; 109(43):17537–17542.
182. Kleinnijenhuis J, Quintin J, Preijers F, Joosten LAB, Jacobs C, Xavier RJ, Meer JWM van der, Crevel R van, Netea MG. BCG-induced trained immunity in NK cells: Role for non-specific protection to infection. Clinical Immunology. **2014**; 155(2):213–219.
183. Quintin J, Saeed S, Martens JHA, Giamarellos-Bourboulis EJ, Ifrim DC, Logie C, Jacobs L, Jansen T, Kullberg BJ, Wijmenga C, Joosten LAB, Xavier RJ, Meer JWM Van Der, Stunnenberg HG, Netea MG. Candida albicans infection affords protection against reinfection via functional reprogramming of monocytes. Cell Host and Microbe. **2012**; 12(2):223–232.
184. Sun JC, Madera S, Bezman NA, Beilke JN, Kaplan MH, Lanier LL. Proinflammatory cytokine signaling required for the generation of natural killer cell memory. Journal of Experimental Medicine. **2012**; 209(5):947–954.
185. Saeed S, Quintin J, Kerstens HHD, et al. Epigenetic programming of monocyte-to-macrophage differentiation and trained innate immunity. Science. **2014**; 345(6204):1251086.
186. Benn CS, Netea MG, Selin LK, Aaby P. A Small Jab - A Big Effect: Nonspecific Immunomodulation By Vaccines. Trends in Immunology. **2013**; 34(9):431–439.
187. Kleinnijenhuis J, Quintin J, Preijers F, Benn CS, Joosten LAB, Jacobs C, Loenhout J Van, Xavier RJ, Aaby P, Meer JWM Van Der, Crevel R Van, Netea MG. Long-lasting effects of bcg vaccination on both heterologous th1/th17 responses and innate trained immunity. Journal of Innate Immunity. **2014**; 6(2):152–158.
188. Prentice S, Nassanga B, Webb EL, et al. BCG-induced non-specific effects on heterologous infectious disease in Ugandan neonates: an investigator-blind randomised controlled trial. The Lancet Infectious Diseases. **2021**; 21(7):993–1003.
189. Castro MJ De, Pardo-Seco J, Martinón-Torres F. Nonspecific (heterologous) protection of neonatal BCG vaccination against hospitalization due to respiratory infection and sepsis. Clinical Infectious Diseases. **2015**; 60(11):1611–1619.
190. Aaby P, Roth A, Ravn H, Napirna BM, Rodrigues A, Lisse IM, Stensballe L, Diness BR, Lausch KR, Lund N, Biering-Sørensen S, Whittle H, Benn CS. Randomized trial of BCG vaccination at birth to low-birth-weight children: Beneficial nonspecific effects in the neonatal period? Journal of Infectious Diseases. **2011**; 204(2):245–252.
191. Stensballe LG, Nante E, Jensen IP, Kofoed PE, Poulsen A, Jensen H, Newport M, Marchant A, Aaby P. Acute lower respiratory tract infections and respiratory syncytial virus in infants in Guinea-Bissau: A beneficial effect of BCG vaccination for girls: Community based case-control study. Vaccine. **2005**; 23(10):1251–1257.
192. Hole CR, Wager CML, Castro-Lopez N, Campuzano A, Cai H, Wozniak KL, Wang Y,

Wormley FL. Induction of memory-like dendritic cell responses in vivo. Nature Communications. **2019**; 10(1):2955.
193. Moorlag SJCFM, Rodriguez-Rosales YA, Gillard J, et al. BCG Vaccination Induces Long-Term Functional Reprogramming of Human Neutrophils. Cell Reports. **2020**; 33(7):108387.
194. Khan N, Downey J, Sanz J, Kaufmann E, Blankenhaus B, Pacis A, Pernet E, Ahmed E, Cardoso S, Nijnik A, Mazer B, Sassetti C, Behr MA, Soares MP, Barreiro LB, Divangahi M. M. tuberculosis Reprograms Hematopoietic Stem Cells to Limit Myelopoiesis and Impair Trained Immunity. Cell. **2020**; 183(3):752–770.e22.
195. Christ A, Günther P, Lauterbach MAR, et al. Western Diet Triggers NLRP3-Dependent Innate Immune Reprogramming. Cell. **2018**; 172(1–2):162–175.e14.
196. Mitroulis I, Ruppova K, Wang B, et al. Modulation of Myelopoiesis Progenitors Is an Integral Component of Trained Immunity. Cell. **2018**; 172(1–2):147–161.e12.
197. Kaufmann E, Sanz J, Dunn JL, et al. BCG Educates Hematopoietic Stem Cells to Generate Protective Innate Immunity against Tuberculosis. Cell. **2018**; 172(1–2):176–190.e19.
198. Netea MG, Domínguez-Andrés J, Barreiro LB, Chavakis T, Divangahi M, Fuchs E, Joosten LAB, Meer JWM van der, Mhlanga MM, Mulder WJM, Riksen NP, Schlitzer A, Schultze JL, Stabell Benn C, Sun JC, Xavier RJ, Latz E. Defining trained immunity and its role in health and disease. Nature Reviews Immunology. **2020**; 20(6):375–388.
199. Arts RJW, Carvalho A, Rocca C La, Palma C, Rodrigues F, Silvestre R, Kleinnijenhuis J, Lachmandas E, Gonçalves LG, Belinha A, Cunha C, Oosting M, Joosten LAB, Matarese G, Crevel R van, Netea MG. Immunometabolic Pathways in BCG-Induced Trained Immunity. Cell Reports. **2016**; 17(10):2562–2571.
200. Yoshida K, Maekawa T, Zhu Y, Renard-Guillet C, Chatton B, Inoue K, Uchiyama T, Ishibashi KI, Yamada T, Ohno N, Shirahige K, Okada-Hatakeyama M, Ishii S. The transcription factor ATF7 mediates lipopolysaccharide-induced epigenetic changes in macrophages involved in innate immunological memory. Nature Immunology. **2015**; 16(10):1034–1043.
201. Arts RJW, Moorlag SJCFM, Novakovic B, Li Y, Wang SY, Oosting M, Kumar V, Xavier RJ, Wijmenga C, Joosten LAB, Reusken CBEM, Benn CS, Aaby P, Koopmans MP, Stunnenberg HG, Crevel R van, Netea MG. BCG Vaccination Protects against Experimental Viral Infection in Humans through the Induction of Cytokines Associated with Trained Immunity. Cell Host and Microbe. **2018**; 23(1):89–100.e5.
202. Uthayakumar D, Paris S, Chapat L, Freyburger L, Poulet H, Luca K De. Non-specific Effects of Vaccines Illustrated Through the BCG Example: From Observations to Demonstrations. Frontiers in Immunology. **2018**; 9:2869.
203. Cheng SC, Quintin J, Cramer RA, et al. MTOR- and HIF-1α-mediated aerobic glycolysis as metabolic basis for trained immunity. Science. **2014**; 345(6204):1250684.
204. Sender R, Fuchs S, Milo R. Revised Estimates for the Number of Human and Bacteria Cells in the Body. PLoS Biology. **2016**; 14(8):e1002533.
205. D'Argenio V, Salvatore F. The role of the gut microbiome in the healthy adult status. Clinica Chimica Acta. **2015**; 451(Pt A):97–102.
206. Methé BA, Nelson KE, Pop M, et al. A framework for human microbiome research. Nature. **2012**; 486(7402):215–221.
207. Donaldson GP, Lee SM, Mazmanian SK. Gut biogeography of the bacterial microbiota. Nature Reviews Microbiology. **2015**; 14(1):20–32.
208. Singh S, Verma N, Taneja N. The human gut resistome: Current concepts & future prospects.

Indian Journal of Medical Research. **2019**; 150(4):345–358.
209. Turnbaugh PJ, Hamady M, Yatsunenko T, Cantarel BL, Duncan A, Ley RE, Sogin ML, Jones WJ, Roe BA, Affourtit JP, Egholm M, Henrissat B, Heath AC, Knight R, Gordon JI. A core gut microbiome in obese and lean twins. Nature. **2009**; 457(7228):480–484.
210. Linehan K, Dempsey EM, Ryan CA, Ross RP, Stanton C. First encounters of the microbial kind: perinatal factors direct infant gut microbiome establishment. Microbiome Research Reports. **2022**; 1(2):10.
211. Bergström A, Skov TH, Bahl MI, Roager HM, Christensen LB, Ejlerskov KT, Mølgaard C, Michaelsen KF, Licht TR. Establishment of intestinal microbiota during early life: A longitudinal, explorative study of a large cohort of Danish infants. Applied and Environmental Microbiology. **2014**; 80(9):2889–2900.
212. Koenig JE, Spor A, Scalfone N, Fricker AD, Stombaugh J, Knight R, Angenent LT, Ley RE. Succession of microbial consortia in the developing infant gut microbiome. Proceedings of the National Academy of Sciences of the United States of America. **2011**; 108(SUPPL. 1):4578–4585.
213. Yatsunenko T, Rey FE, Manary MJ, et al. Human gut microbiome viewed across age and geography. Nature. **2012**; 486(7402):222–227.
214. Hill L, Sharma R, Hart L, Popov J, Moshkovich M, Pai N. The neonatal microbiome in utero and beyond: Perinatal influences and long-term impacts. Journal of Laboratory Medicine. **2021**; 45(6):275–291.
215. Boskey ER, Cone RA, Whaley KJ, Moench TR. Origins of vaginal acidity: High D/L lactate ratio is consistent with bacteria being the primary source. Human Reproduction. **2001**; 16(9):1809–1813.
216. Petrova MI, Reid G, Vaneechoutte M, Lebeer S. Lactobacillus iners: Friend or Foe? Trends in Microbiology. **2017**; 25(3):182–191.
217. Pantoja-Feliciano IG, Clemente JC, Costello EK, Perez ME, Blaser MJ, Knight R, Dominguez-Bello MG. Biphasic assembly of the murine intestinal microbiota during early development. ISME Journal. **2013**; 7(6):1112–1115.
218. Pinto Coelho GD, Arial Ayres LF, Barreto DS, Henriques BD, Cardoso Prado MRM, Passos CM Dos. Acquisition of microbiota according to the type of birth: An integrative review. Revista Latino-Americana de Enfermagem. **2021**; 29:e3446.
219. Azad MB, Konya T, Maughan H, Guttman DS, Field CJ, Chari RS, Sears MR, Becker AB, Scott JA, Kozyrskyj AL. Gut microbiota of healthy Canadian infants: Profiles by mode of delivery and infant diet at 4 months. CMAJ Canadian Medical Association Journal. **2013**; 185(5):385–394.
220. Rutayisire E, Huang K, Liu Y, Tao F. The mode of delivery affects the diversity and colonization pattern of the gut microbiota during the first year of infants' life: A systematic review. BMC Gastroenterology. **2016**; 16(1):86.
221. Hu J, Nomura Y, Bashir A, Fernandez-Hernandez H, Itzkowitz S, Pei Z, Stone J, Loudon H, Peter I. Diversified microbiota of meconium is affected by maternal diabetes status. PLoS ONE. **2013**; 8(11):e78257.
222. Hill CJ, Lynch DB, Murphy K, Ulaszewska M, Jeffery IB, O'Shea CA, Watkins C, Dempsey E, Mattivi F, Tuohy K, Paul Ross R, Anthony Ryan C, O' Toole PW, Stanton C. Evolution of gut microbiota composition from birth to 24 weeks in the INFANTMET Cohort. Microbiome. **2017**; 5(1):4.
223. Akagawa S, Tsuji S, Onuma C, Akagawa Y, Yamaguchi T, Yamagishi M, Yamanouchi S,

Kimata T, Sekiya SI, Ohashi A, Hashiyada M, Akane A, Kaneko K. Effect of delivery mode and nutrition on gut microbiota in Neonates. Annals of Nutrition and Metabolism. **2019**; 74(2):132–139.
224. Salminen S, Gibson GR, McCartney AL, Isolauri E. Influence of mode of delivery on gut microbiota composition in seven year old children. Gut. **2004**; 53(9):1388–1389.
225. Jakobsson HE, Abrahamsson TR, Jenmalm MC, Harris K, Quince C, Jernberg C, Björkstén B, Engstrand L, Andersson AF. Decreased gut microbiota diversity, delayed Bacteroidetes colonisation and reduced Th1 responses in infants delivered by Caesarean section. Gut. **2014**; 63(4):559–566.
226. Roswall J, Olsson LM, Kovatcheva-Datchary P, Nilsson S, Tremaroli V, Simon MC, Kiilerich P, Akrami R, Krämer M, Uhlén M, Gummesson A, Kristiansen K, Dahlgren J, Bäckhed F. Developmental trajectory of the healthy human gut microbiota during the first 5 years of life. Cell Host and Microbe. **2021**; 29(5):765–776.e3.
227. Willyard C. Could baby's first bacteria take root before birth? Nature. **2018**; 553(7688):264–266.
228. Mishra A, Lai GC, Yao LJ, et al. Microbial exposure during early human development primes fetal immune cells. Cell. **2021**; 184(13):3394–3409.e20.
229. Stout MJ, Conlon B, Landeau M, Lee I, Bower C, Zhao Q, Roehl KA, Nelson DM, MacOnes GA, Mysorekar IU. Identification of intracellular bacteria in the basal plate of the human placenta in term and preterm gestations. American Journal of Obstetrics and Gynecology. **2013**; 208(3):226.e1-226.e7.
230. Aagaard K, Ma J, Antony KM, Ganu R, Petrosino J, Versalovic J. The placenta harbors a unique microbiome. Science Translational Medicine. **2014**; 6(237):237ra65.
231. Funkhouser LJ, Bordenstein SR. Mom Knows Best: The Universality of Maternal Microbial Transmission. PLoS Biology. **2013**; 11(8):e1001631.
232. Rackaityte E, Halkias J, Fukui EM, Mendoza VF, Hayzelden C, Crawford ED, Fujimura KE, Burt TD, Lynch S V. Viable bacterial colonization is highly limited in the human intestine in utero. Nature Medicine. **2020**; 26(4):599–607.
233. Kennedy KM, Gerlach MJ, Adam T, Heimesaat MM, Rossi L, Surette MG, Sloboda DM, Braun T. Fetal meconium does not have a detectable microbiota before birth. Nature Microbiology. **2021**; 6(7):865–873.
234. Gschwind R, Fournier T, Kennedy S, Tsatsaris V, Cordier AG, Barbut F, Butel MJ, WydauDematteis S. Evidence for contamination as the origin for bacteria found in human placenta rather than a microbiota. PLoS ONE. **2020**; 15(8):e0237232.
235. Patel A, Badhoniya N, Khadse S, Senarath U, Agho KE, Dibley MJ, Roy SK, Kabir I, Pandey S, Tiwari K, Godakandage SSP, Jayawickrama H, Hazir T, Akram DS, Mihrshahi S. Infant and young child feeding indicators and determinants of poor feeding practices in India: Secondary data analysis of National Family Health Survey 2005-06. Food and Nutrition Bulletin. **2010**; 31(2):314–333.
236. Boquien CY. Human milk: An ideal food for nutrition of preterm newborn. Frontiers in Pediatrics. **2018**; 6:295.
237. Jost T, Lacroix C, Braegger C, Chassard C. Assessment of bacterial diversity in breast milk using culture-dependent and culture-independent approaches. British Journal of Nutrition. **2013**; 110(7):1253–1262.
238. Martín R, Langa S, Reviriego C, Jiménez E, Marín ML, Xaus J, Fernández L, Rodríguez JM. Human milk is a source of lactic acid bacteria for the infant gut. Journal of Pediatrics.

2003; 143(6):754–758.
239. Benno Y, Mitsuoka T. Development of Intestinal Microflora in Humans and Animals. Bifidobacteria and Microflora. **1986**; 5(1):13–25.
240. Jiménez E, Delgado S, Maldonado A, Arroyo R, Albújar M, García N, Jariod M, Fernández L, Gómez A, Rodríguez JM. Staphylococcus epidermidis: A differential trait of the fecal microbiota of breast-fed infants. BMC Microbiology. **2008**; 8:143.
241. Martín V, Maldonado-Barragán A, Moles L, Rodriguez-Baños M, Campo R Del, Fernández L, Rodríguez JM, Jiménez E. Sharing of bacterial strains between breast milk and infant feces. Journal of Human Lactation. **2012**; 28(1):36–44.
242. Olivares M, Díaz-Ropero MP, Martín R, Rodríguez JM, Xaus J. Antimicrobial potential of four Lactobacillus strains isolated from breast milk. Journal of Applied Microbiology. **2006**; 101(1):72–79.
243. Heikkilä MP, Saris PEJ. Inhibition of Staphylococcus aureus by the commensal bacteria of human milk. Journal of Applied Microbiology. **2003**; 95(3):471–478.
244. Maldonado J, Cañabate F, Sempere L, Vela F, Sánchez AR, Narbona E, López-Huertas E, Geerlings A, Valero AD, Olivares M, Lara-Villoslada F. Human milk probiotic lactobacillus fermentum CECT5716 reduces the incidence of gastrointestinal and upper respiratory tract infections in infants. Journal of Pediatric Gastroenterology and Nutrition. **2012**; 54(1):55–61.
245. Fernández L, Langa S, Martín V, Maldonado A, Jiménez E, Martín R, Rodríguez JM. The human milk microbiota: Origin and potential roles in health and disease. Pharmacological Research. **2013**; 69(1):1–10.
246. Martín V, Maldonado A, Fernández L, Rodríguez JM, Connor RI. Inhibition of human immunodeficiency virus type 1 by lactic acid bacteria from human breastmilk. Breastfeeding Medicine. **2010**; 5(4):153–158.
247. Zivkovic AM, German JB, Lebrilla CB, Mills DA. Human milk glycobiome and its impact on the infant gastrointestinal microbiota. Proceedings of the National Academy of Sciences of the United States of America. **2011**; 108(SUPPL. 1):4653–4658.
248. Newburg DS, Ruiz-Palacios GM, Morrow AL. Human milk glycans protect infants against enteric pathogens. Annual Review of Nutrition. **2005**; 25:37–58.
249. Rogier EW, Frantz AL, Bruno MEC, Wedlund L, Cohen DA, Stromberg AJ, Kaetzel CS. Secretory antibodies in breast milk promote long-term intestinal homeostasis by regulating the gut microbiota and host gene expression. Proceedings of the National Academy of Sciences of the United States of America. **2014**; 111(8):3074–3079.
250. Bezirtzoglou E, Tsiotsias A, Welling GW. Microbiota profile in feces of breast- and formula-fed newborns by using fluorescence in situ hybridization (FISH). Anaerobe. **2011**; 17(6):478–482.
251. Fallani M, Young D, Scott J, Norin E, Amarri S, Adam R, Aguilera M, Khanna S, Gil A, Edwards CA, Doré J. Intestinal microbiota of 6-week-old infants across Europe: Geographic influence beyond delivery mode, breast-feeding, and antibiotics. Journal of Pediatric Gastroenterology and Nutrition. **2010**; 51(1):77–84.
252. Bäckhed F, Roswall J, Peng Y, et al. Dynamics and stabilization of the human gut microbiome during the first year of life. Cell Host and Microbe. **2015**; 17(5):690–703.
253. Laursen MF, Bahl MI, Michaelsen KF, Licht TR. First foods and gut microbes. Frontiers in Microbiology. **2017**; 8:356.
254. Korpela K, Blakstad EW, Moltu SJ, Strømmen K, Nakstad B, Rønnestad AE, Brække K,

Iversen PO, Drevon CA, Vos W de. Intestinal microbiota development and gestational age in preterm neonates. Scientific Reports. **2018**; 8(1):2453.
255. Zwittink RD, Zoeren-Grobben D Van, Martin R, Lingen RA Van, Jebbink LJG, Boeren S, Renes IB, Elburg RM Van, Belzer C, Knol J. Metaproteomics reveals functional differences in intestinal microbiota development of preterm infants. Molecular and Cellular Proteomics. **2017**; 16(9):1610–1620.
256. Kim CS, Claud EC. Necrotizing Enterocolitis Pathophysiology: How Microbiome Data Alter Our Understanding. Clinics in Perinatology. **2019**; 46(1):29–38.
257. Lee CC, Feng Y, Yeh YM, Lien R, Chen CL, Zhou YL, Chiu CH. Gut Dysbiosis, Bacterial Colonization and Translocation, and Neonatal Sepsis in Very-Low-Birth-Weight Preterm Infants. Frontiers in Microbiology. **2021**; 12:746111.
258. Dethlefsen L, Relman DA. Incomplete recovery and individualized responses of the human distal gut microbiota to repeated antibiotic perturbation. Proceedings of the National Academy of Sciences of the United States of America. **2011**; 108(SUPPL. 1):4554–4561.
259. Dethlefsen L, Huse S, Sogin ML, Relman DA. The pervasive effects of an antibiotic on the human gut microbiota, as revealed by deep 16s rRNA sequencing. PLoS Biology. **2008**; 6(11):2383–2400.
260. Bokulich NA, Chung J, Battaglia T, Henderson N, Jay M, Li H, Lieber AD, Wu F, Perez-Perez GI, Chen Y, Schweizer W, Zheng X, Contreras M, Dominguez-Bello MG, Blaser MJ. Antibiotics, birth mode, and diet shape microbiome maturation during early life. Science Translational Medicine. **2016**; 8(343):343ra82.
261. Reyman M, Houten MA van, Watson RL, Chu MLJN, Arp K, Waal WJ de, Schiering I, Plötz FB, Willems RJL, Schaik W van, Sanders EAM, Bogaert D. Effects of early-life antibiotics on the developing infant gut microbiome and resistome: a randomized trial. Nature Communications. **2022**; 13(1):893.
262. Neuman H, Forsythe P, Uzan A, Avni O, Koren O. Antibiotics in early life: dysbiosis and the damage done. FEMS Microbiology Reviews. **2018**; 42(4):489–499.
263. Chu D, Antony K, Ma J, Prince A, Moller M, Boggan B, Aagaard K. 114: A maternal high fat diet (HFD) during gestation alters the neonatal gut microbiome in a human population based longitudinal cohort. American Journal of Obstetrics and Gynecology. **2016**; 214(1):S79.
264. Lundgren SN, Madan JC, Emond JA, Morrison HG, Christensen BC, Karagas MR, Hoen AG. Maternal diet during pregnancy is related with the infant stool microbiome in a delivery mode-dependent manner. Microbiome. **2018**; 6(1):109.
265. Seferovic MD, Mohammad M, Pace RM, Engevik M, Versalovic J, Bode L, Haymond M, Aagaard KM. Maternal diet alters human milk oligosaccharide composition with implications for the milk metagenome. Scientific Reports. **2020**; 10(1):22092.
266. Miyoshi J, Hisamatsu T. The impact of maternal exposure to antibiotics on the development of child gut microbiome. Immunological Medicine. **2022**; 45(2):63–68.
267. Galley JD, Bailey M, Dush CK, Schoppe-Sullivan S, Christian LM. Maternal obesity is associated with alterations in the gut microbiome in toddlers. PLoS ONE. **2014**; 9(11):e113026.
268. Soderborg TK, Clark SE, Mulligan CE, Janssen RC, Babcock L, Ir D, Lemas DJ, Johnson LK, Weir T, Lenz LL, Frank DN, Hernandez TL, Kuhn KA, D'Alessandro A, Barbour LA, Kasmi KC El, Friedman JE. The gut microbiota in infants of obese mothers increases inflammation and susceptibility to NAFLD. Nature Communications. **2018**; 9(1):4462.

269. Falony G, Joossens M, Vieira-Silva S, et al. Population-level analysis of gut microbiome variation. Science. **2016**; 352(6285):560–564.
270. Filippo C De, Cavalieri D, Paola M Di, Ramazzotti M, Poullet JB, Massart S, Collini S, Pieraccini G, Lionetti P. Impact of diet in shaping gut microbiota revealed by a comparative study in children from Europe and rural Africa. Proceedings of the National Academy of Sciences of the United States of America. **2010**; 107(33):14691–14696.
271. Frank DN, Robertson CE, Hamm CM, Kpadeh Z, Zhang T, Chen H, Zhu W, Sartor RB, Boedeker EC, Harpaz N, Pace NR, Li E. Disease phenotype and genotype are associated with shifts in intestinal-associated microbiota in inflammatory bowel diseases. Inflammatory Bowel Diseases. **2011**; 17(1):179–184.
272. Rehman A, Sina C, Gavrilova O, Häsler R, Ott S, Baines JF, Schreiber S, Rosenstiel P. Nod2 is essential for temporal development of intestinal microbial communities. Gut. **2011**; 60(10):1354–1362.
273. Rausch P, Rehman A, Künzel S, Häsler R, Ott SJ, Schreiber S, Rosenstiel P, Franke A, Baines JF. Colonic mucosa-associated microbiota is influenced by an interaction of crohn disease and FUT2 (Secretor) genotype. Proceedings of the National Academy of Sciences of the United States of America. **2011**; 108(47):19030–19035.
274. Qin Y, Havulinna AS, Liu Y, et al. Combined effects of host genetics and diet on human gut microbiota and incident disease in a single population cohort. Nature Genetics. **2022**; 54(2):134–142.
275. Goodrich JK, Waters JL, Poole AC, Sutter JL, Koren O, Blekhman R, Beaumont M, Treuren W Van, Knight R, Bell JT, Spector TD, Clark AG, Ley RE. Human genetics shape the gut microbiome. Cell. **2014**; 159(4):789–799.
276. Drago L, Toscano M, Grandi R De, Grossi E, Padovani EM, Peroni DG. Microbiota network and mathematic microbe mutualism in colostrum and mature milk collected in two different geographic areas: Italy versus Burundi. ISME Journal. **2017**; 11(4):875–884.
277. Assimakopoulos SF, Triantos C, Maroulis I, Gogos C. The Role of the Gut Barrier Function in Health and Disease. Gastroenterology Research. **2018**; 11(4):261–263.
278. Muniz LR, Knosp C, Yeretssian G. Intestinal antimicrobial peptides during homeostasis, infection, and disease. Frontiers in Immunology. **2012**; 3:310.
279. Buckley A, Turner JR. Cell biology of tight junction barrier regulation and mucosal disease. Cold Spring Harbor Perspectives in Biology. **2018**; 10(1):a029314.
280. Frenkel ES, Ribbeck K. Salivary mucins in host defense and disease prevention. Journal of Oral Microbiology. **2015**; 7(1):29759.
281. Tytgat KMAJ, Büller HA, Opdam FJM, Kim YS, Einerhand AWC, Dekker J. Biosynthesis of human colonic mucin: Muc2 is the prominent secretory mucin. Gastroenterology. **1994**; 107(5):1352–1363.
282. Longman RJ, Douthwaite J, Sylvester PA, Poulsom R, Corfield AP, Thomas MG, Wright NA. Coordinated localisation of mucins and trefoil peptides in the ulcer associated cell lineage and the gastrointestinal mucosa. Gut. **2000**; 47(6):792–800.
283. Paone P, Cani PD. Mucus barrier, mucins and gut microbiota: The expected slimy partners? Gut. **2020**; 69(12):2232–2243.
284. Johansson MEV, Phillipson M, Petersson J, Velcich A, Holm L, Hansson GC. The inner of the two Muc2 mucin-dependent mucus layers in colon is devoid of bacteria. Proceedings of the National Academy of Sciences of the United States of America. **2008**; 105(39):15064–15069.

285. Sluis M Van der, Koning BAE De, Bruijn ACJM De, Velcich A, Meijerink JPP, Goudoever JB Van, Büller HA, Dekker J, Seuningen I Van, Renes IB, Einerhand AWC. Muc2-Deficient Mice Spontaneously Develop Colitis, Indicating That MUC2 Is Critical for Colonic Protection. Gastroenterology. **2006**; 131(1):117–129.
286. Johansson MEV, Holmén Larsson JM, Hansson GC. The two mucus layers of colon are organized by the MUC2 mucin, whereas the outer layer is a legislator of host-microbial interactions. Proceedings of the National Academy of Sciences of the United States of America. **2011**; 108(SUPPL. 1):4659–4665.
287. Kim JM. Antimicrobial Proteins in Intestine and Inflammatory Bowel Diseases. Intestinal Research. **2014**; 12(1):20.
288. Huan Y, Kong Q, Mou H, Yi H. Antimicrobial Peptides: Classification, Design, Application and Research Progress in Multiple Fields. Frontiers in Microbiology. **2020**; 11:582779.
289. Eberl G, Lochner M. The development of intestinal lymphoid tissues at the interface of self and microbiota. Mucosal Immunology. **2009**; 2(6):478–485.
290. Kraehenbuhl JP, Neutra MR. Epithelial M cells: Differentiation and function. Annual Review of Cell and Developmental Biology. **2000**; 16:301–332.
291. Goodman T, Lefrançois L. Expression of the γ-δ T-cell receptor on intestinal CD8+ intraepithelial lymphocytes. Nature. **1988**; 333(6176):855–858.
292. Guy-Grand D, Cerf-Bensussan N, Malissen B, Malassis-Seris M, Briottet C, Vassalli P. Two gut intraepithelial CD8+ lymphocyte populations with different T cell receptors: A role for the gut epithelium in T cell differentiation. Journal of Experimental Medicine. **1991**; 173(2):471–481.
293. Cheroutre H, Lambolez F, Mucida D. The light and dark sides of intestinal intraepithelial lymphocytes. Nature Reviews Immunology. **2011**; 11(7):445–456.
294. Qiu Y, Yang H. Effects of intraepithelial lymphocyte-derived cytokines on intestinal mucosal barrier function. Journal of Interferon and Cytokine Research. **2013**; 33(10):551–562.
295. Costello CM, Willsey GG, Richards AF, Kim J, Pizzuto MS, Jaconi S, Benigni F, Corti D, Mantis NJ, March JC. Transcytosis of IgA Attenuates Salmonella Invasion in Human Enteroids and Intestinal Organoids. Infection and Immunity. **2022**; 90(6):e00041-22.
296. Stadtmueller BM, Huey-Tubman KE, López CJ, Yang Z, Hubbell WL, Bjorkman PJ. The structure and dynamics of secretory component and its interactions with polymeric immunoglobulins. eLife. **2016**; 5:e10640.
297. Woof JM, Russell MW. Structure and function relationships in IgA. Mucosal Immunology. **2011**; 4(6):590–597.
298. Turula H, Wobus CE. The role of the polymeric immunoglobulin receptor and secretory immunoglobulins during mucosal infection and immunity. Viruses. **2018**; 10(5):237.
299. O'Mahony L, Mccarthy J, Kelly P, Hurley G, Luo F, Chen K, O'Sullivan GC, Kiely B, Collins JK, Shanahan F, Quigley EMM. Lactobacillus and Bifidobacterium in irritable bowel syndrome: Symptom responses and relationship to cytokine profiles. Gastroenterology. **2005**; 128(3):541–551.
300. Zeng J, Li YQ, Zuo XL, Zhen YB, Yang J, Liu CH. Clinical trial: Effect of active lactic acid bacteria on mucosal barrier function in patients with diarrhoea-predominant irritable bowel syndrome. Alimentary Pharmacology and Therapeutics. **2008**; 28(8):994–1002.
301. Kajander K, Myllyluoma E, Rajilić-Stojanović M, Kyrönpalo S, Rasmussen M, Järvenpää S, Zoetendal EG, Vos WM De, Vapaatalo H, Korpela R. Clinical trial: Multispecies

probiotic supplementation alleviates the symptoms of irritable bowel syndrome and stabilizes intestinal microbiota. Alimentary Pharmacology and Therapeutics. **2008**; 27(1):48–57.
302. Tan C, Ling Z, Huang Y, Cao Y, Liu Q, Cai T, Yuan H, Liu C, Li Y, Xu K. Dysbiosis of intestinal microbiota associated with inflammation involved in the progression of acute pancreatitis. Pancreas. **2015**; 44(6):868–875.
303. Winkler P, Ghadimi D, Schrezenmeir J, Kraehenbuhl JP. Molecular and cellular basis of microflora-host interactions. Journal of Nutrition. **2007**; 137(3 Suppl 2):756S–72S.
304. Li X, Zhang S, Guo G, Han J, Yu J. Gut microbiome in modulating immune checkpoint inhibitors. eBioMedicine. **2022**; 82:104163.
305. Coombes JL, Powrie F. Dendritic cells in intestinal immune regulation. Nature Reviews Immunology. **2008**; 8(6):435–446.
306. Akira S, Uematsu S, Takeuchi O. Pathogen recognition and innate immunity. Cell. **2006**; 124(4):783–801.
307. Hooper L V. Bacterial contributions to mammalian gut development. Trends in Microbiology. **2004**; 12(3):129–134.
308. Turroni F, Rizzo SM, Ventura M, Bernasconi S. Cross-talk between the infant/maternal gut microbiota and the endocrine system: a promising topic of research. Microbiome Research Reports. **2022**; 1(2):14.
309. Pluznick JL. Gut microbes and host physiology: What happens when you host billions of guests? Frontiers in Endocrinology. **2014**; 5:91.
310. Andoh A. Physiological role of gut microbiota for maintaining human health. Digestion. **2016**; 93(3):176–181.
311. Thaiss CA, Zmora N, Levy M, Elinav E. The microbiome and innate immunity. Nature. **2016**; 535(7610):65–74.
312. Josefowicz SZ, Niec RE, Kim HY, Treuting P, Chinen T, Zheng Y, Umetsu DT, Rudensky AY. Extrathymically generated regulatory T cells control mucosal TH2 inflammation. Nature. **2012**; 482(7385):395–399.
313. Nakanishi Y, Ikebuchi R, Chtanova T, Kusumoto Y, Okuyama H, Moriya T, Honda T, Kabashima K, Watanabe T, Sakai Y, Tomura M. Regulatory T cells with superior immunosuppressive capacity emigrate from the inflamed colon to draining lymph nodes. Mucosal Immunology. **2018**; 11(2):437–448.
314. Lochner M, Bérard M, Sawa S, Hauer S, Gaboriau-Routhiau V, Fernandez TD, Snel J, Bousso P, Cerf-Bensussan N, Eberl G. Restricted Microbiota and Absence of Cognate TCR Antigen Leads to an Unbalanced Generation of Th17 Cells. The Journal of Immunology. **2011**; 186(3):1531–1537.
315. Campbell C, McKenney PT, Konstantinovsky D, Isaeva OI, Schizas M, Verter J, Mai C, Jin WB, Guo CJ, Violante S, Ramos RJ, Cross JR, Kadaveru K, Hambor J, Rudensky AY. Bacterial metabolism of bile acids promotes generation of peripheral regulatory T cells. Nature. **2020**; 581(7809):475–479.
316. Smith PM, Howitt MR, Panikov N, Michaud M, Gallini CA, Bohlooly-Y M, Glickman JN, Garrett WS. The microbial metabolites, short-chain fatty acids, regulate colonic T reg cell homeostasis. Science. **2013**; 341(6145):569–573.
317. Lathrop SK, Bloom SM, Rao SM, Nutsch K, Lio CW, Santacruz N, Peterson DA, Stappenbeck TS, Hsieh CS. Peripheral education of the immune system by colonic commensal microbiota. Nature. **2011**; 478(7368):250–254.

318. Cosovanu C, Neumann C. The Many Functions of Foxp3+ Regulatory T Cells in the Intestine. Frontiers in Immunology. **2020**; 11:600973.
319. Tsuji M, Komatsu N, Kawamoto S, Suzuki K, Kanagawa O, Honjo T, Hori S, Fagarasan S. Preferential generation of follicular B helper T cells from Foxp3 + T cells in gut Peyer's patches. Science. **2009**; 323(5920):1488–1492.
320. Cong Y, Feng T, Fujihashi K, Schoeb TR, Elson CO. A dominant, coordinated T regulatory cell-IgA response to the intestinal microbiota. Proceedings of the National Academy of Sciences of the United States of America. **2009**; 106(46):19256–19261.
321. Thome JJC, Bickham KL, Ohmura Y, Kubota M, Matsuoka N, Gordon C, Granot T, Griesemer A, Lerner H, Kato T, Farber DL. Early-life compartmentalization of human T cell differentiation and regulatory function in mucosal and lymphoid tissues. Nature Medicine. **2016**; 22(1):72–77.
322. Sonnenberg GF, Artis D. Innate Lymphoid Cell Interactions with Microbiota: Implications for Intestinal Health and Disease. Immunity. **2012**; 37(4):601–610.
323. Sawa S, Lochner M, Satoh-Takayama N, Dulauroy S, Bérard M, Kleinschek M, Cua D, Santo JP Di, Eberl G. RORγt+ innate lymphoid cells regulate intestinal homeostasis by integrating negative signals from the symbiotic microbiota. Nature Immunology. **2011**; 12(4):320–328.
324. Hepworth MR, Monticelli LA, Fung TC, Ziegler CGK, Grunberg S, Sinha R, Mantegazza AR, Ma HL, Crawford A, Angelosanto JM, John Wherry E, Koni PA, Bushman FD, Elson CO, Eberl G, Artis D, Sonnenberg GF. Innate lymphoid cells regulate CD4 + T-cell responses to intestinal commensal bacteria. Nature. **2013**; 498(7452):113–117.
325. Hepworth MR, Fung TC, Masur SH, Kelsen JR, McConnell FM, Dubrot J, Withers DR, Hugues S, Farrar MA, Reith W, Eberl G, Baldassano RN, Laufer TM, Elson CO, Sonnenberg GF. Group 3 innate lymphoid cells mediate intestinal selection of commensal bacteria-specific CD4+ T cells. Science. **2015**; 348(6238):1031–1035.
326. Lyu M, Suzuki H, Kang L, et al. ILC3s select microbiota-specific regulatory T cells to establish tolerance in the gut. Nature. **2022**; 610(7933):744–751.
327. Spits H, Artis D, Colonna M, Diefenbach A, Santo JP Di, Eberl G, Koyasu S, Locksley RM, McKenzie ANJ, Mebius RE, Powrie F, Vivier E. Innate lymphoid cells - a proposal for uniform nomenclature. Nature Reviews Immunology. **2013**; 13(2):145–149.
328. Jarade A, Garcia Z, Marie S, Demera A, Prinz I, Bousso P, Santo JP Di, Serafini N. Inflammation triggers ILC3 patrolling of the intestinal barrier. Nature Immunology. Springer US; **2022**; 23(9):1317–1323.
329. Coombes JL, Siddiqui KRR, Arancibia-Cárcamo C V., Hall J, Sun CM, Belkaid Y, Powrie F. A functionally specialized population of mucosal CD103+ DCs induces Foxp3+ regulatory T cells via a TGF-β -and retinoic acid-dependent mechanism. Journal of Experimental Medicine. **2007**; 204(8):1757–1764.
330. Broere F, Pré MF du, Berkel LA van, Garssen J, Schmidt-Weber CB, Lambrecht BN, Hendriks RW, Nieuwenhuis EES, Kraal G, Samsom JN. Cyclooxygenase-2 in mucosal DC mediates induction of regulatory T cells in the intestine through suppression of IL-4. Mucosal Immunology. **2009**; 2(3):254–264.
331. Round JL, Mazmanian SK. Erratum: The gut microbiota shapes intestinal immune responses during health and disease. Nature Reviews Immunology. **2009**; 9:313–323.
332. Bouskra D, Brézillon C, Bérard M, Werts C, Varona R, Boneca IG, Eberl G. Lymphoid tissue genesis induced by commensals through NOD1 regulates intestinal homeostasis.

Nature. **2008**; 456(7221):507–510.
333. Cheng Z, Taylor B, Ourthiague DR, Hoffmann A. Distinct single-cell signaling characteristics are conferred by the MyD88 and TRIF pathways during TLR4 activation. Science Signaling. **2015**; 8(385):ra69.
334. Zeuthen LH, Fink LN, Frokiaer H. Epithelial cells prime the immune response to an array of gut-derived commensals towards a tolerogenic phenotype through distinct actions of thymic stromal lymphopoietin and transforming growth factor-β. Immunology. **2008**; 123(2):197–208.
335. Shang L, Fukata M, Thirunarayanan N, Martin AP, Arnaboldi P, Maussang D, Berin C, Unkeless JC, Mayer L, Abreu MT, Lira SA. Toll-Like Receptor Signaling in Small Intestinal Epithelium Promotes B-Cell Recruitment and IgA Production in Lamina Propria. Gastroenterology. **2008**; 135(2):529–38.
336. Kim CH. Control of lymphocyte functions by gut microbiota-derived short-chain fatty acids. Cellular and Molecular Immunology. **2021**; 18(5):1161–1171.
337. Kelly CJ, Zheng L, Campbell EL, Saeedi B, Scholz CC, Bayless AJ, Wilson KE, Glover LE, Kominsky DJ, Magnuson A, Weir TL, Ehrentraut SF, Pickel C, Kuhn KA, Lanis JM, Nguyen V, Taylor CT, Colgan SP. Crosstalk between microbiota-derived short-chain fatty acids and intestinal epithelial HIF augments tissue barrier function. Cell Host and Microbe. **2015**; 17(5):662–671.
338. Furusawa Y, Obata Y, Fukuda S, et al. Commensal microbe-derived butyrate induces the differentiation of colonic regulatory T cells. Nature. **2013**; 504(7480):446–450.
339. Arpaia N, Campbell C, Fan X, Dikiy S, Veeken J Van Der, Deroos P, Liu H, Cross JR, Pfeffer K, Coffer PJ, Rudensky AY. Metabolites produced by commensal bacteria promote peripheral regulatory T-cell generation. Nature. **2013**; 504(7480):451–455.
340. Singh N, Gurav A, Sivaprakasam S, Brady E, Padia R, Shi H, Thangaraju M, Prasad PD, Manicassamy S, Munn DH, Lee JR, Offermanns S, Ganapathy V. Activation of Gpr109a, receptor for niacin and the commensal metabolite butyrate, suppresses colonic inflammation and carcinogenesis. Immunity. **2014**; 40(1):128–139.
341. Kimura I, Ozawa K, Inoue D, Imamura T, Kimura K, Maeda T, Terasawa K, Kashihara D, Hirano K, Tani T, Takahashi T, Miyauchi S, Shioi G, Inoue H, Tsujimoto G. The gut microbiota suppresses insulin-mediated fat accumulation via the short-chain fatty acid receptor GPR43. Nature Communications. **2013**; 4:1829.
342. Round JL, Mazmanian SK. Inducible Foxp3+ regulatory T-cell development by a commensal bacterium of the intestinal microbiota. Proceedings of the National Academy of Sciences of the United States of America. **2010**; 107(27):12204–12209.
343. Kullberg MC, Jankovic D, Gorelick PL, Caspar P, Letterio JJ, Cheever AW, Sher A. Bacteria-triggered CD4+ T regulatory cells suppress Helicobacter hepaticus-induced colitis. Journal of Experimental Medicine. **2002**; 196(4):505–515.
344. Atarashi K, Tanoue T, Shima T, Imaoka A, Kuwahara T, Momose Y, Cheng G, Yamasaki S, Saito T, Ohba Y, Taniguchi T, Takeda K, Hori S, Ivanov II, Umesaki Y, Itoh K, Honda K. Induction of colonic regulatory T cells by indigenous Clostridium species. Science. **2011**; 331(6015):337–341.
345. Karimi K, Inman MD, Bienenstock J, Forsythe P. Lactobacillus reuteri-induced regulatory T cells protect against an allergic airway response in mice. American Journal of Respiratory and Critical Care Medicine. **2009**; 179(3):186–193.
346. Lavasani S, Dzhambazov B, Nouri M, Fåk F, Buske S, Molin G, Thorlacius H, Alenfall J,

Jeppsson B, Weström B. A novel probiotic mixture exerts a therapeutic effect on experimental autoimmune encephalomyelitis mediated by IL-10 producing regulatory T cells. PLoS ONE. **2010**; 5(2):e9009.
347. O'Mahony C, Scully P, O'Mahony D, Murphy S, O'Brien F, Lyons A, Sherlock G, MacSharry J, Kiely B, Shanahan F, O'Mahony L. Commensal-induced regulatory T cells mediate protection against pathogen-stimulated NF-κB activation. PLoS Pathogens. **2008**; 4(8):e1000112.
348. Lyons A, O'Mahony D, O'Brien F, MacSharry J, Sheil B, Ceddia M, Russell WM, Forsythe P, Bienenstock J, Kiely B, Shanahan F, O'Mahony L. Bacterial strain-specific induction of Foxp3+ T regulatory cells is protective in murine allergy models. Clinical and Experimental Allergy. **2010**; 40(5):811–819.
349. López P, González-Rodríguez I, Gueimonde M, Margolles A, Suárez A. Immune response to Bifidobacterium bifidum strains support Treg/Th17 plasticity. PLoS ONE. **2011**; 6(9):e24776.
350. Sun S, Luo L, Liang W, Yin Q, Guo J, Rush AM, Lv Z, Liang Q, Fischbach MA, Sonnenburg JL, Dodd D, Davis MM, Wang F. Bifidobacterium alters the gut microbiota and modulates the functional metabolism of T regulatory cells in the context of immune checkpoint blockade. Proceedings of the National Academy of Sciences of the United States of America. **2020**; 117(44):27509–27515.
351. Li D, Cheng J, Zhu Z, Catalfamo M, Goerlitz D, Lawless OJ, Tallon L, Sadzewicz L, Calderone R, Bellanti JA. Treg–inducing capacity of genomic DNA of Bifidobacterium longum subsp. infantis. Allergy and Asthma Proceedings. **2020**; 41(5):372–385.
352. Fujimura KE, Sitarik AR, Havstad S, Lin DL, Levan S, Fadrosh D, Panzer AR, Lamere B, Rackaityte E, Lukacs NW, Wegienka G, Boushey HA, Ownby DR, Zoratti EM, Levin AM, Johnson CC, Lynch S V. Neonatal gut microbiota associates with childhood multisensitized atopy and T cell differentiation. Nature Medicine. **2016**; 22(10):1187–1191.
353. Ni J, Wu GD, Albenberg L, Tomov VT. Gut microbiota and IBD: Causation or correlation? Nature Reviews Gastroenterology and Hepatology. **2017**; 14(10):573–584.
354. Fan Y, Pedersen O. Gut microbiota in human metabolic health and disease. Nature Reviews Microbiology. **2021**; 19(1):55–71.
355. Stiemsma LT, Arrieta MC, Dimitriu PA, Cheng J, Thorson L, Lefebvre DL, Azad MB, Subbarao P, Mandhane P, Becker A, Sears MR, Kollmann TR, Mohn WW, Finlay BB, Turvey SE. Shifts in Lachnospira and Clostridium sp. in the 3-month stool microbiome are associated with preschool age asthma. Clinical Science. **2016**; 130(23):2199–2207.
356. Arrieta MC, Stiemsma LT, Dimitriu PA, et al. Early infancy microbial and metabolic alterations affect risk of childhood asthma. Science Translational Medicine. **2015**; 7(307):307ra152.
357. Penders J, Thijs C, Brandt PA Van Den, Kummeling I, Snijders B, Stelma F, Adams H, Ree R Van, Stobberingh EE. Gut microbiota composition and development of atopic manifestations in infancy: The KOALA birth cohort study. Gut. **2007**; 56(5):661–667.
358. Wang M, Karlsson C, Olsson C, Adlerberth I, Wold AE, Strachan DP, Martricardi PM, Åberg N, Perkin MR, Tripodi S, Coates AR, Hesselmar B, Saalman R, Molin G, Ahrné S. Reduced diversity in the early fecal microbiota of infants with atopic eczema. Journal of Allergy and Clinical Immunology. **2008**; 121(1):129–134.
359. Nylund L, Nermes M, Isolauri E, Salminen S, Vos WM De, Satokari R. Severity of atopic disease inversely correlates with intestinal microbiota diversity and butyrate-producing

bacteria. Allergy: European Journal of Allergy and Clinical Immunology. **2015**; 70(2):241–244.
360. Alsharairi NA. The role of short-chain fatty acids in the interplay between a very low-calorie ketogenic diet and the infant gut microbiota and its therapeutic implications for reducing asthma. International Journal of Molecular Sciences. **2020**; 21(24):1–21.
361. Kim HK, Rutten NBMM, Besseling-van der Vaart I, Niers LEM, Choi YH, Rijkers GT, Hemert S van. Probiotic supplementation influences faecal short chain fatty acids in infants at high risk for eczema. Beneficial Microbes. **2015**; 6(6):783–790.
362. Akiyama T, Miyamoto H, Fukuda K, Sano N, Katagiri N, Shobuike T, Kukita A, Yamashita Y, Taniguchi H, Goto M. Development of a novel PCR method to comprehensively analyze salivary bacterial flora and its application to patients with odontogenic infections. Oral Surgery, Oral Medicine, Oral Pathology, Oral Radiology and Endodontology. **2010**; 109(5):669–676.
363. Yoshimura K, Morotomi N, Fukuda K, Nakano M, Kashimura M, Hachisuga T, Taniguchi H. Intravaginal microbial flora by the 16S rRNA gene sequencing. American Journal of Obstetrics and Gynecology. **2011**; 205(3):235.e1-235.e9.
364. Claesson MJ, Wang Q, O'Sullivan O, Greene-Diniz R, Cole JR, Ross RP, O'Toole PW. Comparison of two next-generation sequencing technologies for resolving highly complex microbiota composition using tandem variable 16S rRNA gene regions. Nucleic Acids Research. **2010**; 38(22):e200.
365. Neefs J marc, Peer Y Van De, Rijk P De, Chapelle S, Wachter R de. Compilation of small ribosomal subunit RNA structures. Nucleic Acids Research. **1993**; 21(13):3025–3049.
366. Hoffman C, Siddiqui NY, Fields I, Gregory WT, Simon HM, Mooney MA, Wolfe AJ, Karstens L. Species-Level Resolution of Female Bladder Microbiota from 16S rRNA Amplicon Sequencing. mSystems. **2021**; 6(5):e0051821.
367. Quince C, Walker AW, Simpson JT, Loman NJ, Segata N. Shotgun metagenomics, from sampling to analysis. Nature Biotechnology. **2017**; 35(9):833–844.
368. Lapidus AL, Korobeynikov AI. Metagenomic Data Assembly – The Way of Decoding Unknown Microorganisms. Frontiers in Microbiology. **2021**; 12:613791.
369. Cho JC, Tiedje JM. Bacterial Species Determination from DNA-DNA Hybridization by Using Genome Fragments and DNA Microarrays. Applied and Environmental Microbiology. **2001**; 67(8):3677–3682.
370. Paliy O, Agans R. Application of phylogenetic microarrays to interrogation of human microbiota. FEMS Microbiology Ecology. **2012**; 79(1):2–11.
371. Mandelbrot L, Landreau-Mascaro A, Rekacewicz C, Berrebi A, Bénifla JL, Burgard M, Lachassine E, Barret B, Chaix ML, Bongain A, Ciraru-Vigneron N, Crenn-Hébert C, Delfraissy JF, Rouzioux C, Mayaux MJ, Blanche S. Lamivudine-zidovudine combination for prevention of maternal-infant transmission of HIV-1. Jama. **2001**; 285(16):2083–2093.
372. Slogrove AL, Powis KM, Johnson LF, Stover J, Mahy M. Global estimates of children HIV exposed and uninfected in the evolving HIV epidemic: 2000 to 2018. Lancet global health. **2020**; 8(1):e67–e75.
373. Marinda E, Humphrey JH, Iliff PJ, et al. Child mortality according to maternal and infant HIV status in Zimbabwe. Pediatric Infectious Disease Journal. **2007**; 26(6):519–526.
374. Slogrove A, Reikie B, Naidoo S, Beer C De, Ho K, Cotton M, Bettinger J, Speert D, Esser M, Kollmann T. HIV-exposed uninfected infants are at increased risk for severe infections in the first year of life. Journal of Tropical Pediatrics. **2012**; 58(6):505–508.

375. Liu L, Johnson HL, Cousens S, Perin J, Scott S, Lawn JE, Rudan I, Campbell H, Cibulskis R, Li M, Mathers C, Black RE. Global, regional, and national causes of child mortality: An updated systematic analysis for 2010 with time trends since 2000. The Lancet. **2012**; 379(9832):2151–2161.
376. Brennan AT, Bonawitz R, Gill CJ, Thea DM, Kleinman M, Useem J, Garrison L, Ceccarelli R, Udokwu C, Long L, Fox MP. A meta-analysis assessing all-cause mortality in HIVexposed uninfected compared with HIV-unexposed uninfected infants and children. AIDS. **2016**; 30(15):2351–2360.
377. Zash R, Souda S, Leidner J, Ribaudo H, Binda K, Moyo S, Powis KM, Petlo C, Mmalane M, Makhema J, Essex M, Lockman S, Shapiro R. HIV-exposed children account for more than half of 24-month mortality in Botswana. BMC Pediatrics. **2016**; 16(1):103.
378. Kuhn L, Kasonde P, Sinkala M, Kankasa C, Semrau K, Scott N, Tsai WY, Vermund SH, Aldrovandi GM, Thea DM. Does severity of HIV disease in HIV-infected mothers affect mortality and morbidity among their uninfected infants? Clinical Infectious Diseases. **2005**; 41(11):1654–1661.
379. Chilongozi D, Wang L, Brown L, Taha T, Valentine M, Emel L, Sinkala M, Kafulafula G, Noor RA, Read JS, Brown ER, Goldenberg RL, Hoffman I. Morbidity and mortality among a cohort of human immunodeficiency virus type 1-infected and uninfected pregnant women and their infants from Malawi, Zambia, and Tanzania. Pediatric Infectious Disease Journal. **2008**; 27(9):808–814.
380. Shapiro RL, Lockman S, Kim S, Smeaton L, Rahkola JT, Thior I, Wester C, Moffat C, Arimi P, Ndase P, Asmelash A, Stevens L, Montano M, Makhema J, Essex M, Janoff EN. Infant morbidity, mortality, and breast milk immunologic profiles among breast-feeding HIV-infected and HIV-uninfected women in Botswana. Journal of Infectious Diseases. **2007**; 196(4):562–569.
381. Brahmbhatt H, Kigozi G, Wabwire-Mangen F, Serwadda D, Lutalo T, Nalugoda F, Sewankambo N, Kiduggavu M, Wawer M, Gray R. Mortality in HIV-infected and uninfected children of HIV-infected and uninfected mothers in rural Uganda. Journal of Acquired Immune Deficiency Syndromes. **2006**; 41(4):504–508.
382. Madhi SA, Nachman S, Violari A, Kim S, Cotton MF, Bobat R, Jean-Philippe P, McSherry G, Mitchell C. Primary Isoniazid Prophylaxis against Tuberculosis in HIV-Exposed Children. New England Journal of Medicine. **2011**; 365(1):21–31.
383. Cranmer LM, Draper HR, Mandalakas AM, Kim S, McSherry G, Krezinski E, Coetzee J, Mitchell C, Nachman S, Linde M van der, Cotton MF, Hesseling AC. High Incidence of Tuberculosis Infection in Hiv-Exposed Children Exiting an Isoniazid Preventive Therapy Trial. Pediatric Infectious Disease Journal. **2018**; 37(10):E254–E256.
384. Zhang X, Justice AC, Hu Y, Wang Z, Zhao H, Wang G, Johnson EO, Emu B, Sutton RE, Krystal JH, Xu K. Epigenome-wide differential DNA methylation between HIV-infected and uninfected individuals. Epigenetics. **2016**; 11(10):750–760.
385. Musimbi ZD, Rono MK, Otieno JR, Kibinge N, Ochola-Oyier LI, Villiers EP de, Nduati EW. Peripheral blood mononuclear cell transcriptomes reveal an over-representation of down-regulated genes associated with immunity in HIV-exposed uninfected infants. Scientific Reports. **2019**; 9(1):1–12.
386. Marsit CJ, Brummel SS, Kacanek D, Seage GR, Spector SA, Armstrong DA, Lester BM, Rich K. Infant peripheral blood repetitive element hypomethylation associated with antiretroviral therapy in utero. Epigenetics. **2015**; 10(8):708–716.

387. Farquhar C, Nduati R, Haigwood N, Sutton W, Mbori-Ngacha D, Richardson B, John-Stewart G. High maternal HIV-1 viral load during pregnancy is associated with reduced placental transfer of measles IgG antibody. Journal of Acquired Immune Deficiency Syndromes. **2005**; 40(4):494–497.
388. Legrand FA, Nixon DF, Loo CP, Ono E, Chapman JM, Miyamoto M, Diaz RS, Santos AMN, Succi RCM, Abadi J, Rosenberg MG, Moraes-Pinto MI de, Kallas EG. Strong HIV-1-specific T cell responses in HIV-1-exposed uninfected infants and neonates revealed after regulatory T cell removal. PLoS ONE. **2006**; 1(1):e102.
389. Kidzeru EB, Hesseling AC, Passmore JAS, Myer L, Gamieldien H, Tchakoute CT, Gray CM, Sodora DL, Jaspan HB. In-utero exposure to maternal HIV infection alters T-cell immune responses to vaccination in HIV-uninfected infants. AIDS. **2014**; 28(10):1421–1430.
390. Zhang M, Lin Y, Iyer D V., Gong J, Abrams JS, Barnes PF. T-cell cytokine responses in human infection with Mycobacterium tuberculosis. Infection and Immunity. **1995**; 63(8):3231–3234.
391. Williams A, Steffens F, Reinecke C, Meyer D. The Th1/Th2/Th17 cytokine profile of HIV-infected individuals: A multivariate cytokinomics approach. Cytokine. **2013**; 61(2):521–526.
392. Gulzar N, Diker B, Balasubramanian S, Jiang JQ, Copeland KFT. Human immunodeficiency virus-1 infection protects against a Tc1-to-Tc2 shift in CD8(+) T cells. Human Immunology. **2011**; 72(11):995–1000.
393. Borges-Almeida E, Milanez HM, Vilela MM, Cunha FGP, Abramczuk BM, Reis-Alves SC, Metze K, Lorand-Metze I. The impact of maternal HIV infection on cord blood lymphocyte subsets and cytokine profile in exposed non-infected newborns. BMC Infectious Diseases. **2011**; 11:38.
394. Sommer F, Bäckhed F. The gut microbiota-masters of host development and physiology. Nature Reviews Microbiology. **2013**; 11(4):227–238.
395. Tamburini S, Shen N, Wu HC, Clemente JC. The microbiome in early life: Implications for health outcomes. Nature Medicine. **2016**; 22(7):713–722.
396. Clerici M, Saresella M, Colombo F, Fossati S, Sala N, Bricalli D, Villa ML, Ferrante P, Dally L, Vigano A. T-lymphocyte maturation abnormalities in uninfected newborns and children with vertical exposure to HIV. Blood. **2000**; 96(12):3866–3871.
397. Nielsen SD, Jeppesen DL, Kolte L, Clark DR, Sørensen TU, Dreves AM, Ersbøll AK, Ryder LP, Valerius NH, Nielsen JO. Impaired progenitor cell function in HIV-negative infants of HIV-positive mothers results in decreased thymic output and low CD4 counts. Blood. **2001**; 98(2):398–404.
398. Smith C, Jalbert E, Almeida V de, et al. Altered natural killer cell function in HIV-exposed uninfected infants. Frontiers in Immunology. **2017**; 8:470.
399. Moraes-Pinto MI De, Almeida ACM, Kenj G, Filgueiras TE, Tobias W, Santos AMN, Carneiro-Sampaio MMS, Farhat CK, Milligan PJM, Johnson PM, Hart CA. Placental transfer and maternally acquired neonatal IgG immunity in human immunodeficiency virus infection. Journal of Infectious Diseases. **1996**; 173(5):1077–1084.
400. Jones CE, Naidoo S, Beer C De, Esser M, Kampmann B, Hesseling AC. Maternal HIV infection and antibody responses against vaccine-preventable diseases in uninfected infants. Jama. **2011**; 305(6):576–584.
401. Mazzola TN, Silva MTN Da, Abramczuk BM, Moreno YMF, Lima SCBS, Zorzeto TQ,

Passeto ASZ, Vilela MMS. Impaired Bacillus Calmette-Guérin cellular immune response in HIV-exposed, uninfected infants. AIDS. **2011**; 25(17):2079–2087.
402. Lewy T, Hong BY, Weiser B, Burger H, Tremain A, Weinstock G, Anastos K, George MD. Oral Microbiome in HIV-Infected Women: Shifts in the Abundance of Pathogenic and Beneficial Bacteria Are Associated with Aging, HIV Load, CD4 Count, and Antiretroviral Therapy. AIDS Research and Human Retroviruses. **2019**; 35(3):276–286.
403. Vujkovic-Cvijin I, Sortino O, Verheij E, Sklar J, Wit FW, Kootstra NA, Sellers B, Brenchley JM, Ananworanich J, Loeff MS van der, Belkaid Y, Reiss P, Sereti I. HIV-associated gut dysbiosis is independent of sexual practice and correlates with noncommunicable diseases. Nature Communications. **2020**; 11(1):2448.
404. Bender JM, Li F, Martelly S, Byrt E, Rouzier V, Leo M, Tobin N, Pannaraj PS, Adisetiyo H, Rollie A, Santiskulvong C, Wang S, Autran C, Bode L, Fitzgerald D, Kuhn L, Aldrovandi GM. Maternal HIV infection influences the microbiome of HIV-uninfected infants. Science Translational Medicine. **2016**; 8(349):349ra100.
405. Grant-Beurmann S, Jumare J, Ndembi N, Matthew O, Shutt A, Omoigberale A, Martin OA, Fraser CM, Charurat M. Dynamics of the infant gut microbiota in the first 18 months of life: the impact of maternal HIV infection and breastfeeding. Microbiome. BioMed Central; **2022**; 10(1):1–18.
406. Amenyogbe N, Dimitriu P, Cho P, Ruck C, Fortuno ES, Cai B, Alimenti A, Côté HCF, Maan EJ, Slogrove AL, Esser M, Marchant A, Goetghebuer T, Shannon CP, Tebbutt SJ, Kollmann TR, Mohn WW, Smolen KK. Innate Immune Responses and Gut Microbiomes Distinguish HIV-Exposed from HIV-Unexposed Children in a Population-Specific Manner. The Journal of Immunology. **2020**; 205(10):2618–2628.
407. Jackson CL, Frank DN, Robertson CE, Ir D, Kofonow JM, Montlha MP, Mutsaerts EAML, Nunes MC, Madhi SA, Ghosh D, Weinberg A. Evolution of the Gut Microbiome in HIV-Exposed Uninfected and Unexposed Infants during the First Year of Life. mBio. **2022**; 13(5):e0122922.
408. Machiavelli A, Duarte RTD, Pires MM d. S, Zárate-Bladés CR, Pinto AR. The impact of in utero HIV exposure on gut microbiota, inflammation, and microbial translocation. Gut Microbes. **2019**; 10(5):599–614.
409. Claassen-Weitz S, Gardner-Lubbe S, Nicol P, Botha G, Mounaud S, Shankar J, Nierman WC, Mulder N, Budree S, Zar HJ, Nicol MP, Kaba M. HIV-exposure, early life feeding practices and delivery mode impacts on faecal bacterial profiles in a South African birth cohort. Scientific Reports. **2018**; 8(1):5078.
410. Jenkins HE, Yuen CM, Rodriguez CA, Nathavitharana RR, McLaughlin MM, Donald P, Marais BJ, Becerra MC. Mortality in children diagnosed with tuberculosis: a systematic review and meta-analysis. The Lancet Infectious Diseases. **2017**; 17(3):285–295.
411. Flynn JAL. Immunology of tuberculosis and implications in vaccine development. Tuberculosis. **2004**; 84(1–2):93–101.
412. Fernandez D, Salami I, Davis J, Mbah F, Kazeem A, Ash A, Babino J, Carter L, Salemi JL, Spooner KK, Olaleye OA, Salihu HM. HIV-TB Coinfection among 57 Million Pregnant Women, Obstetric Complications, Alcohol Use, Drug Abuse, and Depression. Journal of Pregnancy. **2018**; 2018:5896901.
413. Gensollen T, Iyer SS, Kasper DL, Blumberg RS. How colonization by microbiota in early life shapes the immune system. Science. **2016**; 352(6285):539–544.
414. UNAIDS. UNAIDS data 2020 [Internet]. 2020 [cited 2023 Feb 21]. Available from:

https://www.unaids.org/en/resources/documents/2020/unaids-data
415. Evans C, Jones CE, Prendergast AJ. HIV-exposed, uninfected infants: new global challenges in the era of paediatric HIV elimination. The Lancet Infectious Diseases. **2016**; 16(6):e92–e107.
416. Jao J, Sun S, Bonner LB, Legbedze J, Mmasa KN, Makhema J, Mmalane M, Kgole S, Masasa G, Moyo S, Gerschenson M, Mohammed T, Abrams EJ, Kurland IJ, Geffner ME, Powis KM. Lower Insulin Sensitivity in Newborns With In Utero HIV and Antiretroviral Exposure Who Are Uninfected in Botswana. The Journal of infectious diseases. **2022**; 226(11):2002–2009.
417. Tchakoute CT, Sainani KL, Osawe S, Datong P, Kiravu A, Rosenthal KL, Gray CM, William Cameron D, Abimiku A le, Jaspan HB. Breastfeeding mitigates the effects of maternal HIV on infant infectious morbidity in the Option B+ era. Aids. **2018**; 32(16):2383–2391.
418. Cranmer LM, Kanyugo M, Jonnalagadda SR, Lohman-Payne B, Sorensen B, Maleche Obimbo E, Wamalwa D, John-Stewart GC. High prevalence of tuberculosis infection in HIV-1 exposed kenyan infants. Pediatric Infectious Disease Journal. **2014**; 33(4):401–406.
419. WHO. Global tuberculosis report 2022 [Internet]. 2022 [cited 2021 Feb 21]. Available from: https://www.who.int/publications/i/item/9789240061729
420. Marchant A, Goldman M. T cell-mediated immune responses in human newborns: Ready to learn? Clinical and Experimental Immunology. **2005**; 141(1):10–18.
421. Anterasian C, Warr AJ, Lacourse SM, Kinuthia J, Richardson BA, Nguyen FK, Matemo D, Maleche-Obimbo E, John Stewart GC, Hawn TR. Non-IFNγ Whole Blood Cytokine Responses to Mycobacterium Tuberculosis Antigens in HIV-exposed Infants. Pediatric Infectious Disease Journal. **2021**; 40(10):922–929.
422. Crook AM, Turkova A, Musiime V, et al. Tuberculosis incidence is high in HIV-infected African children but is reduced by co-trimoxazole and time on antiretroviral therapy. BMC Medicine. **2016**; 14(1):50.
423. Subramanian S, Blanton L V., Frese SA, Charbonneau M, Mills DA, Gordon JI. Cultivating healthy growth and nutrition through the gut microbiota. Cell. **2015**; 161(1):36–48.
424. Slogrove AL, Powis KM, Johnson LF, Stover J, Mahy M. Estimates of the global population of children who are HIV-exposed and uninfected, 2000–18: a modelling study. The Lancet Global Health. **2020**; 8(1):e67–e75.
425. Cohen C, Moyes J, Tempia S, Groome M, Walaza S, Pretorius M, Naby F, Mekgoe O, Kahn K, Gottberg A Von, Wolter N, Cohen AL, Mollendorf C Von, Venter M, Madhi SA. Epidemiology of acute lower respiratory tract infection in HIV exposed uninfected infants. Pediatrics. **2016**; 137(4):e20153272.
426. Smith C, Moraka NO, Ibrahim M, Moyo S, Mayondi G, Kammerer B, Leidner J, Gaseitsiwe S, Li S, Shapiro R, Lockman S, Weinberg A. Human immunodeficiency virus exposure but not early cytomegalovirus infection is associated with increased hospitalization and decreased memory T-cell responses to tetanus vaccine. Journal of Infectious Diseases. **2020**; 221(7):1167–1175.
427. Abu-Raya B, Smolen KK, Willems F, Kollmann TR, Marchant A. Transfer of maternal antimicrobial immunity to HIV-exposed uninfected newborns. Frontiers in Immunology. **2016**; 7:338.
428. Zimmermann P, Curtis N. Factors that influence the immune response to vaccination. Clinical Microbiology Reviews. **2019**; 32(2):e00084-18.

429. Hagan T, Cortese M, Rouphael N, et al. Antibiotics-Driven Gut Microbiome Perturbation Alters Immunity to Vaccines in Humans. Cell. **2019**; 178(6):1313–1328.e13.
430. Huda MN, Lewis Z, Kalanetra KM, Rashid M, Ahmad SM, Raqib R, Qadri F, Underwood MA, Mills DA, Stephensen CB. Stool microbiota and vaccine responses of infants. Pediatrics. **2014**; 134(2):e362–e372.
431. South African National Department of Health. National consolidated guidelines for the prevention of mother-to-child transmission of HIV [Internet]. 2015 [cited 2023 Mar 7]. Available from: https://sahivsoc.org/Files/ART Guidelines 15052015.pdf
432. Federal Ministry of Health. National Guidelines for HIV Prevention, Treatment and Care, National AIDS and STI's Control Programme [Internet]. 2016 [cited 2023 Mar 7]. Available from: https://www.prepwatch.org/wp-content/uploads/2017/08/nigeria_national_guidelines_2016.pdf
433. WHO. Consolidated Guidelines on the use of antiretroviral drugs for treating and preventing HIV infection [Internet]. 2015 [cited 2023 Mar 7]. Available from: https://apps.who.int/iris/bitstream/handle/10665/198064/9789241509893_eng.pdf
434. Kuhn L, Aldrovandi GM, Sinkala M, Kankasa C, Semrau K, Kasonde P, Mwiya M, Tsai WY, Thea DM. Differential effects of early weaning for HIV-free survival of children born to HIV-infected mothers by severity of maternal disease. PLoS ONE. **2009**; 4(6):e6059.
435. Yuan S, Cohen DB, Ravel J, Abdo Z, Forney LJ. Evaluation of methods for the extraction and purification of DNA from the human microbiome. PLoS ONE. **2012**; 7(3):e33865.
436. Dabee S, Tanko RF, Brown BP, Bunjun R, Balle C, Feng C, Konstantinus IN, Jaumdally SZ, Onono M, Nair G, Palanee-Phillips T, Gill K, Baeten JM, Bekker LG, Passmore JAS, Heffron R, Jaspan HB, Happel AU. Comparison of Female Genital Tract Cytokine and Microbiota Signatures Induced by Initiation of Intramuscular DMPA and NET-EN Hormonal Contraceptives - a Prospective Cohort Analysis. Frontiers in Immunology. **2021**; 12:760504.
437. Martin M. Cutadapt removes adapter sequences from high-throughput sequencing reads. EMBnet Journal. **2011**; 17(1):10.
438. Callahan BJ, McMurdie PJ, Rosen MJ, Han AW, Johnson AJA, Holmes SP. DADA2: High-resolution sample inference from Illumina amplicon data. Nature Methods. **2016**; 13(7):581–583.
439. R Core Team. A Language and Environment for Statistical Computing [Internet]. R Foundation for Statistical Computing. 2020. Available from: http://www.r-project.org
440. Quast C, Pruesse E, Yilmaz P, Gerken J, Schweer T, Yarza P, Peplies J, Glöckner FO. The SILVA ribosomal RNA gene database project: Improved data processing and web-based tools. Nucleic Acids Research. **2013**; 41(D1):D590–D596.
441. Brown BP. Updated 16S databases for marker gene taxonomic assignment [Internet]. Github. 2021 [cited 2023 Mar 24]. Available from: https://github.com/itsmisterbrown/updated_16S_dbs
442. Davis NM, Proctor DiM, Holmes SP, Relman DA, Callahan BJ. Simple statistical identification and removal of contaminant sequences in marker-gene and metagenomics data. Microbiome. **2018**; 6(1):226.
443. McMurdie PJ, Holmes S. Phyloseq: An R Package for Reproducible Interactive Analysis and Graphics of Microbiome Census Data. PLoS ONE. **2013**; 8(4):e61217.
444. Oksanen J, Simpson GL, Blanchet FG, et al. Vegan: Community Ecology Package [Internet]. 2022 [cited 2023 Mar 7]. Available from: https://cran.r-

project.org/web/packages/vegan/index.html
445. Maechler M, Rousseeuw P, Struyf A, Hubert M, Hornik K, Studer M, Roudier P, Gonzalez J, Kozlowski K, Schubert E, Murphy K. cluster: Cluster Analysis Basics and Extensions [Internet]. 2019 [cited 2023 Mar 7]. Available from: https://cran.r-project.org/web/packages/cluster/index.html
446. Lin H, Peddada S Das. Analysis of compositions of microbiomes with bias correction. Nature Communications. **2020**; 11(1):3514.
447. Friedman J, Hastie T, Tibshirani R. Regularization paths for generalized linear models via coordinate descent. Journal of Statistical Software. **2010**; 33(1):1–22.
448. Callahan BJ, Sankaran K, Fukuyama JA, McMurdie PJ, Holmes SP. Bioconductor Workflow for Microbiome Data Analysis: from raw reads to community analyses. F1000Research. **2016**; 5:1492.
449. Chen J, Wright K, Davis JM, Jeraldo P, Marietta E V., Murray J, Nelson H, Matteson EL, Taneja V. An expansion of rare lineage intestinal microbes characterizes rheumatoid arthritis. Genome Medicine. **2016**; 8(1):43.
450. Perlaza-Jiménez L, Wu Q, Torres VVL, Zhang X, Li J, Rocker A, Lithgow T, Zhou T, Vijaykrishna D. Forensic genomics of a novel klebsiella quasipneumoniae type from a neonatal intensive care unit in China reveals patterns of colonization, evolution and epidemiology. Microbial Genomics. **2020**; 6(10):1–10.
451. Western Cape Government. Circular H 117/2020: Introduction of tetanus toxoid vaccination during pregnancy [Internet]. 2020 [cited 2023 Mar 21]. Available from: https://www.westerncape.gov.za/assets/departments/health/h117_2020_covid-19_introduction_of_tetanus_toxoid_vaccination.pdf
452. Jones C, Pollock L, Barnett SM, Battersby A, Kampmann B. The relationship between concentration of specific antibody at birth and subsequent response to primary immunization. Vaccine. **2014**; 32(8):996–1002.
453. Dogra SK, Chung CK, Wang D, Sakwinska O, Mottaz SC, Sprenger N. Nurturing the early life gut microbiome and immune maturation for long term health. Microorganisms. **2021**; 9(10):2110.
454. Collado MC, Rautava S, Aakko J, Isolauri E, Salminen S. Human gut colonisation may be initiated in utero by distinct microbial communities in the placenta and amniotic fluid. Scientific Reports. **2016**; 6:23129.
455. Solís G, los Reyes-Gavilan CG de, Fernández N, Margolles A, Gueimonde M. Establishment and development of lactic acid bacteria and bifidobacteria microbiota in breast-milk and the infant gut. Anaerobe. **2010**; 16(3):307–310.
456. Chen J, Chen X, Ho CL. Recent Development of Probiotic Bifidobacteria for Treating Human Diseases. Frontiers in Bioengineering and Biotechnology. **2021**; 9:770248.
457. Kaci G, Goudercourt D, Dennin V, Pot B, Doré J, Ehrlich SD, Renault P, Blottière HM, Daniel C, Delorme C. Anti-inflammatory properties of Streptococcus salivarius, a commensal bacterium of the oral cavity and digestive tract. Applied and Environmental Microbiology. **2014**; 80(3):928–934.
458. Han SM, Derraik JGB, Binia A, Sprenger N, Vickers MH, Cutfield WS. Maternal and Infant Factors Influencing Human Milk Oligosaccharide Composition: Beyond Maternal Genetics. Journal of Nutrition. **2021**; 151(6):1383–1393.
459. Cabrera-Rubio R, Collado MC, Laitinen K, Salminen S, Isolauri E, Mira A. The human milk microbiome changes over lactation and is shaped by maternal weight and mode of

delivery. American Journal of Clinical Nutrition. **2012**; 96(3):544–551.
460. Banwo K, Oyeyipo A, Mishra L, Sarkar D, Shetty K. Improving phenolic bioactive-linked functional qualities of traditional cereal-based fermented food (Ogi) of Nigeria using compatible food synergies with underutilized edible plants. NFS Journal. **2022**; 27:1–12.
461. Spies HC, Nel M, Walsh CM. Adherence to the Mediterranean Diet of Pregnant Women in Central South Africa: The NuEMI Study. Nutrition and Metabolic Insights. **2022**; 15:1–8.
462. Nigeria Population Commission, ICF. Nigeria Demographic and Health Survey 2018 [Internet]. National Population Commission. 2019 [cited 2023 Dec 28]. Available from: https://dhsprogram.com/pubs/pdf/FR359/FR359.pdf
463. Samani RJ, Tajbakhsh E, Momtaz H, Samani MK. Prevalence of Virulence Genes and Antibiotic Resistance Pattern in Enterococcus Faecalis Isolated from Urinary Tract Infection in Shahrekord, Iran. Reports of Biochemistry and Molecular Biology. **2021**; 10(1):50–59.
464. Kleinnijenhuis J, Quintin J, Preijers F, Joosten LAB, Ifrim DC, Saeed S, Jacobs C, Loenhout J Van, Jong D De, Hendrik S, Xavier RJ, Meer JWM Van Der, Crevel R Van, Netea MG. Bacille Calmette-Guérin induces NOD2-dependent nonspecific protection from reinfection via epigenetic reprogramming of monocytes. Proceedings of the National Academy of Sciences of the United States of America. **2012**; 109(43):17537–17542.
465. Chen J, Gao L, Wu X, Fan Y, Liu M, Peng L, Song J, Li B, Liu A, Bao F. BCG-induced trained immunity: history, mechanisms and potential applications. Journal of Translational Medicine. **2023**; 21(1):106.
466. Arts RJW, Novakovic B, Horst R ter, et al. Glutaminolysis and Fumarate Accumulation Integrate Immunometabolic and Epigenetic Programs in Trained Immunity. Cell Metabolism. **2016**; 24(6):807–819.
467. Schlums H, Cichocki F, Tesi B, Theorell J, Beziat V, Holmes TD, Han H, Chiang SCC, Foley B, Mattsson K, Larsson S, Schaffer M, Malmberg KJ, Ljunggren HG, Miller JS, Bryceson YT. Cytomegalovirus infection drives adaptive epigenetic diversification of NK cells with altered signaling and effector function. Immunity. **2015**; 42(3):443–456.
468. Lee J, Zhang T, Hwang I, Kim A, Nitschke L, Kim MJ, Scott JM, Kamimura Y, Lanier LL, Kim S. Epigenetic modification and antibody-dependent expansion of memory-like NK cells in human cytomegalovirus-infected individuals. Immunity. **2015**; 42(3):431–442.
469. Buffen K, Oosting M, Quintin J, et al. Autophagy Controls BCG-Induced Trained Immunity and the Response to Intravesical BCG Therapy for Bladder Cancer. PLoS Pathogens. **2014**; 10(10):e1004485.
470. Jensen KJ, Larsen N, Sørensen SB, Andersen A, Eriksen HB, Monteiro I, Hougaard D, Aaby P, Netea MG, Flanagan KL, Benn CS. Heterologous immunological effects of early BCG vaccination in low-birth-weight infants in guinea-bissau: A randomized-controlled trial. Journal of Infectious Diseases. **2015**; 211(6):956–967.
471. Freyne B, Donath S, Germano S, Gardiner K, Casalaz D, Robins-Browne RM, Amenyogbe N, Messina NL, Netea MG, Flanagan KL, Kollmann T, Curtis N. Neonatal BCG vaccination influences cytokine responses to toll-like receptor ligands and heterologous antigens. Journal of Infectious Diseases. **2018**; 217(11):1798–1808.
472. Rie A Van, Madhi SA, Heera JR, Meddows-Taylor S, Wendelboe AM, Anthony F, Violari A, Tiemessen CT. Gamma interferon production in response to Mycobacterium bovis BCG and Mycobacterium tuberculosis antigens in infants born to human immunodeficiency virus-infected mothers. Clinical and Vaccine Immunology. **2006**; 13(2):246–252.

473. Landt SG, Marinov GK, Kundaje A, et al. ChIP-seq guidelines and practices of the ENCODE and modENCODE consortia. Genome Research. **2012**; 22(9):1813–1831.
474. Jung YL, Luquette LJ, Ho JWK, Ferrari F, Tolstorukov M, Minoda A, Issner R, Epstein CB, Karpen GH, Kuroda MI, Park PJ. Impact of sequencing depth in ChIP-seq experiments. Nucleic Acids Research. **2014**; 42(9):e74.
475. Tchakoute CT, Hesseling AC, Kidzeru EB, Gamieldien H, Passmore JAS, Jones CE, Gray CM, Sodora DL, Jaspan HB. Delaying BCG vaccination until 8 weeks of age results in robust BCG-specific T-cell responses in HIV-exposed infants. Journal of Infectious Diseases. **2015**; 211(3):338–346.
476. Blakney AK, Tchakoute CT, Hesseling AC, Kidzeru EB, Jones CE, Passmore JAS, Sodora DL, Gray CM, Jaspan HB. Delayed BCG vaccination results in minimal alterations in T cell immunogenicity of acellular pertussis and tetanus immunizations in HIV-exposed infants. Vaccine. **2015**; 33(38):4782–4789.
477. Gasper MA, Hesseling AC, Mohar I, Myer L, Azenkot T, Passmore JAS, Hanekom W, Cotton MF, Crispe IN, Sodora DL, Jaspan HB. BCG vaccination induces HIV target cell activation in HIV-exposed infants in a randomized trial. JCI Insight. **2017**; 2(7):e91963.
478. Stinson K, Goemaere E, Coetzee D, Cutsem G Van, Hilderbrand K, Osler M, Hennessey C, Wilkinson L, Patten G, Cragg C, Mathee S, Cox V, Boulle A. Cohort profile: The Khayelitsha antiretroviral programme, Cape Town, South Africa. International Journal of Epidemiology. **2017**; 46(2):e21.
479. Kaya-Okur H, Henikoff S, Henikoff S. Bench top CUT&Tag V.3 [Internet]. Protocols.io. 2020 [cited 2023 Sep 30]. Available from: https://www.protocols.io/view/bench-top-cut-amp-tag-kqdg34qdpl25/v3?version_warning=no
480. Buenrostro JD, Wu B, Litzenburger UM, Ruff D, Gonzales ML, Snyder MP, Chang HY, Greenleaf WJ. Single-cell chromatin accessibility reveals principles of regulatory variation. Nature. **2015**; 523(7561):486–490.
481. Zheng Y, Ahmad K, Henikoff S. CUT&Tag Data Processing and Analysis Tutorial [Internet]. Protocol.io. 2020 [cited 2023 Jul 24]. Available from: https://dx.doi.org/10.17504/protocols.io.bjk2kkye
482. Andrews S. FastQC [Internet]. Babraham Bioinformatics. 2010 [cited 2023 Sep 30]. Available from: https://www.bioinformatics.babraham.ac.uk/projects/fastqc/
483. Consortium GR. Genome Reference Consortium Human Building 37 (GRCh37) [Internet]. 2009 [cited 2023 Apr 21]. Available from: http://hgdownload.cse.ucsc.edu/goldenpath/hg19/chromosomes/
484. Langmead B, Salzberg SL. Fast gapped-read alignment with Bowtie 2. Nature Methods. **2012**; 9(4):357–359.
485. Broad Institute M and H. Picard [Internet]. Github. [cited 2023 Apr 21]. Available from: http://broadinstitute.github.io/picard/
486. Li H, Durbin R. Fast and accurate long-read alignment with Burrows-Wheeler transform. Bioinformatics. **2010**; 26(5):589–595.
487. Quinlan AR, Hall IM. BEDTools: A flexible suite of utilities for comparing genomic features. Bioinformatics. **2010**; 26(6):841–842.
488. Zhang Y, Liu T, Meyer CA, Eeckhoute J, Johnson DS, Bernstein BE, Nussbaum C, Myers RM, Brown M, Li W, Shirley XS. Model-based analysis of ChIP-Seq (MACS). Genome Biology. **2008**; 9(9):R137.
489. Meers MP, Tenenbaum D, Henikoff S. Peak calling by Sparse Enrichment Analysis for

CUT&RUN chromatin profiling. Epigenetics and Chromatin. **2019**; 12(1):42.
490. Robinson JT, Thorvaldsdóttir H, Winckler W, Guttman M, Lander ES, Getz G, Mesirov JP. Integrative genomics viewer. Nature Biotechnology. **2011**; 29(1):24–26.
491. Yu G, Wang LG, He QY. ChIP seeker: An R/Bioconductor package for ChIP peak annotation, comparison and visualization. Bioinformatics. **2015**; 31(14):2382–2383.
492. Team BC, Maintainer BP. TxDb.Rnorvegicus.UCSC.rn6.refGene: Annotation package for TxDb object(s) [Internet]. R package version 3.4.6. 2019 [cited 2023 Apr 22]. Available from: https://bioconductor.org/packages/release/data/annotation/html/TxDb.Rnorvegicus.UCSC.rn6.refGene.html
493. Stark R, Brown GD. Differential analysis of ChIP-Seq peak data [Internet]. Bioconductor. 2012 [cited 2023 Apr 21]. Available from: https://bioconductor.org/packages/release/bioc/html/DiffBind.html
494. Amemiya HM, Kundaje A, Boyle AP. The ENCODE Blacklist: Identification of Problematic Regions of the Genome. Scientific Reports. **2019**; 9(1):9354.
495. Yu G, Wang LG, Han Y, He QY. ClusterProfiler: An R package for comparing biological themes among gene clusters. OMICS A Journal of Integrative Biology. **2012**; 16(5):284–287.
496. Wu T, Hu E, Xu S, Chen M, Guo P, Dai Z, Feng T, Zhou L, Tang W, Zhan L, Fu X, Liu S, Bo X, Yu G. clusterProfiler 4.0: A universal enrichment tool for interpreting omics data. Innovation. **2021**; 2(3):100141.
497. Carlson M, Carlson M., Carlson M. org.Hs.eg.db: Genome wide annotation for Human (R package version 3.8.2.) [Internet]. Bioconducter. 2019 [cited 2023 Sep 30]. Available from: https://bioconductor.org/packages/release/data/annotation/html/org.Hs.eg.db.html
498. EpiCypher. CUTANA CUT&Tag Protocol (version 1.7) [Internet]. 2022 [cited 2023 Jul 25]. Available from: https://www.epicypher.com/resources/protocols/
499. Meers MP, Tenenbaum D. SEACR [Internet]. Github. 2020 [cited 2023 Aug 2]. Available from: https://github.com/FredHutch/SEACR
500. Mikkelsen TS, Ku M, Jaffe DB, et al. Genome-wide maps of chromatin state in pluripotent and lineage-committed cells. Nature. **2007**; 448(7153):553–560.
501. Hartenstein V, Martinez P. Phagocytosis in cellular defense and nutrition: a food-centered approach to the evolution of macrophages. Cell and Tissue Research. **2019**; 377(3):527–547.
502. Maul-Pavicic A, Chiang SCC, Rensing-Ehl A, et al. ORAI1-mediated calcium influx is required for human cytotoxic lymphocyte degranulation and target cell lysis. Proceedings of the National Academy of Sciences of the United States of America. **2011**; 108(8):3324–3329.
503. Creyghton MP, Cheng AW, Welstead GG, Kooistra T, Carey BW, Steine EJ, Hanna J, Lodato MA, Frampton GM, Sharp PA, Boyer LA, Young RA, Jaenisch R. Histone H3K27ac separates active from poised enhancers and predicts developmental state. Proceedings of the National Academy of Sciences of the United States of America. **2010**; 107(50):21931–21936.
504. Zhao W, Xu Y, Wang Y, Gao D, King J, Xu Y, Liang F Sen. Investigating crosstalk between H3K27 acetylation and H3K4 trimethylation in CRISPR/dCas-based epigenome editing and gene activation. Scientific Reports. **2021**; 11(1):15912.
505. Sims D, Sudbery I, Ilott NE, Heger A, Ponting CP. Sequencing depth and coverage: Key

considerations in genomic analyses. Nature Reviews Genetics. **2014**; 15(2):121–132.
506. Almeida JS, Casanova JM, Santos-Rosa M, Tarazona R, Solana R, Rodrigues-Santos P. Natural Killer T-like Cells: Immunobiology and Role in Disease. International Journal of Molecular Sciences. **2023**; 24(3):2743.
507. Morandi B, Bougras G, Muller WA, Ferlazzo G, Münz C. NK cells of human secondary lymphoid tissues enhance T cell polarization via IFN-γ secretion. European Journal of Immunology. **2006**; 36(9):2394–2400.
508. Martín-Fontecha A, Thomsen LL, Brett S, Gerard C, Lipp M, Lanzavecchia A, Sallusto F. Induced recruitment of NK cells to lymph nodes provides IFN-γ for TH1 priming. Nature Immunology. **2004**; 5(12):1260–1265.
509. Mertz PM, DeWitt DL, Stetler-Stevenson WG, Wahl LM. Interleukin 10 suppression of monocyte prostaglandin H synthase-2. Mechanism of inhibition of prostaglandin-dependent matrix metalloproteinase production. Journal of Biological Chemistry. **1994**; 269(33):21322–21329.
510. Fu Q, Yan S, Wang L, Duan X, Wang L, Wang Y, Wu T, Wang X, An J, Zhang Y, Zhou Q, Zhan L. Hepatic NK cell-mediated hypersensitivity to ConA-induced liver injury in mouse liver expressing hepatitis C virus polyprotein. Oncotarget. **2017**; 8(32):52178–52192.
511. Daniels B, Kuhn L, Spooner E, Mulol H, Goga A, Feucht U, Essack SY, Coutsoudis A. Cotrimoxazole guidelines for infants who are HIV-exposed but uninfected: a call for a public health and ethics approach to the evidence. The Lancet Global Health. **2022**; 10(8):e1198–e1203.
512. South African National Department of Health. Guideline for the Prevention of Vertical Transmission of Communicable Infections 2023 [Internet]. 2023 [cited 2023 Mar 15]. Available from: https://knowledgehub.health.gov.za/system/files/elibdownloads/2023-09/2023 Vertical Transmission Prevention Guideline 04092023 signed WEB_1.pdf
513. Mellqvist H, Saggers RT, Elfvin A, Hentz E, Ballot DE. The effects of exposure to HIV in neonates at a referral hospital in South Africa. BMC Pediatrics. **2021**; 21(1):485.
514. Koyanagi A, Humphrey JH, Ntozini R, Nathoo K, Moulton LH, Iliff P, Mutasa K, Ruff A, Ward B. Morbidity among human immunodeficiency virus-exposed but uninfected, human immunodeficiency virus-infected, and human immunodeficiency virus-unexposed infants in zimbabwe before availability of highly active antiretroviral therapy. Pediatric Infectious Disease Journal. **2011**; 30(1):45–51.
515. Brennan AT, Bonawitz R, Gill CJ, Thea DM, Kleinman M, Long L, McCallum C, Fox MP. A Meta-analysis Assessing Diarrhea and Pneumonia in HIV-Exposed Uninfected Compared with HIV-Unexposed Uninfected Infants and Children. Journal of Acquired Immune Deficiency Syndromes. **2019**; 82(1):1–8.
516. Roux DM Le, Nicol MP, Myer L, Vanker A, Stadler JAM, Delft E Von, Zar HJ. Lower Respiratory Tract Infections in Children in a Well-vaccinated South African Birth Cohort: Spectrum of Disease and Risk Factors. Clinical Infectious Diseases. **2019**; 69(9):1588–1596.
517. Rupérez M, González R, Maculuve S, Quintó L, López-Varela E, Augusto O, Vala A, Nhacolo A, Sevene E, Naniche D, Menéndez C. Maternal HIV infection is an important health determinant in non-HIV-infected infants. AIDS. **2017**; 31(11):1545–1553.
518. Roux SM le, Abrams EJ, Donald KA, Brittain K, Phillips TK, Zerbe A, Roux DM le, Kroon M, Myer L. Infectious morbidity of breastfed, HIV-exposed uninfected infants under conditions of universal antiretroviral therapy in South Africa: a prospective cohort study. The Lancet Child and Adolescent Health. **2020**; 4(3):220–231.

519. Mollendorf C Von, Gottberg A Von, Tempia S, Meiring S, Gouveia L De, Quan V, Lengana S, Avenant T, Plessis N Du, Eley B, Finlayson H, Reubenson G, Moshe M, O'Brien KL, Klugman KP, Whitney CG, Cohen C. Increased risk for and mortality from invasive pneumococcal disease in HIV-exposed but uninfected infants aged <1 year in South Africa, 2009-2013. Clinical Infectious Diseases. **2015**; 60(9):1346–1356.
520. Doherty T, Jackson D, Swanevelder S, Lombard C, Engebretsen IMS, Tylleskär T, Goga A, Ekström EC, Sanders D, PROMISE EBF study group. Severe events in the first 6 months of life in a cohort of HIV-unexposed infants from South Africa: effects of low birthweight and breastfeeding status. Tropical medicine & international health. **2014**; 19(10):1162–1169.
521. Abu-Raya B, Kollmann TR, Marchant A, MacGillivray DM. The immune system of HIV-exposed uninfected infants. Frontiers in Immunology. **2016**; 7:383.
522. Afran L, Jambo KC, Nedi W, Miles DJC, Kiran A, Banda DH, Kamg'Ona R, Tembo D, Pachnio A, Nastouli E, Ferne B, Mwandumba HC, Moss P, Goldblatt D, Rowland-Jones S, Finn A, Heyderman RS. Defective Monocyte Enzymatic Function and an Inhibitory Immune Phenotype in Human Immunodeficiency Virus-Exposed Uninfected African Infants in the Era of Antiretroviral Therapy. Journal of Infectious Diseases. **2022**; 226(7):1243–1255.
523. Lacourse SM, Richardson BA, Kinuthia J, Warr AJ, Maleche-Obimbo E, Matemo D, Cranmer LM, Mecha J, Escudero JN, Hawn TR, John-Stewart G. A Randomized Controlled Trial of Isoniazid to Prevent Mycobacterium tuberculosis Infection in Kenyan Human Immunodeficiency Virus-Exposed Uninfected Infants. Clinical Infectious Diseases. **2021**; 73(2):E337–E344.
524. Warr AJ, Anterasian C, Shah JA, Rosa SC De, Nguyen FK, Maleche-Obimbo E, Cranmer LM, Matemo D, Mecha J, Kinuthia J, LaCourse SM, John-Stewart GC, Hawn TR. A CD4+ TNF+ monofunctional memory T-cell response to BCG vaccination is associated with Mycobacterium tuberculosis infection in infants exposed to HIV. eBioMedicine. **2022**; 80:104023.
525. Mazurek GH, Jereb J, Vernon A, LoBue P, Goldberg S, Castro K, IGRA Expert Committee, Centers for Disease Control and Prevention (CDC). Updated guidelines for using Interferon Gamma Release Assays to detect Mycobacterium tuberculosis infection - United States, 2010. MMWR Recommendations and reports : Morbidity and mortality weekly report Recommendations and reports. **2010**; 59(RR-5):1–25.
526. Martinez L, Cords O, Horsburgh CR, et al. The risk of tuberculosis in children after close exposure: a systematic review and individual-participant meta-analysis. The Lancet. **2020**; 395(10228):973–984.
527. Ruhwald M, Ravn P. Biomarkers of latent TB infection. Expert Review of Respiratory Medicine. **2009**; 3(4):387–401.
528. Anterasian C, Warr AJ, Lacourse SM, Kinuthia J, Richardson BA, Nguyen FK, Matemo D, Maleche-Obimbo E, John Stewart GC, Hawn TR. Non-IFNγ Whole Blood Cytokine Responses to Mycobacterium Tuberculosis Antigens in HIV-exposed Infants. Pediatric Infectious Disease Journal. NIH Public Access; **2021**; 40(10):922–929.
529. Mao L, LaCourse SM, Kim S, Liu C, Ning B, Bao D, Fan J, Lyon CJ, Sun Z, Nachman S, Mitchell CD, Hu TY. Evaluation of a serum-based antigen test for tuberculosis in HIV-exposed infants: a diagnostic accuracy study. BMC Medicine. **2021**; 19(1):113.
530. Harris VC, Haak BW, Boele van Hensbroek M, Wiersinga WJ. The Intestinal Microbiome

in Infectious Diseases: The Clinical Relevance of a Rapidly Emerging Field. Open Forum Infectious Diseases. **2017**; 4(3):ofx144.
531. Gaufin T, Tobin NH, Aldrovandi GM. The importance of the microbiome in pediatrics and pediatric infectious diseases. Current Opinion in Pediatrics. **2018**; 30(1):117–124.
532. Libertucci J, Young VB. The role of the microbiota in infectious diseases. Nature Microbiology. **2019**; 4(1):35–45.
533. Niekerk E van, Autran CA, Nel DG, Kirsten GF, Blaauw R, Bode L. Human milk oligosaccharides differ between HIV-infected and HIV-uninfected mothers and are related to necrotizing enterocolitis incidence in their preterm very-low-birth-weight infants. Journal of Nutrition. **2014**; 144(8):1227–1233.
534. D'Souza AW, Moodley-Govender E, Berla B, Kelkar T, Wang B, Sun X, Daniels B, Coutsoudis A, Trehan I, Dantas G. Cotrimoxazole prophylaxis increases resistance gene prevalence and α-diversity but decreases β-diversity in the gut microbiome of human immunodeficiency virus–exposed, uninfected infants. Clinical Infectious Diseases. **2020**; 71(11):2858–2868.
535. Powis KM, Souda S, Lockman S, Ajibola G, Bennett K, Leidner J, Hughes MD, Moyo S, Widenfelt E Van, Jibril HB, Makhema J, Essex M, Shapiro RL. Cotrimoxazole prophylaxis was associated with enteric commensal bacterial resistance among HIV-exposed infants in a randomized controlled trial, Botswana. Journal of the International AIDS Society. **2017**; 20(3):e25021.
536. Nguyen Thi PL, Yassibanda S, Aidara A, Bouguénec C Le, Germani Y. Enteropathogenic Klebsiella pneumoniae in HIV-infected adults, Africa. Emerging Infectious Diseases. **2003**; 9(1):135–137.
537. Wanyiri JW, Kanyi H, Maina S, Wang DE, Ngugi P, O'Connor R, Kamau T, Waithera T, Kimani G, Wamae CN, Mwamburi M, Ward HD. Infectious diarrhoea in antiretroviral therapy-naïve HIV/AIDS patients in Kenya. Transactions of the Royal Society of Tropical Medicine and Hygiene. **2013**; 107(10):631–638.
538. Weinberg A, Mussi-Pinhata MM, Yu Q, Cohen RA, Almeida VC, Amaral F, Pinto J, Teixeira MLB, Succi RCM, Freimanis L, Read JS, Siberry G. Excess respiratory viral infections and low antibody responses among HIV-exposed, uninfected infants. Aids. **2017**; 31(5):669–679.
539. Reikie BA, Naidoo S, Ruck CE, Slogrove AL, Beer C De, Grange H La, Adams RCM, Ho K, Smolen K, Speert DP, Cotton MF, Preiser W, Esser M, Kollmann TR. Antibody responses to vaccination among South African HIV-exposed and unexposed uninfected infants during the first 2 years of life. Clinical and Vaccine Immunology. **2013**; 20(1):33–38.
540. Bashir MF, Elechi HA, Ashir MG, Rabasa AI, Bukbuk DN, Usman AB, Mustapha MG, Alhaji MA. Neonatal tetanus immunity in Nigeria: The effect of HIV infection on serum levels and transplacental transfer of antibodies. Journal of Tropical Medicine. **2016**; 2016:7439605.
541. Crowe J. Influence of maternal antibodies on neonatal immunization against respiratory viruses. Clinical Infectious Diseases. **2001**; 33(10):1720–1727.
542. Nziza N, Jung W, Mendu M, Chen T, McNamara RP, Fortune SM, Franken KLMC, Ottenhoff THM, Bryson B, Ngonzi J, Bebell LM, Alter G. Maternal HIV infection drives altered placental Mtb-specific antibody transfer. Frontiers in Microbiology. **2023**; 14:1171990.

543. Zhang X, Chen B di, Zhao L dan, Li H. The Gut Microbiota: Emerging Evidence in Autoimmune Diseases. Trends in Molecular Medicine. **2020**; 26(9):862–873.
544. Kim CH. B cell-helping functions of gut microbial metabolites. Microbial Cell. **2016**; 3(10):529–531.
545. Kim M, Qie Y, Park J, Kim CH. Gut Microbial Metabolites Fuel Host Antibody Responses. Cell Host and Microbe. **2016**; 20(2):202–214.
546. Goetghebuer T, Smolen KK, Adler C, Das J, Mcbride T, Smits G, Lecomte S, Haelterman E, Barlow P, Piedra PA, Klis F Van Der, Kollmann TR, Lauffenburger DA, Alter G, Levy J, Marchant A. Initiation of Antiretroviral Therapy Before Pregnancy Reduces the Risk of Infection-related Hospitalization in Human Immunodeficiency Virus-exposed Uninfected Infants Born in a High-income Country. Clinical Infectious Diseases. **2019**; 68(7):1193–1203.
547. Ajibola G, Bennett K, Powis KM, Hughes MD, Leidner J, Kgole S, Batlang O, Mmalane M, Makhema J, Lockman S, Shapiro R. Decreased diarrheal and respiratory disease in HIV exposed uninfected children following vaccination with rotavirus and pneumococcal conjugate vaccines. PLoS ONE. **2021**; 15(12):e0244100.
548. Statistics South Africa. Khayelitsha [Internet]. 2011 [cited 2024 Mar 24]. Available from: https://www.statssa.gov.za/?page_id=4286&id=328
549. Western Cape Government. Settlement Profile [Internet]. [cited 2024 Mar 24]. Available from: https://www.westerncape.gov.za/assets/departments/human-settlements/docs/issp/sp_cederberg_final_edited_lr.pdf
550. City Population. Nigeria: Administrative Division - Jos North [Internet]. 2022 [cited 2024 Mar 24]. Available from: https://www.citypopulation.de/en/nigeria/admin/
551. Oxfam. Inequality in Nigeria: Exploring the Drivers [Internet]. Oxfam International. 2017 [cited 2024 Mar 24]. Available from: https://www-cdn.oxfam.org/s3fs-public/file_attachments/cr-inequality-in-nigeria-170517-en.pdf
552. WHO Regional Office for Africa. Report on malaria in Nigeria 2022 [Internet]. 2023. Available from: https://www.afro.who.int/countries/nigeria/publication/report-malaria-nigeria-2022#:~:text=Malaria is a major public,of the global malaria burden.
553. Statistics Botswana. 2022 Population and Housing Census Preliminary Results V2 [Internet]. 2022 [cited 2024 Mar 24]. Available from: https://www.statsbots.org.bw/sites/default/files/2022 Population and Housing Census Preliminary Results.pdf
554. Tiam A, Kassaye SG, MacHekano R, Tukei V, Gill MM, Mokone M, Letsie M, Tsietso M, Seipati I, Barasa J, Isavwa A, Tylleskär T, Guay L. Comparison of 6-week PMTCT outcomes for HIV-exposed and HIV-unexposed infants in the era of lifelong ART: Results from an observational prospective cohort study. PLoS ONE. **2019**; 14(12):e0226339.
555. Ramokolo V, Goga AE, Lombard C, Doherty T, Jackson DJ, Engebretsen IMS. In Utero ART Exposure and Birth and Early Growth Outcomes among HIV-Exposed Uninfected Infants Attending Immunization Services: Results from National PMTCT Surveillance, South Africa. Open Forum Infectious Diseases. **2017**; 4(4):ofx187.
556. Piske M, Qiu AQ, Maan EJ, Sauvé LJ, Forbes JC, Alimenti A, Janssen PA, Money DM, Côté HCF. Preterm Birth and Antiretroviral Exposure in Infants HIV-exposed Uninfected. Pediatric Infectious Disease Journal. **2021**; 40(3):245–250.
557. Anderson K, Kalk E, Madlala HP, Nyemba DC, Kassanjee R, Jacob N, Slogrove A, Smith M, Eley BS, Cotton MF, Muloiwa R, Spittal G, Kroon M, Boulle A, Myer L, Davies MA.

Increased infectious-cause hospitalization among infants who are HIV-exposed uninfected compared with HIV-unexposed. AIDS. **2021**; 35(14):2327–2339.
558. Polin RA, Papile LA, Baley JE, Benitz W, Carlo WA, Cummings J, Kumar P, Tan RC, Wang KS, Watterberg KL, Bhutani VK. Management of Neonates with Suspected or Proven Early-Onset Bacterial Sepsis. Pediatrics. **2012**; 129(5):1006–1015.
559. Steiner L, Diesner SC, Voitl P. Risk of infection in the first year of life in preterm children: An Austrian observational study. PLoS ONE. **2019**; 14(12):e0224766.

APPENDICES

Appendix A. Inclusion and exclusion criteria of the InFANT study (parent study).

	Inclusion Criteria	Exclusion Criteria
Maternal Factors	1) Mother with known HIV status. 2) Age of mother ≥ 18 years. 3) Mother has self-chosen to breastfeed her infant. 4) Mother is able and willing to do the follow up assessments and provide informed consent.	1) Complications during pregnancy and delivery such as chorioamnionitis and eclampsia. 2) Mother with TB or a cough. 3) Mother who is planning to move away from Khayelitsha in the next 12 months with her infant.
Infant Factors	1) Gestational age ≥ 35 weeks. 2) Birth weight ≥ 2.0 kg. 3) For the HIV-exposed infants, negative HIV DNA PCR test at six weeks after birth.	1) Hypoxic injury/ seizures/ sepsis/ intrauterine growth retardation.

Abbreviations: HIV, human immunodeficiency virus; PCR, polymerase chain reaction; TB, tuberculosis.

Appendix B. Inclusion and exclusion criteria of the Karabo study (parent study: Tshilo Dikotla).

	Inclusion Criteria	Exclusion Criteria
Maternal Factors	1) Mother with known HIV status. 2) Age of mother ≥ 18 years. 3) Botswana citizens. 4) Mother able to provide informed consent for themselves and their infant to participate in the study. 5) Willing to exclusively breastfeed for the first six months of life. 6) For mother with HIV, they must be on TDF/3TC or FTC/EFV or TDF/3TC or FTC/Dolutegravir at time of study enrollment or willing to initiate this treatment and continue throughout the period of breastfeeding, if not for their lifetime.	1) Mother with TB symptoms or is on treatment of active TB at delivery. 2) Pre-existing maternal diabetes mellitus. 3) The mother is presently incarcerated.
Infant Factors	1) The infant has a birth weight of ≥ 2 kilograms and a gestational age ≥ 32 weeks. 2) The infant has documentation of receiving a BCG vaccine within 72 hours of birth. 3) The infant enrolled in Tshilo Dikotla has not reached 14 months of age or completed the 9-12 months Tshilo Dikotla study visit.	1) The infant is born with major congenital anomalies. 2) The infant is documented to have experienced severe birth complications including birth asphyxia or seizures.

Abbreviations: BCG, Bacillus Calmette-Guérin; EFV, efavirenz; FTC, emtricitabine; HIV, human immunodeficiency virus; 3TC, lamivudine; TDF, tenofovir disoproxil fumarate; TB, tuberculosis.

Appendix C. Sensitivity analysis result.

	conversion.rate	reversion.rate	prevalence.at.12mo	significance.proportion
1	0	0	0.02	0.00000
2	0.02	0.02	0.02	0.00000
3	0.02	0.02	0.04	0.00000
4	0.02	0.02	0.06	0.00000
5	0.02	0.02	0.08	0.00000
6	0.02	0.02	0.1	0.00000
7	0.02	0.02	0.12	0.00000
8	0.02	0.02	0.14	0.00000
9	0.02	0.02	0.16	0.00000
10	0.02	0.02	0.18	0.00000
11	0.02	0.02	0.2	0.00000
12	0.02	0.04	0.02	0.00020
13	0.02	0.04	0.04	0.00040
14	0.02	0.04	0.06	0.00000
15	0.02	0.04	0.08	0.00020
16	0.02	0.04	0.1	0.00020
17	0.02	0.04	0.12	0.00020
18	0.02	0.04	0.14	0.00000
19	0.02	0.04	0.16	0.00000
20	0.02	0.04	0.18	0.00040
21	0.02	0.04	0.2	0.00020
22	0.02	0.06	0.02	0.00020
23	0.02	0.06	0.04	0.00000
24	0.02	0.06	0.06	0.00020
25	0.02	0.06	0.08	0.00040
26	0.02	0.06	0.1	0.00040
27	0.02	0.06	0.12	0.00020
28	0.02	0.06	0.14	0.00020
29	0.02	0.06	0.16	0.00020
30	0.02	0.06	0.18	0.00000
31	0.02	0.06	0.2	0.00000
32	0.02	0.08	0.02	0.00040
33	0.02	0.08	0.04	0.00100
34	0.02	0.08	0.06	0.00000
35	0.02	0.08	0.08	0.00040
36	0.02	0.08	0.1	0.00060
37	0.02	0.08	0.12	0.00040
38	0.02	0.08	0.14	0.00020
39	0.02	0.08	0.16	0.00080
40	0.02	0.08	0.18	0.00080
41	0.02	0.08	0.2	0.00080
42	0.02	0.1	0.02	0.00040
43	0.02	0.1	0.04	0.00060
44	0.02	0.1	0.06	0.00040
45	0.02	0.1	0.08	0.00140
46	0.02	0.1	0.1	0.00100
47	0.02	0.1	0.12	0.00080
48	0.02	0.1	0.14	0.00140

49	0.02	0.1	0.16	0.00100
50	0.02	0.1	0.18	0.00080
51	0.02	0.1	0.2	0.00100
52	0.02	0.12	0.02	0.00080
53	0.02	0.12	0.04	0.00080
54	0.02	0.12	0.06	0.00060
55	0.02	0.12	0.08	0.00100
56	0.02	0.12	0.1	0.00040
57	0.02	0.12	0.12	0.00080
58	0.02	0.12	0.14	0.00100
59	0.02	0.12	0.16	0.00160
60	0.02	0.12	0.18	0.00160
61	0.02	0.12	0.2	0.00240
62	0.02	0.14	0.02	0.00120
63	0.02	0.14	0.04	0.00060
64	0.02	0.14	0.06	0.00080
65	0.02	0.14	0.08	0.00060
66	0.02	0.14	0.1	0.00120
67	0.02	0.14	0.12	0.00140
68	0.02	0.14	0.14	0.00140
69	0.02	0.14	0.16	0.00240
70	0.02	0.14	0.18	0.00160
71	0.02	0.14	0.2	0.00180
72	0.02	0.16	0.02	0.00140
73	0.02	0.16	0.04	0.00180
74	0.02	0.16	0.06	0.00100
75	0.02	0.16	0.08	0.00140
76	0.02	0.16	0.1	0.00140
77	0.02	0.16	0.12	0.00140
78	0.02	0.16	0.14	0.00280
79	0.02	0.16	0.16	0.00260
80	0.02	0.16	0.18	0.00400
81	0.02	0.16	0.2	0.00320
82	0.02	0.18	0.02	0.00200
83	0.02	0.18	0.04	0.00200
84	0.02	0.18	0.06	0.00140
85	0.02	0.18	0.08	0.00240
86	0.02	0.18	0.1	0.00300
87	0.02	0.18	0.12	0.00160
88	0.02	0.18	0.14	0.00320
89	0.02	0.18	0.16	0.00200
90	0.02	0.18	0.18	0.00380
91	0.02	0.18	0.2	0.00540
92	0.02	0.2	0.02	0.00180
93	0.02	0.2	0.04	0.00120
94	0.02	0.2	0.06	0.00240
95	0.02	0.2	0.08	0.00220
96	0.02	0.2	0.1	0.00380
97	0.02	0.2	0.12	0.00300
98	0.02	0.2	0.14	0.00280
99	0.02	0.2	0.16	0.00420

100	0.02	0.2	0.18	0.00520
101	0.02	0.2	0.2	0.00540
102	0.04	0.02	0.02	0.00120
103	0.04	0.02	0.04	0.00160
104	0.04	0.02	0.06	0.00100
105	0.04	0.02	0.08	0.00020
106	0.04	0.02	0.1	0.00060
107	0.04	0.02	0.12	0.00080
108	0.04	0.02	0.14	0.00060
109	0.04	0.02	0.16	0.00040
110	0.04	0.02	0.18	0.00060
111	0.04	0.02	0.2	0.00080
112	0.04	0.04	0.02	0.00140
113	0.04	0.04	0.04	0.00100
114	0.04	0.04	0.06	0.00060
115	0.04	0.04	0.08	0.00140
116	0.04	0.04	0.1	0.00160
117	0.04	0.04	0.12	0.00080
118	0.04	0.04	0.14	0.00120
119	0.04	0.04	0.16	0.00060
120	0.04	0.04	0.18	0.00040
121	0.04	0.04	0.2	0.00040
122	0.04	0.06	0.02	0.00140
123	0.04	0.06	0.04	0.00140
124	0.04	0.06	0.06	0.00260
125	0.04	0.06	0.08	0.00080
126	0.04	0.06	0.1	0.00120
127	0.04	0.06	0.12	0.00120
128	0.04	0.06	0.14	0.00080
129	0.04	0.06	0.16	0.00100
130	0.04	0.06	0.18	0.00180
131	0.04	0.06	0.2	0.00040
132	0.04	0.08	0.02	0.00180
133	0.04	0.08	0.04	0.00220
134	0.04	0.08	0.06	0.00220
135	0.04	0.08	0.08	0.00180
136	0.04	0.08	0.1	0.00220
137	0.04	0.08	0.12	0.00220
138	0.04	0.08	0.14	0.00280
139	0.04	0.08	0.16	0.00240
140	0.04	0.08	0.18	0.00200
141	0.04	0.08	0.2	0.00180
142	0.04	0.1	0.02	0.00180
143	0.04	0.1	0.04	0.00240
144	0.04	0.1	0.06	0.00180
145	0.04	0.1	0.08	0.00220
146	0.04	0.1	0.1	0.00220
147	0.04	0.1	0.12	0.00240
148	0.04	0.1	0.14	0.00320
149	0.04	0.1	0.16	0.00320
150	0.04	0.1	0.18	0.00400

151	0.04	0.1	0.2	0.00340
152	0.04	0.12	0.02	0.00240
153	0.04	0.12	0.04	0.00200
154	0.04	0.12	0.06	0.00280
155	0.04	0.12	0.08	0.00340
156	0.04	0.12	0.1	0.00360
157	0.04	0.12	0.12	0.00320
158	0.04	0.12	0.14	0.00340
159	0.04	0.12	0.16	0.00300
160	0.04	0.12	0.18	0.00340
161	0.04	0.12	0.2	0.00220
162	0.04	0.14	0.02	0.00320
163	0.04	0.14	0.04	0.00360
164	0.04	0.14	0.06	0.00480
165	0.04	0.14	0.08	0.00440
166	0.04	0.14	0.1	0.00440
167	0.04	0.14	0.12	0.00560
168	0.04	0.14	0.14	0.00600
169	0.04	0.14	0.16	0.00480
170	0.04	0.14	0.18	0.00440
171	0.04	0.14	0.2	0.00540
172	0.04	0.16	0.02	0.00260
173	0.04	0.16	0.04	0.00520
174	0.04	0.16	0.06	0.00440
175	0.04	0.16	0.08	0.00560
176	0.04	0.16	0.1	0.00480
177	0.04	0.16	0.12	0.00620
178	0.04	0.16	0.14	0.00560
179	0.04	0.16	0.16	0.00480
180	0.04	0.16	0.18	0.00500
181	0.04	0.16	0.2	0.00660
182	0.04	0.18	0.02	0.00460
183	0.04	0.18	0.04	0.00400
184	0.04	0.18	0.06	0.00220
185	0.04	0.18	0.08	0.00740
186	0.04	0.18	0.1	0.00540
187	0.04	0.18	0.12	0.00600
188	0.04	0.18	0.14	0.01040
189	0.04	0.18	0.16	0.00900
190	0.04	0.18	0.18	0.00700
191	0.04	0.18	0.2	0.00640
192	0.04	0.2	0.02	0.00580
193	0.04	0.2	0.04	0.00560
194	0.04	0.2	0.06	0.00740
195	0.04	0.2	0.08	0.01020
196	0.04	0.2	0.1	0.00760
197	0.04	0.2	0.12	0.00800
198	0.04	0.2	0.14	0.01000
199	0.04	0.2	0.16	0.01220
200	0.04	0.2	0.18	0.01000

Full simulation results available at: https://doi.org/10.1093/cid/ciad356

Appendix D. Prediction of factors associated with TT vaccine response among South African infants by LASSO regression.

Explanatory variables	Coefficients
(Intercept)	1.10177
Anti-tetanus IgG titer at W1	0
[W1 ASV1] *Bifidobacterium longum*	0
[W1 ASV2] *Streptococcus salivarius*	0
[W1 ASV3] *Escherichia-Shigella coli*	0
[W1 ASV4] *Bifidobacterium longum*	0
[W1 ASV5] *Enterococcus faecalis*	0
[W1 ASV6] *Collinsella aerofacien*s	0
[W1 ASV7] *Enterococcus faecium*	0
[W1 ASV8] *Bifidobacterium catenulatum*	0
[W1 ASV9] *Streptococcus lutetiensis*	0
[W1 ASV10] *Bifidobacterium breve*	0
[W1 ASV11] *Staphylococcus caprae*	0
[W1 ASV16] *Bifidobacterium bifidum*	0
[W1 ASV19] *Streptococcus* (unclassified)	0
[W1 ASV20] *Lactobacillus gasseri*	0
[W1 ASV21] *Ruminococcus gnavus* group (unclassified)	0
[W1 ASV24] *Veillonella dispar*	0
[W1 ASV25] *Collinsella aerofaciens*	0.01536
[W1 ASV26] *Escherichia-Shigella* (unclassified)	0
[W1 ASV32] *Bacteroides vulgatus*	0
[W1 ASV36] *Klebsiella quasipneumoniae*	0
[W1 ASV38] *Veillonella atypica*	0
[W1 ASV39] *Klebsiella pneumoniae*	0
[W1 ASV40] *Enterococcus* (unclassified)	0
[W1 ASV41] *Staphylococcus* (unclassified)	-0.0061
[W1 ASV46] *Klebsiella variicola*	0
[W1 ASV53] *Holdemanella* (unclassified)	0
[W1 ASV55] *Bacteroides vulgatus*	0
[W1 ASV59] *Blautia obeum*	0
[W1 ASV60] *Bacteroides fragilis*	0
[W1 ASV61] *Bifidobacterium adolescentis*	0
[W1 ASV69] *Clostridium sensu stricto 1* (unclassified)	0
[W1 ASV70] *Erysipelatoclostridium ramosum*	0
[W1 ASV72] *Streptococcus peroris*	0.01018
[W1 ASV73] *Streptococcus parasanguinis*	0
[W1 ASV75] *Ruminococcus torques* group (unclassified)	0.00485
[W1 ASV76] *Sutterella wadsworthensis*	-0.01084
[W1 ASV82] *Streptococcus salivarius*	0.03789

[W1 ASV83] *Bacteroides vulgatus*	0
[W1 ASV91] *Campylobacter jejuni*	0
[W1 ASV114] *Streptococcus salivarius*	0
[W1 ASV116] *Phascolarctobacterium faecium*	0
[W1 ASV155] *Arthrobacter* (unclassified)	0
[W1 ASV159] *Veillonella parvula*	0
[W1 ASV161] *Lactobacillus gasseri*	0
[W1 ASV175] *Clostridium sensu stricto 1 butyricum*	0
[W1 ASV182] *Bacteroides dorei*	0.01568
[W1 ASV194] *Clostridium sensu stricto 1* (unclassified)	0
[W1 ASV239] *Prevotella copri*	0
[W1 ASV330] *Bifidobacterium dentium*	0
[W1 ASV603] *Bordetella pseudohinzii*	0
HIV-exposure status (iHEU)	-0.44265

The top 50 rank-transformed bacterial taxa at week 1, HIV exposure status, and anti-tetanus IgG titers at week 1 were included as explanatory variables. Coefficients of each variable after penalization with a value of lambda that gives the minimum mean of cross-validated error (lambda.min) are indicated. Abbreviations: HIV, human immunodeficiency virus; TT, tetanus toxoid; W1, 1 week of age; ASV, amplicon sequence variant; iHEU, infants who are HIV-exposed uninfected; LASSO, Least Absolute Shrinkage and Selection Operator.

Appendix E. Prediction of factors associated with TT vaccine response among Nigerian infants by LASSO regression.

Explanatory variables	Coefficients
(Intercept)	1.207
[W15 ASV1] *Bifidobacterium longum*	0
[W15 ASV2] *Streptococcus salivarius*	0.00532
[W15 ASV3] *Escherichia-Shigella coli*	0
[W15 ASV4] *Bifidobacterium longum*	0
[W15 ASV5] *Enterococcus faecalis*	0
[W15 ASV6] *Collinsella aerofaciens*	0
[W15 ASV7] *Enterococcus faecium*	0
[W15 ASV9] *Streptococcus lutetiensis*	0
[W15 ASV10] *Bifidobacterium breve*	0
[W15 ASV11] *Staphylococcus caprae*	0
[W15 ASV12] *Staphylococcus saprophyticus*	0
[W15 ASV13] *Kocuria carniphila*	-0.00694
[W15 ASV15] *Staphylococcus aureus*	0
[W15 ASV16] *Bifidobacterium bifidum*	0
[W15 ASV18] *Staphylococcus haemolyticus*	0
[W15 ASV19] *Streptococcus* (unclassified)	0
[W15 ASV22] *Staphylococcus saprophyticus*	0
[W15 ASV23] *Pediococcus pentosaceus*	0
[W15 ASV26] *Escherichia-Shigella* (unclassified)	0
[W15 ASV28] *Bifidobacterium longum*	0
[W15 ASV29] *Pseudomonas azotoformans*	0
[W15 ASV30] *Kocuria palustris*	-0.00028
[W15 ASV31] *Micrococcus luteus*	-0.00037
[W15 ASV35] *Libanicoccus* (unclassified)	0
[W15 ASV36] *Klebsiella quasipneumoniae*	0
[W15 ASV37] *Staphylococcus equorum*	0
[W15 ASV43] *Staphylococcus haemolyticus*	0
[W15 ASV45] *Rhodococcus erythropolis*	0.03079
[W15 ASV48] *Jeotgalicoccus* (unclassified)	0
[W15 ASV49] *Oceanobacillus oncorhynchi*	0
[W15 ASV57] *Globicatella* (unclassified)	0
[W15 ASV67] *Staphylococcus haemolyticus*	0
[W15 ASV68] *Staphylococcus haemolyticus*	0
[W15 ASV74] *Brevundimonas mediterranea*	0
[W15 ASV78] *Micrococcus luteus*	0
[W15 ASV80] *Enterococcus gallinarum*	0
[W15 ASV81] *Enterococcus faecalis*	0
[W15 ASV85] *Brachybacterium* (unclassified)	0

[W15 ASV86] *Oceanobacillus* (unclassified)	0
[W15 ASV88] *Enterococcus faecalis*	0
[W15 ASV94] *Oceanobacillus profundus*	0
[W15 ASV111] *Clostridium sensu stricto 1* (unclassified)	0
[W15 ASV129] *Macrococcus caseolyticus*	0
[W15 ASV131] *Staphylococcus lentus*	0
[W15 ASV187] *Staphylococcus* (unclassified)	0
[W15 ASV202] *Enterococcus casseliflavus*	0
[W15 ASV255] *Staphylococcus kloosii*	0
[W15 ASV294] *Dietzia* (unclassified)	0
[W15 ASV310] *Staphylococcus succinus*	0
[W15 ASV582] *Staphylococcus sciuri*	0
HIV-exposure status (iHEU)	-0.02089

The top 50 rank-transformed bacterial taxa at week 15 and HIV exposure status were included as explanatory variables. Coefficients of each variable after penalization with a value of lambda that gives the minimum mean of cross-validated error (lambda.min) are indicated. Abbreviations: HIV, human immunodeficiency virus; TT, tetanus toxoid; W15, 15 weeks of age; ASV, amplicon sequence variant; iHEU, infants who are HIV-exposed uninfected; LASSO, Least Absolute Shrinkage and Selection Operator.

Appendix F. Inclusion and exclusion criteria for the early vs. delayed BCG vaccination randomized trial ("BCG study").

	Inclusion Criteria	Exclusion Criteria
Maternal Factors	1) Mother living with HIV. 2) Mother (legal guardian) is able and willing to do the follow up assessments and provide informed consent.	1) No actual illness or pregnancy or delivery complications. 2) No known current maternal TB or known TB exposure in the household.
Infant Factors	1) Gestational age ≥ 36 weeks. 2) Birth weight ≥ 2.4 kg.	

Abbreviations: HIV, human immunodeficiency virus; TB, tuberculosis.

Appendix G. Decision-making rules for histone markers.

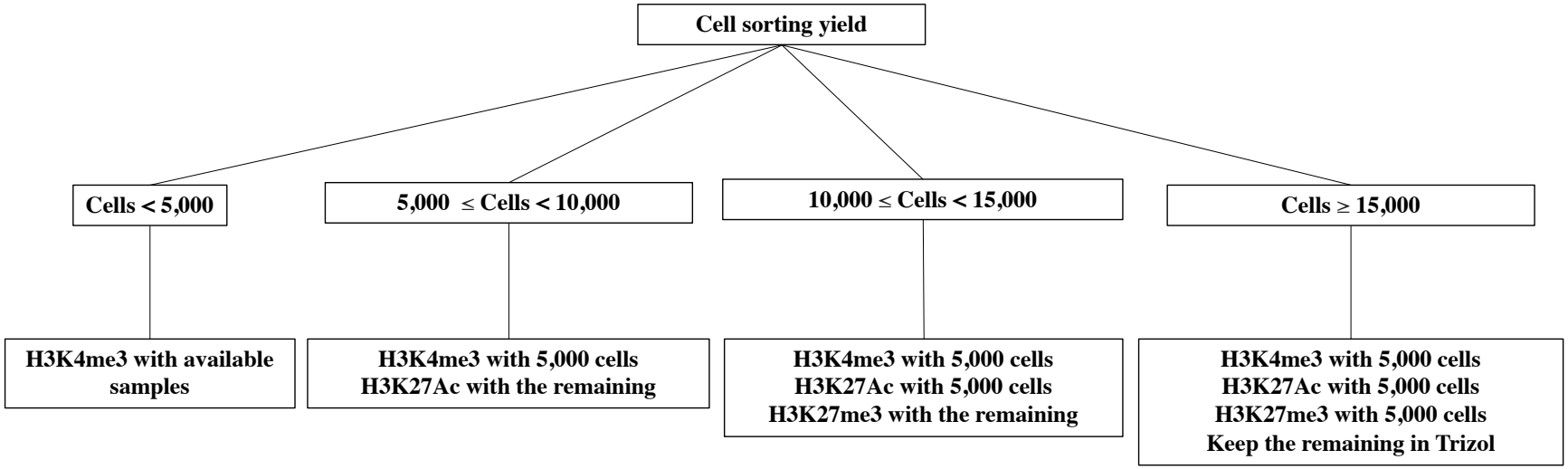

Abbreviations: H3K27Ac, acetylation of histone H3 at lysine 27; H3K4me3, trimethylation of histone H3 at lysine 4; H3K27me3, trimethylation of histone H3 at lysine 27.

Appendix H. Codes used for downstream analysis in Chapter 4.

<Alignment to the reference genome>

```
bowtie2 --end-to-end --very-sensitive --no-mixed --no-discordant --phred33 \
    -I 10 -X 700 \
    -p 8 \
    -x ref.index \
    -1 R1.fastq.gz -2 R2.fastq.gz \
    -S bowtie2.sam &> bowtie2.output.txt
```

<PCR duplicate removal>

```
(1)

java -jar /usr/local/Cellar/picard-tools/2.25.1/libexec/picard.jar SortSam \
    I=bowtie2.sam \
    O=bowtie2.sorted.sam \
    SORT_ORDER=coordinate

(2)

java -jar /usr/local/Cellar/picard-tools/2.25.1/libexec/picard.jar MarkDuplicates \
    I=bowtie2.sorted.sam \
    O=bowtie2.sorted.rmDup.sam \
    M=marked_dup_metrics.txt

(3)

java -jar /usr/local/Cellar/picard-tools/2.25.1/libexec/picard.jar MarkDuplicates \
    I=bowtie2.sorted.sam \
    O=bowtie2.sorted.rmDup.sam \
    REMOVE_DUPLICATES=true\
    METRICS_FILE= picard.rmDup.txt
```

<Fragment size check>

```
samtools view -F 0x04 bowtie2.sorted.rmDup.sam | awk -F'\t' 'function abs(x){return ((x < 0.0) ? -x : x)}
{print abs($9)}' | sort | uniq -c | awk -v OFS="\t" '{print $2, $1/2}' >  fragmentLen.rmDup.txt
```

<Read filtering>

```
samtools view -h -q 2 bowtie2.sorted.rmDup.sam > bowtie2.sorted.rmDup.qualityScore2.sam
```

<File conversion>

```
(1)
```

```
samtools view -bS -F 0x04 bowtie2.sorted.rmDup.qualityScore2.sam >
bowtie2.rmDup.qualityScore2.mapped.bam

(2)

samtools sort -n bowtie2.rmDup.qualityScore2.mapped.bam -o
bowtie2.rmDup.qualityScore2.mapped.sorted.bam

(3)

samtools index bowtie2.rmDup.qualityScore2.mapped.sorted.bam

(4)

bedtools bamtobed -i bowtie2.rmDup.qualityScore2.mapped.sorted.bam -bedpe > bowtie2.bed

(5)

awk '$1==$4 && $6-$2 < 1000 {print $0}' bowtie2.bed > bowtie2.clean.bed

(6)

cut -f 1,2,6 bowtie2.clean.bed | sort -k1,1 -k2,2n -k3,3n > bowtie2.fragments.bed
```

<Peak calling with MACS2>

```
macs2 callpeak \
-t bowtie2.rmDup.qualityScore2.mapped.sorted.bam \
-f BAM \
-g hs \
-n outname \
--broad \
--broad-cutoff 0.1 \
--nomodel \
--outdir outdir \
-n outname 2> macs2.log
```

<Peak calling with SEACR>

```
bedtools genomecov \
-bg \
-i bowtie2.fragments.bed \
-g hg38chromsizes.bed > bowtie2.fragments.bedgraph

# SEACR condition 1: Relaxed peak calling mode and using IgG as normalization control
```

```
bash $seacr \
bowtie2.fragments.bedgraph\
E27-S1-Mono-IgG_bowtie2.fragments.bedgraph \
norm relaxed seacr_control.peaks

# SEACR condition 2: Relaxed peak calling mode and selection of the top 1% of peaks

bash $seacr \
bowtie2.fragments.bedgraph \
0.01 non relaxed seacr_top0.01.peaks\

# SEACR condition 3: Stringent peak calling mode and using IgG as normalization control

bash $seacr \
bowtie2.fragments.bedgraph \
E27-S1-Mono-IgG_bowtie2.fragments.bedgraph \
norm stringent seacr_control.peaks

# SEACR condition 4: Stringent peak calling mode and selecting the top 1% of peaks

bash $seacr \
bowtie2.fragments.bedgraph \
0.01 non stringent seacr_top0.01.peaks\
```

Appendix I. CUT&Tag sequencing results.

Sample name	Cell type	Histone marker	Library conc. (ng/µl)	PCR duplication rate (%)	Read depth (million reads)	MACS2		SEACR			
						Narrow peak mode	Broad peak mode	Relaxed mode & IgG control	Relaxed mode & top 1% peaks	Stringent mode & IgG control	Stringent mode & top 1% peaks
E27-S1-Mono-H3K27Ac	Monocytes	H3K27Ac	5.5	72.45	5.9	389	1,214	136,861	821,160	136,861	8,122
E27-S1-Mono-H3K27me3	Monocytes	H3K27me3	7.83	65.1	6.5	1,944	3,349	4,107	682,681	3,015	5,992
E27-S1-Mono-H3K4me3	Monocytes	H3K4me3	4.18	76.6	4.7	1,857	5,352	5,513	471,942	3,471	4,704
E27-S1-Mono-IgG	Monocytes	IgG	0.03	90.55	0.4	na	na	na	na	na	na
E27-S1-NK-H3K27Ac	NK cells	H3K27Ac	1.84	88.1	6.3	1	1	18,457	244,582	18,457	2,447
E27-S1-NK-H3K27me3	NK cells	H3K27me3	3.48	82.9	7	2	4	792	393,364	353	3,709
E27-S1-NK-H3K4me3	NK cells	H3K4me3	0.93	86.7	5.1	1	1	12,742	115,670	12,742	1,162
E27-S2-Mono-H3K27Ac	Monocytes	H3K27Ac	4.63	74.65	6.1	344	1,005	125,893	702,074	125,893	6,939

E27-S2-Mono-H3K27me3	Monocytes	H3K27me3	5	78.9	5.7	12	18	2,526	281,237	986	2,711
E27-S2-Mono-H3K4me3	Monocytes	H3K4me3	4.23	82.15	7.2	3,678	6,848	2,745	255,151	1,350	2,643
E27-S2-NK-H3K27Ac	NK cells	H3K27Ac	2.04	87.9	5.3	1	1	14,487	222,148	14,487	2,217
E27-S2-NK-H3K27me3	NK cells	H3K27me3	2.51	81.5	4.3	2	2	35,577	233,202	35,566	2,249
E27-S2-NK-H3K4me3	NK cells	H3K4me3	1.92	86.6	6.6	356	1,391	25,589	197,290	25,589	1,987
E28-S1-Mono-H3K4me3	Monocytes	H3K4me3	1.7	87.8	11.3	1,337	3,097	1,670	130,604	101	1,342
E28-S1-NK-H3K27Ac	NK cells	H3K27Ac	1.24	89.2	7	2	2	18,021	199,399	18,017	1,994
E28-S1-NK-H3K27me3	NK cells	H3K27me3	2.9	86.05	7.7	1	1	803	282,896	99	2,708
E28-S1-NK-H3K4me3	NK cells	H3K4me3	1.19	88.15	6	14	31	14,170	75,027	14,170	763
E28-S2-Mono-H3K4me3	Monocytes	H3K4me3	3.53	83.85	10.5	6,616	9,954	4,468	205,362	2,098	2,210

E28-S2-NK-H3K4me3	NK cells	H3K4me3	0.02	84.8	0.2	-	-	409	9,485	409	94
E30-S1-Mono-H3K27Ac	Monocytes	H3K27Ac	0.8	88.9	5.6	2	2	7,431	180,765	7,431	1,781
E30-S1-Mono-H3K27me3	Monocytes	H3K27me3	5.76	68.55	6.5	2,479	4,041	5,019	502,215	3,223	4,986
E30-S1-Mono-H3K4me3	Monocytes	H3K4me3	1.83	80.25	4.9	1,534	3,644	2,670	282,040	1,265	2,840
E30-S1-NK-H3K27Ac	NK cells	H3K27Ac	0.25	89.85	2.5	1	1	1,519	49,308	1,519	485
E30-S1-NK-H3K27me3	NK cells	H3K27me3	1.97	81.95	3.8	1	1	38,576	293,254	38,576	2,870
E30-S1-NK-H3K4me3	NK cells	H3K4me3	0.55	90.9	5.4	1	1	3,360	67,430	3,360	664
E30-S2-Mono-H3K27Ac	Monocytes	H3K27Ac	0.02	92.45	18.3	14	16	84	300,413	45	2,993
E30-S2-Mono-H3K27me3	Monocytes	H3K27me3	3.89	61.6	4.8	3,079	4,630	6,397	593,641	4,800	5,500
E30-S2-Mono-H3K4me3	Monocytes	H3K4me3	1.71	86.85	5.2	20	50	19,487	212,066	19,487	2,123

E30-S2-NK-H3K27Ac	NK cells	H3K27Ac	0.54	91.3	6.9	1	2	4,368	116,208	4,368	1,151
E30-S2-NK-H3K27me3	NK cells	H3K27me3	4.59	70.1	3.4	2	2	74,033	505,883	74,033	4,813
E30-S2-NK-H3K4me3	NK cells	H3K4me3	0.36	89.35	4.1	1	1	3,939	103,151	3,939	1,023
E30-S3-Mono-H3K4me3	Monocytes	H3K4me3	2.24	83.05	5.9	3,794	7,169	2,938	188,370	298	1,932
E30-S3-NK-H3K27Ac	NK cells	H3K27Ac	0.4	91.35	4	1	1	2,309	66,479	2,309	654
E30-S3-NK-H3K27me3	NK cells	H3K27me3	3.13	83.75	4.2	1	1	33,777	244,304	33,777	2,366
E30-S3-NK-H3K4me3	NK cells	H3K4me3	0.67	88.55	4.7	19	109	12,396	74,219	12,396	751
E30-S4-Mono-H3K27me3	Monocytes	H3K27me3	7.76	69.85	5.3	155	483	2,754	446,321	1,480	4,219
E30-S4-Mono-IgG	Monocytes	IgG	0	88.7	0	-	-	3	412	3	3
E31-S1-Mono-H3K27Ac	Monocytes	H3K27Ac	3.46	62.55	3.3	11,134	15,117	2,584	576,672	1,348	5,760
E31-S1-Mono-H3K27me3	Monocytes	H3K27me3	5.87	49.55	5.9	5,345	7,668	8,493	1,009,579	6,611	8,569

E31-S1-Mono-H3K4me3	Monocytes	H3K4me3	6.77	63.8	6.1	18,999	22,458	13,471	344,652	11,664	4,963
E31-S1-NK-H3K27Ac	NK cells	H3K27Ac	1.74	86.6	6.1	98	206	27,783	302,082	27,783	3,011
E31-S1-NK-H3K27me3	NK cells	H3K27me3	8.5	56.9	5.9	657	1,967	3,191	1,117,905	2,091	9,951
E31-S1-NK-H3K4me3	NK cells	H3K4me3	0.88	80.15	3.2	5,748	7,727	1,585	150,560	644	1,532
E31-S2-Mono-H3K4me3	Monocytes	H3K4me3	0.33	87.05	2.9	-	-	5,354	37,864	5,354	379
E31-S2-NK-H3K27Ac	NK cells	H3K27Ac	1	87.85	6	1	1	18,589	265,380	18,589	2,656
E31-S2-NK-H3K27me3	NK cells	H3K27me3	4.79	79.9	5.8	2	2	1,280	451,286	217	4,254
E31-S2-NK-H3K4me3	NK cells	H3K4me3	3.57	81.2	5.6	7,944	10,150	2,561	162,248	1,005	1,752
E31-S3-Mono-H3K27Ac	Monocytes	H3K27Ac	7.84	57.9	4.7	8,512	12,162	4,609	873,678	999	8,775
E31-S3-Mono-H3K27me3	Monocytes	H3K27me3	7.58	69.45	7.8	743	1,846	4,813	738,304	2,848	6,590

E31-S3-Mono-H3K4me3	Monocytes	H3K4me3	6.06	64.55	5.1	19,209	20,528	7,530	270,068	4,146	3,700
E31-S3-NK-H3K27Ac	NK cells	H3K27Ac	3.49	78.65	5.2	60	157	60,809	459,639	60,809	4,599
E31-S3-NK-H3K27me3	NK cells	H3K27me3	4.96	79.1	6.8	3	4	104,613	576,353	104,613	5,351
E31-S3-NK-H3K4me3	NK cells	H3K4me3	2.33	86.8	9.2	4,450	7,572	4,208	131,056	672	1,381
E33-S1-Mono-H3K27Ac	Monocytes	H3K27Ac	4.61	77.8	6.2	549	1,400	104,430	638,993	104,430	6,368
E33-S1-Mono-H3K27me3	Monocytes	H3K27me3	4.33	78.05	6.8	240	690	3,417	491,787	1,434	4,531
E33-S1-Mono-H3K4me3	Monocytes	H3K4me3	6.04	75.55	7.3	14,320	16,844	6,756	364,182	3,293	4,214
E33-S1-NK-H3K27Ac	NK cells	H3K27Ac	0.5	87.25	4.4	1	1	6,218	163,855	6,218	1,618
E33-S1-NK-H3K27me3	NK cells	H3K27me3	2.54	82.55	7.1	29	99	475	452,585	209	4,207
E33-S1-NK-H3K4me3	NK cells	H3K4me3	1.13	87.65	5.4	28	106	17,975	212,558	17,975	2,111

E33-S2-Mono-H3K27Ac	Monocytes	H3K27Ac	1.54	86.7	15.5	265	715	3,731	759,271	1,100	7,471
E33-S2-Mono-H3K27me3	Monocytes	H3K27me3	1.99	85.4	10	14	25	2,816	344,100	1,128	3,238
E33-S2-Mono-H3K4me3	Monocytes	H3K4me3	4.23	79.1	6	5,581	8,364	5,356	387,734	2,783	3,901
E33-S2-NK-H3K27Ac	NK cells	H3K27Ac	1.32	90.7	7.6	1	1	11,384	195,128	11,384	1,950
E33-S2-NK-H3K27me3	NK cells	H3K27me3	3.24	85.8	6.6	1	1	45,589	285,136	45,516	2,676
E33-S2-NK-H3K4me3	NK cells	H3K4me3	1.82	86.1	6	2,339	4,455	5,302	170,102	1,807	1,726
E33-S3-Mono-H3K27Ac	Monocytes	H3K27Ac	4.32	80.75	7.2	572	1,528	92,954	567,191	92,954	5,687
E33-S3-Mono-H3K27me3	Monocytes	H3K27me3	9.2	70.9	4.4	492	1,153	3,277	371,976	1,351	3,731
E33-S3-Mono-H3K4me3	Monocytes	H3K4me3	5.43	76.5	5.3	9,241	12,262	4,308	226,076	2,104	2,492
E33-S3-NK-H3K27Ac	NK cells	H3K27Ac	1.63	88.95	6.6	1	1	16,658	239,916	16,658	2,394

E33-S3-NK-H3K27me3	NK cells	H3K27me3	5.23	81.4	6.8	12	34	1,413	433,911	760	4,075
E33-S3-NK-H3K4me3	NK cells	H3K4me3	0.32	92	18.1	77	529	1,354	170,413	625	1,709
E33-S4-Mono-H3K27Ac	Monocytes	H3K27Ac	3.16	81.95	6	335	1,799	67,538	458,604	67,538	4,579
E33-S4-Mono-H3K27me3	Monocytes	H3K27me3	4.4	76.75	5.4	74	226	3,171	343,196	1,445	3,265
E33-S4-Mono-H3K4me3	Monocytes	H3K4me3	5.1	80.9	6.9	9,116	11,808	7,067	252,830	2,783	2,765
E33-S4-NK-H3K27Ac	NK cells	H3K27Ac	3.05	85.1	6.3	3	5	42,799	380,846	42,799	3,811
E33-S4-NK-H3K27me3	NK cells	H3K27me3	6.36	77.3	6.6	23	102	3,197	545,084	1,466	5,002
E33-S4-NK-H3K4me3	NK cells	H3K4me3	1.97	86.55	7.1	1,920	4,280	484	141,469	153	1,437

Abbreviations: H3K27Ac, acetylation of histone H3 at lysine 27; SEACR; Sparse Enrichment Analysis for CUT&RUN, MACS2; Model-based Analysis of ChIP-Seq 2, NK cells; Natural killer cells, PCR; Polymerase chain reaction; H3K4me3, trimethylation of histone H3 at lysine 4; H3K27me3, trimethylation of histone H3 at lysine 27.

Appendix J. Included publication (1).

Clinical Infectious Diseases

BRIEF REPORT

T-SPOT.TB Reactivity in Southern African Children With and Without *in Utero* HIV Exposure

Saori C. Iwase,[1,2] Paul T. Edlefsen,[3] Lynnette Bhebhe,[4] Kesego Motsumi,[4] Sikhulile Moyo,[4,5] Anna-Ursula Happel,[1,2] Danica Shao,[3] Nicholas Mmasa,[6] Sara Schenkel,[7] Melanie A. Gasper,[8] Melanie Dubois,[7,9] Megan A. Files,[10] Chetan Seshadri,[10] Fergal Duffy,[8] John Aitchison,[8,©] Mihai G. Netea,[11,12] Jennifer Jao,[4,13] Donald W. Cameron,[14] Clive M. Gray,[1,2,15] Heather B. Jaspan,[1,2,8] and Kathleen M. Powis[4,5,16]

[1]Division of Immunology, Department of Pathology, University of Cape Town, Cape Town, South Africa; [2]Institute of Infectious Disease and Molecular Medicine, University of Cape Town, Cape Town, South Africa; [3]Vaccine and Infectious Disease Division, Statistical Center for HIV/AIDS Research and Prevention, Fred Hutchinson Cancer Research Center, Seattle, USA; [4]Botswana Harvard AIDS Institute Partnership, Gaborone, Botswana; [5]Department of Immunology and Infectious Diseases, Harvard T.H. Chan School of Public Health, Boston, USA; [6]Surgical Department, County Durham and Darlington NHS Trust, Darlington Memorial Hospital, Darlington, United Kingdom; [7]Division of Pediatric Global Health, Massachusetts General Hospital, Boston, USA; [8]Center for Global Infectious Disease Research, Seattle Children's Research Institute, Seattle, USA; [9]Division of Infectious Diseases, Department of Pediatrics, Boston Children's Hospital, Boston, USA; [10]Department of Medicine, University of Washington School of Medicine, Seattle, USA; [11]Department of Internal Medicine and Radboud Center for Infectious Diseases, Radboud University Medical Center, Nijmegen, The Netherlands; [12]Department of Immunology and Metabolism, Life & Medical Sciences Institute, University of Bonn, Bonn, Germany; [13]Department of Pediatrics, Department of Medicine, Northwestern University Feinberg School of Medicine, Chicago, USA; [14]Divisions of Infectious Diseases and Respirology, University of Ottawa at the Ottawa Hospital, Ottawa, Canada; [15]Division of Molecular Biology and Human Genetics, Biomedical Research Institute, Stellenbosch University, Cape Town, South Africa; and [16]Departments of Internal Medicine and Pediatrics, Massachusetts General Hospital, Boston, USA

Infants who are human immunodeficiency virus (HIV)-exposed uninfected (iHEU) experience higher risk of infectious morbidity than infants HIV-unexposed uninfected (iHUU). We compared tuberculosis (TB) infection prevalence in 418 Bacillus Calmette-Guérin vaccinated sub-Saharan African iHEU and iHUU aged 9–18 months using T-SPOT.TB. Prevalence of TB infection was low and did not differ by HIV exposure status.

Keywords. TB infection; Southern Africa; infants; HIV exposure; T-SPOT.TB.

Children under 5 years of age experience high risk of progression to tuberculosis (TB) disease if untreated [1]. In sub-Saharan Africa, about 25% of persons of childbearing potential are living with human immunodeficiency virus (HIV) [2]. Successful antiretroviral treatment (ART) scale-up for pregnant persons living with HIV has resulted in an increasing number of infants born HIV-exposed uninfected (iHEU).The iHEU experience greater risk of infectious morbidity than infants born HIV-unexposed uninfected (iHUU) [3].

Bacillus Calmette-Guérin (BCG) vaccine prevents severe TB disease. BCG vaccination induces T-cell interferon-gamma (IFN-γ) production, an important component of protection against TB [4]. We previously found a significantly lower proportion of BCG-specific IFN-γ producing $CD4^+$ T cells among iHEU, suggesting that iHEU may not achieve equivalent BCG immune protection compared to iHUU [5]. Therefore, we investigated TB infection prevalence by HIV exposure status among BCG-vaccinated infants in Botswana and South Africa (SA), 2 high burden HIV and TB settings.

METHODS

Study Design

The study was nested within 2 prospective observational cohort studies enrolling pregnant women with and without HIV and their infants. The Tshilo Dikotla study and the Innate Factors Associated with Nursing Transmission (InFANT) study recruited participants from government antenatal clinics in Botswana and SA between 2013 and 2020 [6, 7]. Infants with severe birth complications, or born to mothers with active TB or TB symptoms were excluded. All infants received BCG vaccination within 72 hours of birth. Participants were followed over 36 months in Botswana and 12 months in SA. Peripheral blood mononuclear cells were collected at 9–12 and 18 months in Botswana, at 9 and 12 months in SA, and stored in liquid nitrogen.

Ethics

This study was approved by the Health Research Development Committee in Botswana, Massachusetts General Hospital's Institutional Review Board, and University of Cape Town's Human Research Ethics Committee. Women provided written informed consent for their participation and that of their infant.

T-SPOT.TB Assay

T-SPOT.TB assays (Oxford Immunotec) were performed and interpreted according to manufacturer's instructions. Samples below the recommended cell number were normalized as previously described [8]. For invalid or borderline results, retesting was performed using an aliquot collected at the same visit or a follow-up visit. If the re-tested result was valid, the valid result was assigned to the initial visit. Infants testing T-SPOT.TB positive were referred to government clinics. We

Received 09 March 2023; editorial decision 01 June 2023; accepted 08 June 2023; published online 9 June 2023

Correspondence: S. C. Iwase, Division of Immunology, Department of Pathology, Institute of Infectious Disease and Molecular Medicine, University of Cape Town, Falmouth Building, Anzio Rd, Observatory, Cape Town 7925, South Africa (saori.christina.iwase@gmail.com).

Clinical Infectious Diseases®

https://doi.org/10.1093/cid/ciad356

defined "TB infection" as T-SPOT.TB positive without TB disease symptoms at the time of specimen draw.

Sensitivity Analysis

Due to timing variation of testing between sites, we simulated results as if all testing was performed at 12 months. For SA infants, we assumed a positive test at month 9 would have a negative at month 12 with probability R (reversion), and infants with a negative or invalid result at month 9 would have a positive at month 12 with probability C (conversion). These probabilities were applied to 12- to 18-months results in the Botswana cohort. We assumed a baseline P (prevalence) at 12 months to calculate the probability of a positive (or negative/invalid) test at 18 months having been negative (or positive) at month 12. For each combination of R, C, and P, ranging from 0% to 20% based on published studies [8, 9], we randomly generated 5000 data sets and performed Fisher exact tests on the pooled month 12 data, comparing the proportion of positive results by infant HIV exposure status.

Statistical Analysis

Data analysis was performed using R (version 4.0.4). Normally distributed continuous variables were compared by *t* test using means with standard deviations. Continuous variables with skewed distributions were compared by Wilcoxon rank-sum test using medians with interquartile ranges. Categorical variables were compared by χ^2 test. TB infection proportions were compared by infant HIV exposure status using Fisher exact test.

Power Calculations

Previous sub-Saharan data reported a prevalence of TB infection of 10.9% (95% confidence interval [CI], 6.1%–17.7%) in 6-month-old iHEU [8]. Thus, we expected that at least 18% of iHEU would test positive by 12 months. Given our study's sample size (125 iHUU and 293 iHEU), we had at least 80% power to detect a 57.5% difference in TB infection at 12 months, assuming a prevalence of ≤ 7.65% among iHUU.

RESULTS

Cohort Characteristics

The study included 418 mother-infant pairs, of which 293 were iHEU (Supplementary Table 1). The proportion of iHEU was higher in Botswana compared to SA. Infant sex and gestational age at birth were similar between HIV exposure groups. Women with HIV were older and had higher gravidity than women without HIV. Among women with HIV, 63.0% were on ART at conception with median CD4 count of 463 cells/mm^3 at enrollment. Fifteen (3.6%) infants had household TB exposure cases (n = 5 in Botswana; n = 10 in SA), including 6 mothers of infants in SA. Household exposure did not differ by HIV exposure status.

Table 1. T-SPOT.TB Reactivity by HIV Exposure Status

		iHUU N = 125	iHEU N = 293
Study site, n (%)	Botswana	33 (26.4)	135 (46.1)
	SA	92 (73.6)	158 (53.9)
Testing time point, n (%)	Month 9	44 (35.2)	117 (39.9)
	Month 12	48 (38.4)	46 (15.7)
	Month 18	33 (26.4)	130 (44.4)
T-SPOT.TB result, n (%)	Positive[a]	4 (3.2)	10 (3.4)
	Negative[b]	115 (92.0)	273 (93.2)
	Borderline[c]	0 (0.0)	1 (0.3)
	Invalid[d,e]	6 (4.8)	9 (3.1)

Abbreviations: HIV, human immunodeficiency virus; iHUU, HIV-unexposed uninfected infants; iHEU, HIV-exposed uninfected infants; PHA, phytohemagglutinin; SA, South Africa; SFCs, spot-forming cells; TB, tuberculosis.

[a]Positive if there were ≥ 8 SFCs above Nil control for at least 1 of TB antigens.

[b]Negative if a test did not fall into any of the interpretations.

[c]Borderline if the difference to Nil control was between 5–7 SFCs for at least 1 of TB antigens.

[d]Invalid if there were PHA < 20 SFCs or Nil control > 10 SFCs.

[e]Reason of invalid: contamination of kits or assay (n = 2); PHA < 20 SFCs (n = 7) and Nil control > 10 SFCs (n = 6).

Prevalence of TB Infection

The 418 infants' results comprised 14 (3.3%) T-SPOT.TB positive, 1 (0.24%) borderline, 15 (3.6%) invalid, and 388 (92.8%) negative (Table 1). T-SPOT.TB reactivity did not differ by infant HIV exposure status (Table 1) or by study site (Supplementary Table 2). No infants who tested positive and were referred for clinical evaluation were diagnosed with TB disease. Two reversions (0.48%) occurred among Botswana iHEU, 1 of which had a household TB contact (Supplementary Table 1). Although spot-forming cells (SFCs) for TB antigens did not differ pre-reversion, SFCs for phytohemagglutinin (positive control) were significantly lower than other positive cases when they reverted (median 165 vs 724, $P = .003$).

We conducted a sensitivity analysis to impute T-SPOT.TB results at 12 months of age across study sites, considering potential conversion and reversion rates over time (Supplementary Table 3). No combination of assumptions gave a statistically significant difference between HIV-exposure groups in T-SPOT.TB positivity more than 5% of the time.

DISCUSSION

In our Southern African cohort, we found a low overall risk of TB infection among infants BCG-vaccinated at birth (3.3%), without variation by HIV exposure status. The lack of difference is important, as iHEU have been reported to be at high risk of infectious morbidity [3]. Although testing was performed between 9 and 18 months of life, with some infants having a longer window of risk for TB exposure, the sensitivity analysis suggests that the prevalence of T-SPOT.TB positivity was robust to conversion and reversion between the observed

time points. Literature investigating TB infection in iHEU using interferon-gamma release assays (IGRAs) like the QuantiFERON-TB or T-SPOT.TB is limited [10], and studies including iHUU as a comparison group are scarce. To our knowledge, this is the largest study comparing TB infection prevalence between Southern African iHEU and iHUU using T-SPOT.TB.

The prevalence of TB infection was lower among infants in this study compared to other studies using IGRA-based approaches [9]. Differences in cohort characteristics likely account for lower IGRA positivity in our study. We excluded mothers with active TB disease. Furthermore, the previously published SA study assessed TB infection in children with a mean age of 3.5 years [9], evaluating a longer exposure window. It was also conducted during a period when SA recorded its highest TB incidence in the last 2 decades [11]. Thus, household TB contact was more common than our study (13.2% vs 3.6%).

We found no difference in T-SPOT.TB reactivity by HIV exposure status. This differs from a Ugandan study where children HEU up to 5 years of age had higher IGRA positivity prevalence than children HUU [10]. Differences in maternal inclusion criteria and longer follow-up period likely explain the higher prevalence reported in Ugandan children who were HEU.

The strengths of this study include a large sample size, with cohorts recruited in neighboring countries, both with high HIV and TB burden, using a common protocol. Pooling of data increased study power. Although the timing of testing varied between sites, we employed a sensitivity analysis to assess for robustness of findings. Given the lower than anticipated T-SPOT.TB positivity prevalence, we did not have sufficient power to conclusively evaluate the association between HIV exposure and TB infection. Because the prevalence of a T-SPOT.TB reactivity in iHEU was 3.4% in our cohort, prevalence among iHUU would had to have been ≤0.175%, a 94.9% reduction, to detect a significant difference. Adequately powered studies would be needed to definitively exclude a higher risk of TB infection in iHEU.

We employed IGRA-based testing, similar to previous studies [9, 10]. Infant T cells have lower IFN-γ producing capacity than adult T cells [12], and perinatal HIV exposure has been associated with altered immunity [13]. Thus, it is unclear whether iHEU and iHUU have similar T-SPOT.TB reactivity. Furthermore, IGRA testing is not recommended for children under 2 years of age, but tuberculin skin testing can result in false positive tests in BCG-vaccinated individuals. Assays targeting non-IFN-γ markers have been proposed as alternatives in BCG-vaccinated children under 2 years of age [14] and may be beneficial to use in future studies in parallel with IGRA testing.

In summary, we showed that the TB infection prevalence among BCG-vaccinated infants from 2 Southern African countries with high HIV and TB prevalence was low and did not vary by fetal HIV exposure status.

Supplementary Data

Supplementary materials are available at *Clinical Infectious Diseases* online. Consisting of data provided by the authors to benefit the reader, the posted materials are not copyedited and are the sole responsibility of the authors, so questions or comments should be addressed to the corresponding author.

Notes

Acknowledgments. The authors thank the mothers and infants who participated in this study, the research and lab staff at Botswana Harvard AIDS Institute Partnership in Gaborone, Botswana, and the clinic Maternal Obstetric Unit in Cape Town, South Africa.

Previously presented. HIV & Pediatrics 2022, Montreal, Canada, July 2022. Abstract number 38. AIDS 2022, Montreal, Canada, August 2022. Abstract number PEMOB32.

Financial support. This work was supported by the National Institute of Allergies and Infectious Disease (NIAID) (grant number R01AI142670 awarded to K. M. P.). The Tshilo Dikotla study was funded by the National Institute of Diabetes and Digestive and Kidney Diseases (grant number R01DK109881 awarded to J. J.). The InFANT study was supported in part by the Global Health Research Initiative (GHRI), a research funding partnership composed of the Canadian Institutes of Health Research, the Canadian International Development Agency, and the International Development Research Centre (grant number THA-118568 awarded to H. B. J. and C. M G.), as well as the NIAID (grant number R01AI120714-01A1 awarded to H. B. J.) and National Institute of Child Health and Human Development (NICHD) (grant number R21HD083344 awarded to H. B. J. and C. M. G.). M. D. was supported by NIAID (grant number T32AI007433). S. C. I. was funded by Yoshida Scholarship Foundation.

Potential conflicts of interest. All authors report no potential conflicts.

All authors have submitted the ICMJE Form for Disclosure of Potential Conflicts of Interest. Conflicts that the editors consider relevant to the content of the manuscript have been disclosed.

References

1. Jenkins HE, Yuen CM, Rodriguez CA, et al. Mortality in children diagnosed with tuberculosis: a systematic review and meta-analysis. Lancet Infect Dis **2017**; 17: 285–95.
2. UNAIDS. UNAIDS data 2020 [Internet]. 2020. Available at: https://www.unaids.org/sites/default/files/media_asset/2020_aids-data-book_en.pdf. Accessed 21 February 2023.
3. Evans C, Jones CE, Prendergast AJ. HIV-exposed, uninfected infants: new global challenges in the era of paediatric HIV elimination. Lancet Infect Dis **2016**; 16: e92–e107.
4. Flynn JL. Immunology of tuberculosis and implications in vaccine development. Tuberculosis (Edinb) **2004**; 84(1–2):93–101.
5. Kidzeru EB, Hesseling AC, Passmore JA, et al. In-utero exposure to maternal HIV infection alters T-cell immune responses to vaccination in HIV-uninfected infants. AIDS **2014**; 28:1421–30.
6. Jao J, Sun S, Bonner LB, et al. Lower insulin sensitivity in newborns with in utero HIV and antiretroviral exposure who are uninfected in Botswana. J Infect Dis **2022**; 226:2002–9.
7. Tchakoute CT, Sainani KL, Osawe S, et al. Breastfeeding mitigates the effects of maternal HIV on infant infectious morbidity in the option BR era. Aids **2018**; 32:2383–91.
8. Cranmer LM, Kanyugo M, Jonnalagadda SR, et al. High prevalence of tuberculosis infection in HIV-1 exposed Kenyan infants. Pediatr Infect Dis J **2014**; 33:401–6.
9. Cranmer LM, Draper HR, Mandalakas AM, et al. High incidence of tuberculosis infection in HIV-exposed children exiting an isoniazid preventive therapy trial. Pediatr Infect Dis J **2018**; 37:e254–6.
10. Marquez C, Chamie G, Achan J, et al. Tuberculosis infection in early childhood and the association with HIV-exposure in HIV-uninfected children in rural Uganda. Pediatr Infect Dis J **2016**; 35:524–9.

11. World Health Organization. Global tuberculosis report 2022 [Internet]. 2022. Geneva: World Health Organization. Available at: https://www.who.int/publications/i/item/9789240061729. Accessed 21 February 2023.
12. Marchant A, Goldman M. T cell-mediated immune responses in human newborns: ready to learn? Clin Exp Immunol **2005**; 141:10–8.
13. Smith C, Jalbert E, de Almeida V, et al. Altered natural killer cell function in HIV-exposed uninfected infants. Front Immunol **2017**; 8:470.
14. Anterasian C, Warr AJ, Lacourse SM, et al. Non-IFNγ whole blood cytokine responses to mycobacterium tuberculosis antigens in HIV-exposed infants. Infect Dis J **2021**; 40:922–9.

Appendix K. Included publication (2).

AMERICAN SOCIETY FOR MICROBIOLOGY | Microbiology Spectrum

| Open Peer Review | Human Microbiome | Research Article

Longitudinal gut microbiota composition of South African and Nigerian infants in relation to tetanus vaccine responses

Saori C. Iwase,[1,2] Sophia Osawe,[3] Anna-Ursula Happel,[1,2] Clive M. Gray,[4] Susan P. Holmes,[5] Jonathan M. Blackburn,[2,6] Alash'le Abimiku,[3,7] Heather B. Jaspan[1,2,8]

AUTHOR AFFILIATIONS See affiliation list on p. 14.

ABSTRACT Infants who are exposed to HIV but uninfected (iHEU) have higher risk of infectious morbidity than infants who are HIV-unexposed and uninfected (iHUU), possibly due to altered immunity. As infant gut microbiota may influence immune development, we evaluated the effects of HIV exposure on infant gut microbiota and its association with tetanus toxoid vaccine responses. We evaluated the gut microbiota of 82 South African (61 iHEU and 21 iHUU) and 196 Nigerian (141 iHEU and 55 iHUU) infants at <1 and 15 weeks of life by 16S rRNA gene sequencing. Anti-tetanus antibodies were measured by enzyme-linked immunosorbent assay at matched time points. Gut microbiota in the 278 included infants and its succession were more strongly influenced by geographical location and age than by HIV exposure. Microbiota of Nigerian infants, who were exclusively breastfed, drastically changed over 15 weeks, becoming dominated by *Bifidobacterium longum* subspecies *infantis*. This change was not observed among South African infants, even when limiting the analysis to exclusively breastfed infants. The Least Absolute Shrinkage and Selection Operator regression suggested that HIV exposure and gut microbiota were independently associated with tetanus titers at week 15, and that high passively transferred antibody levels, as seen in the Nigerian cohort, may mitigate these effects. In conclusion, in two African cohorts, HIV exposure minimally altered the infant gut microbiota compared to age and setting, but both specific gut microbes and HIV exposure independently predicted humoral tetanus vaccine responses.

IMPORTANCE Gut microbiota plays an essential role in immune system development. Since infants HIV-exposed and uninfected (iHEU) are more vulnerable to infectious diseases than unexposed infants, we explored the impact of HIV exposure on gut microbiota and its association with vaccine responses. This study was conducted in two African countries with rapidly increasing numbers of iHEU. Infant HIV exposure did not substantially affect gut microbial succession, but geographic location had a strong effect. However, both the relative abundance of specific gut microbes and HIV exposure were independently associated with tetanus titers, which were also influenced by baseline tetanus titers (maternal transfer). Our findings provide insight into the effect of HIV exposure, passive maternal antibody, and gut microbiota on infant humoral vaccine responses.

KEYWORDS HIV-exposed uninfected infants, South Africa, Nigeria, gut microbiota, tetanus toxoid, vaccine response

The mutualistic relationship between microbes and humans begins in early life. Emerging evidence suggests that the colonization of microbes in the gut facilitates the development of the immune system and growth trajectories (1, 2). Due to the successful prevention of vertical transmission programs, the number of infants who are

Editor Laxmi Yeruva, USDA-ARS Arkansas Children's Nutrition Center, Little Rock, Arkansas, USA

Address correspondence to Heather B. Jaspan, HBJaspan@gmail.com.

Saori C. Iwase and Sophia Osawe contributed equally to this article. Order of authors was determined on primary manuscript contribution.

The authors declare no conflict of interest.

See the funding table on p. 14.

Received 29 August 2023
Accepted 20 December 2023
Published 17 January 2024

HIV-exposed yet uninfected (iHEU) has been increasing, particularly in sub-Saharan Africa (3). Compared to infants who are HIV-unexposed and uninfected (iHUU), iHEU are at higher risk of morbidity and mortality, predominantly due to infectious diseases (4). This is thought to be linked to their altered immunity (5, 6), which may be secondary to altered gut microbiota. To our knowledge, there are limited longitudinal studies comparing gut microbiota between iHEU and iHUU, and most of them were conducted in a single country (7–10). Some studies have found few differences (8, 10, 11), whereas clear differences in microbiota profile were observed in Haitian (7) and Nigerian iHEU (9). Thus far, only one cross-sectional study compared the gut microbiota between iHEU and iHUU in multiple countries, including Belgium, Canada, and South Africa, and suggested that the difference in microbiota by HIV exposure status may be population-specific (12). Therefore, the effect of geography and HIV exposure on infant gut microbiota requires further investigation.

Vaccines are critical for protecting infants from infectious diseases and consequent morbidity and mortality. However, multiple factors can influence vaccine immunogenicity, including genetics, nutritional status, and pre-existing immunity (13). In addition, emerging evidence points to a possible role of the gut microbiome in influencing vaccine response (14). In Bangladeshi infants, CD4+ T cell proliferation and IgG against tetanus toxoid (TT) vaccination were positively associated with abundance of Actinobacteria, particularly *Bifidobacterium longum,* until at least 2 years of age (15, 16). Conversely, vaccine-induced CD4+ T cell proliferation against TT vaccine was negatively associated with the abundance of *Enterobacteriales* and *Pseudomonadales* (15).

To evaluate the contribution of gut microbiota to observed differences in immunity between iHEU and iHUU, we longitudinally compared the gut microbiota of South African and Nigerian infants exposed and unexposed to HIV, and correlated these with TT vaccine responses.

MATERIALS AND METHODS

Study participants

Mothers with and without HIV and their neonates were recruited into a multicenter longitudinal study between September 2013 and November 2017 (17). Mother-infant pairs were enrolled during the first week post-delivery at the Khayelitsha Site B Midwife Obstetric Unit in Cape Town, South Africa, and the Plateau State Specialist Hospital in Jos, Nigeria. Clinical and demographic data and samples (including stool and blood) were collected. All mothers with HIV received antiretroviral therapy according to local guidelines, and their infants were confirmed as HIV negative by polymerase chain reaction (PCR) at birth and later time points (18, 19). In addition, all iHEU received nevirapine post-exposure prophylaxis after birth, and co-trimoxazole was recommended at 6 weeks of age as per country-specific guidelines (18, 20). Exclusive breastfeeding was advised to all mothers for 6 months. Feeding data were collected using a structured questionnaire validated in similar settings (21). Feeding practices were categorized as "exclusive breastfeeding," defined as receiving only breastmilk or prescribed medicines since birth, or "mixed feeding," defined as receiving breastmilk supplemented with other liquids or food or receiving formula. In this analysis, we included stool and plasma collected from term infants during the first and at 15 weeks of life born to mothers without complications during pregnancy or delivery.

Immunization

Routine childhood vaccinations were given to all infants according to the World Health Organization Expanded Program on Immunization (22). In both countries, infants were vaccinated against tetanus at 6, 10, and 14 weeks. South African infants received DTaP [diphtheria toxoid (DT), TT, and acellular pertussis (aP)], while Nigerian infants received DTwP [DT, TT, and whole-cell pertussis (wP)]. Pregnant mothers were given booster TT vaccination (Serum Institute of India Pvt. Ltd.) in Nigeria.

Sample collection, DNA extraction, and 16S rRNA gene sequencing

Fecal samples were collected from diapers, avoiding the surface. Samples were placed on ice immediately, transferred to the lab within 6 hours, and stored at −40 to −20°C until analysis. Samples were thawed and treated with a cocktail of mutanolysin (300 U/mL, Sigma Aldrich), lysozyme (45,000 U/mL, Sigma Aldrich), and lysostaphin (24 U/mL, Sigma Aldrich) in 300 µL phosphate buffered solution (PBS) for 1 hour at 37°C. Samples were then mechanically disrupted by bead-beating at 50 Hz for 10 minutes using the Qiagen TissueLyser LT (23). DNA was extracted using the PowerSoil DNA extraction kit (Qiagen), following the manufacturer's protocol. For cross-contamination filtering, genomic DNA was extracted from mock bacterial community cells with equal colony-forming units from each of the 22 known species (HM-280, Biodefense and Emerging Infections Research Resources Repository [BEI]). Extracted genomic DNA was subjected to PCR amplification in triplicate using primers targeting the V3–V4 region (357F/806R primers) of the 16S rRNA gene, as described previously (24). Negative controls for DNA extraction and PCR were included. Amplified libraries were purified using AMPure XP beads (Beckman Coulter), quantitated using Quant-iT dsDNA High Sensitivity Assay Kits (ThermoFisher), pooled in equal molar amounts, and paired-end sequenced using a MiSeq Reagent Kit V3 (600-cycle, Illumina). Following demultiplexing, barcode primers were removed using Cutadapt (version 3.4) (25), and reads were processed using DADA2 (version 1.19.2) (26) within the R framework (R version 4.0.4) (27). Taxonomic classification of amplicon sequence variants (ASVs) was done using an updated SILVA training set (version 132) (28), available at https://github.com/itsmisterbrown/updated_16S_dbs (29). Contaminant ASVs were identified and removed using the decontam package (version 1.16.0) (30). Samples with less than 2,000 filtered reads were excluded from the downstream analysis.

Plasma IgG anti-tetanus antibodies

Blood samples were obtained from infants at 1 and 15 weeks and from Nigerian mothers at 1 week postpartum. All blood samples were collected in heparinized tubes and transported to the lab within 6 hours for sample processing. Plasma was removed prior to cell isolation using Ficoll density-gradient separation medium (Sigma Aldrich) and stored at −80°C until analysis. Plasma anti-tetanus IgG was measured by enzyme-linked immunosorbent assay (ELISA) following the manufacturer's protocol (TECAN, IBL International GmbH). The optical density at 450 nm was measured using an ELISA microplate reader (BioTek ELx808 absorbance plate reader), and a standard curve was generated using the readings from the calibrators included on each plate and used to calculate the individual titers (IU/mL). To validate each assay, we considered only calibration curves for each plate with a coefficient of determination (r^2) above 0.95. Calibration curves that had an r^2 below 0.95 were repeated. The manufacturer provided the intra-assay and inter-assay coefficient of variation (CV%) as 6.9 and 10.4, respectively. Samples on each plate were run in duplicate and averaged. Previously tested positive samples were incorporated into subsequent runs as in-house controls.

Data analysis

Differences in study cohort characteristics were assessed using the Student's *t*-test (parametric continuous variables), Wilcoxon signed-rank test (non-parametric continuous variables), and χ^2 test (parametric categorical variables). Spearman's rank correlation coefficient (*R*) was used to analyze associations between groups. Bacterial community analysis was done using the phyloseq (version 1.40.0) (31) and vegan (version 2.4.6) (32) packages. The ASV table was normalized (i.e., transformed to relative abundance * median sample read depth) and filtered so that each ASV had at least 10 counts in at least 20% of the samples or had a total relative abundance of at least 0.1%. Shannon index was calculated as a measure of α-diversity. Comparison of microbial community composition between groups was evaluated by principal coordinate analysis (PCoA) and

permutational multivariate analysis of variance (PERMANOVA) using the adonis2 function in the vegan package (32), based on the Bray-Curtis dissimilarity and 999 permutations. Partitioning around medoids (PAM) clustering was applied to determine the optimal *k* using the cluster package (version 2.1.4) (33). Analysis of Compositions of Microbiomes with Bias Correction (ANCOM-BC; version 1.6.4) (34) was used to identify significantly differentially abundant ASVs through pair-wise comparisons with an adjusted *P*-value of <0.05, and $\log_e$ fold change of >0.5 or <−0.5. *P*-values of anti-tetanus IgG titers were compared by Wilcoxon signed-rank tests and adjusted for multiple comparisons using the Benjamini-Hochberg method. To identify factors associated with infant anti-tetanus IgG titers at 15 weeks of age, we applied the Least Absolute Shrinkage and Selection Operator (LASSO) regression using the glmnet package (version 4.1.4) (35). Since microbiome compositional data are often highly skewed, we employed rank-based transformation (36) for the regression analysis using the top 50 ASVs among infants who had microbiota data available at both week 1 and week 15. After the transformation, the most abundant bacterial taxon within the sample was given the highest score of 50, and the least abundant bacterial taxon was given a score of 1. The rank-transformed ASVs, infant anti-tetanus IgG titers at 1 week of age (indicative of passive maternal antibody transfer), and HIV exposure status were used as explanatory variables. Models were created according to the infant's age and geographical location separately. The predictive models were validated by 10-fold cross-validation using the cv.glmnet() function in the glmnet package (35). Lambda value that gave the lowest model error was used as a tuning parameter. Variables that fitted within the regression model were considered to be predictor variables for the TT vaccine response. *P*-values <0.05 and 95% confidence intervals were used to assess statistical significance.

RESULTS

Cohort characteristics

Overall, there were 278 mother-infant pairs included in this analysis; 82 were from South Africa and 196 were Nigerian. Several demographic and socioeconomic characteristics differed by study site (Table 1). At enrolment, Nigerian mothers were older [mean age 31 (standard deviation (SD) ±5.31) versus 28 (SD ±5.38) years, $P = 0.001$] with higher gravidity [median 2 (interquartile range (IQR): 1–4) versus 1 (IQR: 1–2), $P < 0.001$] and lower body weight [mean 62.87 (SD ±11.51) versus 72.69 (SD ±13.86) kg, $P < 0.001$] than South African mothers. While electricity was equally available for participants from both countries, significantly more mothers in South Africa had a refrigerator and running water at home, and significantly more Nigerian mothers lived in formal housing (all $P < 0.001$). The weight-for-length z score (wflz) of Nigerian infants was significantly lower than that of South African infants at 15 weeks of age (0.54 versus 0.86, $P = 0.023$). All Nigerian infants were exclusively breastfed (EBF) until 15 weeks of life, whereas only 58.5% of South African mothers reported still EBF at 15 weeks postpartum ($P < 0.001$). Among the South African mothers who reported "mixed feeding," 58.8% ($n = 19$) introduced formula feeding or solid food while continuing breastfeeding, and 41.2% ($n = 14$) completely switched to formula feeding during the course of the study (median breastfeeding duration: 32 days). Mothers of iHUU had higher formal education than mothers of iHEU ($P = 0.002$; Table S1). History of antibiotic use was higher among iHEU due to co-trimoxazole prophylaxis (86.6% iHEU versus 6.6% iHUU, $P < 0.001$). Significantly fewer South African iHEU reported co-trimoxazole prophylaxis than Nigerian iHEU (55.7% versus 100%, $P < 0.001$).

Gut microbiota differs substantially between South African and Nigerian infants in the first week of life

Of the 524 samples sequenced, 442 samples passed the quality filtering of requiring at least 2,000 filtered reads. Thus, 164 (47 South African and 117 Nigerian) out of the 278 infants had gut microbiota data available at both 1 and 15 weeks of life. Gut microbiota

TABLE 1 Cohort characteristics[c]

		South Africa (*N* = 82)	Nigeria (*N* = 196)	*P*
Maternal characteristics				
Mother's age at delivery [years; mean (SD)]		28 (5.38)	31 (5.31)	0.001
Education (*n*; %)	None	0 (0.0)	2 (1.0)	<0.001
	Elementary	5 (6.1)	65 (33.2)	
	Secondary	72 (87.8)	73 (37.2)	
	Higher	5 (6.1)	56 (28.6)	
Unemployed (*n*; %)		59 (72.0)	6 (3.1)	<0.001
Formal housing (*n*; %)		33 (40.2)	185 (94.4)	<0.001
Electricity (*n*; %)		78 (95.1)	178 (90.8)	0.332
Refrigerator (*n*; %)		70 (85.4)	96 (49.0)	<0.001
Running water (*n*; %)		38 (46.3)	48 (24.5)	0.001
Marital status (*n*; %)	Married/living together	25 (30.5)	186 (94.9)	<0.001
	Single	57 (69.5)	10 (5.1)	
Gravidity [*n*; median (IQR)]		1 [1, 2]	2 [1, 4]	<0.001
Mother's weight at enrollment [kg; mean (SD)][a]		72.69 (13.86)	62.87 (11.51)	<0.001
Infant characteristics				
iHEU (*n*; %)		61 (74.4)	141 (71.9)	0.787
Male (*n*; %)		41 (50.0)	94 (48.0)	0.858
Gestational age at delivery [weeks; median (IQR)]		39.30 [38.02, 40.38]	39.95 [38.98, 40.62]	0.011
Vaginal delivery (*n*; %)		82 (100.0)	167 (85.2)	0.001
Wflz at W15 [median (IQR)][b]		0.86 [0.32, 1.90]	0.54 [−0.64, 1.42]	0.023
Mode of feeding at W15 (*n*; %)	Exclusive breastfeeding	48 (58.5)	196 (100.0)	<0.001
	Mixed feeding	34 (41.5)	0 (0.0)	
Reported antibiotic use (*n*; %)	Co-trimoxazole	34 (41.5)	141 (71.9)	<0.001
	Other	2 (2.4)	3 (1.5)	

[a]Missing data from five Nigerian participants.
[b]Missing data from 41 participants (South Africa, *n* = 16; Nigeria, *n* = 25).
[c]IQR, interquartile range; SD, standard deviation; iHEU, infants who are HIV-exposed yet uninfected; W15, 15 weeks of age; wflz, weight-for-length z score.

composition differed significantly by study site during the first week of life (Fig. 1A). Within-sample microbial diversity (Shannon index) was higher among South African than Nigerian infants [median 2.23 (IQR: 1.96–2.62) versus 1.13 (IQR: 0.77–1.68), $P < 0.0001$; Fig. 1B]. In addition, microbial community composition was significantly different by geographical location, although the site only explained 6% of the community composition (Fig. 1C; PERMANOVA $P < 0.001$). Geographical location remained significantly associated with α- and β-diversity after adjusting for sequencing batch or in separate models adjusting for demographic factors that significantly differed between countries, namely maternal marital status, weight, age, gravity, education level, occupation, type of house, access to a refrigerator or running water, mode of delivery, or infant gestational age ($P < 0.001$ for both α- and β-diversity). Moreover, α- and β-diversity remained significantly different by the geographic location when the comparison was made strictly among samples collected on the first day of life ($n = 147$; Fig. S1).

At baseline, most South African infants had gut microbiota consisting of (i) Actinomycetota, including several *Bifidobacterium* species (such as *B. longum* subspecies *longum*, *Bifidobacterium catenulatum,* and *Bifidobacterium breve*) and *Collinsella aerofaciens,* (ii)

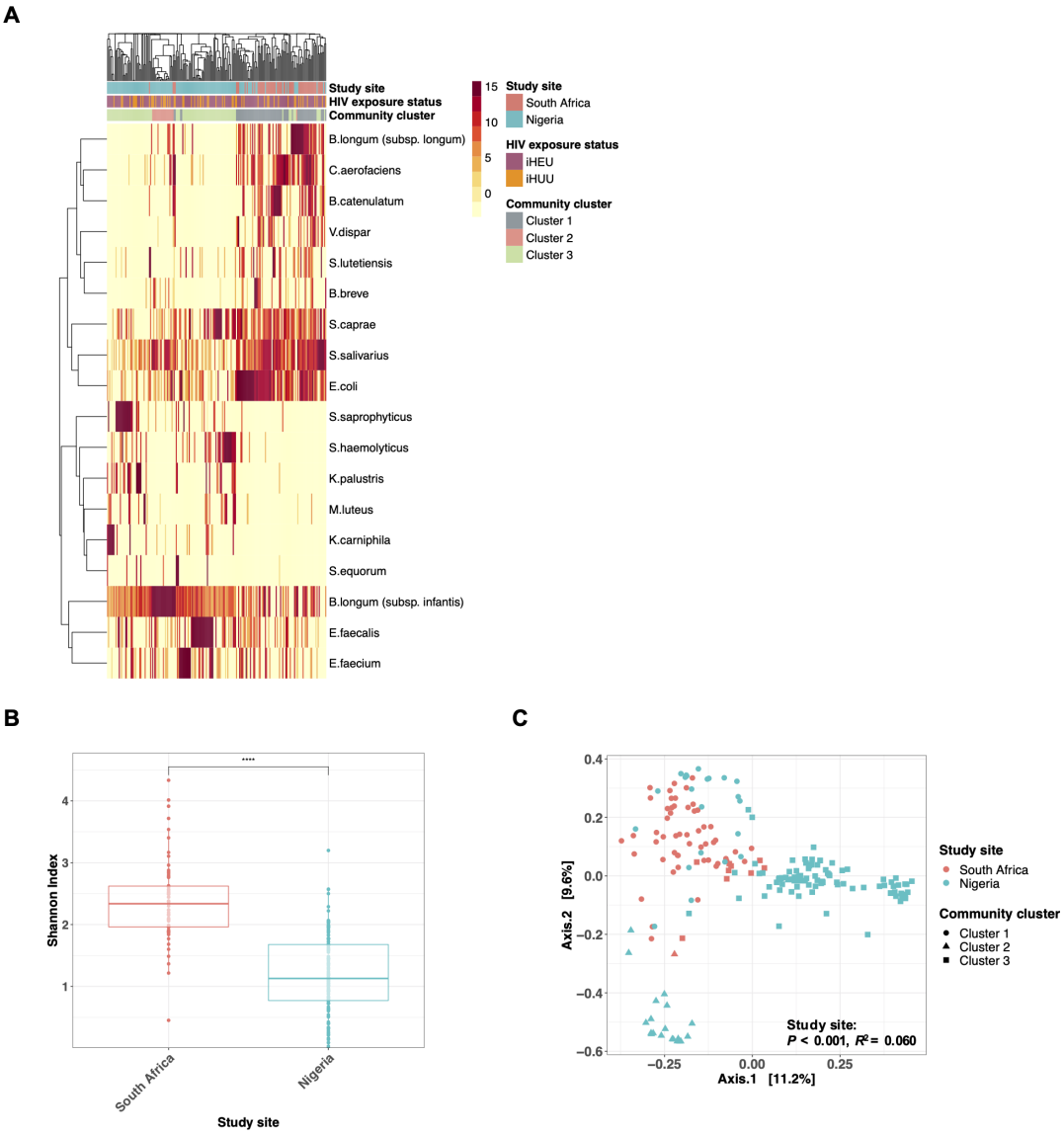

FIG 1 Geographical location strongly affects gut microbiota among African infants in the first week of life. (A) Heatmap of the top 20 taxa in the gut microbiota of South African (n = 63) and Nigerian (n = 141) infants in the first week of age. Study site, HIV exposure status, and community cluster types (based on PAM clustering; k = 3) are shown in annotation bars. (B) Comparison of α-diversity (Shannon index) between South African (n = 63) and Nigerian (n = 141) infants during the first week of life. (C) PCoA and PERMANOVA (Bray-Curtis dissimilarity) of gut microbiota during the first week of age (South African, n = 63; Nigerian, n = 141), colored by study site and shaped by community groups, based on PAM clustering (k = 3). ****P < 0.0001.

Firmicutes, including *Streptococcus* species (such as *Streptococcus salivarius*, *Streptococcus caprae*, and *Streptococcus lutetiensis*) and *Veillonella dispar,* and (iii) Proteobacteria which mainly consist of *Escherichia coli*, which was named "cluster 1" identified by PAM

clustering (Fig. 1A). On the other hand, the majority of Nigerian infants' microbiota was classified as community cluster 3, dominated by (i) Actinomycetota, mainly *B. longum* subspecies *infantis* and (ii) Firmicutes, including *Staphylococcus* species (such as *Staphylococcus haemolyticus* and *Staphylococcus saprophyticus*) and *Enterococcus* species (such as *Enterococcus faecalis* and *Enterococcus faecium*).

Age is a major driver of microbiota development, but microbial succession differs between sites

We next assessed gut microbiota longitudinally. The α-diversity in South African infants increased significantly from week 1 to week 15 [median 2.33 (IQR: 1.96–2.62) versus 2.54 (IQR: 2.26–2.77), $P = 0.036$], while α-diversity in Nigerian infants significantly decreased [median 1.13 (IQR: 0.77–1.68) versus 0.87 (IQR: 0.51–1.166), $P < 0.0001$] (Fig. 2A), further exacerbating the differences in α-diversity between sites. There was distinct microbial community composition among Nigerian samples by age, which was less evident for South African infants (Fig. 2B). In agreement, the dominant bacterial changed only marginally from week 1 to week 15 among South African infants, while Nigerian infants experienced a shift from a Firmicutes-dominated microbiota (cluster 3) to one dominated by *Bifidobacterium infantis* and *Streptococcus salivarius* (cluster 2) at 15 weeks of age (Fig. 2C; Fig. 3). Given the differences in delivery mode and proportion of exclusively breastfed infants between sites, we also performed the analysis restricting to EBF ($n = 212$) or vaginally delivered ($n = 249$) infants. The significant differences observed between countries in α- and β-diversity remained over the 15 weeks when the comparison was strictly among EBF infants or vaginally delivered infants (Fig. S2 and S3).

HIV exposure has a subtle effect on the gut microbiota regardless of the geographical location

There were no significant differences in α-diversity (Fig. S4A), β-diversity (Fig. S4B), or PAM cluster transition (Fig. S4C and D) by HIV exposure status in either country. Differential abundance testing using ANCOM-BC was performed adjusting for feeding mode at the week 15 time point (34). Several bacterial taxa were significantly associated with HIV exposure status in South Africa (Table 2). Several *Enterococcus* species were significantly more abundant in iHEU than iHUU at week 1 (*E. faecium*; LFC: 0.57) and week 15 [*E. faecalis*, *Enterococcus gilvus,* and *Enterococcus raffinosus*; LFC: 0.61, 1.02, and 0.76, respectively). Moreover, *Collinsella aerofaciens* (LFC: 0.72 at week 1 and 1.18 at week 15) and *Klebsiella quasipneumoniae* (LFC: 0.84 at both week 1 and week 15), which are known to be pathobionts (37, 38), were consistently more abundant in iHEU during the first 15 weeks of life. In contrast, no bacterial taxa were differentially abundant by HIV exposure in the Nigerian cohort. To disentangle the effects of co-trimoxazole and HIV exposure on infant gut microbiota, we assessed the gut microbiota based on reported co-trimoxazole prophylaxis history. We did not see any effects of co-trimoxazole on α- and β-diversity among South African iHEU at 15 weeks of age (Fig. S5). We further explored whether co-trimoxazole partially contributed to the differentially enriched bacterial taxa that were identified in South African iHEU. When adjusting the ANCOM-BC for reported co-trimoxazole prophylaxis, several bacterial taxa were no longer enriched in iHEU (Table S2), including *Enterococcus* species (*E. faecalis* and unclassified species), *Veillonella atypica*, and *Staphylococcus* (unclassified species).

Maternal HIV status and infant gut microbes are associated with infant TT vaccine response

Among the 278 infants, plasma IgG anti-tetanus antibody data were available from 77 South African (59 iHEU and 18 iHUU) and 192 Nigerian infants (138 iHEU and 54 iHUU). In Nigeria, it is recommended that pregnant women receive TT booster vaccinations, whereas this is not policy in the Western Cape, South Africa (39). Therefore, not surprisingly, infant anti-tetanus IgG concentrations in the first week of life, representing

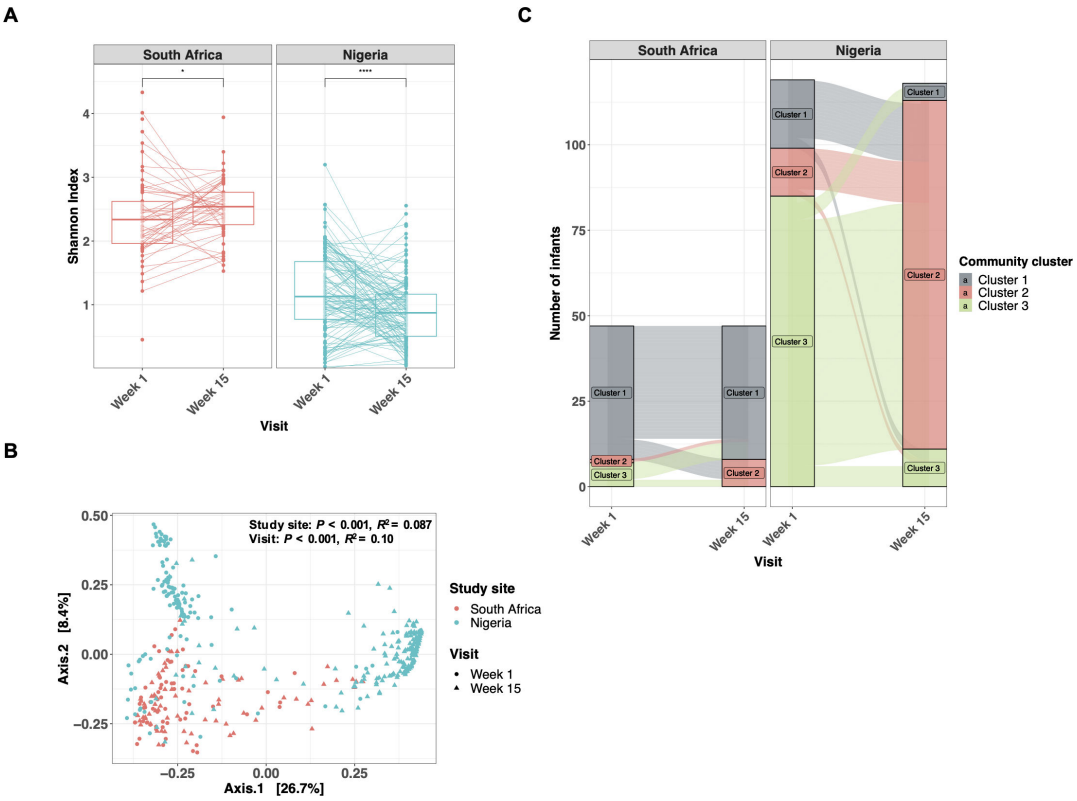

FIG 2 Longitudinal transition of gut microbiota is distinct among infants in South Africa and Nigeria. (A) The transition of α-diversity (Shannon index) of infant gut microbiota over the first 15 weeks of age in South Africa (n = 82) and Nigeria (n = 196). (B) PCoA and PERMANOVA (Bray-Curtis dissimilarity) of gut microbiota at 1 week and 15 weeks of age, colored by study site and shaped by visit (South African, n = 82; Nigerian, n = 196). (C) Alluvial plot showing the transition of cluster groups from week 1 to week 15 at each study site (South African, n = 82; Nigerian, n = 196). Samples were grouped according to PAM clustering (k = 3), indicated by color. *P < 0.05; ****P < 0.0001.

maternally transferred antibodies, were significantly lower among South African infants than Nigerian infants [median 1.0 (IQR: 0.55–2.2) versus 1.5 (IQR: 0.9–4.1) IU/mL, adj P = 0.002; Fig. S6A]. In contrast, titers did not differ between South African and Nigerian infants at 15 weeks of age [median 1.9 (IQR: 0.65–2.5) versus 1.6 (IQR: 1.0–3.9) IU/mL, adj P = 0.280]. We investigated the correlation of TT vaccine response between mother and infant pairs living in Nigeria (n = 191). Anti-tetanus titers were strongly correlated at week 1. However, iHEU mother-infant anti-tetanus titers showed a lower Pearson's correlation coefficient compared to iHUU [R: 0.72 (P < 0.001) versus 0.95 (P < 0.001)] (Fig. 4A). The correlation between maternal and infant anti-tetanus IgG levels was no longer evident by 15 weeks of age in either iHEU or iHUU (Fig. S6B). We did not see any difference in anti-tetanus IgG titers among Nigerian mothers by their HIV status (Fig. S6C). However, iHEU had significantly lower anti-tetanus IgG concentrations than iHUU at 15 weeks of life (P = 0.016), and this remained significant after adjusting for multiple comparisons (adj P = 0.031; Fig. 4B). The difference between iHEU and iHUU at week 15 was no longer statistically significant when infants were compared separately by study site (adj P = 0.290 in South Africa and adj P = 0.180 in Nigeria; Fig. S6D).

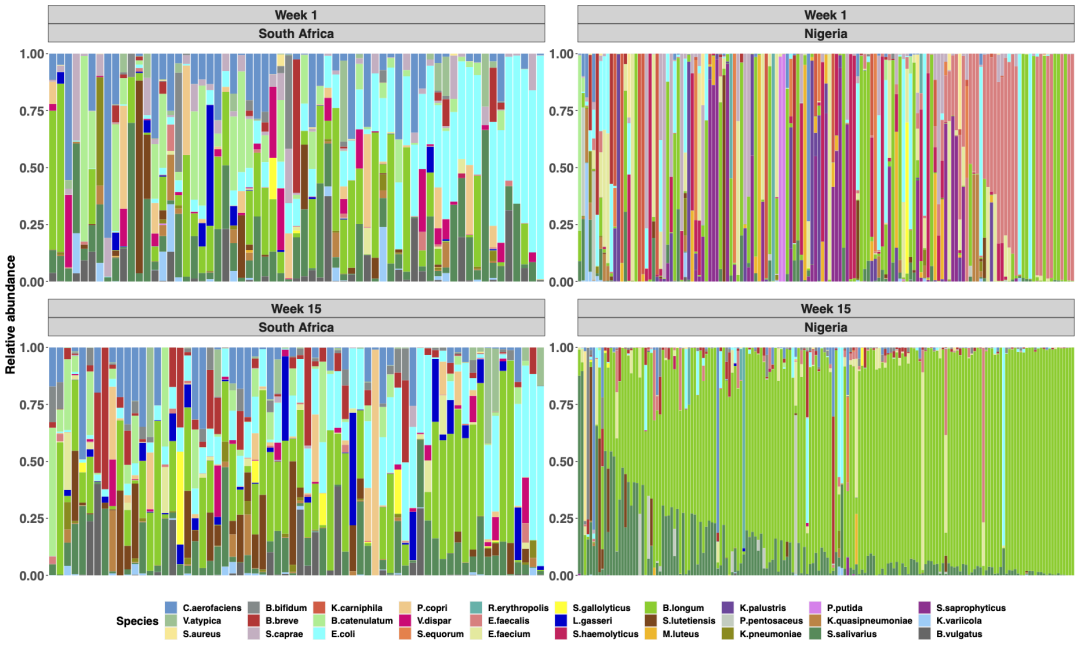

FIG 3 Infants' gut microbial succession over the first 15 weeks differs substantially between the study sites. Relative abundance plot of most abundant 30 taxa of South African (n = 82) and Nigerian (n = 196) infants at the 1 week and 15 weeks of age. Each column represents individual participants. *B. longum* subspecies *infantis* and *B. longum* subspecies *longum* are indicated as the same color (green).

Since gut microbiome is thought to modulate the development of the immune system (15), we investigated the relationship between infant gut microbiota and TT vaccine response at week 15, a week after infants complete their primary TT series. We did not see consistent correlations between 15-week anti-tetanus IgG titers and Shannon diversity at 1 or 15 weeks (Fig. 5A). To further explore factors associated with infant TT vaccine response at week 15, we conducted a LASSO regression. Rank-transformed top 50 ASVs at either week 1 or week 15, HIV exposure status, and anti-tetanus IgG titers at week 1 were included as explanatory variables to investigate the predictor, TT vaccine response at 15 weeks of age. In South Africa, infant HIV exposure status showed a strong negative association with 15-week TT vaccine response (β-coefficient = −0.44), and the rank-transformed taxon abundance at week 1 of some bacterial species, including *Streptococcus salivarius* (β-coefficient = 0.038), *Bacteroides dorei* (β-coefficient = 0.016), *Collinsella aerofaciens* (β-coefficient = 0.015), and *Sutterella wadsworthensis* (β-coefficient = −0.011) were independently associated with vaccine response, albeit with weaker β-coefficients than HIV-exposure (Fig. 5B; Table S3A). In contrast, no variables were selected as predictors of the TT vaccine response in the Nigerian cohort. Previously, it has been shown that passively transferred maternal antibody interferes with infant TT vaccination response (40). Since Nigerian infants showed significantly higher maternal antibodies than South African infants at week 1 (Fig. S6A), we speculated that these maternal anti-tetanus antibodies may have masked any associations underlying the infant TT vaccine response at week 15 of life. For this reason, we re-assessed the LASSO regression without including week 1 anti-tetanus IgG data in the explanatory variables (Fig. S7; Table S3B). Although there was no change in the result for the South African infants (Fig. S7A), HIV exposure and several bacteria present at 15 weeks of age, including *S. salivarius*, were independently associated with the TT vaccine response in Nigerian

TABLE 2 ANCOM-BC analysis of iHEU and iHUU living in South Africa[b]

Taxonomy (genus, species)	Taxon ID	LFC[a]
At 1 week of age		
Klebsiella variicola	ASV46	1.22
Sutterella (unclassified)	ASV150	1.02
Holdemanella (unclassified)	ASV53	1.00
Parabacteroides merdae	ASV101	0.98
Catenibacterium (unclassified)	ASV218	0.96
Blautia obeum	ASV59	0.93
Senegalimassilia (unclassified)	ASV145	0.87
Bifidobacterium breve	ASV10	0.84
Klebsiella quasipneumoniae	ASV36	0.84
Libanicoccus (unclassified)	ASV153	0.81
Blautia (unclassified)	ASV225	0.80
Ruminococcus torques group (unclassified)	ASV75	0.72
Collinsella aerofaciens	ASV25	0.72
Subdoligranulum (unclassified)	ASV251	0.70
Bacteroides vulgatus	ASV83	0.70
Sutterella (unclassified)	ASV496	0.67
Klebsiella pneumoniae	ASV39	0.66
Megamonas (unclassified)	ASV169	0.65
Romboutsia ilealis	ASV93	0.64
Senegalimassilia (unclassified)	ASV171	0.64
Faecalibacterium (unclassified)	ASV505	0.58
Fusobacterium mortiferum	ASV278	0.57
Enterococcus faecium	ASV7	0.57
Parabacteroides distasonis	ASV138	0.54
Actinomyces (unclassified)	ASV668	−0.54
Parabacteroides distasonis	ASV203	−0.57
At 15 weeks of age		
Streptococcus gallolyticus	ASV44	1.33
Collinsella aerofaciens	ASV25	1.18
Clostridium innocuum group (unclassified)	ASV336	1.13
Enterococcus gilvus	ASV157	1.02
Klebsiella quasipneumoniae	ASV42	0.84
Veillonella atypica	ASV163	0.83
Enterococcus raffinosus	ASV338	0.76
Enterococcus (unclassified)	ASV40	0.71
Bifidobacterium adolescentis	ASV296	0.71
Enterococcus raffinosus	ASV51	0.71
Lactococcus lactis	ASV206	0.66
Enterococcus faecalis	ASV5	0.61
Granulicatella (unclassified)	ASV681	0.59
Dorea formicigenerans	ASV229	0.59
Faecalibacterium prausnitzii	ASV103	0.52
Staphylococcus (unclassified)	ASV41	0.51
Lactobacillus rhamnosus	ASV191	−0.51
Klebsiella michiganensis	ASV266	−0.51
Lactobacillus gasseri	ASV161	−0.53
Prevotella copri	ASV405	−0.55
Megasphaera elsdenii	ASV167	−0.58
Olsenella (unclassified)	ASV97	−0.58
Prevotella (unclassified)	ASV176	−0.83
Bacteroides caccae	ASV552	−0.93

(*Continued on next page*)

TABLE 2 ANCOM-BC analysis of iHEU and iHUU living in South Africa[b] (*Continued*)

Taxonomy (genus, species)	Taxon ID	LFC[a]
Olsenella (unclassified)	ASV120	−1.89
Ruminococcus torques group (unclassified)	ASV75	−2.43

[a]Abundance in iHEU in relation to iHUU. ANCOM-BC, Analysis of Compositions of Microbiomes with Bias Correction; LFC, $\log_e$ fold change; ASV, amplicon sequence variant; iHEU, infants who are HIV-exposed uninfected; iHUU, infants who are HIV-unexposed uninfected.
[b]Differentially abundant ASVs (adj $P < 0.05$) among iHEU relative to iHUU at 1 week or 15 weeks of age in South Africa (n = 82). Data at week 15 were adjusted by mode of feeding. Positive LFC values indicate higher abundance among iHEU, whereas negative LFC values indicate higher abundance among iHUU. No differentially abundant bacterial taxa were identified among Nigerian infants.

infants (Fig. S7B). However, the β-coefficients for all selected predictors were small, including HIV exposure status.

DISCUSSION

This is one of the largest studies that longitudinally compared the gut microbiota between iHEU and iHUU in two settings and investigated the association with their vaccine responses. Our findings suggest that the country of origin was the most influential factor in the infants' gut microbiota at week 1, which also strongly affected its succession over the first 15 weeks of life. Both feeding and delivery modes have been shown to influence infant gut microbiota (41). Since these demographic characteristics significantly differed between our South African and Nigerian cohorts, we explored their potential effects on the infant gut microbiota. A comparison restricted to infants still EBF at 15 weeks showed that α- and β-diversity at that time point remained significantly different between the countries. Similarly, the difference was independent of mode of delivery. Analysis of stool samples collected shortly after birth suggested that the difference in gut microbiota profile was already prominent before feeding was established. Collectively, these data indicate that geographical location strongly

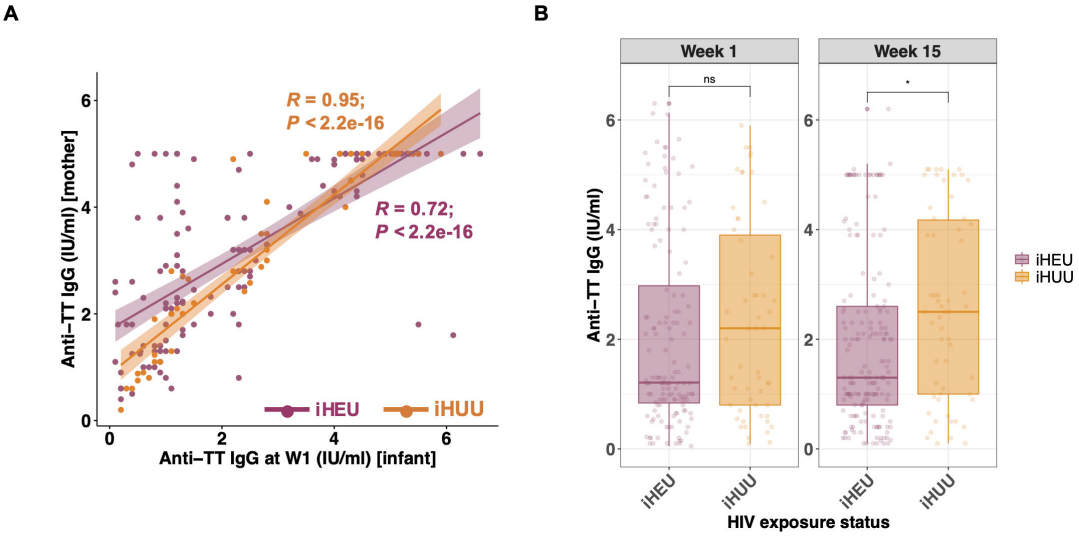

FIG 4 Passive maternal antibody and HIV exposure are both associated with infant TT vaccine response. (A) Scatter plot and Spearman's rank correlation coefficients (*R*) of anti-tetanus IgG titers (IU/mL) between Nigerian mothers (y-axis; *n* = 191) and their infants at week 1 (x-axis; *n* = 191). Dots and lines of best fit are colored by HIV exposure status. (B) Comparison of anti-tetanus IgG titers between iHEU (*n* = 197) and iHUU (*n* = 72) at week 1 and week 15. *P*-values comparing anti-tetanus IgG titers were adjusted for multiple comparisons using the Benjamini-Hochberg method. W1, 1 week of age; ns, not significant. *$P < 0.05$.

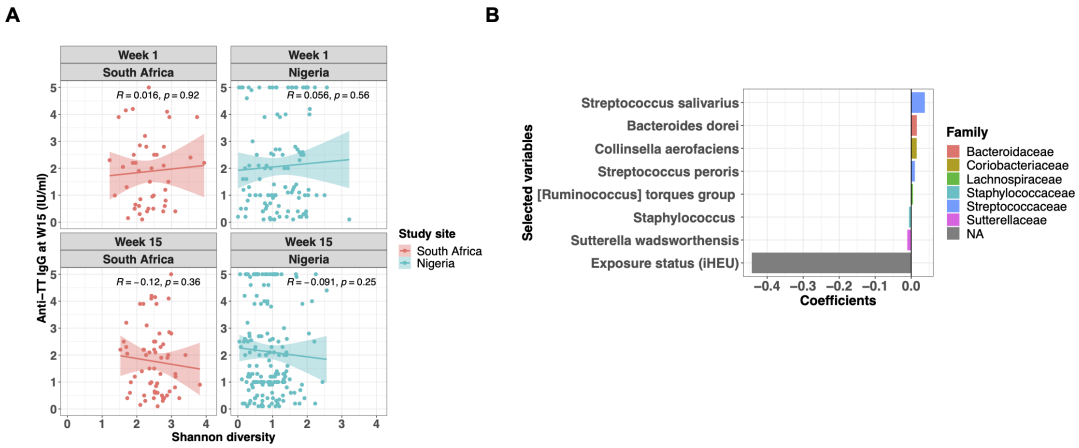

FIG 5 HIV exposure status and gut microbiota are independently associated with TT vaccine response. (A) Correlation analysis of infants' anti-tetanus IgG titers (IU/mL) measured at 15 weeks of age and α-diversity (Shannon index) at each study site and visit (South African, *n* = 65; Nigerian, *n* = 170). Spearman's rank correlation coefficients (*R*) are indicated on each panel. (B) Rank-transformed top 50 ASVs (at either week 1 or week 15), HIV exposure status, and anti-tetanus IgG titer data at week 1 were used as explanatory variables for the LASSO regression to assess the association with TT vaccine response at 15 weeks of age. Each model was constructed separately based on geographical location and time point. The optimal coefficient tuning parameter (lambda.min) was chosen using 10-fold cross-validation. Selected variables and their glmnet coefficients were plotted. Color of the bars represents taxonomy at the family level. Week 1 ASVs and HIV exposure status were associated with week 15 TT vaccine response among South African infants. No variables were selected for the Nigerian cohort. W15, 15 weeks of age.

influences the initial seeding of gut microbes, and this affects the trajectory of microbiota regardless of feeding practices. Notably, the term "geography" includes not only the physical location (rural versus urban) but also extends to socioeconomics, genetics, diet, climate, and ethnicity, among others.

Microbiota among Nigerian infants transitioned drastically over the first 15 weeks of life, such that at 15 weeks, *B. infantis* was the dominant taxon, with some *S. salivarius*. Both are commonly found in breast milk and gut microbiota among breastfed infants (42). *Bifidobacteria* benefit human health and are often used as probiotics (43). Moreover, *Streptococcus salivarius*, classified as a lactic acid bacterium, has been shown to have probiotic properties (44). However, the drastic changes in microbiota over the 15 weeks only occurred mostly among the Nigerian infants and far less in the South African infants. Plausible explanations for this may be the difference in profiles of maternal gut and breastmilk microbiota and human milk oligosaccharides influenced by genetics, ethnicity, diet, and body mass index (BMI) (45). For instance, a higher maternal BMI is associated with reduced *Bifidobacterium* in breastmilk (46), which might suggest that South African mothers, who had higher mean weight, had less *Bifidobacterium* in their breastmilk than Nigerian mothers, leading to less *Bifidobacterium* in their infants' gut. An additional explanation is that Nigerian mothers in this setting have a diet rich in fermented foods, whereas South African mothers may have a more Westernized diet (47, 48). South African infants also had higher relative abundance of *B. longum* but lower relative abundance of *B. infantis* at baseline.

Nigerian infants had significantly higher anti-tetanus titers at week 1, likely due to maternal immunization and consequent high passive maternal antibody transfer compared to South African infants (49). In contrast, in the Western Cape region where our South African cohort was recruited, there was no routine TT booster vaccination for pregnant women due to the prolonged absence of neonatal tetanus cases in the province (39). Notably, anti-tetanus IgG levels post-vaccination among Nigerian infants remained similar to those at week 1 and were comparable with South African infants.

This inferior induction of anti-tetanus IgG titers observed in Nigerian infants may be explained by the inhibition of TT vaccine response by passively transferred high maternal antibodies, as previously described (40).

We identified several bacterial taxa that exhibited differential abundance in iHEU compared to iHUU, including several pathobionts. Whether these identified bacterial taxa contribute to increased risk of infectious morbidity in iHEU is unknown. Moreover, several bacterial enrichments in iHEU may, in part, be attributed to co-trimoxazole prophylaxis recommended for this population. For example, *E. faecalis* frequently carries co-trimoxazole resistance (50). Supporting this, our differential abundance analysis showed that the enrichment of *E. faecalis* was no longer evident in 15-week-old iHEU after adjusting for reported co-trimoxazole prophylaxis use. Of note, there was a significant difference in reported co-trimoxazole use among iHEU between the countries in our study. Since the record of co-trimoxazole treatment was sorely relied on mothers' recall at each follow-up visit, it is possible that the accuracy of reported antibiotics records among iHEU may be underestimated.

LASSO regression models also suggested that *in utero* HIV exposure and relative abundance of several bacterial taxa at week 1 were independently associated with later TT vaccine response in South Africa but not Nigeria. The higher passive antibody levels observed in Nigerian infants may have mitigated the effects of HIV exposure and microbiota on the infant vaccine response. In fact, excluding the week 1 titer data from the regression model indicated that the HIV exposure and several microbes found at 15 weeks of age were independently associated with the infant TT vaccine response among Nigerian infants. In line with our assumption, removing week 1 titer data from the regression model did not change the LASSO regression result in South African infants, who showed much lower passive maternal antibody transfer. Interestingly, *S. salivarius* relative abundance was predictive of improved anti-tetanus IgG titers in both cohorts. Since the microbiota at week 1 among South African infants was associated with TT vaccine response at week 15, this suggests that in some settings, vaccine responses could potentially be modified using an early-life microbiome intervention where maternal vaccination is not possible.

There are several limitations in our study. Firstly, we did not have comprehensive records of maternal lifestyle and dietary information, which are known to have an impact on gut microbiota composition. In addition, co-trimoxazole adherence among iHEU was not extensively captured. All iHEU received nevirapine post-exposure prophylaxis; therefore, the effects of HIV exposure versus antiretroviral exposure cannot be disentangled. Lastly, additional data, both maternal (such as vaginal and breastmilk microbiota) and infant (such as gut metabolomics, metatranscriptomics, and metagenomics), could have provided more insights into our study.

Conclusions

This study showed that the transition of infant gut microbiota was strongly dependent on geographical location and age, while effect of *in utero* HIV exposure was modest. However, maternal HIV status was negatively associated with the passive maternal anti-tetanus antibody transfer, and the negative effect of HIV exposure on TT vaccine response persisted over the first 15 weeks of life among iHEU. In addition, there were independent associations of specific gut microbes and HIV exposure with infant humoral response to TT vaccine at 15 weeks of age.

ACKNOWLEDGMENTS

We would like to thank the mothers and infants who participated in this study, the clinic staff at the Plateau State Specialist Hospital, Jos, Nigeria, and the Khayelitsha Site B Clinic in Cape Town, South Africa, and the InFANT study lab technologists.

This work was funded by the Canadian Institutes of Health Research (CIHR) (01044–000 awarded to C.M.G.) and the U.S. National Institutes of Health (NIH), Eunice Kennedy

Shriver National Institute of Child Health and Human Development (NICHD), and the National Human Genome Research Institute (NHGRI) (U01HD094658 to A.A.). S.C.I. was funded by the Yoshida Scholarship Foundation.

C.M.G., A.A., J.M.B., and H.B.J. contributed to the conception and design of the study. S.O. was responsible for the acquisition of anti-tetanus IgG data. S.C.I. was responsible for acquiring and analyzing microbiome data and making graphs, tables, and additional files. S.C.I., H.B.J., A.H., and S.P.H. were involved in data interpretation. S.C.I., H.B.J., and A.H. wrote the manuscript. All authors participated in drafting and revising the manuscript and approved the final version of the manuscript.

AUTHOR AFFILIATIONS

[1]Division of Immunology, Department of Pathology, University of Cape Town, Cape Town, South Africa
[2]Institute of Infectious Disease and Molecular Medicine, University of Cape Town, Cape Town, South Africa
[3]Institute of Human Virology-Nigeria, Abuja, Nigeria
[4]Division of Molecular Biology and Human Genetics, Biomedical Research Institute, Stellenbosch University, Cape Town, South Africa
[5]Department of Statistics, Stanford University, Stanford, California, USA
[6]Division of Chemical and Systems Biology, University of Cape Town, Cape Town, South Africa
[7]Institute of Human Virology, University of Maryland, School of Medicine, Baltimore, Maryland, USA
[8]Seattle Children's Research Institute, Center for Global Infectious Disease Research, Seattle, Washington, USA

AUTHOR ORCIDs

Saori C. Iwase http://orcid.org/0009-0009-6481-0305
Sophia Osawe http://orcid.org/0000-0001-7998-9680
Anna-Ursula Happel http://orcid.org/0000-0003-3658-8638
Heather B. Jaspan http://orcid.org/0000-0002-0745-6073

FUNDING

Funder	Grant(s)	Author(s)
HHS | NIH | Eunice Kennedy Shriver National Institute of Child Health and Human Development (NICHD)	U01HD094658	Alash'le Abimiku
Gouvernement du Canada | Canadian Institutes of Health Research (IRSC)	OCB034114	Heather B. Jaspan
Yoshida Scholarship Foundation (YSF)		Saori C. Iwase
HHS | NIH | National Institute of Allergy and Infectious Diseases (NIAID)	R01AI120714	Heather B. Jaspan

AUTHOR CONTRIBUTIONS

Saori C. Iwase, Data curation, Formal analysis, Investigation, Visualization, Writing – original draft | Sophia Osawe, Data curation, Formal analysis, Supervision, Writing – review and editing | Anna-Ursula Happel, Data curation, Formal analysis, Investigation, Supervision, Writing – review and editing | Clive M. Gray, Conceptualization, Writing – review and editing | Susan P. Holmes, Methodology, Supervision, Writing – review and editing | Jonathan M. Blackburn, Conceptualization, Writing – review and editing | Alash'le Abimiku, Conceptualization, Funding acquisition, Supervision, Writing – review and editing.

DATA AVAILABILITY

Sequencing reads from the 16S rRNA gene profiling are available at the Sequence Read Archive repository hosted by NCBI (accession number PRJNA976299). Scripts and related data sets can be found at https://github.com/saiwase/BEAMING_GUT_MICROBIOME.

ETHICS APPROVAL

The study was conducted under the Declaration of Helsinki. The protocol was approved by the Ethics Committee of the University of Cape Town (HREC 285/2012), the Institutional Review Board of Seattle Children's Hospital (Study # 15690), and the Human Research Committee of the Plateau State Hospital Jos (PSSS/ADM/ETHC/2015/004). Written informed consent was obtained from all mothers in their preferred language prior to enrolment.

ADDITIONAL FILES

The following material is available online.

Supplemental Material

Fig. S1 (Spectrum03190-23-s0001.pdf). α-diversity of meconium samples differs significantly by study site.
Fig. S2 (Spectrum03190-23-s0002.pdf). α- and β-diversity significantly differ between the countries in exclusively breastfed infants.
Fig. S3 (Spectrum03190-23-s0003.pdf). α- and β-diversity significantly differ between the countries in vaginally delivered infants.
Fig. S4 (Spectrum03190-23-s0004.pdf). HIV exposure has a subtle effect on gut microbiota across two African countries.
Fig. S5 (Spectrum03190-23-s0005.pdf). The effect of co-trimoxazole on α- and β-diversity of gut microbiota is marginal.
Fig. S6 (Spectrum03190-23-s0006.pdf). Association of infant anti-tetanus titer with age, HIV exposure status and mother's anti-tetanus titer.
Fig. S7 (Spectrum03190-23-s0007.pdf). Maternal antibodies may mask the effect of HIV exposure and microbiota on infant vaccine response.
SupplementalMaterials (Spectrum03190-23-s0008.docx). Supplemental tables and figure legends.

Open Peer Review

PEER REVIEW HISTORY (review-history.pdf). An accounting of the reviewer comments and feedback.

REFERENCES

1. Gensollen T, Iyer SS, Kasper DL, Blumberg RS. 2016. How colonization by microbiota in early life shapes the immune system. Science 352:539–544. https://doi.org/10.1126/science.aad9378
2. Subramanian S, Blanton LV, Frese SA, Charbonneau M, Mills DA, Gordon JI. 2015. Cultivating healthy growth and nutrition through the gut microbiota. Cell 161:36–48. https://doi.org/10.1016/j.cell.2015.03.013
3. Slogrove AL, Powis KM, Johnson LF, Stover J, Mahy M. 2020. Estimates of the global population of children who are HIV-exposed and uninfected, 2000–18: a modelling study. Lancet Glob Health 8:e67–e75. https://doi.org/10.1016/S2214-109X(19)30448-6
4. Cohen C, Moyes J, Tempia S, Groome M, Walaza S, Pretorius M, Naby F, Mekgoe O, Kahn K, von Gottberg A, Wolter N, Cohen AL, von Mollendorf C, Venter M, Madhi SA. 2016. Epidemiology of acute lower respiratory tract infection in HIV-exposed uninfected infants. Pediatrics 137:e20153272. https://doi.org/10.1542/peds.2015-3272
5. Smith C, Moraka NO, Ibrahim M, Moyo S, Mayondi G, Kammerer B, Leidner J, Gaseitsiwe S, Li S, Shapiro R, Lockman S, Weinberg A. 2020. Human immunodeficiency virus exposure but not early cytomegalovirus infection is associated with increased hospitalization and decreased memory T-cell responses to tetanus vaccine. J Infect Dis 221:1167–1175. https://doi.org/10.1093/infdis/jiz590
6. Abu-Raya B, Smolen KK, Willems F, Kollmann TR, Marchant A. 2016. Transfer of maternal antimicrobial immunity to HIV-exposed uninfected newborns. Front Immunol 7:338. https://doi.org/10.3389/fimmu.2016.00338
7. Bender JM, Li F, Martelly S, Byrt E, Rouzier V, Leo M, Tobin N, Pannaraj PS, Adisetiyo H, Rollie A, Santiskulvong C, Wang S, Autran C, Bode L, Fitzgerald D, Kuhn L, Aldrovandi GM. 2016. Maternal HIV infection influences the microbiome of HIV-uninfected infants. Sci Transl Med 8:349ra100. https://doi.org/10.1126/scitranslmed.aaf5103
8. Jackson CL, Frank DN, Robertson CE, Ir D, Kofonow JM, Montlha MP, Mutsaerts E, Nunes MC, Madhi SA, Ghosh D, Weinberg A, Messaoudi I. 2022. Evolution of the gut microbiome in HIV-exposed uninfected and

unexposed infants during the first year of life. mBio 13:e0122922. https://doi.org/10.1128/mbio.01229-22
9. Grant-Beurmann S, Jumare J, Ndembi N, Matthew O, Shutt A, Omoigberale A, Martin OA, Fraser CM, Charurat M. 2022. Dynamics of the infant gut microbiota in the first 18 months of life: The impact of maternal HIV infection and breastfeeding. Microbiome 10:61. https://doi.org/10.1186/s40168-022-01230-1
10. Claassen-Weitz S, Gardner-Lubbe S, Nicol P, Botha G, Mounaud S, Shankar J, Nierman WC, Mulder N, Budree S, Zar HJ, Nicol MP, Kaba M. 2018. HIV-exposure, early life feeding practices and delivery mode impacts on faecal bacterial profiles in a South African birth cohort. Sci Rep 8:5078. https://doi.org/10.1038/s41598-018-22244-6
11. Machiavelli A, Duarte RTD, Pires MM de S, Zárate-Bladés CR, Pinto AR. 2019. The impact of in utero HIV exposure on gut microbiota, inflammation, and microbial translocation. Gut Microbes 10:599–614. https://doi.org/10.1080/19490976.2018.1560768
12. Amenyogbe N, Dimitriu P, Cho P, Ruck C, Fortuno ES, Cai B, Alimenti A, Côté HCF, Maan EJ, Slogrove AL, Esser M, Marchant A, Goetghebuer T, Shannon CP, Tebbutt SJ, Kollmann TR, Mohn WW, Smolen KK. 2020. Innate immune responses and gut microbiomes distinguish HIV-exposed from HIV-unexposed children in a population-specific manner. J Immunol 205:2618–2628. https://doi.org/10.4049/jimmunol.2000040
13. Zimmermann P, Curtis N. 2019. Factors that influence the immune response to vaccination. Clin Microbiol Rev 32:e00084-18. https://doi.org/10.1128/CMR.00084-18
14. Chong FS, O'Sullivan MG, Kerry JP, Moloney AP, Methven L, Gordon AW, Hagan TD, Farmer LJ. 2020. Understanding consumer liking of beef using hierarchical cluster analysis and external preference mapping. J Sci Food Agric 100:245–257. https://doi.org/10.1002/jsfa.10032
15. Huda MN, Lewis Z, Kalanetra KM, Rashid M, Ahmad SM, Raqib R, Qadri F, Underwood MA, Mills DA, Stephensen CB. 2014. Stool microbiota and vaccine responses of infants. Pediatrics 134:e362–72. https://doi.org/10.1542/peds.2013-3937
16. Huda MN, Ahmad SM, Alam MJ, Khanam A, Kalanetra KM, Taft DH, Raqib R, Underwood MA, Mills DA, Stephensen CB. 2019. Bifidobacterium abundance in early infancy and vaccine response at 2 years of age. Pediatrics 143:e20181489. https://doi.org/10.1542/peds.2018-1489
17. Tchakoute CT, Sainani KL, Osawe S, Datong P, Kiravu A, Rosenthal KL, Gray CM, Cameron DW, Abimiku A, Jaspan HB, INFANT study team. 2018. Breastfeeding mitigates the effects of maternal HIV on infant infectious morbidity in the option BR era. AIDS 32:2383–2391. https://doi.org/10.1097/QAD.0000000000001974
18. Department of Health, Republic of South Africa. 2015. National consolidated guidelines for the prevention of mother-to-child transmission of HIV. Available from: https://www.knowledgehub.org.za/system/files/elibdownloads/2019-07/National%2520consolidated%2520guidelines%25202015.pdf
19. Federal Ministry of Health. 2016. National guidelines for HIV prevention, treatment and care. National AIDS and STI's Control Programme. Available from: https://www.prepwatch.org/wp-content/uploads/2017/08/nigeria_national_guidelines_2016.pdf
20. WHO. 2015. Service delivery (Consolidated guidelines on the use of antiretroviral drugs for treating and preventing HIV infection). World Health Organisation (WHO). https://apps.who.int/iris/bitstream/handle/10665/198064/9789241509893_eng.pdf.
21. Kuhn L, Aldrovandi GM, Sinkala M, Kankasa C, Semrau K, Kasonde P, Mwiya M, Tsai W-Y, Thea DM, Zambia Exclusive Breastfeeding Study (ZEBS). 2009. Differential effects of early weaning for HIV-free survival of children born to HIV-infected mothers by severity of maternal disease. PLoS ONE 4:e6059. https://doi.org/10.1371/journal.pone.0006059
22. Machingaidze S, Wiysonge CS, Hussey GD. 2013. Strengthening the expanded programme on immunization in Africa: looking beyond 2015. PLoS Med. 10:e1001405. https://doi.org/10.1371/journal.pmed.1001405
23. Yuan S, Cohen DB, Ravel J, Abdo Z, Forney LJ, Gilbert JA. 2012. Evaluation of methods for the extraction and purification of DNA from the human microbiome. PLoS One 7:e33865. https://doi.org/10.1371/journal.pone.0033865
24. Dabee S, Tanko RF, Brown BP, Bunjun R, Balle C, Feng C, Konstantinus IN, Jaumdally SZ, Onono M, Nair G, Palanee-Phillips T, Gill K, Baeten JM, Bekker LG, Passmore JAS, Heffron R, Jaspan HB, Happel AU. 2021. Comparison of female genital tract cytokine and microbiota signatures induced by initiation of Intramuscular DMPA and NET-EN hormonal contraceptives - a prospective cohort analysis. Front Immunol 12:760504. https://doi.org/10.3389/fimmu.2021.760504
25. Martin M. 2011. Cutadapt removes adapter sequences from high-throughput sequencing reads. EMBnet j 17:10. https://doi.org/10.14806/ej.17.1.200
26. Callahan BJ, McMurdie PJ, Rosen MJ, Han AW, Johnson AJA, Holmes SP. 2016. DADA2: high-resolution sample inference from illumina amplicon data. Nat Methods 13:581–583. https://doi.org/10.1038/nmeth.3869
27. 3.6.3 RDCT. 2020. A language and environment for statistical computing. R foundation for statistical computing. Vienna, Austria
28. Quast C, Pruesse E, Yilmaz P, Gerken J, Schweer T, Yarza P, Peplies J, Glöckner FO. 2013. The SILVA Ribosomal RNA gene database project: improved data processing and web-based tools. Nucleic Acids Res. 41:D590–6. https://doi.org/10.1093/nar/gks1219
29. Brown BP. 2021. Updated 16S databases for marker gene Taxonomic assignment. Available from: https://github.com/itsmisterbrown/updated_16S_dbs
30. Davis NM, Proctor DM, Holmes SP, Relman DA, Callahan BJ. 2018. Simple statistical identification and removal of contaminant sequences in marker-gene and metagenomics data. Microbiome 6:226. https://doi.org/10.1186/s40168-018-0605-2
31. McMurdie PJ, Holmes S. 2013. Phyloseq: An R package for reproducible interactive analysis and graphics of microbiome census data. PLoS One 8:e61217. https://doi.org/10.1371/journal.pone.0061217
32. Simpson GL, Blanchet FG, Solymos P, Stevens MHH, Szoecs E, Wagner H, Barbour M, Bedward M, Bolker B, et al. 2022. vegan: community ecology package. Cran.R project. Available from: https://cran.r-project.org/web/packages/vegan/index.html
33. Liang D, Seyfried TN. 2001. Genes differentially expressed in the kindled Mouse brain. Brain Res Mol Brain Res 96:94–102. https://doi.org/10.1016/s0169-328x(01)00287-x
34. Lin H, Peddada SD. 2020. Analysis of compositions of microbiomes with bias correction. Nat Commun 11:3514. https://doi.org/10.1038/s41467-020-17041-7
35. Friedman J, Hastie T, Tibshirani R. 2010. Regularization paths for generalized linear models via coordinate descent. J Stat Softw 33:1–22.
36. Callahan BJ, Sankaran K, Fukuyama JA, McMurdie PJ, Holmes SP. 2016. Bioconductor workflow for microbiome data analysis: from raw reads to community analyses. F1000Res 5:1492. https://doi.org/10.12688/f1000research.8986.2
37. Chen J, Wright K, Davis JM, Jeraldo P, Marietta EV, Murray J, Nelson H, Matteson EL, Taneja V. 2016. An expansion of rare lineage intestinal microbes characterizes rheumatoid arthritis. Genome Med 8:43. https://doi.org/10.1186/s13073-016-0299-7
38. Perlaza-Jiménez L, Wu Q, Torres VVL, Zhang X, Li J, Rocker A, Lithgow T, Zhou T, Vijaykrishna D. 2020. Forensic genomics of a novel Klebsiella quasipneumoniae type from a neonatal intensive care unit in China reveals patterns of colonization, evolution and epidemiology. Microb Genom 6:1–10. https://doi.org/10.1099/mgen.0.000433
39. Western Cape Government. 2020. Circular H 117/2020: Introduction of tetanus toxoid vaccination during pregnancy. Available from: https://www.westerncape.gov.za/assets/departments/health/h117_2020_covid-19_introduction_of_tetanus_toxoid_vaccination.pdf
40. Jones C, Pollock L, Barnett SM, Battersby A, Kampmann B. 2014. The relationship between concentration of specific antibody at birth and subsequent response to primary immunization. Vaccine 32:996–1002. https://doi.org/10.1016/j.vaccine.2013.11.104
41. Dogra SK, Kwong Chung C, Wang D, Sakwinska O, Colombo Mottaz S, Sprenger N. 2021. Nurturing the early life gut microbiome and immune maturation for long term health. Microorganisms 9:2110. https://doi.org/10.3390/microorganisms9102110
42. Solís G, de Los Reyes-Gavilan CG, Fernández N, Margolles A, Gueimonde M. 2010. Establishment and development of lactic acid bacteria and bifidobacteria microbiota in breast-milk and the infant gut. Anaerobe 16:307–310. https://doi.org/10.1016/j.anaerobe.2010.02.004
43. Chen J, Chen X, Ho CL. 2021. Recent development of probiotic bifidobacteria for treating human diseases. Front Bioeng Biotechnol 9:770248. https://doi.org/10.3389/fbioe.2021.770248
44. Kaci G, Goudercourt D, Dennin V, Pot B, Doré J, Ehrlich SD, Renault P, Blottière HM, Daniel C, Delorme C. 2014. Anti-inflammatory properties of

Streptococcus salivarius, a commensal bacterium of the oral cavity and digestive tract. Appl Environ Microbiol 80:928–934. https://doi.org/10.1128/AEM.03133-13
45. Han SM, Derraik JGB, Binia A, Sprenger N, Vickers MH, Cutfield WS. 2021. Maternal and infant factors influencing human milk oligosaccharide composition: beyond maternal genetics. J Nutr 151:1383–1393. https://doi.org/10.1093/jn/nxab028
46. Cabrera-Rubio R, Collado MC, Laitinen K, Salminen S, Isolauri E, Mira A. 2012. The human milk microbiome changes over lactation and is shaped by maternal weight and mode of delivery. Am J Clin Nutr 96:544–551. https://doi.org/10.3945/ajcn.112.037382
47. Banwo K, Oyeyipo A, Mishra L, Sarkar D, Shetty K. 2022. Improving phenolic bioactive-linked functional qualities of traditional cereal-based fermented food (OGI) of *Nigeria* using compatible food synergies with underutilized edible plants. NFS Journal 27:1–12. https://doi.org/10.1016/j.nfs.2022.03.001
48. Spies HC, Nel M, Walsh CM. 2022. Adherence to the mediterranean diet of pregnant women in central South Africa: the nuemi study. Nutr Metab Insights 15:11786388221107801. https://doi.org/10.1177/-11786388221107801
49. National Population Commission (NPC) [Nigeria] and ICF. 2019. Nigeria demographic and health survey 2018. Available from: https://dhsprogram.com/pubs/pdf/FR359/FR359.pdf
50. Jafarzadeh Samani R, Tajbakhsh E, Momtaz H, Kabiri Samani M. 2021. Prevalence of virulence genes and antibiotic resistance pattern in enterococcus faecalis isolated from urinary tract infection in Shahrekord, Iran. Rep Biochem Mol Biol 10:50–59. https://doi.org/10.52547/rbmb.10.1.50